ABSTRACT

Title of Dissertation:	DIARYL NITRENIUM IONS: ELECTRONIC STATE REACTIONS, MECHANISTIC STUDIES, AND PEPTIDE LABELING
	Edward Samuel Chinn, Doctor of Philosophy, 2025
Dissertation directed by:	Professor Daniel E. Falvey Department of Chemistry and Biochemistry

Nitrenium ions are studied for their electronic properties, synthetic reactions, and their labeling of biomolecules. Diaryl nitrenium ions have sufficient conjugation to allow the nitrenium ions to both exist as a discrete structure and be directly observed by laser flash photolysis. In this dissertation the mechanisms and reactions of diaryl nitrenium ions will be examined. Further, the peptide WWCNDGR will be selectively labeled with a diaryl nitrenium ion.

Chapter 1 reviews relevant photochemistry fundamentals and nitrenium ion basics. Chapter 2 describes the 10,11-dihydrodibenzo[b,f]azepinyl nitrenium ion **2** in comparison to the diphenyl nitrenium ion **1**. It will be found that although the ethylene bridge 10,11-dihydrodibenzo[b,f]azepinyl nitrenium ion **2** raises the triplet state energy by approximately 8 kcal/mol, it's singlet state reaction rates are only minorly decreased. Chapter 3 investigates diaryl nitrenium ions' mechanism with H-atom donors as the parent amine has been reported in the literature as evidence of

triplet state reactivity. It is concluded there are alternative mechanisms for formation of the parent amine through either reducing the nitrenium ion to the neutral radical or through direct hydrogen atom abstraction from the singlet state. Chapter 4 examines the antiaromaticity of 3,6-dibromocarbazolyl nitrenium ion's mechanism with different electron donors and nucleophiles. It is concluded that the 3,6-dibromocarbazolyl nitrenium ion either gets trapped by a nucleophile or it gets reduced by an electron donor or the parent pyridinium ion to form the neutral radical. The neutral radical either gets protonated to form the parent amine or dimerizes to form the N-N dimer. Finally, chapter 5 shows that the diaryl nitrenium ion, *N*-(4,4'-dibromodiphenyl)nitrenium ion, can selectively label tryptophan on the peptide WWCNDGR.

DIARYL NITRENIUM IONS: ELECTRONIC STATE REACTIONS, MECHANISTIC STUDIES, AND PEPTIDE LABELING

by

Edward Samuel Chinn

Dissertation submitted to the Faculty of the Graduate School of the
University of Maryland, College Park, in partial fulfillment
of the requirements for the degree of
Doctor of Philosophy
2025

Advisory Committee:
Professor Daniel E. Falvey, Chair
Professor Jeffery Davis
Professor Myles Poulin
Professor Mercedes Taylor
Professor Jordan Goodman, Dean's Representative

Dedication

This dissertation is dedicated to my wife Laurelia Chinn, and my children Abigail Chinn and Steven Chinn. Thank you for always supporting me and being proud of me.

Acknowledgements

I would like to thank Dr. Falvey for the countless times he has helped me over the years. I am grateful for him always being willing to drop what he is doing to help me. Further, he has always been patient in teaching me, and has always respected my insights as a true scientist. None of this would be possible without his consistent help.

I would like to also thank my other committee members, Dr. Davis, Dr. Poulin, Dr. Taylor, and Dr. Goodman for their time and support. I am grateful for all the knowledge and time each of you have given to me to develop me into a better chemist over the years. Further, I want to thank the other faculty members and staff that have been instrumental over the years in teaching and developing my projects, Dr. Shi, Dr. Li, and Dr. Isaacs.

Thank you also to everyone I had the pleasure of serving as a teaching assistant for, Dr. Koppel, Dr. Friedman, Dr. Stocker, Dr. Montague-Smith, Dr. Falvey, Dr. Hirschauer, Dr. Dixon, and Dr. Davis. All of you have been good mentors to me in my teaching assistant assignments over the years, and I have enjoyed working with all of you.

I would also like to thank the members of the Falvey Group, both past and present, namely Dr. Andrea Zeppuhar, Donald Hong, Nicholas Simms, Yantong Li, Abigail Joyce, Abigail Svoysky, Mikael Daniel, Athra Goshtasbi-Gowharrizi, Swapno Chaudhuri, Logan Kallini, and Emma Talbot for their insights, encouragements, and friendship over the years as well.

Finally, I would like to thank my family and friends who have always encouraged me to chase after my dreams and achieve my goals no matter the hurdles.

Table of Contents

List of Tables

List of Figures

Chapter 1: Introduction to Organic Photochemistry and Nitrenium Ions

Chapter 2: Photochemical Generation and Characterization of the 5-endo-10,11-Dihydrodibenzoazepine Nitrenium Ion

Chapter 3 H-atom Donors with Diaryl Nitrenium Ions

Chapter 4: Generation of the Antiaromatic 3,6-Dibromocarbazolyl Nitrenium Ion: Mechanistic Studies and Alkene Trapping

List of Schemes

Chapter 1: Introduction to Organic Photochemistry and Nitrenium Ions

Chapter 2: Photochemical Generation and Characterization of the 5-endo-10,11-Dihydrodibenzoazepine Nitrenium Ion

Chapter 3 H-atom Donors with Diaryl Nitrenium Ions

Chapter 4: Generation of the Antiaromatic 3,6-Dibromocarbazolyl Nitrenium Ion: Mechanistic Studies and Alkene Trapping

List of Abbreviations

AMP	Adenosine Monophosphate
B3LYP	Becke, Three-parameter, Lee-Yang-Parr Functional
BDE	Bond Dissociation Energy
4-BrPhOH	4-Bromophenol
CD_3CN	Acetonitrile-d3
CH_3CN	Acetonitrile
CHD	1,4-Cyclohexadiene
CID	Collision-Induced Dissociation
4-CNPhOH	4-Cyanophenol
D_2O	Water-d2
DABCO	1,4-Diazabicyclo[2.2.2]octane
DART	Direct Analysis in Real Time
DCM	Dichloromethane
ΔE_{ST}	Singlet-Triplet Energy Gap
DFT	Density Functional Theory
DMA	*N*,*N*-Dimethylaniline
DMB	1,4-Dimethoxybenzene
DMF	Dimethylformamide
DMSO	Dimethyl Sulfoxide-d6
DNA	Deoxyribonucleic Acid
dsDNA	Double-Stranded Deoxyribonucleic Acid
EE	Electronic Energy
E_{ox}	Oxidation Potential
ESI-TOF	Electrospray Ionization Time of Flight
EVE	Ethyl Vinyl Ether
GMP	Guanosine Monophosphate
H-atom	Hydrogen Atom
H_2O	Water
HOMO	Highest Occupied Molecular Orbital
HQSC	Heteronuclear Single Quantum Coherence
k_0	Projected Decay Rate Constant in the Absence of Trap
k_2	2nd Order Rate Constant
k_{diff}	Diffusion Limited 2nd Order Rate Constant in Acetonitrile
k_H	2nd Order Rate Constant with Respect to H-atom Abstraction
KIE	Kinetic Isotope Effect
k_{obs}	Observed Pseudo First Order Rate Constant
k_{trap}	2nd Order Rate Constant with Respect to Trap
LFP	Laser Flash Photolysis
LUMO	Lowest Unoccupied Molecular Orbital
M06-2x	Minnesota 06 Functional
MALDI	Matrix Assisted Laser Desorption/Ionization
MeOD	Methanol-d4
MeOH	Methanol

MS	Mass Spectrometry
Nd:YAG	Neodymium-Doped Yttrium Aluminum Garnet
NMR	Nuclear Magnetic Resonance
NT	Nitrogen Terminus
OD	Optical density
$PhCH_3$	Toluene
PhOD	Phenol-d1
PhOH	Phenol
PMT	Photomultiplier Tube
R	Gas Constant
RBF	Round Bottom Flask
RNA	Ribose Nucleic Acid
RT	Room Temperature
SCE	Saturated Calomel Electrode
SET	Single Electron Transfer
SMD	Solvation Model Based on Density
ssDNA	Single-Stranded Deoxyribonucleic Acid
T	Temperature
TBACl	Tetra(n-butyl)ammonium Chloride
TD-DFT	Time-Dependent Density Functional Theory
THF	Tetrahydrofuran
TMB	1,3,5-Trimethoxybenzene
TMS	Trimethylsilyl
UV	Ultraviolet
Vis	Visible
WWCNDGR	Peptide: Tryptophan-Tryptophan-Cysteine-Asparagine-Aspartic Acid-Glycine-Arginine
ZPVE	Zero Point Vibrational Energy

Chapter 1: Introduction to Organic Photochemistry and Nitrenium Ions

1.1 Nitrenium Ion Definition

Nitrenium ions are hypovalent nitrogens that are isolobal and isoelectronic with carbenes. As such nitrenium ions possess a formal Lewis structure which has 2 sigma bonds to R groups, a lone pair, and a positive charge on the nitrogen as seen in Figure 1.1.[1–4] Since nitrenium ions do not possess an octet, they tend to be high energy intermediates which can undergo a number of different reactions. These reactions include combining with nucleophiles, oxidizing electron donors, H-atom abstraction, or hydride abstraction.[2,3,5–17]

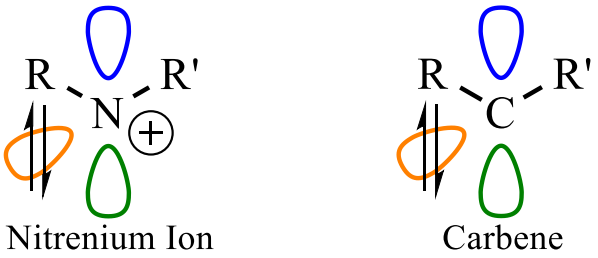

Figure 1.1. Lewis structures of a nitrenium ion and a carbene.

1.2 Alkyl vs. Aryl Nitrenium Ions

The parent nitrenium ion NH_2^+ is a nitrenium ion that has been well studied in relation to its fundamental structural properties. It is a ground state triplet with a singlet-triplet energy gap (ΔE_{ST}) of + 29.9 kcal/mol in favor of the triplet state.[18–21] However, when alkyl groups are added to the nitrenium ion, the energy barrier to methyl or hydride rearrangement does not have a local minimum. For example, the CH_3NH^+ nitrenium ion has no energy minimum, so it does not exist

as a discrete structure.[22] Other alkyl nitrenium ions have extremely low energy barriers to rearrangement. For instance, the $(CH_3)_2N^+$ nitrenium ion does not exist as a discrete structure as the energy well is below the zero-point vibrational energy of 0.11 kcal/mol.[22] Nearly all alkyl nitrenium ions have low barriers for hydride or methyl rearrangement. This along with a lack of a chromophore makes them practically impossible to directly observe by LFP. Alkyl nitrenium ions have been studied primarily through calculated energies, energy barriers, and transition states. Direct observation of alkyl nitrenium ions has not yet been reported.

The vinyl nitrenium ions have local energy minima making them true intermediates. The amount of energy needed for 1,2-alkyl rearrangement of the t-butyl vinyl nitrenium ion is only about 1.4 kcal/mol.[22] The methyl vinyl nitrenium ion has a larger 1,2-hydride shift barrier of 13.8 kcal/mol. Without greater conjugation, the vinyl nitrenium ions do not absorb high enough wavelength light to be studied by LFP. Extending conjugation by adding phenyl/aryl groups allows the energy well of the nitrenium ion to be lowered enough to be characterized.[22] For example, the phenyl methyl nitrenium ion has a 1,2-hydride shift rearrangement barrier of 22.8 kcal/mol.[22] This allows for the nitrenium to have lifetimes of hundreds of ns to μs. This makes aryl nitrenium ions desirable to study as this deeper energy well means a longer lifetime for the nitrenium ion which in turn leads to the possibility of direct characterization.

Aryl nitrenium ions have been extensively studied over the past several decades, both experimentally and through computational methods. Interest in these intermediates can be attributed to the role of aryl nitrenium ions in DNA damaging reactions,[4,23–31] but also because of potential applications as electrophilic nitrogen species in synthetic reactions,[32–42] photoaffinity agents, as well as interest in their carbene-like electronic structure.[42–50]

In general, aryl nitrenium ions react with alcohols, halide ions and water through addition to the aryl ring, rather than the formally positively charged nitrogen.[5–9,51] However electron-rich arenes, including the DNA base, guanine, can also provide N-adducts. Other reactions include H-atom or hydride donation to the nitrogen center as well as electron transfer from readily oxidized donors. One interesting trend is that para-substitution on the aryl ring attenuates aryl nitrenium reactivity toward oxygen centered nucleophiles, without significantly affecting the rate at which arenes react at the N center.[5,44,52–54] (Scheme 1.1)

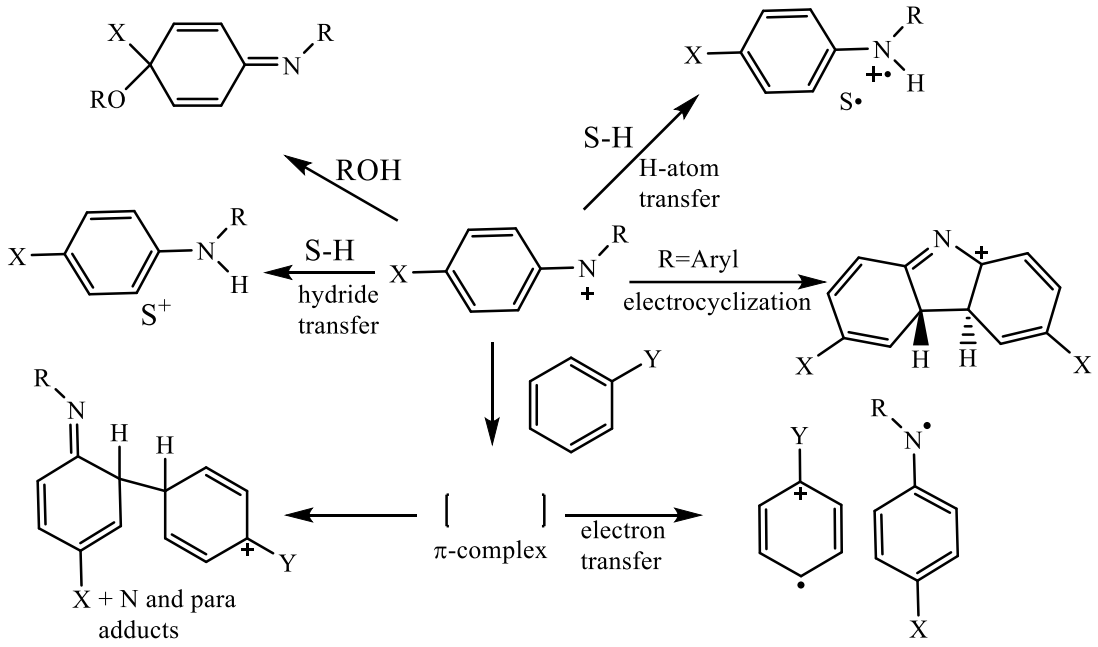

Scheme 1.1. Reactions of an aryl nitrenium ion.

Simple aryl nitrenium ions have singlet ground states due to delocalization of the charge from the nitrogen into the aromatic ring. However calculations predict that the states can be inverted when sufficiently electron-withdrawing substituents are included in the ring and/or the C-N-C central bond angle is large.[2,11,17,55] Alternatively nitrenium ions with strongly donating meta substituents also can have triplet ground states.[12,43,56] In these cases the triplet state results

from an electronic structure that involves formal transfer of an electron from the donor to the nitrogen center, creating a non-disjoint diradical ion state, analogous to the meta-xylylene diradical. The electronic spin states of a singlet and triplet nitrenium ion are given in Figure 1.2.

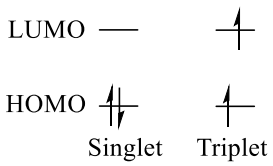

Figure 1.2. Electronic states of a singlet or triplet molecule. Only the electrons in the HOMO are shown.

Diaryl nitrenium ions are studied because the aryl rings greatly increase the lifetime of the nitrenium ions. Further the additional aryl ring increases the conjugation of the parent pyridinium ion leading to a red shifted absorbance allowing the parent pyridinium ion to have a higher molar absorptivity at 355 nm. These properties allow a high enough concentration of nitrenium ion to accumulate in solution with a laser pulse to obtain accurate pseudo first order rate constant measurements and transient absorption spectra of diaryl nitrenium ions via laser flash photolysis (LFP). Controlling when nitrenium ions are generated allows their kinetics to be studied. These two properties make LFP of pyridinium ion precursors the ideal way to generate and study diaryl nitrenium ions.

In order to support a claim that a new aryl nitrenium ion has been generated, three properties are usually shown: 1. The nitrenium ion has a different absorption spectrum than the parent compound, in our case a pyridinium ion.[8–10,12–14,17,18,57–63] 2. The nitrenium ion intermediate is shown to be distinct from the radical and the cation radical of the parent aryl amine.[11,17] 3. Product analysis of the photolyzed aryl pyridinium ion can be analyzed to determine and infer that the aryl nitrenium ion was the necessary intermediate to give rise to all

the products.[8,9,11,13,18,50,62,64–66] Additionally, aryl nitrenium ions' reactivity are characterized with 2nd order rate constants. Usually, they react at or near diffusion limit with tetra(n-butyl)ammonium chloride (TBACl) and react several orders of magnitude slower with either water or methanol.[8–11,17,62]

1.3 Aryl Nitrenium Ions and Carcinogenicity

Nitrenium ions are one of the possible intermediates in the oxidation of aromatic amines to aromatic nitro groups. It was previously shown that nitrenium ions can bond to guanosine in DNA and that these adducts have been found in cells which were exposed to a sufficiently high concentration of aromatic amines.[4,26,27,29,30,67] One example, clozapine, a drug prescribed to patients with schizophrenia, leads to the death of mice when given in sufficient concentrations, due to a covalent bond with guanosine.[4] The high effectiveness of clozapine as a therapeutic drug has produced interest in synthesizing a derivative which is effective as a therapeutic drug, without the carcinogenicity of the aryl nitrenium ion. Therefore, a predictive model for toxicity in aryl nitrenium ions would greatly benefit the drug discovery process.[4]

This predictive model would require a sufficient number of nitrenium ions to correlate the lifetime of the nitrenium ions with carcinogenic behavior in cells and/or animals. The end goal would be to find a range of reactivity which is dependent on lifetime, reactions with water, guanosine, and other biomolecules in which carcinogenic behavior is observed. Further, understanding how the substituents on the aryl rings effect the lifetime and reactivity of a nitrenium ion would allow for a predictive model to change the reactivity of these nitrenium ions.

This predictable model for nitrenium ions would allow for researchers in drug discovery to modify a toxic drug candidate like clozapine to remove the toxicity of the nitrenium ion by either adding or removing substituents. This end goal is still many years in the future. The short-term work to properly build this predictive model is to understand nitrenium ion reactivity with proteins, RNA, ssDNA, dsDNA, and other biomolecules.

1.4 Photochemistry Fundamentals

Most of the experiments discussed below involve the use of photochemical methods to generate nitrenium ions. There are five photochemical fundamentals important to understanding nitrenium ion chemistry. These five fundamentals include: the first and second laws of photochemistry, quantum yields, Jablonski diagrams, and LFP.

The first law of photochemistry, sometimes called the Grotthuss-Draper Law, is that a molecule must absorb a photon in order for a photochemical reaction to occur.[68] This is relevant in photochemically generating nitrenium ions because their parent pyridinium ion precursor must absorb the wavelength of irradiation (355-390 nm). The second law of photochemistry, sometimes called the Stark-Einstein law, is that for each photon of light absorbed by a chemical system, only one molecule is activated for subsequent reactions.[69]

A Quantum yield is the defined by the Equation 1.1.

$$\varphi = \frac{n_{molecules}}{n_{photons}} \qquad \text{(Equation 1.1)}$$

φ is the quantum yield, $n_{molecules}$ is the number of molecules that proceed through the investigated pathway, and $n_{photons}$ is the total number of photons absorbed by the molecule of interest.[70] The main area quantum yields will be relevant in this work is in photolysis of *N*-aminopyridinium ions to yield nitrenium ions.

1.5 Jablonski Diagram

Jablonski diagrams are a fundamental tool for understanding the movement of electrons through different electronic, vibrational, and rotational states. Figure 1.3 shows the Jablonski diagram relevant to all of the compounds studied in this dissertation.

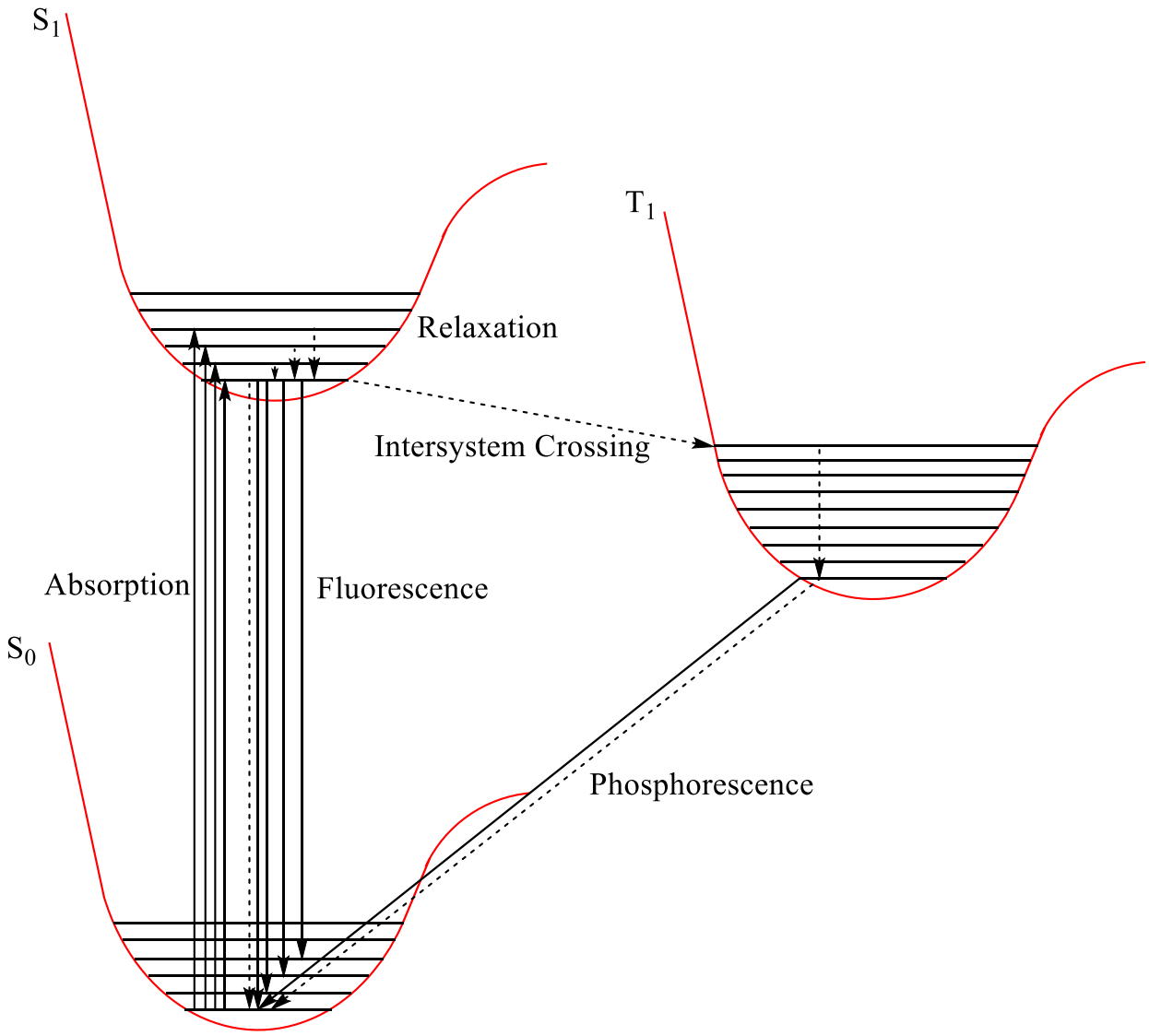

Figure 1.3. The Jablonski diagram for a molecule that is a ground state singlet and whose triplet state has some sort of geometric change to it.[71] Only electronic states and vibrational states are shown for simplification.

The surface (red lines) of each electronic state is a Morse potential. In the S_0 state, both electrons in the highest occupied molecular orbital (HOMO) are paired and it is not until a photon with an energy equal to or greater than the difference in energy between the HOMO and the lowest unoccupied molecular orbital (LUMO) that an electron is promoted from the HOMO to the LUMO resulting in an electronic configuration change from the S_0 state to the S_1 state. Once the S_1 electronic state is achieved, there is potential for a photochemical reaction. A number of things can happen from the S_1 state: fluorescence, internal conversion, intersystem crossing, vibrational relaxation, or photochemical reactions.[71] Intersystem crossing results in the electronic state of the molecule to crossover from the singlet S_1 to the triplet T_1. From this triplet state both phosphorescence and triplet state reactions are possible.

In this work the main molecules photolyzed are n-aminopyridinium ions. When N-aminopyridinium ions are photolyzed they get excited from the S_0 state to the S_1 state. From the S_1 state their N-N bond heterolytically breaks with both electrons ending up on the collidine. This generates a nitrenium ion in the S_0 electronic state. It is believed that for aryl nitrenium ions there is an equilibrium between the S_0 ground state and the T_1 state. This equilibrium requires a spin forbidden transition for the intersystem crossing to occur as seen in Figure 1.4. All aryl nitrenium ions described in this work are generated through this process.

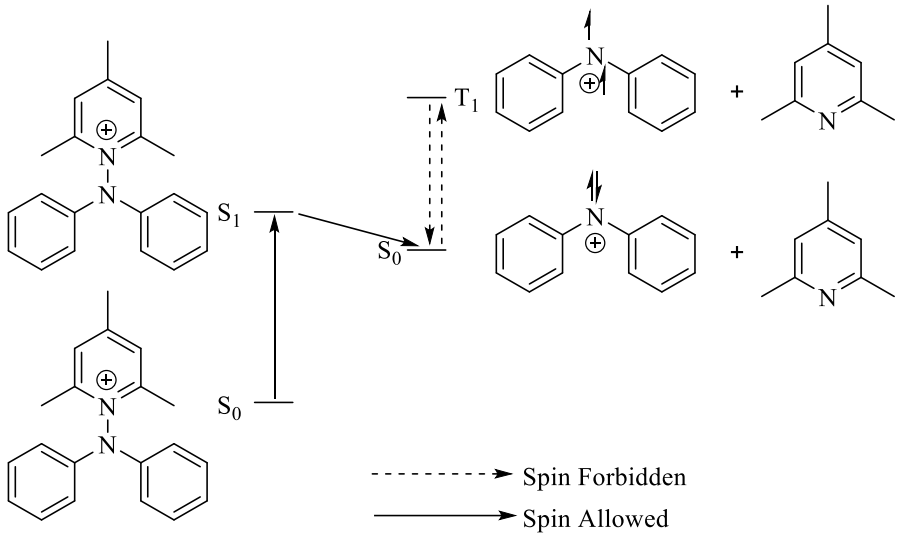

Figure 1.4. *N*-(diphenylamino)-2,4,6-trimethylpyridin-1-ium photolyzed to generate the singlet diphenyl nitrenium ion **1**. The *N*-(diphenylamino)-2,4,6-trimethylpyridin-1-ium is representative of all diaryl nitrenium ions for this process.

1.6 Laser Flash Photolysis and Transient Absorption Spectroscopy

Laser flash photolysis (LFP) is the main analytical technique used for directly studying nitrenium ions. LFP is a time-resolved spectroscopic technique which can characterize and distinguish between different short-lived intermediates such as nitrenium ions, cation radicals, and radicals. LFP will be heavily used in this text to characterize nitrenium ions and their rates of reactions with other species.

The experimental setup used to obtain LFP data is shown in Figure 1.5. The excitation source is a neodymium-doped yttrium aluminum garnet ($Nd:Y_3Al_5O_{12}$, Nd:YAG) laser. The Nd:YAG laser is capable of emitting light at 1064 nm, 532 nm, 355 nm, and 266 nm with a pulse duration of 4-6 ns. The laser beam is passed through a cylindrical lens and spread evenly across the sample cuvette. The probe beam used is a 350 W xenon-arc lamp and this provides a continuous broad spectrum of light. The probe beam is used to characterize the absorption spectrum of the transient species. The laser and the probe beam are positioned perpendicular to

each other to minimize light scattering from the laser to the monochromator. A shutter is positioned in front of the probe beam and is in sync with the laser pulses in order to minimize excess light exposure to the sample. The probe beam is focused through two lenses, one before the sample cuvette to concentrate its light source, and one after the cuvette to concentrate the light into the monochromator. After passing through the monochromator, the light reaches a photomultiplier tube (PMT) which amplifies the signal. The signal is then measured using an oscilloscope. The raw signal measured by the oscilloscope is converted to a change in optical density (ΔOD) by computer software. A positive ΔOD indicates the transient species has a greater absorbance than the ground state species being excited. The ΔOD at a given wavelength can be measured as a function of time to produce a kinetic trace. The kinetic traces can be collected at multiple wavelengths and combined to generate transient absorption spectra. The experimental spectrum can be compared with those found in literature and/or calculated by time-dependent density functional theory (TD-DFT) to determine the identity of the transient species. The reactivity of the transient species can be studied by monitoring the spectral changes upon addition of oxygen, nucleophiles, electron donors/acceptors, and hydrogen atom (H-atom) donors.

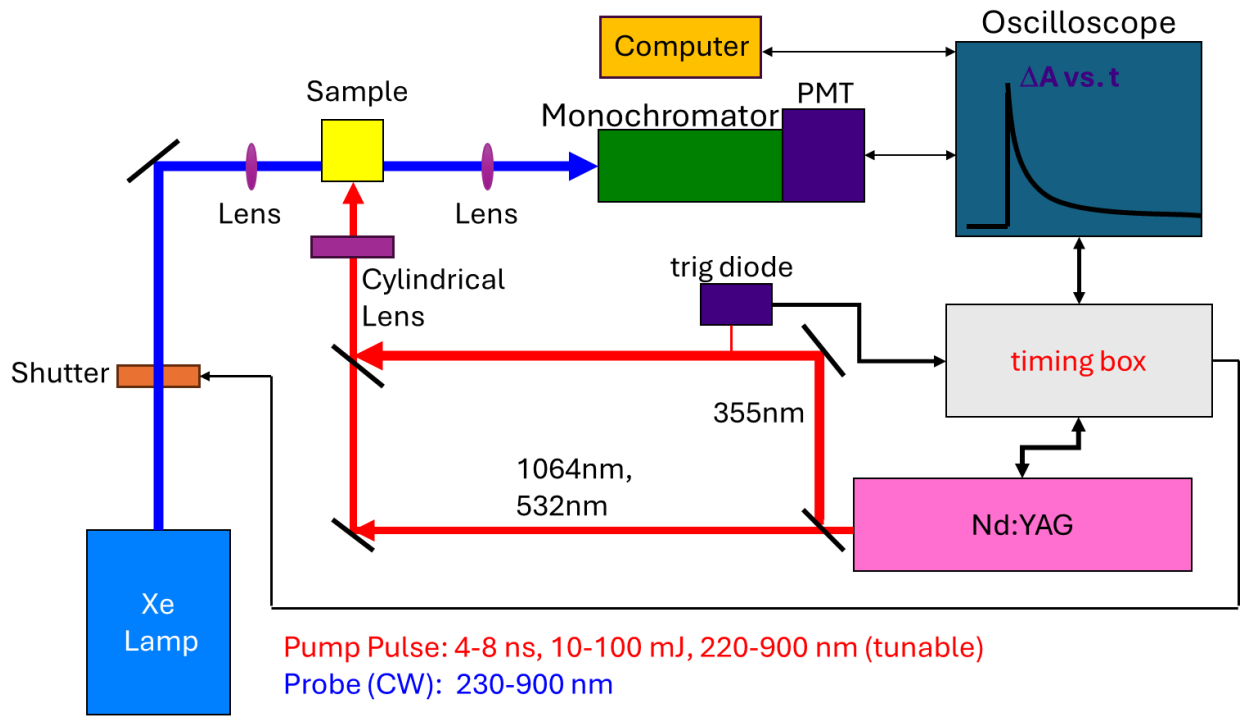

Figure 1.5. Experimental Setup to run Laser Flash Photolysis Experiments.

Practically, the best LFP results required the samples used for photolysis to have absorbances at 355 nm between 0.75 and 2 so that the sample absorbs all the light within the width of the probe beam. The pulse rate of the Nd:YAG laser was 1 Hz, and 20-30 pulses were averaged for each LFP measurement. The main limitation to the experimental setup used are transient intermediates must have lifetimes greater than 10 ns because of inherent signal to noise ratios.

LFP allows the study of long-lived singlet states and most triplet states. Further, LFP has been used to study aryl nitrenium ions for quite some time. Generally, LFP is used to measure the transient absorption spectra of nitrenium ions, the quenching of nitrenium ions, and identify other intermediates that can be formed from nitrenium ions including cation radicals or neutral

radicals.[53,63,72–78] This allows us to unambiguously assign nitrenium ions and other short-lived intermediates making LFP a powerful tool to understand aryl nitrenium ions.

Chapter 2: Photochemical Generation and Characterization of the 5-endo-10,11-Dihydrodibenzoazepine Nitrenium Ion

The majority of the work in this chapter has been published.[10]

Chinn, E. S.; Falvey, D. E. Photochemical Generation and Characterization of the 5-Endo-10,11-Dihydrodibenzoazepine Nitrenium Ion. Photochemical & Photobiological Sciences *2022,* 21, *1907–1914.*

2.1 Comparing diphenyl nitrenium ion to 5-endo-10,11-dihydrodibenzoazepine nitrenium ion

Aryl nitrenium ions are nitrenium ions in which one of the two substituents is an aryl ring. Diaryl nitrenium ions are nitrenium ions in which both of the substituents are aryl rings as seen in Figure 2.1.

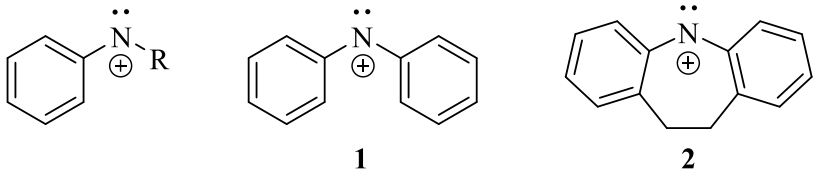

1 **2**

Figure 2.1. Important aryl and diaryl nitrenium ions. Aryl nitrenium ion (left), diphenyl nitrenium ion **1** (center), and 5-endo-10,11-dihydrodibenzo[b,f]azepinyl nitrenium ion **2**.

The diaryl nitrenium ions, like diphenyl nitrenium ion (**1**) show similar reactivity to the aryl series. However, there is an additional decay pathway available to the diaryl nitrenium ions which is electrocyclization, ultimately leading to the formation of carbazole derivatives.[13,51] The second ring destabilizes the (nominally) sp^2 orbital on the nitrogen by rotating this ring out of plane. This tends to decrease the singlet-triplet gap by approximately 10 kcal/mol relative to

phenyl nitrenium ion (approximately 20 kcal/mol). In most cases the diaryls have singlet ground states (i.e. a $-\Delta E_{ST}$).

As part of a long-term effort to understand the effects of structure on the behavior of nitrenium ions, the current study was aimed at the 5-endo-10,11-dihydrodibenzo[b,f]azepinyl nitrenium ion **2**. This species differs from diphenyl nitrenium ion (**1)** in having a two-carbon bridge that connects the aryl rings at their respective ortho positions. It was anticipated that this feature would inhibit the electrocyclization leading to carbazole, leading to a longer lifetime. The weakly electron donating alkyl groups in the ortho-position were also expected to inhibit reaction with external nucleophiles, such as H_2O and methanol. For the singlet-triplet energy splitting there are two competing effects. The increased C–N–C bond angle enforced by the bridge would tend to stabilize the triplet state relative to the singlet. On the other hand, the bridge is also expected to keep the two aromatics rings nearly coplanar. This effect would tend to destabilize the triplet state.

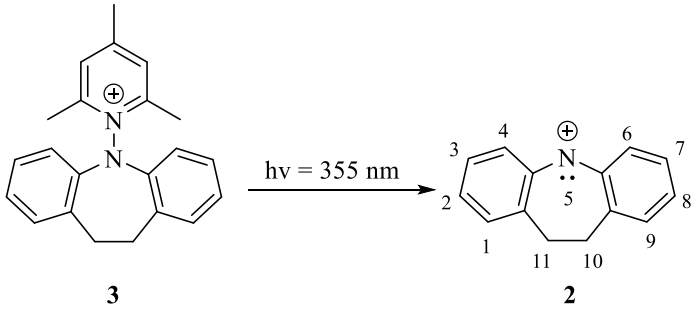

3 **2**

Scheme 2.1. Generation of nitrenium ion **2**.

A combination of calculations, photoproduct analysis, and LFP experiments were therefore carried out on 1-(10,11-dihydro-dibenzo[*b*,*f*]azepin-5-yl)-2,4,6-trimethylpyridin-1-ium tetraflouroborate (**3**), a photoprecursor to nitrenium ion **2** (see Scheme 2.1). These studies show

that **2** (a) has a singlet ground state with a more substantial energy gap than **1** (b) has a significantly longer lifetime than **1** due to inhibition of the electrocyclization reactions (c) shows a modest decrease in reactivity toward both hydroxylic and aromatic nucleophiles.

2.2 Computational comparison of diphenyl nitrenium ion to 5-endo-10,11-dihydrodibenzoazepine nitrenium ion

Calculations, using density functional theory (DFT – (u)M062x/6-311G(d,p)), were used to predict the geometries and electronic characteristics of nitrenium ion **2**. To the extent experimental data are available, DFT methods have been shown to provide reasonably accurate predictions of geometries, spectra, and singlet-triplet energy gaps for carbenes, nitrenium ions and related reactive intermediates. Minimized geometries for the singlet state and the triplet state are illustrated in Figure 2.2. The singlet state shows a central (C-N-C) bond angle of 132.4 deg and the aryl rings deviate from coplanarity by 20.6 deg. The triplet, which lies 18.5 kcal/mol above the singlet, shows a larger central angle of 144.4 deg and the aryl rings are 34.8 deg away from coplanarity.

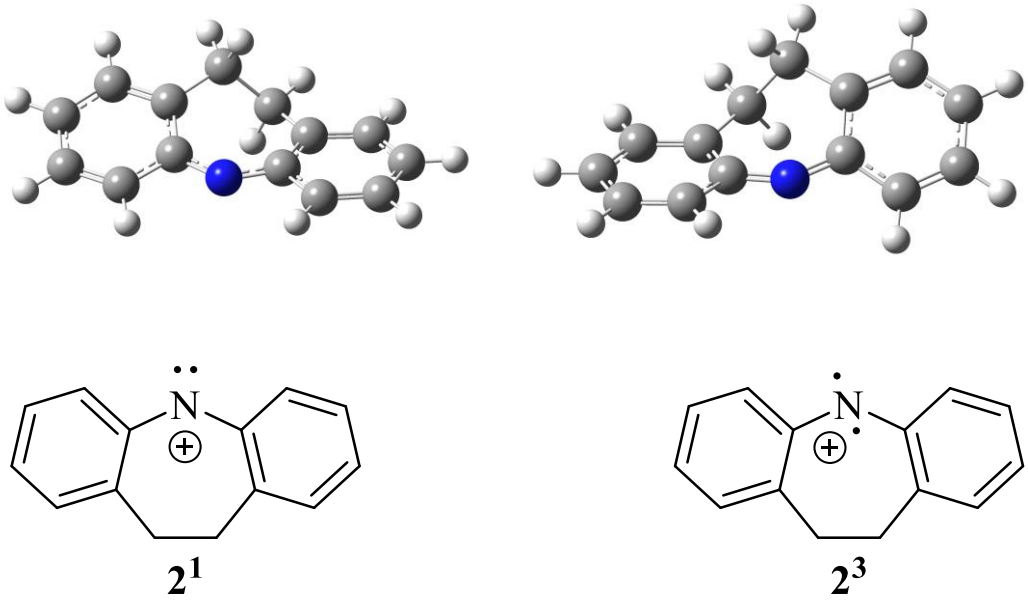

2^1 2^3

(a) (b)

Figure 2.2. DFT-calculated Geometries and Structures for (a) Singlet and (b) Triplet **2**.

The effect of the 2-carbon bridge can be assessed by comparing these geometric parameters to those of the unconstrained diphenyl nitrenium ion **1**. In the latter case, the singlet state shows a slightly more acute bond angle of 124.4 deg, as well as a slightly larger deviation from planarity. A more dramatic example is seen with the triplet state. The bridge forces triplet **2** to lie closer to co-planarity (34.8 deg) whereas in the unconstrained diphenyl system the rings are nearly perpendicular (74.6 deg). Similarly, **1**'s triplet state can adopt a C-N-C bond angle of 147 deg.

Table 2.1. Comparison of DFT Calculated Geometries and Electronic Properties of Nitrenium Ions **2** and **1**.

	2	**1**
ΔE_{ST} (kcal/mol)	-18.5	-10.0
λ_{max} (nm)	385 (s) 487 (w) 618 (w)	353 (s) 502 (w) 645 (s)
Singlet C–N–C angle (deg)	132.4	124.4
Singlet Aryl dihedral (deg)	20.6	31.2
Triplet C–N–C angle (deg)	144.4	147.0
Triplet Aryl dihedral	34.8	74.6

In all, the 2–carbon bridge distorts, and presumably destabilizes, the triplet state far more than it does the singlet state. For this reason, the singlet-triplet gap increases from -10.0 kcal/mol in **1** (favoring the singlet) to -18.5 kcal/mol for **2** as a consequence of the greater ring strain on the triplet.

2.3 Characterization of the 5-endo-10,11-dihydrodibenzoazepine nitrenium ion

The photochemical precursor to **2** is the N-amino-pyridinium ion **3**. The latter was prepared from 10,11-dihydro-dibenzoazepine **4** by subjecting that compound to nitrosation, reduction and condensation with 2,4,6-trimethylpyryllium tetrafluoroborate, following a previously described approach.[13,17] The identity of the product was confirmed by standard spectroscopic methods. Characterization data and detailed procedures are provided in the supporting information. The UV-Vis spectrum of the compound is provided in Figure 2.3. Similar to other examples of N-aminopyridinium ions, **3** shows a high wavelength absorption maximum in the near UV at 395 nm.

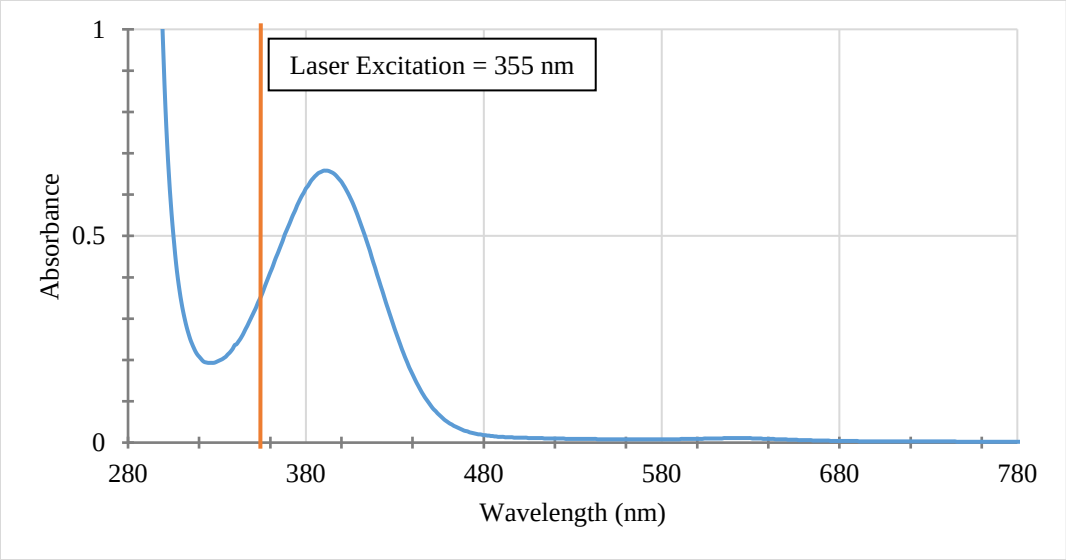

Figure 2.3. UV-Vis absorption spectrum of **3** in CH_3CN.

Consistent with previous examples, photolysis of the current pyridinium salt **3** generates stable products consistent with the formation of a short-lived nitrenium ion. For example, photolysis (390 nm) of **3** with TBACl in CH_3CN provides the corresponding adduct **5** that would result from nucleophilic addition to the 2-position (i.e. *para* to the nitrogen) followed by a net 1,5 hydrogen shift. This product was isolated by column chromatography and characterized by standard spectroscopic methods. (See Scheme 2.2)

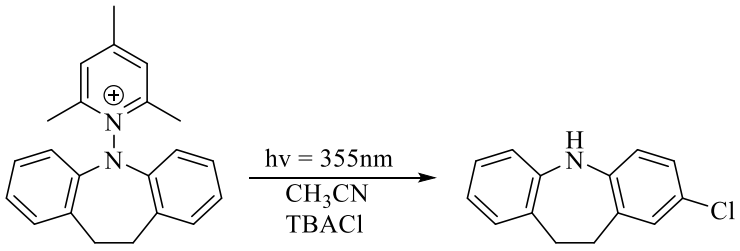

3 **5**

Scheme 2.2. Trapping nitrenium ion **2** with Cl^- to form a chloro-adduct **5**.

Similarly, photolysis (370 nm) of the pyridinium ion **3** in $CDCl_3$ solutions containing 1,4-cyclohexadiene (CHD, a reactive H-atom donor) were photolyzed. Product analysis by ^1H NMR spectroscopy showed clean formation of the corresponding amine **4**, accompanied by benzene (from oxidation of the CHD). Below will be presented spectroscopic evidence supporting a stepwise H atom transfer mechanism for this process.

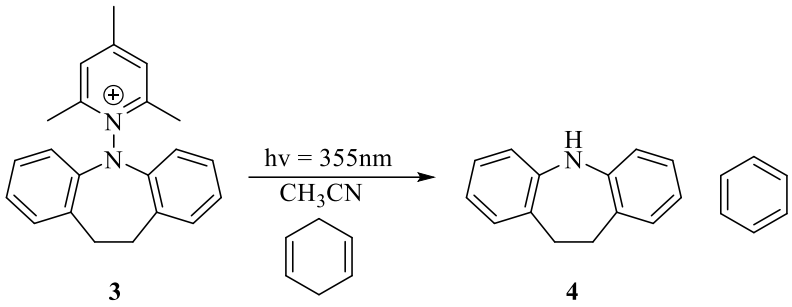

Scheme 2.3. Trapping nitrenium ion **2** with CHD to form the parent amine through H-atom transfer.

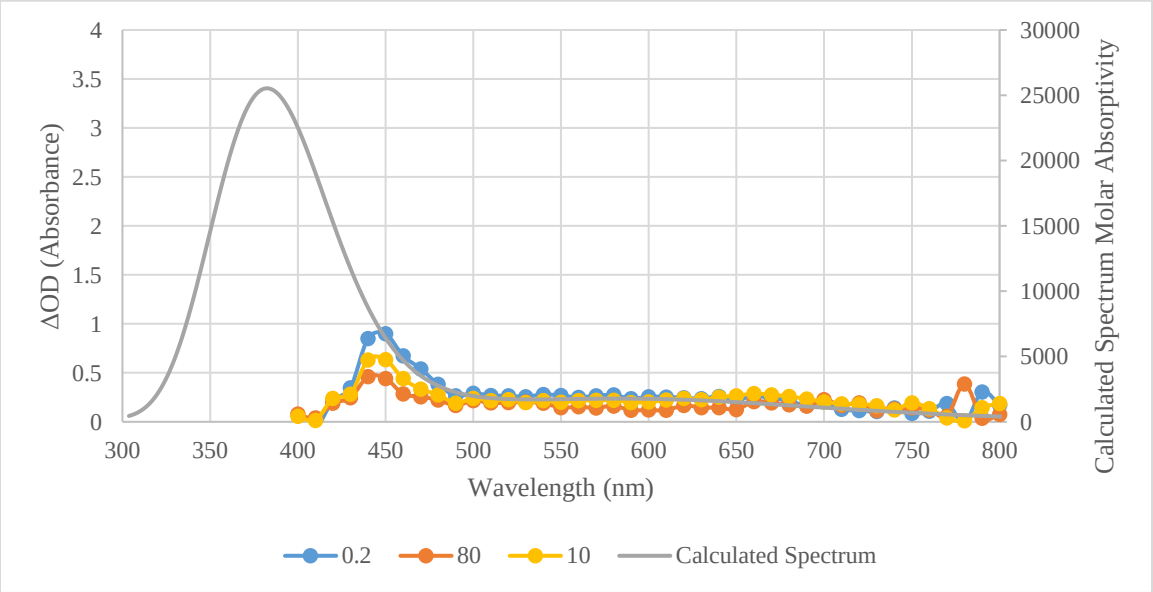

Figure 2.4. Transient spectra from LFP (355 nm, 7 ns, 40 mJ/pulse) of pyridinium ion **3** in CH_3CN solution taken 200 ns, 10 μs, and 80 μs following the excitation pulse. This difference spectrum should give the absorption spectrum of **2** which can be compared to the TD-DFT modeled UV-VIS spectrum of **2**.

LFP experiments were used to characterize the nitrenium ion intermediate **2**. Shown in Figure 2.4 are transient spectra measured following pulsed laser excitation (355 nm, 7 ns, 40 mJ) of pyridinium ion **3** in CH_3CN solution. A strong absorbance with an apparent maximum of 450 nm appears immediately following the excitation pulse and decays in a kinetically complex manner, persisting for over 100 μs following the excitation pulse. A nearly identical spectrum and decay profile were also obtained in DCM.

The assignment of the signal to nitrenium ion **2** is supported by the following observations: (1) The 450 nm decay profile is not significantly changed when the experiment is carried out with N_2 saturated or air-equilibrated solutions. Generally speaking, aryl and diaryl nitrenium ions, being ground state singlets, are unreactive toward oxygen. (2) The lifetime of the 450 nm signal, however, is diminished when nucleophiles known to react with similar aryl nitrenium ions such as chloride ions, and methanol are added to the solution (see Table 2.2). (3) The transient spectrum in Figure 2.4 shows reasonable agreement with a UV-VIS spectrum calculated by time-dependent density functional theory (TD-DFT) (Figure 2.4). The latter predicts a significant peak at 395 nm and a weaker absorption at 618 nm. It should be noted that the transient spectrum in Figure 2.4 is a difference spectrum. Depletion of the photoprecursor **3** at 405 nm (see Figure 2.2) subtracts from the positive signal for the photoproduct. Thus, the true experimental maximum could be at significantly lower wavelengths than the apparent maximum at 450 nm.

The substantially increased lifetime of **2** compared to **1** and other diaryl nitrenium ions can be attributed to the inhibition of the electrocyclization reaction. Under comparable conditions, **1** lives for ca. 1.5 μs and has been shown to produce carbazole along with oligomeric species when generated in the absence of added nucleophiles. Generation of **2** under similar

conditions also generates complex-colored mixtures which we assume to result from oligomerization processes similar to what was reported previously.[17,51] However, no product analogous to carbazole was identified.

2.4 Reactivity of the 5-endo-10,11-dihydrodibenzoazepine nitrenium ion

The reactivity of nitrenium ion **2** was ascertained by measuring the dependence of the pseudo-first order decay rate constants k_{obs} on the concentrations of the various trapping agents [Trap] listed in Table 2.2. In all cases the rate constants agreed reasonably well with Equation 2.1, where k_0 reflects the projected decay rate constant absent the trap and k_{trap} is the second order rate constant.

$$k_{obs} = k_0 + k_{trap}[Trap] \qquad \text{(Equation 2.1)}$$

Table 2.2. Rate constants and predicted products for reactions of nitrenium ion **2** and nitrenium ion **1** in CH_3CN with various trapping agents determined by LFP. (AMP = Adenosine Monophosphate. GMP = Guanosine Monophosphate.)

Trapping Agent	k_{trap} (M^{-1} s^{-1}) with 2	Predicted Product from 2	k_{trap} (M^{-1} s^{-1}) with 1	Predicted Product from 1
TBACl	2.57 x 10^{10}	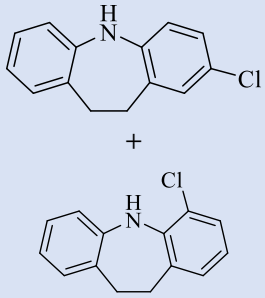	1.0 x 10^{10}	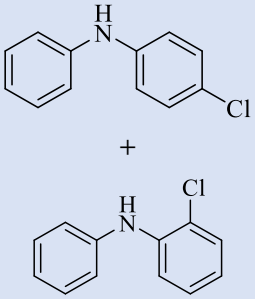
MeOH	5.46 x 10^{5}	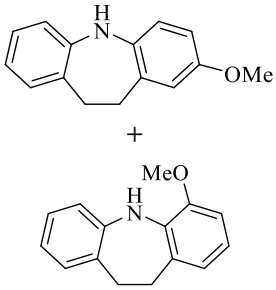	5.2 x 10^{10}	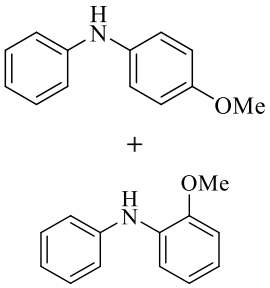
H_2O	3.97 x 10^{4}	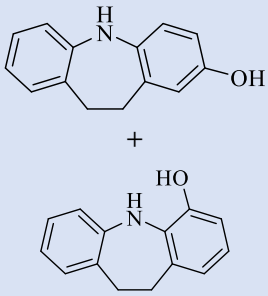	6.1 x 10^{10}	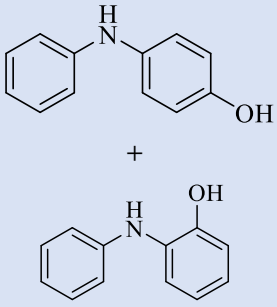
AMP	4.46 x 10^{7}	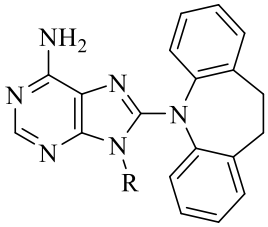		
GMP	9.60 x 10^{7}	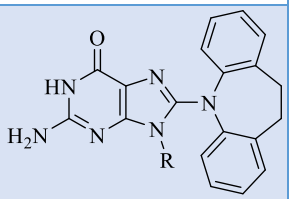		
L-cysteine	3.95 x 10^{8}			

L-tryptophan	2.52×10^9			
L-methionine	8.63×10^8			
L-tyrosine	2.10×10^7			
L-arginine	6.49×10^7			
L-lysine	3.72×10^7			

A general trend that emerges from these rate data is the diminished reactivity of nitrenium ion **2** toward typical nucleophiles. For example, the rate constant of reaction with water is ca. 4×10^4 $M^{-1}s^{-1}$, which about 20 times slower than the reaction of **1** with the same nucleophile (6.1×10^5 $M^{-1}s^{-1}$).[17] In contrast the electron rich amino acid, tryptophan, reacts at near the diffusion limit in H_2O with both nitrenium ions. This effect is similar to the reactivity of the para-substituted dihalo-diphenyl nitrenium ions with H_2O. The most electrophilic position on the diarylnitrenium ions is the para position, but the rate constant of the reaction with water is the same order of magnitude for **2** as well as for the para-dihalo-diphenyl nitrenium ions. Therefore, the decreased rate constant with of the reaction with water is primarily due to restricting one of the electrophilic ortho sites on the aryl rings.

Calculations (M062x/6-311G(d,p) including implicit CH_3CN solvation simulated using the SMD model) on the transition states for addition of water to **2** and **1** are consistent with the experimental trends (Figure 2.5). The Gibbs free energy of activation for addition of H_2O to **2** is 8.6 kcal/mol, this is ca. 2 kcal/mol higher than that for addition to **1** (6.4 kcal/mol). However, it should be noted that in both cases the addition reactions are expected to be endergonic. However, under experimental conditions these can occur with concerted deprotonation to other water

molecules resulting in the net exergonic addition of hydroxide. More extensive simulations using explicit solvent molecules would be needed to quantitatively model this reaction.

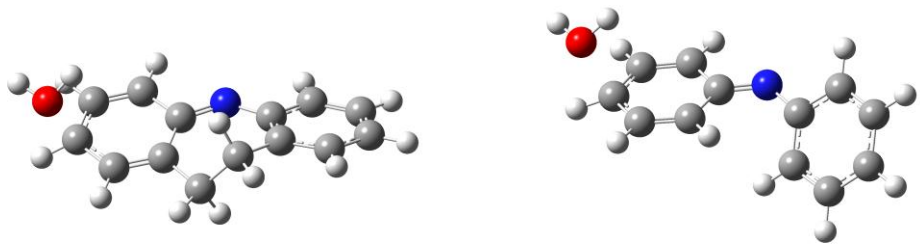

Figure 2.5. Transition state geometries (M062x/6-311G(d,p)- SMD) for addition of H_2O to **2** and **1** in CH_3CN.

Nitrenium ion **2** reacts with the H-atom donor, CHD, with a rate constant of 1.8 x 10^5 $M^{-1}s^{-1}$. LFP experiments show that this reaction happens through a H atom transfer mechanism. Figure 2.6 shows transient spectra taken following LFP of **3** in the presence of 0.5 M of CHD. Following the decay of the nitrenium ion signal (450 nm) there appears weaker, but persistent, signals at 520 nm and 690 nm. These agree well with the transient spectrum of the **2b** cation radical generated independently by using LFP to photolyze the 5-Nitroso-10,11-dihydro-dibenzo[b,f]azepine in the presence of acid (Figure 6.1). Further, the rate constant of **2** with CHD is around 20 times lower than the rate constant of diphenyl nitrenium ion with CHD or the dihalo-diphenyl nitrenium ions with CHD. This would suggest that although **2** is similar to the dihalo-diphenyl nitrenium ions in regards to its reactivity to nucleophiles, it has a greater difference in its 2^{nd} order rate constants with H-atom donors than do the dihalo-diphenyl nitrenium ions. This is evidence that indeed the triplet state of the nitrenium ion is destabilized for **2** in comparison to diphenyl nitrenium ion, but the reactivity of the singlet state is

approximately the same as the dihalo-diphenyl nitrenium ions as measured through 2nd order rate constants with different nucleophiles.

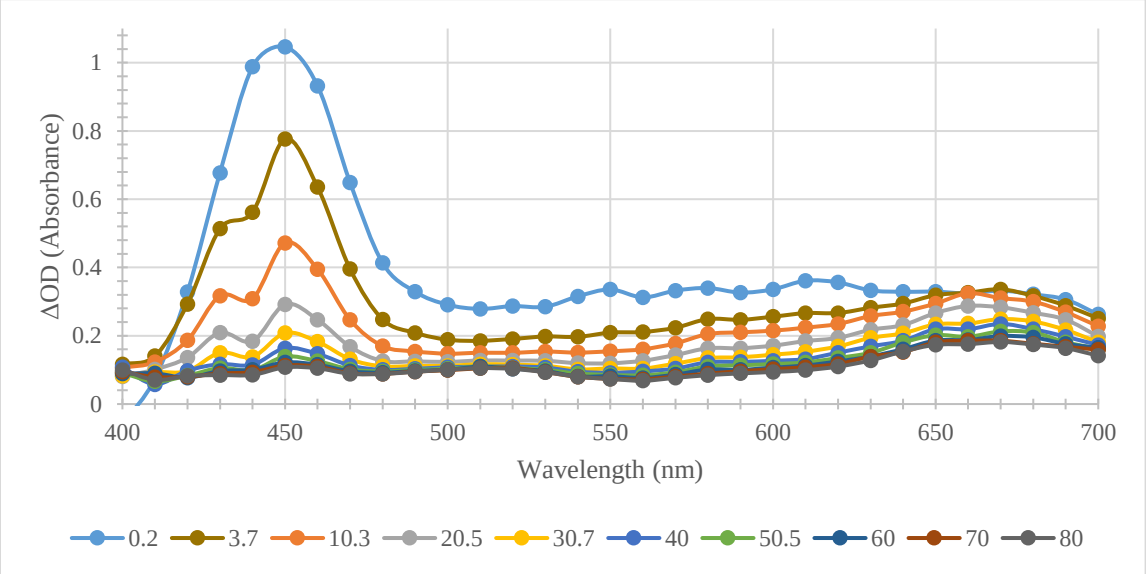

Figure 2.6. Transient spectra resulting from LFP (355 nm, 7 ns, 40 mJ) of **3** and CHD in CH_3CN. Nitrenium ion **2** Max at 450 nm can be seen decaying into cation radical max at 670 nm and radical max at 430 nm.

Previous studies of other diaryl nitrenium ions have shown some level of radical cation formation under certain conditions.[61] These have been attributed to reactions of nitrenium ion triplet states and/or branching from the initially formed pyridinium excited states. This example further establishes this pathway in a case where the nitrenium ion triplet state is even more energetically separated from the singlet. The large ΔE_{ST} value for **2** tends to exclude H atom transfer via the equilibrated triplet state. One possibility is that the singlet abstracts H atoms directly. Additional studies would be needed to test this hypothesis.

2.5 Conclusions

When comparing nitrenium ion **2** to **1**, the most significant effect of the saturated two-carbon bridge is to destabilize the triplet state relative to the singlet, further increasing the ΔE_{ST}.

Analysis of the geometries shows that the second ring in **1** is able to rotate out of planarity and destabilize the filled sp^2 non-bonded orbital on nitrogen. The bridge makes this impossible and the two aryl rings lie nearly coplanar. The bridge significantly extends the lifetime of **2** by inhibiting the electrocyclization reaction leading to carbazole in the case of **2**. The bridge also shows a modest effect on reaction with nucleophiles, inhibiting the addition of H_2O to the ring by ca. a factor of 10. This supports the idea that singlet state of **2** is not greatly affected by the two-carbon bridge as its reactivity with nucleophiles is not greatly affected.

Chapter 3: H-atom Donors with Diaryl Nitrenium Ions

3.1 Parent Methylene Carbene

Nitrenium ions are isoelectronic and isolobal with carbenes. Both nitrenium ions and carbenes have two non-bonding electrons which can be assigned to give either a triplet state or a singlet state as shown in Figure 3.1. The difference between nitrenium ions and carbenes is seen in the formal positive charge on the nitrogen. Therefore, precedents in carbene chemistry have been used for nitrenium ion chemistry.

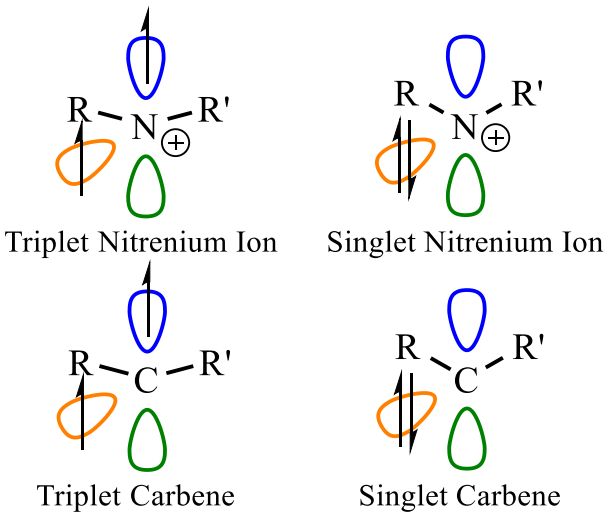

Figure 3.1. Singlet and triplet states of nitrenium ions and carbenes.

Methylene carbene (CH_2) **6** has been extensively studied and it is accepted that two different electron configurations are relevant. These are the $^1A_1$ and $^3B_2$ states and both can be distinguished spectroscopically and have distinct chemistries.[79–85] These observations have led to Skell-Woodworth's rules which essentially state that the electron spins states are conserved throughout a simple reaction step. These predict that for any given carbene, if its electrons are in the $^1A_1$ state then it will generate singlet products and if they are in the $^3B_2$ state then it will

generate triplet products.[86,87] Often there is an equilibrium between the $^1A_1$ and $^3B_2$ states. In that case, the ratio of singlet and triplet products depend on the singlet-triplet energy gap (ΔE_{ST}). It is assumed that this equilibrium is fast enough that no matter which state is initially formed, the product distribution is determined by the ΔE_{ST}. For methylene carbene and most aryl carbenes the $^3B_2$ state is the ground state.

3.2 Parent Nitrenium Ion

The parent nitrenium ion (NH_2^+) **7** is the nitrenium ion equivalent of methylene carbene. It can be generated through the photolysis of a N-amino(2,4,6-triphenylpyridinium ion **8**.[18] It has a calculated ΔE_{ST} of + 29.9 kcal/mol and a measured energy gap of 30.1 kcal/mol.[19–21]

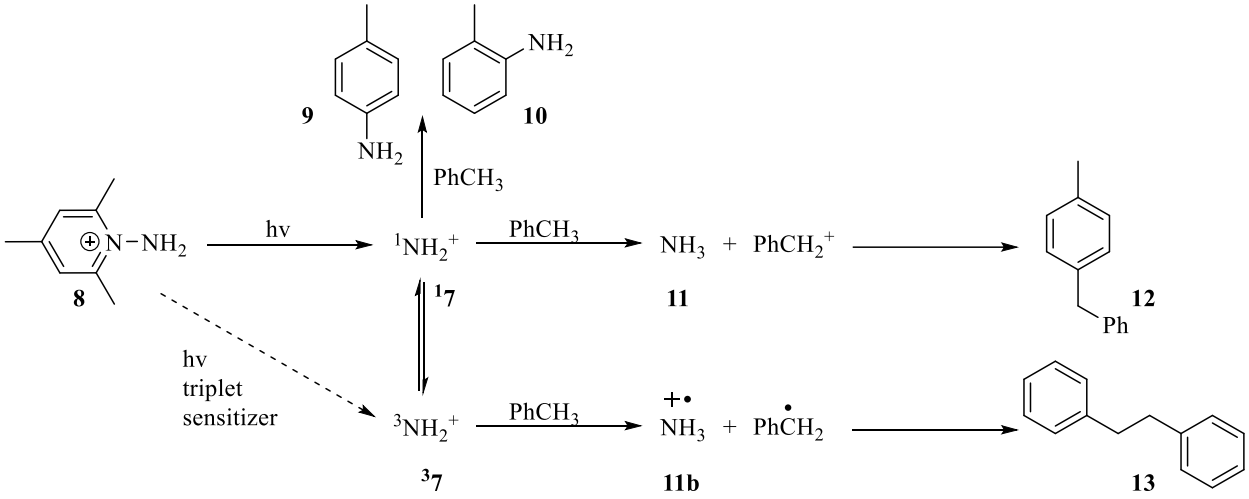

Scheme 3.1.[66] Important reactions and generations of parent nitrenium ion NH_2^+ **7**.

The singlet reactivity has been established through the reactions of **^{1}7** with toluene. Toluene reacts with the singlet **^{1}7** to give 4-benzyltoluene **12**. The mechanism is hydride abstraction from the benzylic C-H, followed by the resulting benzyl cation reacting with a toluene molecule.[66] Further ortho and para amino adducts to toluene **9** and **10** were also identified. The triplet

reaction of ^{3}**7** was identified as H-atom abstraction from toluene. In this case the benzylic radical dimerizes to give bibenzyl **13**.[66] Support for the H-atom abstraction pathway resulting from the triplet was provided by experiments where a triplet sensitizer was used to generate the triplet nitrenium ion ^{3}**7** directly. This resulted in higher yields of **13** compared to **12**.[66] On the basis of this study, it has been assumed that nitrenium ions are analogous to carbenes in that the singlet nitrenium ions react with nucleophiles and the triplet nitrenium ions react as diradicals.

3.3 Diaryl Carbene Mechanistic Pathways

The Skell-Woodworth rules applied to diaryl carbenes rely on a preequilibrium between the singlet and the triplet carbene **14** to predict the products ratios of **14** with trapping agents. We define this mechanism as the preequilibrium model. Two examples of triplet traps would be an H-atom donor like CHD or triplet O_2, and an example of a singlet trap would be methanol.

It is observed that diphenyl carbene inserts into methanol to make the ether adduct as shown in Scheme 3.2.[88]

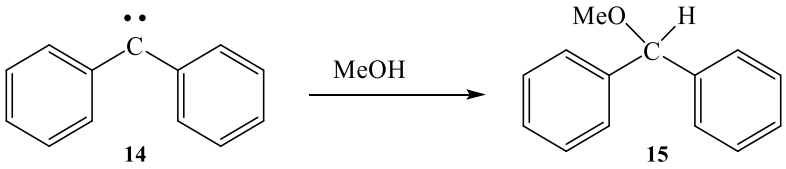

14 **15**

Scheme 3.2. Reaction of diphenyl carbene with methanol.

The electronic ground state for **14** is the triplet state.[89] The ether adduct **15** appears to result from a concerted O-H insertion forming the ether. Triplet carbenes normally react like diradicals following stepwise pathways involving radical pairs. Therefore, the methanol insertion mechanism must occur by one of two pathways: Either it proceeds through the preequilibrium pathway or the ground triplet state directly reacts with methanol and undergoes intersystem

crossing in the transition state, sometimes referred to as the surface crossing mechanism.[90] as is depicted in Scheme 3.3.

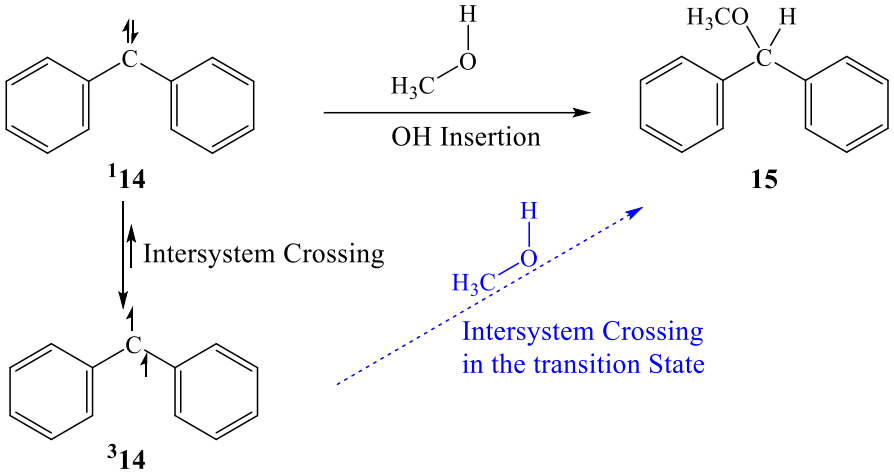

Scheme 3.3. Preequilibrium mechanism in which there is an equilibrium between the triplet ground state of the carbene **14** and the first excited singlet state (**black**). The insertion of methanol directly into the triplet carbene with intersystem crossing in the transition state (**blue**).

The alternative mechanism by which **14** reacts with methanol is that there is a preequilibrium between the ground state triplet and the singlet state, followed by a reaction between the singlet state and methanol.

The equations that govern the preequilibrium mechanism depend on steady state kinetics and a prior rapid equilibrium between the singlet state carbene and the triplet state carbene. This equilibrium is governed by the ΔE_{ST}. The equilibrium constant K_{eq} is given by Equation 3.1.

$$K_{eq} = \frac{[S]}{[T]} \qquad \text{(Equation 3.1)}$$

The observed rate constant is related to the second order rate constant by Equation 3.2.

$$k_{obs} = k_2 K_{eq} \qquad \text{(Equation 3.2)}$$

Equations 3.1 and 3.2 can combine to form Equation 3.3.

$$k_{obs} = k_2 \frac{[S]}{[T]} \qquad \text{(Equation 3.3)}$$

Therefore, the observed rate constant is heavily dependent on the concentration of singlet carbene from the K_{eq}. [S] is the concentration of singlet carbene and [T] is the concentration of triplet carbene. k_2 is the 2nd order rate constant of the singlet carbene reacting with methanol and the k_{obs} is the observed rate constant of the system.

The preequilibrium mechanism has a predicted apparent barrier for the reaction of diphenyl carbene with methanol of 5-7 kcal/mol.[90] However, Griller, Nazran, and Scaiano measured kinetic barriers ranging from 1.17 to 3.61 kcal/mol depending on the solvent used.[90] There are two different proposed explanations given for this lower projected kinetic barrier.

The first proposal is that the measured kinetic barrier is lower than projected. Using Equation 3.4

$$\Delta G^{\neq} = \Delta H^{\neq} - T\Delta S^{\neq} \qquad \text{(Equation 3.4)}$$

where the $\Delta H^{\neq}$ is equal to the ΔE_{ST}, the T is the temperature, and the $\Delta S^{\neq}$ is assumed to be Rln(3)[90] where the R is the gas constant and the "3" is for the three different possible triplet states, it is possible that the entropy term is greater than the assumed Rln(3). This greater entropy term is because the singlet carbene has some zwitterionic character with a filled sp^2 orbital and an empty p orbital. This zwitterionic carbene would require a greater amount of order for solvation than the triplet state. Therefore, if the entropy is greater than projected, the predicted ΔG_{ST} is lower which could account for the lowered measured energy barriers. If this theory is correct, then adding either a para-substituted electron donating group or a para-substituted electron withdrawing group should lower or raise the energy barrier respectively by reducing the zwitterionic character of the carbene. This trend, however, is not observed.[91]

The second proposal offered by Griller *et. al.* is that the mechanism of this reaction does not proceed by the preequilibrium mechanism, but rather by a surface crossing mechanism.[90] In

this mechanism, the transition state of the triplet reacting with methanol and the transition state of the singlet reacting with methanol have very similar geometries allowing for the diphenyl carbene to insert into methanol and undergo an intersystem crossing in the transition state to form the ether adduct. This theory has the benefit of explaining why the energy barriers are lower than expected although it seemingly contradicts the Skell-Woodworth rules.

3.4 Aryl Nitrenium Ions

Aryl nitrenium ions have long been known to produce their parent amines as a byproduct.[11,14,57–60,63,92,93] The mechanism for generating the amine has never been studied in great detail, but it has always been observed when a parent pyridinium ion is photolyzed in an inert solvent. There are three examples: *N*,*N*-di(4-bromophenyl)nitrenium ion **16**, *N*,*N*-di(4-chlorophenyl)nitrenium ion **17**,[17] and 3,6-dibromocarbazolyl nitrenium ion **18**.[94] All three of these nitrenium ions are para-substituted diaryl nitrenium ions and produce the N-N dimer instead. The non-halogenated versions diphenyl nitrenium ion **1** and carbazolyl nitrenium ion **19** still produce the parent amine. The parent amines for the dihalogenated nitrenium ions are exclusively observed when an H-atom donor such as CHD, phenol (PhOH), 4-bromophenol (4-BrPhOH), or 4-cyanophenol (4-CNPhOH) are used to trap the nitrenium ion. The proposed mechanism is the nitrenium ion abstracts an H-atom to form the cation radical and then an electron to form the parent amine.[17,94] H-atom abstraction is possible from the singlet state of the diaryl nitrenium ions, but has historically been ignored since singlet nitrenium ions generally have other reactive pathways available to it, but triplet nitrenium ions do not. Because of both the precedent from the Skell-Woodworth rules in carbene chemistry and the multiple pathways available to singlet nitrenium ions, the presence of the parent amine product has been attributed to triplet nitrenium ion chemistry.[9,10,17,66,93,95]

Most aryl and diaryl nitrenium ions are ground state singlets[50], and nearly all known aryl nitrenium ions generated through photolysis of an *N*-amino-2,4,6-trimethylpyridinium ions or *N*-amino-2,4,6-triphenylpyridinium ions initially produce singlet nitrenium ions. Therefore, the equilibrium between the singlet nitrenium ion and the triplet nitrenium ion would be the pathway expected to produce triplet nitrenium ions to abstract H-atoms. If this assumption is correct the measured 2nd order rate constants between different diaryl nitrenium ions with different H-atom donors should be dependent on the ΔE_{ST}. The latter is difficult to measure, but can be calculated via DFT. Converting the ΔE_{ST} to ΔG_{ST} will give a minimum energy barrier for the H-atom abstraction for all ground state singlet nitrenium ions, and the ΔG_{ST} can be used to predict maximum k_2 for the different H-atom donor traps.

Alternatively, it is possible for the diaryl nitrenium ions to oxidize H-atom donors to form neutral radicals. Neutral radicals can then form cation radical via protonation. The cation radicals then are reduced to the parent amines as is seen in Scheme 3.4. This mechanism is considered in chapter 4 of this dissertation.

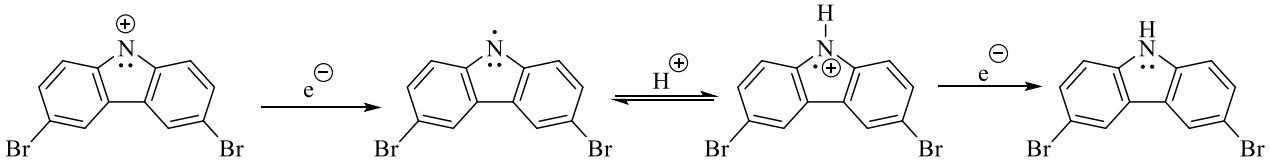

Scheme 3.4. Mechanism to form parent amine through an initial electron transfer step.

Although nitrenium ions and carbenes share many similar properties, two important differences between diaryl nitrenium ions and diaryl carbenes exist. First, nitrenium ions have a formal positive charge and carbenes are neutral. Second, diaryl nitrenium ions' ground state is the singlet state as opposed to the diaryl carbenes' ground state which is the triplet state.

Both diphenyl carbene **14** and diphenyl nitrenium ion **1** have been studied extensively[90,96–98], and it has been noted that diaryl nitrenium ion reactions with CHD has a higher 2nd order rate constant than is predicted by using ΔE_{ST} values obtained with DFT calculations.[96] This suggests that the triplet state of the diaryl nitrenium ions is not the only mechanism to produce the parent amine. We propose singlet state diaryl nitrenium ions can react directly with H-atom donors to produce the parent amine. Further that some diaryl nitrenium ions can oxidize H-atom donors to form neutral radicals and follow the mechanism in Scheme 3.4 above. Therefore, observation of the parent amine product cannot be used to conclude that a triplet state was involved.

The mechanism for diaryl nitrenium ions' reaction with H-atom donors can be determined by a combination of the 2nd order rate constants of different H-atom donors and kinetic isotope effect (KIE) experiments with phenol (PhOH)/phenol-d1 (PhOD). If the diaryl nitrenium ions quenching by H-atom donors is governed by triplet state reactivity, then the k_2's should correspond to ΔE_{ST} can be used to estimate the upper limit on k_2. If the observed rates are faster than the ΔE_{ST} values would allow, then different mechanism(s) are able to produce the parent amine product. A KIE experiment can distinguish between H-atom abstraction from the singlet state and electron transfer mechanism. A normal KIE would indicate that the nitrenium ion abstracts an H-atom. If no KIE is observed with PhOH/PhOD, then an alternative mechanism is responsible for the final parent amine product such as electron transfer (Scheme 3.4).

Several nitrenium ions will be generated by irradiating *N*-(arylamino)-2,4,6-trimethylpyridinium ions with 355 nm light. Irradiation with 355 nm light cleaves the N-N bond heterolytically which results in the generation of diaryl nitrenium ion and 2,4,6-collidine **20** as can be seen in Scheme 3.5.

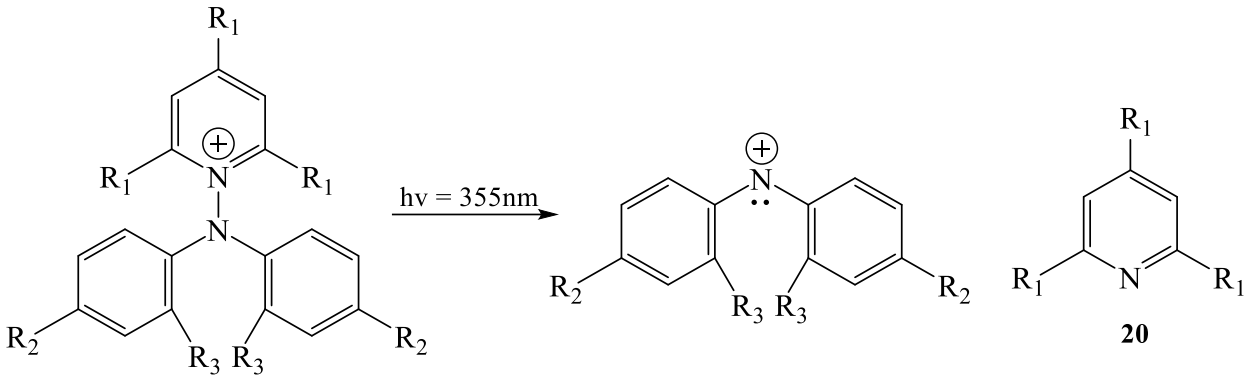

R_1 = Me or Ph
R_2 = H, Br, Cl
R_3 = H, -CH_2CH_2-, -

Scheme 3.5. Different diaryl pyridinium ions which will be photolyzed to make diaryl nitrenium ions.

Several chemical and spectroscopic properties of diaryl nitrenium ions have been previously established.[9–11,61,93,95,96] The list of nitrenium ions studied can be seen in Figure 3.2.

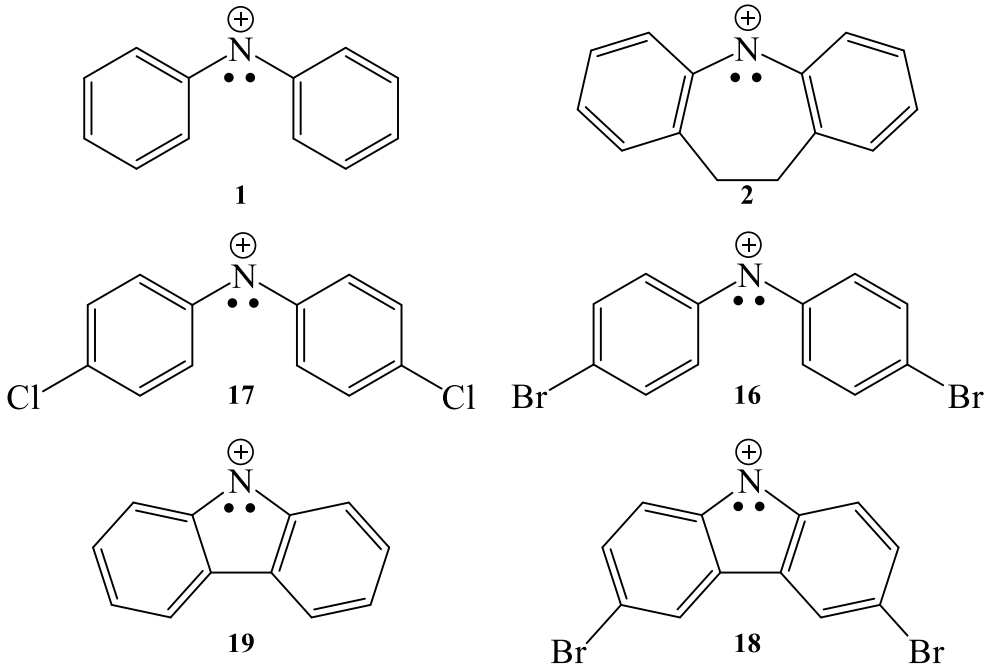

Figure 3.2. Diaryl nitrenium ions used to test mechanism with H-atom donors. Diphenyl nitrenium ion **1**, 10,11-dihydro-dibenzoazepinyl nitrenium ion **2**, *N*,*N*-Di(4-chlorophenyl)nitrenium ion **17**, and *N*,*N*-di(4-bromophenyl)nitrenium ion **16**, carbazolyl nitrenium ion **19**, and 3,6-dibromocarbazolyl nitrenium ion **18**.

3.5 2nd Order Rate Constants of Nitrenium Ions with H-atom Donors

Since the generation of these nitrenium ions have been previously established,[8–11,17] trapping with H-atom donors and KIE experiments can test if parent amine formation is through the triplet state. The experimental and predicted results for the H-atom donors with the diaryl nitrenium ions can be seen in Table 3.1.

Table 3.1. Singlet-triplet energy gaps of different nitrenium ions compared to experimental second order rate constants and predicted second order rate constants with H-atom donors. The equation governing the relationship between ΔE_{ST} and k_H is $k_H = k_{diff} e^{\frac{\Delta G}{RT}}$, and $\Delta G = \Delta E_{ST} - RTln(3)$,[99] where k_H is the measured 2nd order rate constant of CHD with the respective nitrenium ion, k_{diff} is the estimated diffusion limited 2nd order rate constant in CH_3CN,[100] R is the gas constant, T is the temperature, and ΔE_{ST} is the singlet-triplet energy gap.

	1	**16**	**17**	**2**	**19**	**18**
Calculated ΔE_{ST} (kcal/mol)	-10.1	-9.7	-9.9	-18.5	-7.8	-9.9
Predicted k_H from ΔE_{ST} ($M^{-1}s^{-1}$)	2.4×10^3	4.6×10^3	3.3×10^3	1.6×10^{-3}	1.1×10^5	3.3×10^3
CHD k_H $M^{-1}s^{-1}$	6.5×10^6	5.13×10^6	5.86×10^6	2.40×10^5	9.1×10^9	8.13×10^9
Inferred ΔE_{ST} from CHD k_H (kcal/mol)	-5.41	-5.55	-5.47	-7.36	-1.12	-1.18
Phenol k_H ($M^{-1}s^{-1}$)		4.73×10^5	6.81×10^5	1.0×10^7	7.98×10^9	1.21×10^9
Inferred ΔE_{ST} from PhOH k_H (kcal/mol)		-6.77	-6.74	-5.15	-1.19	-2.32
4-BrPhOH k_H ($M^{-1}s^{-1}$)		4.89×10^5	3.76×10^5	6.4×10^6	6.38×10^8	1.25×10^9
Inferred ΔE_{ST} from 4-BrPhOH k_H (kcal/mol)		-6.96	-7.09	-5.42	-2.69	-2.27
4-CNPhOH k_H ($M^{-1}s^{-1}$)		4.89×10^5	3.31×10^5	$< 1 \times 10^5$		$< 1 \times 10^5$
Inferred ΔE_{ST} from 4-CNPhOH k_H (kcal/mol)		-6.94	-7.17	< -7.88		< -7.88

It can be seen from Table 3.1 that the calculated ΔE_{ST} for nitrenium ion **1** is -10.1 kcal/mol. Using the equations in the description of Table 3.1, this corresponds to a maximum k_H of 2.4×10^3 $M^{-1}s^{-1}$. Adding halogens to the para positions of **1** minimally effects the ΔE_{ST} with

nitrenium ion **16**'s ΔE_{ST} = -9.7 kcal/mol and nitrenium ion **17**'s ΔE_{ST} = -9.9 kcal/mol. This would correspond to maximum k_H of 4.6 x 10^3 $M^{-1}s^{-1}$ or 3.3 x 10^3 $M^{-1}s^{-1}$ respectively. Adding an ethylene bridge to the ortho positions of nitrenium ion **1** increases the ΔE_{ST} from -10.1 kcal/mol to -18.5 kcal/mol in nitrenium ion **2**. This would have a predicted maximum k_H = 1.6 x 10^{-3} $M^{-1}s^{-1}$. With such a large ΔE_{ST} nitrenium ion **2** should not be able to observably populate its triplet state. Thus, reactions via the triplet state can be excluded. The carbazolyl nitrenium ions have ΔE_{ST} = -7.8 kcal/mol and -9.9 kcal/mol for carbazolyl nitrenium ion **19** and 3,6-dibromocarbazolyl nitrenium ion **18** respectively. The maximum k_H for **19** and **18** based off of their ΔE_{ST} is predicted to be 1.1 x 10^5 kcal/mol and 3.3 x 10^3 kcal/mol.

CHD, PhOH, 4-BrPhOH, and 4-CNPhOH are used to trap each of the nitrenium ions as each have low bond dissociation energy BDE so they are good H-atom donors (see Table 3.2). Each of these traps are observed to produce the parent amine as the major product. Nitrenium ion **1** has a measured k_H with CHD of 6.5 x 10^6 $M^{-1}s^{-1}$ which implies a ΔE_{ST} of -5.41 kcal/mol. This trend of greater rate constants holds true for nitrenium ions **16** and **17** with measured k_H's of 5.13 x 10^6 $M^{-1}s^{-1}$ and 5.86 x 10^6 $M^{-1}s^{-1}$. The trend shows that nitrenium ions **1**, **16**, and **17** all react about 3 orders of magnitude faster than the predicted maximum k_H. It is possible that CHD is reacting with these nitrenium ions as a hydride donor instead of an H-atom donor, so H-atom donor traps PhOH, 4-BrPhOH, and 4-CNPhOH were used as they would all be poor hydride donors. Nitrenium ions **16**, and **17** have k_H's with PhOH of 4.73 x 10^5 and 6.81 x 10^5, 4-BrPhOH of 4.89 x 10^5 and 3.76 x 10^5, and 4-CNPhOH of 4.89 x 10^5 and 3.31 x 10^5. These observed k_H's are still 2 orders of magnitude faster than the predicted k_H.

Nitrenium ion **2** was predicted to not be able to practically react through its triplet state, but still had k_H's with CHD of 2.40 x 10^5, with PhOH of 1.0 x 10^7, and 4-BrPhOH of 6.4 x 10^6.

4-CNPhOH was unable to quench nitrenium ion **2** so its k_H was < 1 x 10^5. Since this limit still allows 7 orders of magnitude of k_H before the rate constant would be consistent with triplet reactivity, we do not consider 4-CNPhOH to be trapping nitrenium ion **2** exclusively from **2**'s triplet state. CHD, PhOH, and 4-BrPhOH all trap nitrenium ion **2** 8-10 orders of magnitude faster than expected. This indicates these traps are not trapping the nitrenium ions through an H-atom transfer mechanism.

The carbazolyl and 3,6-dibromocarbazolyl nitrenium ions **19** and **18** were respectively trapped at near diffusion rates by CHD with k_H of 9.1 x 10^9, PhOH with k_H of 7.98 x 10^9 and 1.21 x 10^9, 4-BrPhOH with k_H of 6.38 x 10^8 and 1.25 x 10^9. Nitrenium ions **19** and **18** still have measured k_H's 3-6 orders of magnitude greater than the predicted k_H based off of the measured ΔE_{ST}. Presumably the antiaromatic character of nitrenium ions **19** and **18** lead to their increased rates of reactivity over nitrenium ions **1**, **16**, **17**, and **2**. Certainly all of the nitrenium ions studied have greater measured k_H's than the predicted k_H's.

The k_H's are significantly greater than expected. Either there is a significant error in how B3LYP calculates ΔE_{ST} of these nitrenium ions, or H-atom abstraction occurs through a pathway not involving the higher energy triplet state. The alternative pathways are hydride abstraction for CHD, electron transfer, or H-atom abstraction from the singlet state of the nitrenium ion.

Nitrenium ion **2**'s transient absorption spectrum has been previously reported to decay into the cation radical in the presence of CHD giving evidence of H-atom abstraction. Although triplet state nitrenium ion abstracting the H-atom cannot be ruled out from these observations, the singlet state diaryl nitrenium ion directly abstracting the H-atom is the simplest explanation. We propose that the singlet state is directly abstracting the H-atom. The mechanism explains the increased 2nd order rate constants of the diphenyl nitrenium ion series (**1**, **2**, **16**, and **17**) relative

to their ΔE_{ST} as shown in Scheme 3.6. It is assumed that nitrenium ions **1**, **16**, and **17** follow the same trend as nitrenium ion **2**, but further experimentation would be needed to establish this.

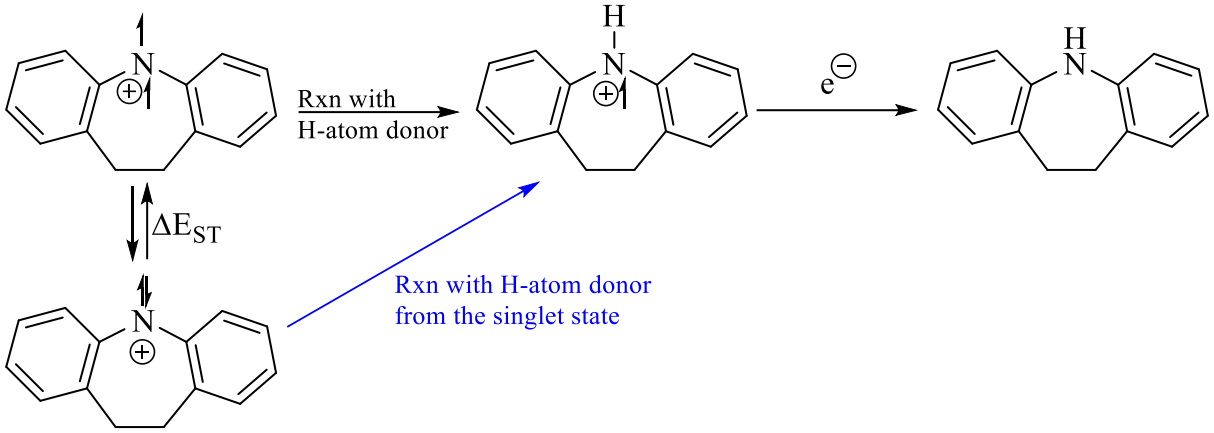

Scheme 3.6. Singlet and triplet state H-atom abstraction for **2** with CHD.

The initial nitrenium ion quenching step is electron transfer for nitrenium ions **18** and **19**. KIE experiments show that nitrenium ion **18** oxidizes an electron donor to produce the radical instead of H-atom abstraction. The neutral radical **18c** then gets protonated to the cation radical **18b**, and finally reduced to the parent amine. A longer discussion of this mechanism is given in Chapter 4.6.

Since all observed diaryl nitrenium ions have 2nd order rate constants significantly higher than the expected 2nd order rate constants, it cannot be assumed that the parent amine product is evidence of the triplet diaryl nitrenium ions. The antiaromatic carbazolyl nitrenium ions (**18** and **19**) are unstable enough to oxidize the phenol derivative traps to form the neutral radical. The phenols are acidic enough to protonate the neutral radicals to forming the cation radical which also get reduced to the parent amine. CHD also reacts significantly faster with the antiaromatic carbazolyl nitrenium ions. The oxidation potential of CHD is close to PhOH and 4-BrPhOH so it may be able to reduce the antiaromatic nitrenium ions. The phenol derivative traps follow such a

pathway as seen in Table 3.2. Alternatively, CHD could react as a hydride donor with nitrenium ions **18** and **19** as has been proposed previously for nitrenium ion **19**.[11] Since the reaction of CHD with antiaromatic nitrenium ions does not occur through an H-atom abstraction, **19**'s exact mechanism for reacting with CHD is not relevant to triplet state nitrenium ions chemistry.

Table 3.2. BDE's and oxidation potentials of the H-atom donors.

	BDE (kcal/mol)	**E_{ox} vs SCE (V)**
CHD	73[101]	1.74
PhOH	90.4[17]	1.63[102]
4-BrPhOH	90.7[17]	1.69[102]
4-CNPhOH	94.2[17]	2.08[102]

It should be noted that triplet aryl nitrenium ions can abstract H-atoms and form the parent amine as has been recently observed via a ground state triplet aryl nitrenium ion.[14] Additionally, it has been previously observed for the parent nitrenium ion NH_2^+ **7** Therefore, if a singlet diaryl nitrenium ion intersystem crosses to the triplet state, it is able to react with H-atom donors. However, the singlet diaryl nitrenium ion is still able to react with the H-atom donor directly from the singlet state or via electron transfer.

3.6 Conclusions

Diaryl nitrenium ions have 2nd order rate constants with H-atom donors which are between 2-10 orders of magnitude greater than those predicted on the basis of DFT calculated singlet-triplet energy gaps. The significantly higher 2nd order rate constants rule out H-atom abstraction from the triplet state as the primary mechanism of parent amine formation as was previously believed. Instead, the data are consistent with the diaryl nitrenium ions reacting directly with H-atom donors from the singlet state either by H-atom transfer or electron transfer.

The future work of this research is in exploring a larger scope of the diaryl nitrenium ions. More diaryl nitrenium ions are needed to investigate which nitrenium ions abstract H atoms and which oxidize H-atom donors. Further, it can be seen that both the **17** and the **18** have the same calculated ΔE_{ST}, but their 2nd order rate constants differ by 3-4 orders of magnitude. This difference in reactivity is related to the difference in mechanism as **17** abstracts an H atom and the **18** gets reduced to the neutral radical. More diaryl nitrenium ions must be investigated to be able to understand this difference in reactivity.

Chapter 4: Generation of the Antiaromatic 3,6-Dibromocarbazolyl Nitrenium Ion: Mechanistic Studies and Alkene Trapping

4.1 Antiaromatic Carbazolyl Nitrenium Ion Previous Characterization

In a previous publication, we described the generation and detection of the antiaromatic carbazolyl nitrenium ion **19** and determined that its lowest energy electronic configuration was a singlet. The important electronic configuration can be seen in Figure 4.1.[11]

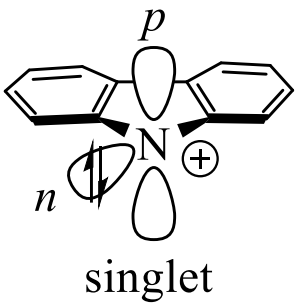

Figure 4.1. Ground state electronic configuration for carbazolyl nitrenium ion **19**.

Recently, carbazolyl nitrenium ion **19** has also been independently characterized by photoelectron spectroscopy and the lowest two energy states measured matched well with the calculated energies of the closed shelled singlet and the triplet.[103] This confirms that the ground state of carbazolyl nitrenium ion **19** is its singlet state. The current work seeks to understand the mechanisms by which antiaromatic carbazolyl nitrenium ion derivatives' react with H-atom donors, electron donors, and related trapping agents.

Carbazolyl nitrenium ion **19** reacts significantly faster with nucleophiles, electron donors, and H-atom donors when compared with diphenyl nitrenium ion **1**. This difference in reactivity is attributed to the antiaromaticity of carbazolyl nitrenium ion **19**. However, it is unknown if the

antiaromaticity of carbazolyl nitrenium ion **19** allows for new reactivity, such as trapping with nucleophiles weaker than H_2O and MeOH. Alternatively, it is possible that the antiaromatic character increases the reduction potential of nitrenium ion **19** and rates of H-atom abstraction to the point that no new aryl nitrenium adducts can be formed.

Practically, the longer the lifetime of the nitrenium ion, the easier it is to measure 2nd order rate constants via LFP trapping experiments and characterize adducts with ^{1}H NMR, ^{13}C NMR, and MS. Carbazolyl nitrenium ion **19** has a lifetime of 0.3 μs. The lifetime is defined as the half-life of the nitrenium ion divided by $\sqrt{2}$. Therefore, a carbazolyl nitrenium ion derivative expected to have a longer lifetime was generated to probe the reaction mechanisms of antiaromatic carbazolyl nitrenium ions.

It has been observed for diphenyl nitrenium ion **1** that if chlorines or bromines are added to the para positions of the phenyl rings then the lifetime of these derivatives is increased by two orders of magnitude.[17] This moves the lifetime of **1** from 1.5 μs to 240 μs (**17)** or 124 (**16**) μs respectively.[17] Therefore, we designed the antiaromatic carbazolyl nitrenium ion derivative to have two bromines added to the two para or the 3,6 positions. It is expected that the antiaromatic nitrenium ion's lifetime will increase from 0.3 μs to around 10 μs as seen in Figure 4.2. This should allow 2nd order rate constants measured through LFP trapping experiments to be measured with less error and require lower amounts of trapping agents for product formations. The synthetic route can be seen in Scheme 4.1. *N*-carbazolyl-(2,4,6-trimethyl)pyridinium ion **24** was synthesized by our previously published method.[11] *N*-carbazolyl-(2,4,6-trimethyl)pyridinium ion **24** was added to 10 equivalents of NBS and stirred at room temperature for 3 days to produce the 3,6-dibromocarbazolyl-(2,4,6-trimethyl)pyridinium ion **25**. **25** was cleaned with AgBF4 and

styrene to ensure no leftover Br_2 or Br^- was still in solution. Pyridinium ion **25** can be photolyzed to generate nitrenium ion **18**.

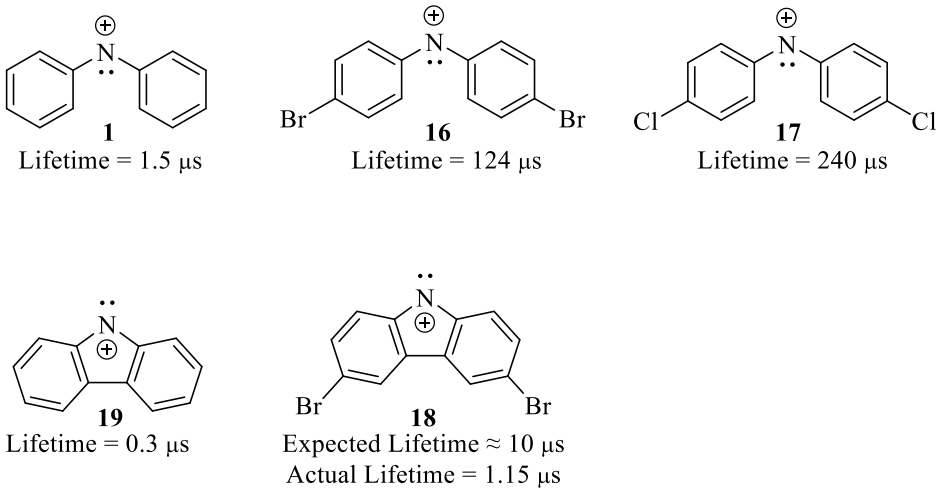

Figure 4.2. Lifetimes of 3,6-dibromocarbazolyl nitrenium ion **18** and other related nitrenium ions.

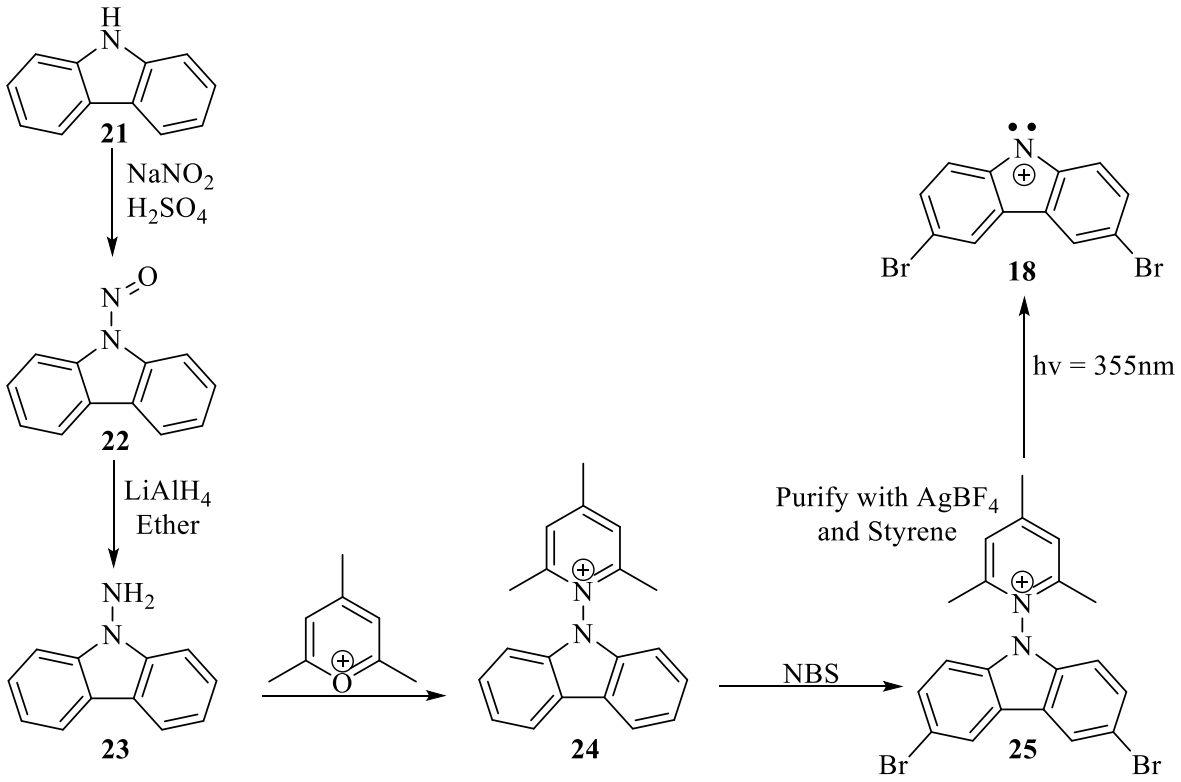

Scheme 4.1. Synthesis of 3,6-dibromocarbazolyl pyridinium ion **25** and generation of 3,6-dibromocarbazolyl nitrenium ion **18**.

4.2 Previous Mechanistic Work for Carbazolyl Nitrenium Ions

Previous mechanistic work with aryl nitrenium ions shows that nucleophiles add predominately to the ortho and para positions of the aromatic ring followed by a tautomerization to regain aromaticity in the ring. Less frequently, nucleophiles will also add to the N position.[11,17] It is been previously observed that the carbazolyl nitrenium ion **19** also forms ortho and para adducts with TBACl (**26** and **27**) and MeOH (**28** and **29**).[11] When a transient absorption spectrum of carbazolyl nitrenium ion **19** in the presence of CHD was reported, the nitrenium ion signal did not decay into the cation radical spectrum expected from H-atom transfer step. Therefore, this reaction was presumed to occur via hydride abstraction. Carbazolyl nitrenium ion **19** has also had its transient absorption spectrum measured in the presences of the electron donors DMA and DMB. In both cases the nitrenium ion **19** absorbance decays into the absorbance of the neutral radical **19c** as well as the known spectrum of the cation radical of DMA or DMB. This gives evidence that electron transfer has occurred as seen in Scheme 4.2.[11] Further, aryl nitrenium ions have long been known to produce their parent amines when photolyzed in an inert solvent.[11,14,57–60,63,92,93]

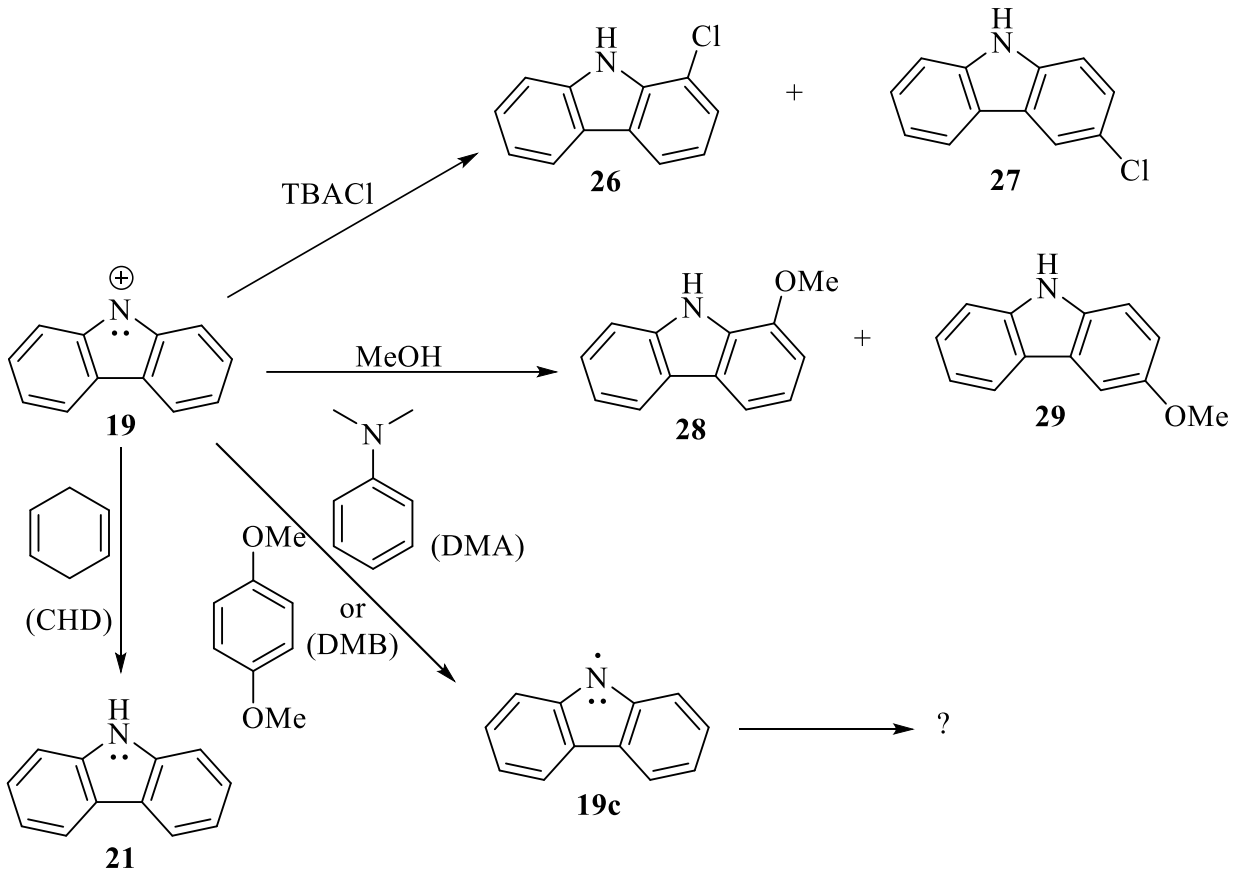

Scheme 4.2. Previous mechanistic work of the carbazolyl nitrenium ion **19**.[11]

The mechanistic work that still needs to be addressed are primarily for the electron donors, the H-atom donors, and the products in inert solvents. For electron donors, the first step of the nitrenium ion oxidizing an electron donor to form the radical is known, but the final product has not been determined. For H-atom donors the final product is established as the parent amine, but whether this happens through electron transfer. H-atom donation, or hydride donation has not been determined. For most diaryl nitrenium ions there is an electrocyclization decay pathway that predominates in inert media. However, the bridge between the two aryl rings in carbazole derivatives rules out this decay pathway. Therefore, both the final products and their formation mechanisms need to be determined. This work seeks to determine all of the

mechanistic pathways and products for the 3,6-dibromocarbazolyl nitrenium ion **18** with H-atom donors and electron donors.

4.3 Targeting Alkenes

Previously, diphenyl nitrenium ion **1** was shown to react with electron rich alkenes. All of the alkenes explored had a trimethylsilyl leaving group on an enol ether or a leaving group on an allylic carbon.[15] It was found that diphenyl nitrenium ion **1** could make covalent bonds through its ortho, para, and N positions.[15] Since we have this precedent with **1**, we chose to explore **18**'s reactivity with alkenes of different electron density as can be seen in Figure 4.3.

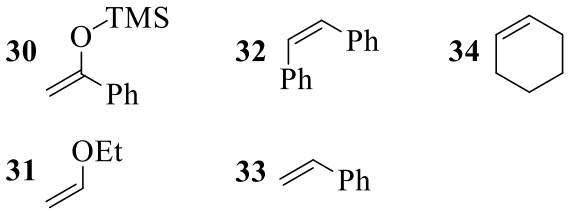

Figure 4.3. Different alkenes for trapping nitrenium ion **18**. From most electron rich to least electron rich: **30**, **31**, **32**, **33**, then **34**.

In this work, we first characterize **18** and measure its 2nd order rate constants with several nucleophilic, electron transfer, and H-atom traps. The measured 2nd order rate constants are slightly slower than carbazolyl nitrenium ion **19** but much faster than *N*,*N*-di(4-bromophenyl)nitrenium ion **16**. The mechanisms of 3,6-dibromocarbazolyl nitrenium ion **18** reacting with different electron donor and H-atom donor traps are investigated as well as **18** in an inert solvent. It was found that the singlet nitrenium ion **18** can be trapped by nucleophilic traps, both H-atom donors and electron donors act as reductants to nitrenium ion **18**, and in inert solvents the pyridinium ion **25** serves as the reductant. Finally, we trapped nitrenium ion **18** with different alkenes to assess if new reactivity can be accessed with nitrenium ions. Out of all the

alkenes studied, only the silyl enol ether **30** could trap the nitrenium ion **18**. Similar behavior has previously been seen with **1**. Therefore, no new alkenes could be used to trap the antiaromatic nitrenium ion.

*4.4 Characterizing 3,6-Dibromocarbazolyl Nitrenium Ion **18***

First, the 3,6-dibromocarbazolyl nitrenium ion **18** was characterized. The pyridinium ion **25** was photolyzed in CH_3CN and the transient absorption spectra can be seen in Figure 4.4.

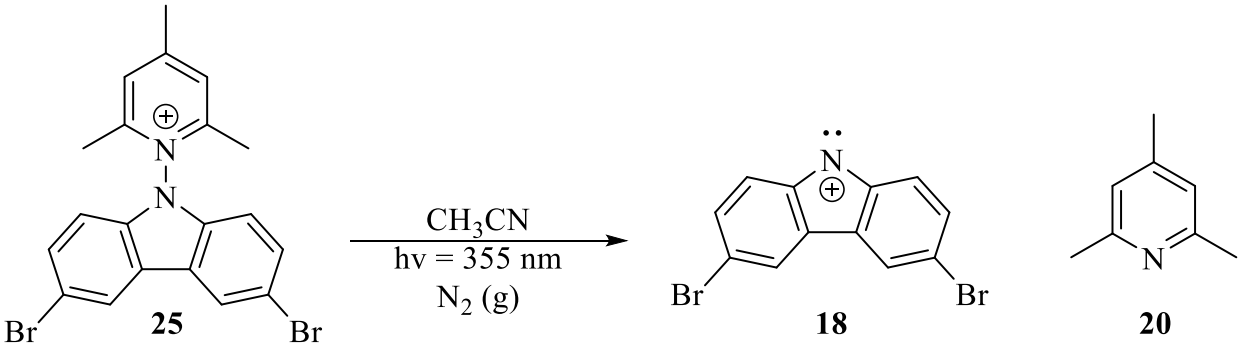

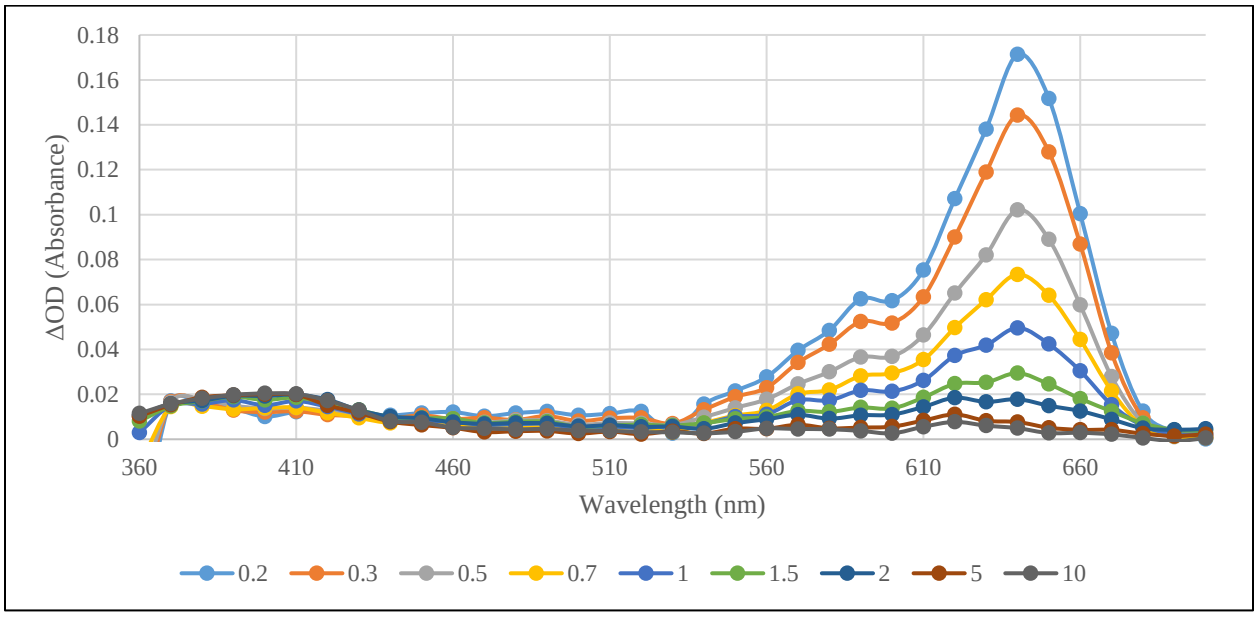

Figure 4.4. LFP of **25** in CH_3CN generates nitrenium ion **18**. The times in the legend are in µs.

The nitrenium ion **18** spectrum can be distinguished from the cation radical spectrum (Figures 6.18-6.21) and the radical spectrum (Figures 6.17). Although the nitrenium ion, cation radical, and the radical spectra all absorb at similar wavelengths, they can be distinguished through their reactivity and lifetimes. A summary of the important high energy intermediates can be seen in Table 4.1. The max absorbances of the nitrenium ion **18** are 590 nm and 640 nm. The radical **18c** and cation radical **18b** both have max absorbances at 570 nm and 620 nm. The distinguishing characteristic between the radical and cation radical spectra are their lifetimes which are 5.87 μs and 30.4 μs respectively. The nitrenium ion **18**'s lifetime in CH_3CN was expected to be about 10 μs, but turned out only to be 1.15 μs. All of the high energy intermediates spectra were calculated with TD-DFT and they differ from their calculated absorptions by approximately 120-160 nm. For most aryl nitrenium ions TD-DFT is able to predict the max absorbances of the nitrenium ions to within 30 nm.[8,10,17] However, with the carbazolyl nitrenium ion **19**, TD-DFT was not able to accurately predict its max absorbance or absorbance profile.[11] Although the source of this significantly greater error in calculated nitrenium ion absorbance spectra is not known, we assume that the same error exists in 3,6-dibromocarbazolyl nitrenium ion **18** as does for the carbazolyl nitrenium ion **19**. A much longer discussion of this error can be found in the journal article on the carbazolyl nitrenium ion.[11]

Table 4.1. Summary of the high energy intermediates related to nitrenium ion **17**.

High Energy Intermediate	Measured Absorptions (nm)	Calculated Absorptions (nm)	Lifetime (μs)	Solvent
Nitrenium Ion **18**	590, 640	433, 522	1.15	CH_3CN
Cation Radical **18b**	570, 620	444, 579	30.4	CH_3CN
Radical **18c**	570, 620	426, 548	5.87	CH_3CN

4.5 Mechanisms of 3,6-Dibromocarbazolyl Nitrenium Ion with Different Traps

To further support that the transient signal in Figure 4.4 is the nitrenium ion, LFP experiments were carried out to determine 2nd order rate constants for reactions of the transient signal with different nucleophiles. The resulting stable adducts were also isolated or compared to authentic samples. The nucleophilic traps used are TBACl, MeOH, H_2O. The 2nd order rate constants of TBACl for other diaryl nitrenium ions are close to diffusion limited rate constant of 2 x 10^{10} $M^{-1}s^{-1}$, MeOH, and H_2O are between 10^4-10^7 $M^{-1}s^{-1}$.[9–11,17] For nitrenium ion **18**, the 2nd order rate constant for TBACl was 2.9 x 10^{10} $M^{-1}s^{-1}$ which is in good agreement with the expected diffusion limited 2nd order rate constant. H_2O gave 2.2 x 10^6 $M^{-1}s^{-1}$ and MeOH gave 1.4 x 10^7 $M^{-1}s^{-1}$ both of which are similar to rate constants for diaryl nitrenium ions. Standard spectroscopic methods are used to characterize the products resulting from nitrenium ion **18** with TBACl and MeOH nucleophilic traps (compounds **35** and **36**). The presence of these adducts shows that the singlet nitrenium ion **18** can be trapped with nucleophiles as was seen for the carbazolyl nitrenium ion **19**.[11]

A summary of all adducts for nitrenium ion **18** can be seen in Scheme 4.3. The 2nd order rate constants measurements obtained by kinetic trace experiments via LFP for nucleophilic traps are shown in Table 4.2.

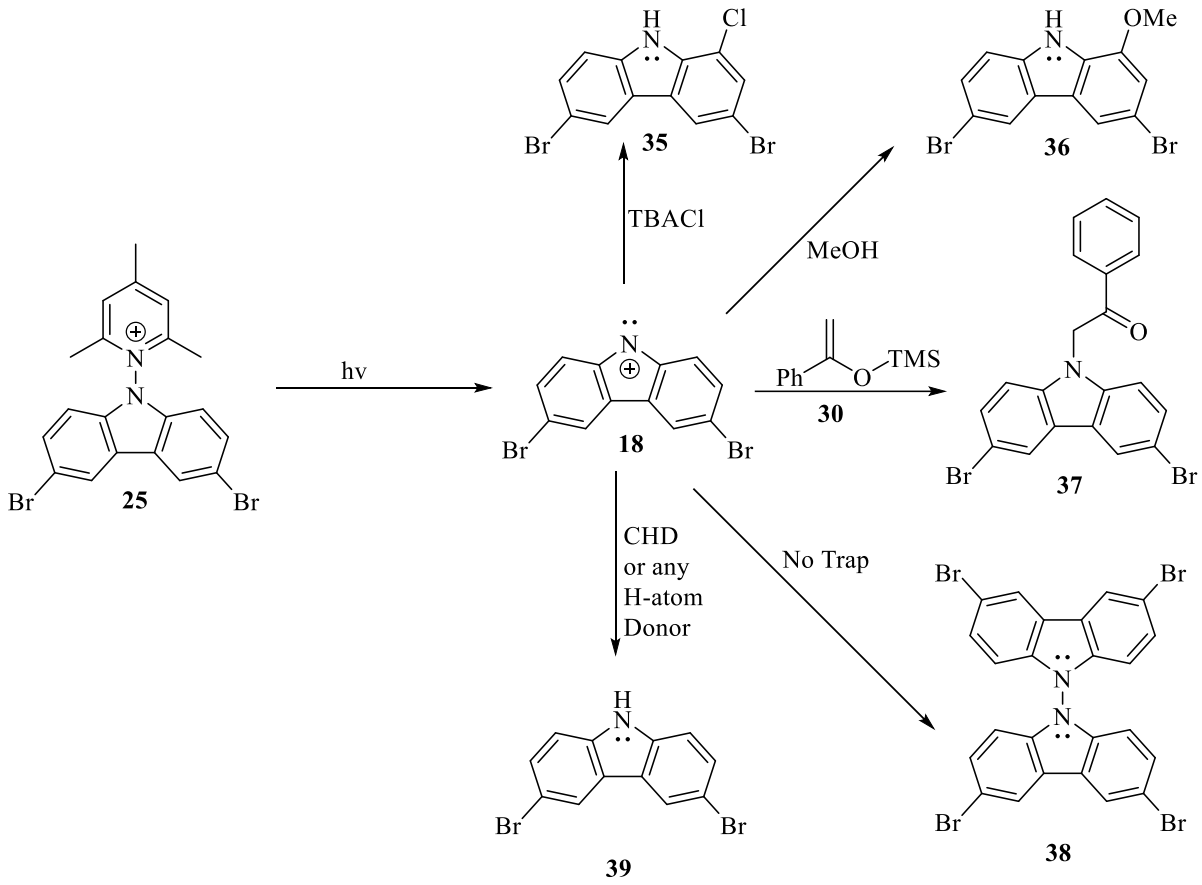

Scheme 4.3. Reactions of nitrenium ion **18**. Compounds **38**, and **39** are compared by ^{1}H NMR to authentic standards.[104,105] Compounds **35**, **36** and **37** are characterized by ^{1}H NMR, ^{13}C NMR, and ESI-MS.

Table 4.2. Nucleophilic traps of nitrenium ion **17** and related nitrenium ions. Carbazolyl nitrenium ion's TBACl and MeOH trapping were previously published[11]

Trap	**19** Carbazolyl Nitrenium Ion[11]	**18** 3,6-Dibromocarbazolyl Nitrenium Ion	**1** Diphenyl Nitrenium Ion[17]	**16** *N*,*N*-di(4-bromophenyl) nitrenium ion [17]
TBACl	*3.5 x 10^{10} M^{-1}s^{-1}*	2.9 x 10^{10} M^{-1}s^{-1}	1.0 x 10^{10} M^{-1}s^{-1}	9.83 x 10^{9} M^{-1}s^{-1}
H_2O	1.1 x 10^{8} M^{-1}s^{-1}	2.2 x 10^{6} M^{-1}s^{-1}	6.1 x 10^{5} M^{-1}s^{-1}	1.12 x 10^{4} M^{-1}s^{-1}
MeOH	*9.8 x 10^{8} M^{-1}s^{-1}*	1.4 x 10^{7} M^{-1}s^{-1}	5.2 x 10^{6} M^{-1}s^{-1}	7.74 x 10^{4} M^{-1}s^{-1}

Nitrenium ions **19** and **18** were then trapped with different electron and H-atom donors and their 2nd order rate constants were measured via LFP. Their reactivity trends and can be seen

in Tables 4.3 and 4.4. Both **19** and **18** trap TMB at 7.2 x 10^9 $M^{-1}s^{-1}$ and 1.3 x 10^{10} $M^{-1}s^{-1}$ which are both close to diffusion limit as is only slightly faster than diphenyl nitrenium ion **1** and *N*,*N*-di(4-bromophenyl) nitrenium ion **16**. A similar trend is seen for DMB with **19** and **18** trapping DMB at 8.1 x 10^9 $M^{-1}s^{-1}$ and 2.5 x 10^9 $M^{-1}s^{-1}$, however, when compared to nitrenium ions **1** and **16** both **19** and **18** trap DMB 1-2 orders of magnitude faster. We attribute this to the antiaromatic character of nitrenium ions **19** and **18**. DMA traps **19** and **18** the fastest at diffusion limited rates of 1.7 x 10^{10} $M^{-1}s^{-1}$ and 2.5 x 10^{10} $M^{-1}s^{-1}$ which is only 1 order of magnitude faster than nitrenium ion **16**. Finally, DABCO is used to trap nitrenium ion **18** to support the mechanism that the radical **18c** can be protonated by an acidic proton to the cation radical **18b**. Since DABCO does not have any acidic proton, two **18c** radical combine to form the N-N dimer **38.**

Table 4.3. Electron donor traps of nitrenium ion **18** and related nitrenium ions. TMB = Trimethoxybenzene. DMA = Dimethylaniline. DMB = Dimethoxybenzene. DABCO = 1,4-Diazabicyclo[2.2.2]octane.

Trap	E_{ox} (V vs SCE)	**19**	**18**	**1**[8]	**16**[17]
TMB	1.49[106]	7.2 x 10^9 $M^{-1}s^{-1}$	1.3 x 10^{10} $M^{-1}s^{-1}$	3.1 x 10^9 $M^{-1}s^{-1}$	5.17 x 10^9 $M^{-1}s^{-1}$
DMA	0.74[102]	1.7 x 10^{10} $M^{-1}s^{-1}$	2.5 x 10^{10} $M^{-1}s^{-1}$		6.01 x 10^9 $M^{-1}s^{-1}$
DMB	1.34[106]	8.1 x 10^9 $M^{-1}s^{-1}$	2.5 x 10^9 $M^{-1}s^{-1}$	3.4 x 10^8 $M^{-1}s^{-1}$	4.03 x 10^7 $M^{-1}s^{-1}$
DABCO	0.69[107]		1.5 x 10^{10} M^{-1} s^{-1}		

Next, **19** and **18** were trapped with different H-atom donors as seen in Table 4.4. Nitrenium ions **19** and **18** were both trapped with CHD at 9.1 x 10^9 $M^{-1}s^{-1}$ and 8.13 x 10^9 $M^{-1}s^{-1}$. Nitrenium ion **19**'s mechanism with CHD has been previously proposed to be by hydride abstraction instead of H-atom abstraction.[11] Both **19** and **18** are trapped by CHD 3 orders of magnitude faster than diphenyl nitrenium ion **1** and *N*,*N*-di(4-bromophenyl) nitrenium ion **16**.

This can be attributed to either **19** and **18** abstracting an electron from CHD or abstracting a hydride as was previously proposed.

Phenol (PhOH) traps both **19** and **18** with rate constants of 7.98 x 10^9 $M^{-1}s^{-1}$ and 1.21 x 10^9 $M^{-1}s^{-1}$ which is 5 orders of magnitude greater than nitrenium ion **16**. Nitrenium ions **19** and **18** are 4-9 kcal/mol more likely to abstract an H-atom from CHD based off of calculated BDE's for nitrenium ions **19**, **18**, **1**, and **16** as seen in Table 4.4, so this increased reactivity could be attributed to either H-atom abstraction or electron transfer. To determine this mechanism, a KIE experiment on trapping nitrenium ion **18** with PhOH and Phenol-d1 (PhOD) is performed as seen in Figure 4.5. Theoretically the KIE between k_H/k_D should be about 7. The kinetic traces obtained via LFP for PhOH vs PhOD are not statistically different, so no KIE is observed. Therefore, **18** does not abstract an H-atom from PhOH, but rather **18** is reduced to the neutral radical **18c**. 4-bromophenol traps **19** and **18** with rate constants of 6.38 x 10^8 $M^{-1}s^{-1}$ and 1.25 x 10^9 $M^{-1}s^{-1}$. These values are still 5 orders of magnitude faster than nitrenium ion **16**. It is assumed that 4-BrPhOH follows the same mechanism as PhOH. The nitrenium ions **19** and **18** react with 4-BrPhOH to initially form neutral radicals. Finally, 4-cyanophenol (4-CNPhOH) was used to trap nitrenium ions **18**. Nitrenium ion **18** was not quenched by 4-CNPhOH which means that the 2^{nd} order rate constant for this reaction is < 1 x 10^5 $M^{-1}s^{-1}$.

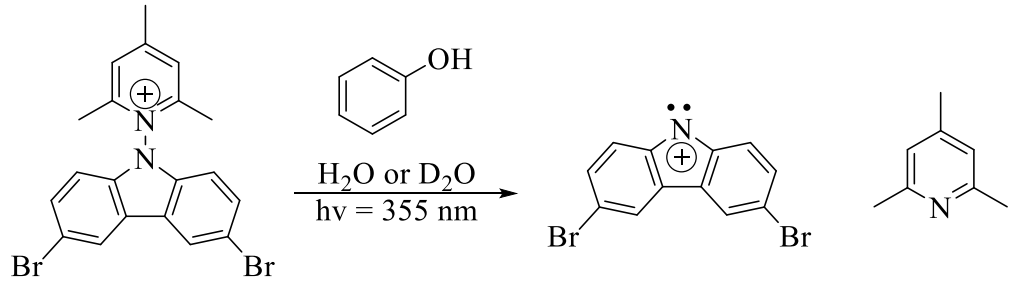

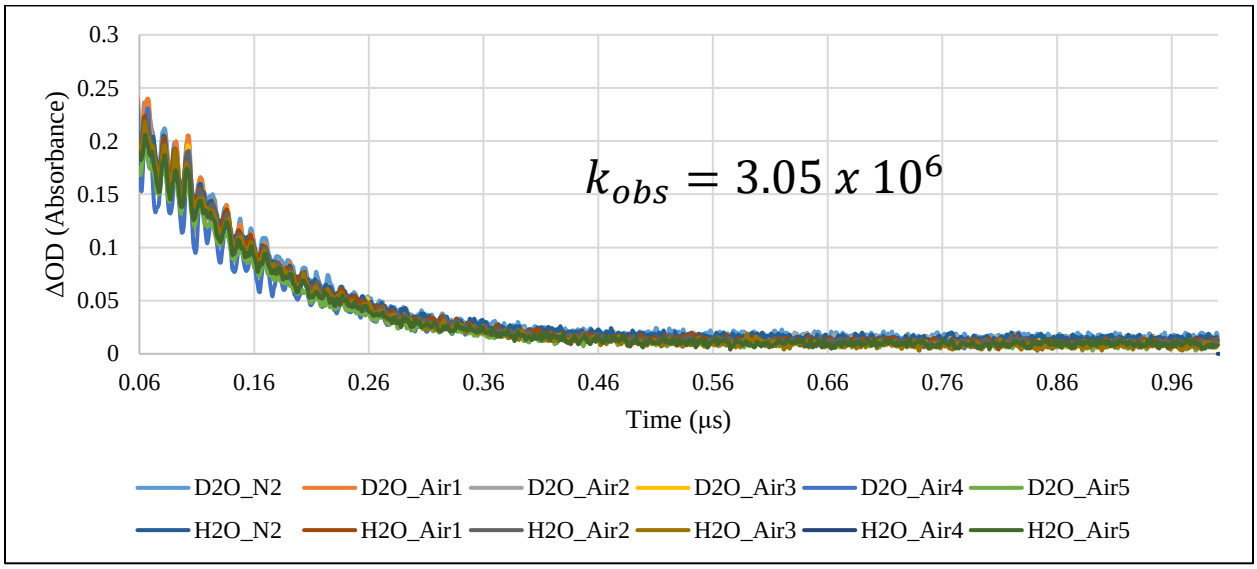

Figure 4.5. Kinetic isotope effect measurements with PhOH vs PhOD. No KIE is observed, so phenol quenches nitrenium ion **18** through electron transfer.

Table 4.4. H-atom donor traps of nitrenium ion **18** and related nitrenium ions. The BDE's are calculated by b3lyp-d3/def2svp EE + ZPVE. Carbazolyl nitrenium ion's CHD trapping was previously published.[11]

Trap	E_{ox} (V vs SCE)	**19**	**18**	**1**[17]	**16**[17]
CHD	1.74[17]	*9.1 x 10^9 M^{-1}s^{-1}*	8.13 x 10^9 M^{-1}s^{-1}	6.5 x 10^6 M^{-1}s^{-1}	5.13 x 10^6 M^{-1}s^{-1}
Phenol	1.63[102]	7.98 x 10^9 M^{-1}s^{-1}	1.21 x 10^9 M^{-1}s^{-1}		4.73 x 10^5 M^{-1}s^{-1}
4-bromo phenol	1.69[102]	6.38 x 10^8 M^{-1}s^{-1}	1.25 x 10^9 M^{-1}s^{-1}		4.89 x 10^5 M^{-1}s^{-1}
4-cyano phenol	2.08[102]		Below Detection Limit or < 1 x 10^6 M^{-1}s^{-1}		
Est. BDE (kcal/mol)		-90.11	-92.3	-85.8	-83.17

Once the 2nd order rate constants are measured, product analysis is used to better understand the mechanism by which nitrenium ion **18** reacts with different traps. NMR tubes with pyridinium ion **25** and different traps were photolyzed and the ^{1}H NMR products from the mixtures were compared to authentic standards as seen in Table 4.5. In the absence of any trap and in an inert solvent, nitrenium ion **18** forms the N-N dimer **38**. However, in the presence of CHD, PhOH, 4-BrPhOH, 4-CNPhOH, and DMA, the product is the parent amine **39**. Surprisingly, in the presence of DMA which is a good electron donor, the final product is also the parent amine **39** instead of the dimer **38**. A plausible mechanism for forming the parent amine **39** for all of the traps in Table 4.5 is that the nitrenium ion **18** is reduced by the traps to form the radical **17c**. When acidic species are present, the radical **18c** is protonated to form the cation radical **18b**. The cation radical **18b** then is reduced again to the parent amine **39** shown in Scheme 4.4.

Table 4.5. NMR experiments of pyridinium ion **25** with different traps. Each sample was photolyzed at 370 nm until all of pyridinium ion **25** was converted. Only the parent amine (**39**) was observed as a product. In the absence of a trap only the dimer (**38**) was observed.

Trap	Products
CHD	**39**
PhOH	**39**
4-BrPhOH	**39**
4-CNPhOH	**39**
DMA	**39**
H_2SO_4 (diluted)	**39**
None	**38**

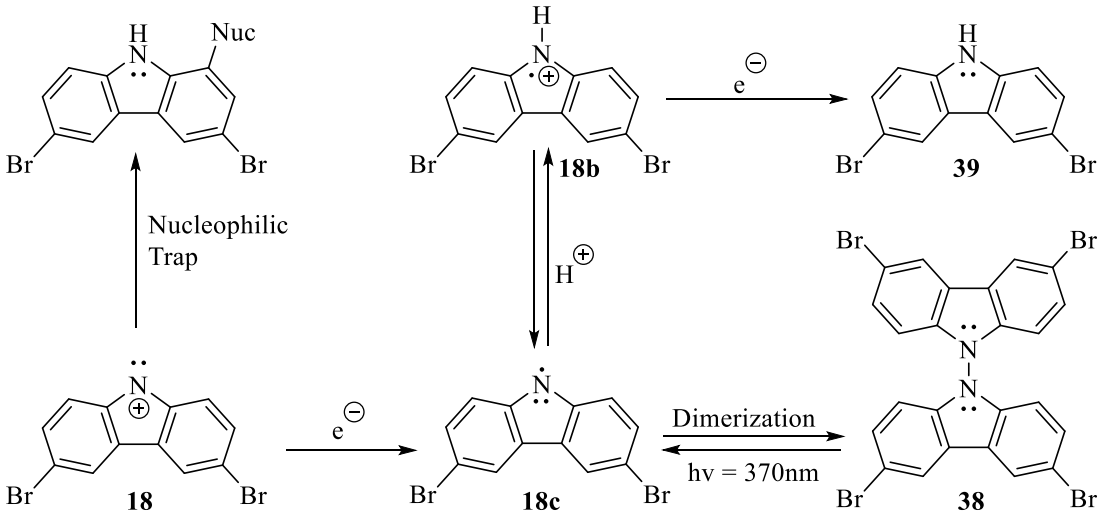

Scheme 4.4. Mechanistic pathway for nitrenium ion **18**. In the presence of TBACl, or MeOH it forms nucleophilic adducts. Nuc = Cl or OMe.

Additional support for the mechanism in Scheme 4.4 was obtained by the NMR experiment with 4-CNPhOH. This step produces the parent amine **39** even though it has no measurable 2nd order rate constant as seen in Table 4.4. The nitrenium ion **18** produces the radical **18c** even in the absence of any trap. 4-CNPhOH serves as an acid and it protonates **18c** to form the cation radical **18b** and eventually the parent amine **39**.

Further support for this mechanism comes from an experiment where a strong acid is added to the photolysis of pyridinium ion **25** in CH_3CH. High yields of parent amine **39** are obtained when **25** is photolyzed in the presence of H_2SO_4 as seen in Table 4.5. The added acid protonates the radical **18c** and causes the major product to be the parent amine **39** instead of the dimer **38**. We do not directly observe the cation radical **18b** accepting an electron to form the parent amine **39**. However, in all reaction conditions where cation radical **18b** is formed, parent amine **39** is observed in the product mixture via ^{1}H NMR.

In neutral conditions, neutral radical **18c** couples to itself to form the dimer **38**. Electron donors which do not easily donate a proton such as DABCO or TMB were able to produce the dimer **38**. It can be seen in Table 4.3 that both DABCO and TMB donate an electron at near diffusion limited rates for nitrenium ion **18**. Further, **18**'s signal in the presence of DABCO clearly gets quenched to make neutral radical **18c** (see Figure 6.22). Photolysis of DABCO and TMB produces the dimer **38** as the primary product and the parent amine **39** as a minor product. The minor product, parent amine **39**, is attributed to prolonged photolysis of the dimer **38**. If the dimer **38** is photolyzed it breaks apart to form **18c**.

The antiaromaticity of the carbazolyl nitrenium ion derivatives destabilizes the nitrenium ions to the extent that they oxidize an electron from the H-atom donor traps to form their corresponding radicals instead of an H-atom to form their corresponding cation radicals. It is unclear whether the antiaromatic nitrenium ions are abstracting an electron or a hydride from CHD as KIE experiments were not done on CHD, but the mechanism for nitrenium ion **18** with traps have been determined.

4.6 Mechanisms of 3,6-Dibromocarbazolyl Nitrenium Ion in the Absence of Traps

With electron donor traps, the nitrenium ion **18** oxidizes trap to form the neutral radical **18c** which combine to make the dimer **38** as seen in Scheme 4.5. However, the dimer **38** is still observed in inert solvents in the absence of trapping agents. The source of electrons in this case must be accounted for. The N-N dimer **38** is very cleanly formed from photolysis of pyridinium ion **25** in the absence of any traps by ^{1}H NMR. Similar N-N dimers were observed with the *N*,*N*-di(4-halophenyl) nitrenium ions **16** and **17**.[17] The question then is what does the nitrenium ion **18** oxidize? There are two different ways to assess the mechanism of nitrenium ion **18** in the absence of any traps. First, LFP can be used to determine the initial mechanistic step. Second, ^{1}H NMR can be used to determine the source of reducing equivalents.

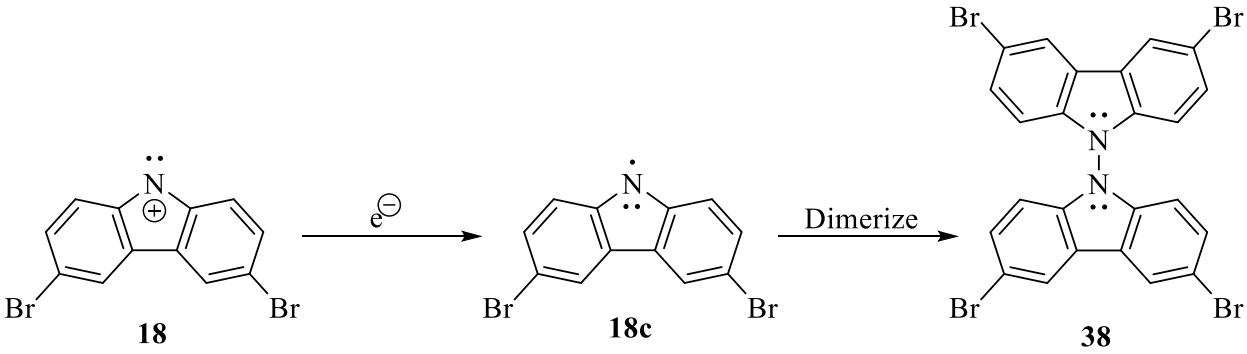

Scheme 4.5. Mechanistic pathway to get from nitrenium ion **18** to dimer **38**.

The initial step of this mechanism is the reduction of nitrenium ion **18** by pyridinium ion **25**. LFP shows that this reaction has a 2nd order rate constant of 3.09 x 10^8 $M^{-1}s^{-1}$ (see Figure 4.6). A closer examination of the transient spectra from LFP shows nitrenium ion **18** decaying to form neutral radical **18c** as seen in Figure 4.4 (in CH_3CN) and Figure 4.8 (in DCM).

We considered the possibility that nitrenium ion **18** might react with the counter ion BF_4^-. Pyridinium ion **25** has a counter ion BF_4^- which could potentially be what nitrenium ion **18** is

oxidizing as increasing concentrations of pyridinium ion **25** also increase the concentration of BF_4^-. To rule out this possibility, LFP experiments with the pyridinium ion **25** and varying concentrations of tetra(n-butyl)ammonium BF_4^- showed that nitrenium ion **18**'s pseudo first order decay was unchanged by differing concentrations of BF_4^- (see Figures 6.26). To further support the pyridinium ion **25** as the initial reductant and not BF_4^- the counter ion was changed from BF_4^- to ClO_4^-. The LFP trapping experiment with nitrenium ion **18** and ClO_4^- again showed there was no difference in rate constant (see Figures 6.27). These experiments exclude the counter ion from reducing nitrenium ion **18**. Therefore, nitrenium ion **18** is trapped by pyridinium ion **25**.

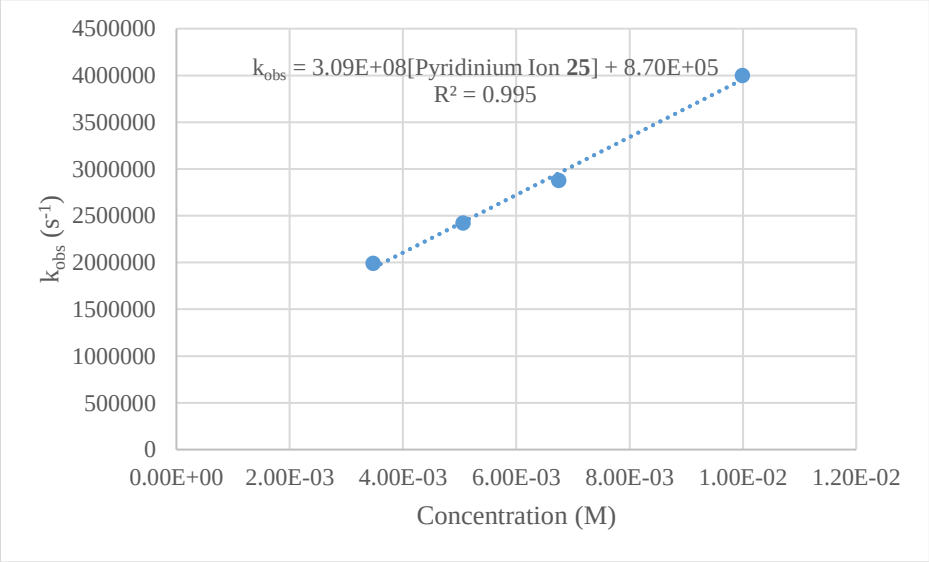

Figure 4.6. LFP trapping experiment shows that nitrenium ion **18** gets trapped by pyridinium ion **25**.

We also examined the possibility of that the solvent quenches nitrenium ion **18**. To test this a KIE experiment using LFP was performed in this experiment, the pyridinium ion **25** was photolyzed in CH_3CN as well as CD_3CN. Since no difference in pseudo-first order rate constants were observed, there is no KIE with CH_3CN/CD_3CN (see Figure 4.7). Therefore, it is unlikely

that nitrenium ion **18** abstracts an H-atom from the solvent. Additionally, the pyridinium ion **25** was photolyzed in both CH_3CN and DCM. The lifetime of the nitrenium ion **18** was the same in both solvents. It is extremely unlikely that both solvents would react at identical rates. Therefore, the solvent is not reducing the nitrenium ion **18** to the neutral radical **18c**. Further, N,N-di(4-bromophenyl)nitrenium ion **16** also makes its N-N dimer, and was found to have consistent lifetimes in CH_3CN, DCM, chlorobenzene, and nitrobenzene as well.[17] Therefore, the solvent has been ruled out as the oxidant, and the pyridinium ion **25** is the initial oxidant.

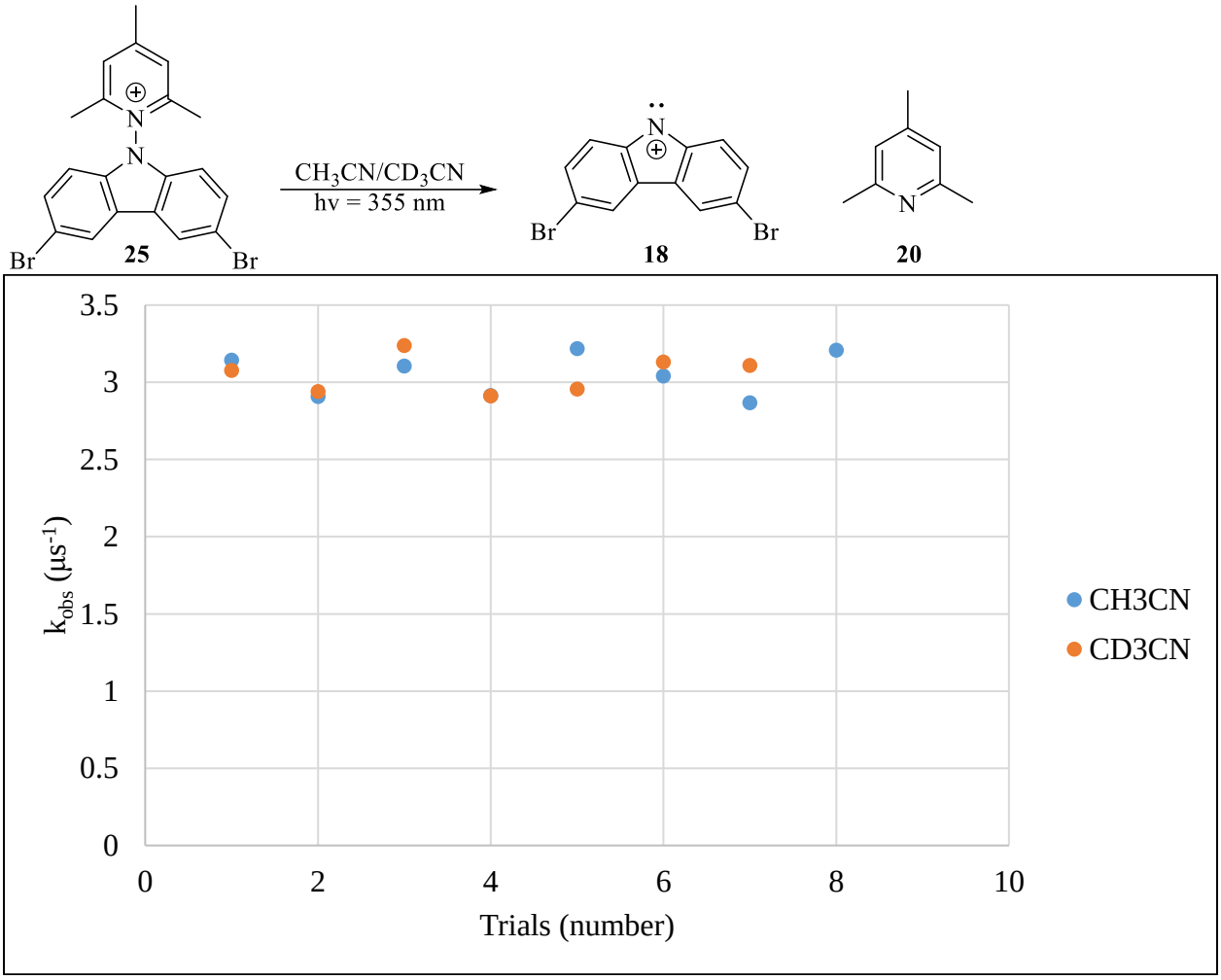

Figure 4.7. Nitrenium ion **18** shows no KIE with the solvent in CH_3CN/CD_3CN.

High yields of collidine exclude this species as the source of reducing equivalent. The photolysis of pyridinium ion **25** in CH_3CN has a ^1H NMR integration ratio of the dimer **38** to collidine **20** of 0.4:1. The collidine **20** yield is between 90-100%, so collidine **20** is discounted as the final donor of electrons.

In contrast to the collidine leaving group, only 40% of the 3,6-dibromocarbazolyl product is accounted for in the yield of dimer **38**. ESI-MS shows a small fragment at m/z 768 with the appropriate isotopic distribution for a nitrenium ion **18** bonded to a pyridinium ion **25**. Another 5% of the 3,6-dibromocarbazolyl product can be attributed to this pyridinium ion adduct **40**, and a possible mechanism and structure is given in Scheme 4.6. The missing 55% of dibromocarbazolyl product is attributed to oligomers similar to what has been previously observed.[51] These oligomers would presumably be oxidized to form persistent cation radicals which would not be observed in ^1H NMR as their unpaired electrons' spin would cause the T_2^* to decrease to the point that it would not be observable in ^1H NMR. Analogous oligomers have been previously observed in MALDI MS.[51] Oligomers of nitrenium ion **18** are what we attribute the final oxidant to be.

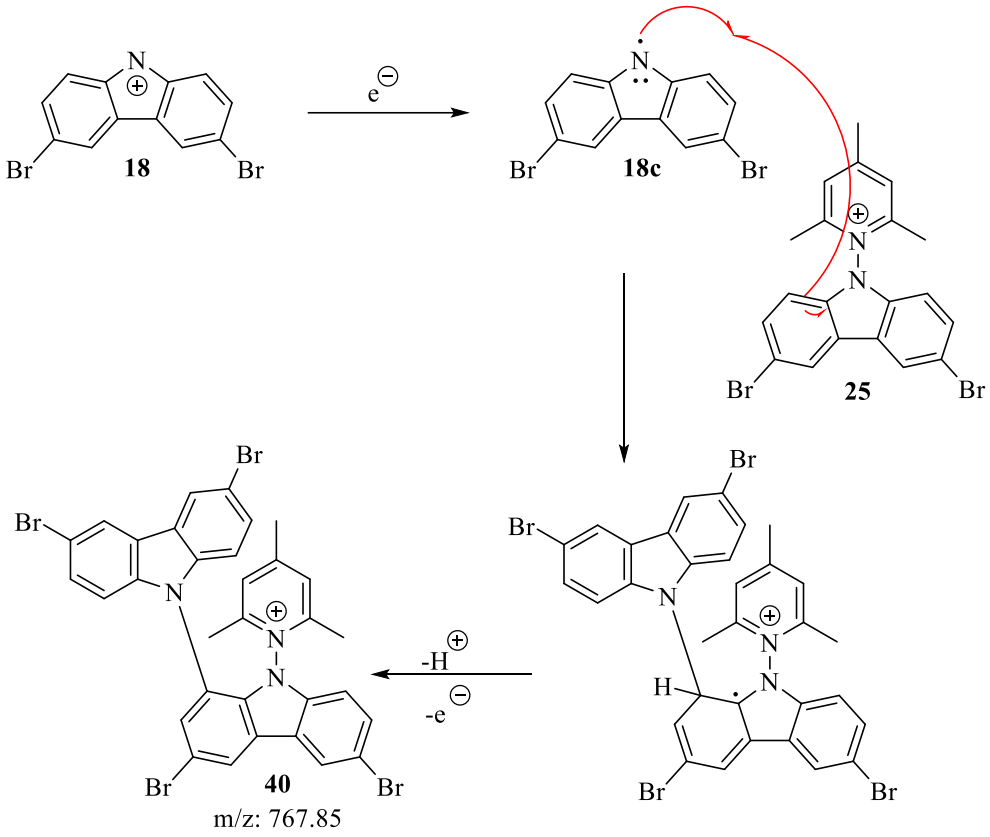

Scheme 4.6. Proposed mechanism of formation of pyridinium-nitrenium ion adduct **40** observed in product mixture by ESI-MS. This product accounts for approximately 5% of the product mixture by ^{1}H NMR impurities. The dimer **38** accounts for 40% of the product mixture.

To discount other possible final electrons sources, BF_4^- is ruled out by using ^{19}F NMR to determine if there is any change in chemical shift of BF_4^- or if any additional peaks grow in. Neither of these are observed (see Chapter 6.4.4). Further, collidine **20** can be ruled out as its yield is between 90-100%.

A mechanism which can account for all the data is shown in Scheme 4.7. In the first step, nitrenium ion **18** oxidizes pyridinium ion **25** to make the neutral radical **18c** and the dicationic pyridinium ion **41**. The formation of the **18c** can be clearly seen by LFP in CH_3CN and in DCM, but is a little clearer in DCM and can be seen in Figure 4.8. Next, two **18c**'s dimerize to give the final dimer product **38**. **41** then pulls an electron from the dimer **38** or oligomeric species to

regenerate the pyridinium ion **25** and either the cation radical of **38** or the cation radical of an oligomeric species. This second step is attributed to the fact that **20** and BF_4^- do not form any side products, and the pyridinium ion **25** can be cleanly converted to make **20**, but only 40% of **38**. The final proposed mechanism is shown in Scheme 4.7.

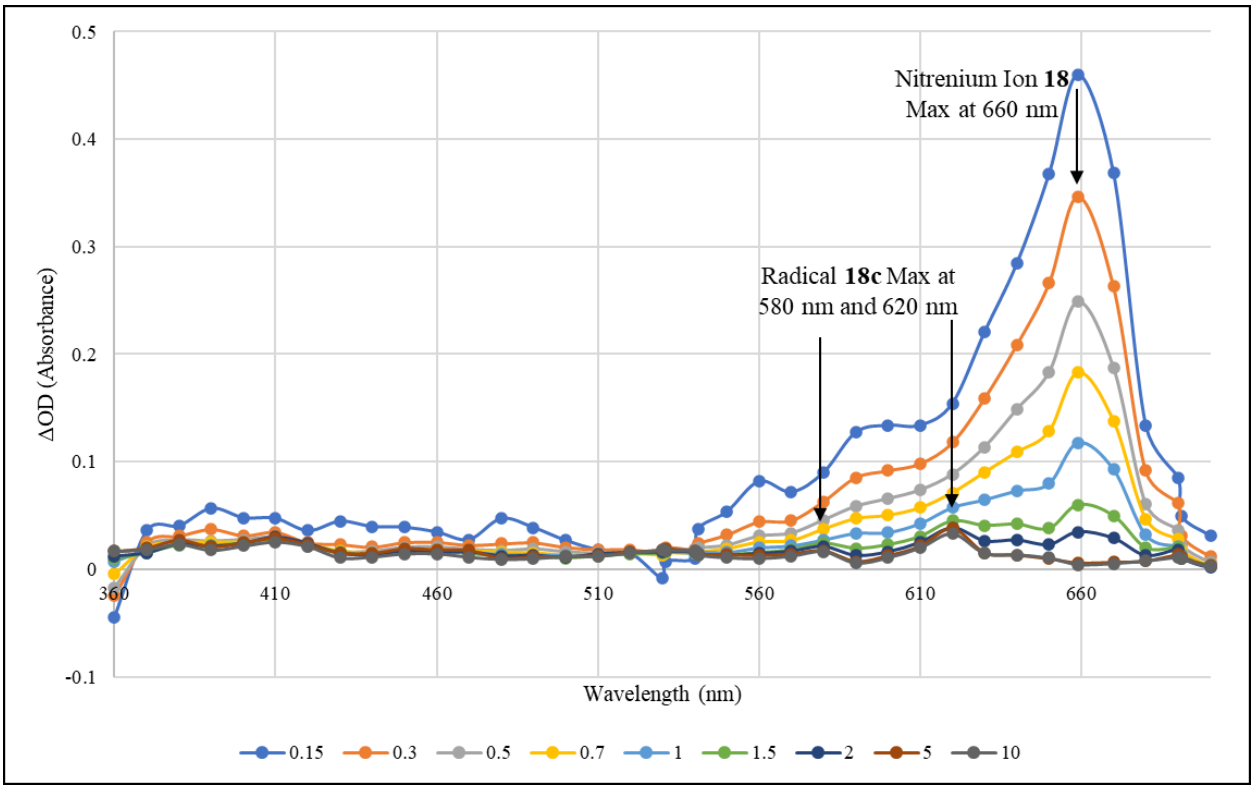

Figure 4.8. Nitrenium ion **18** decaying into neutral radical **18c**. Solvent is DCM. Times are in μs. **18c** is clearly visible at 1.5 μs and still visible when the nitrenium ion is completely decayed at 5 μs.

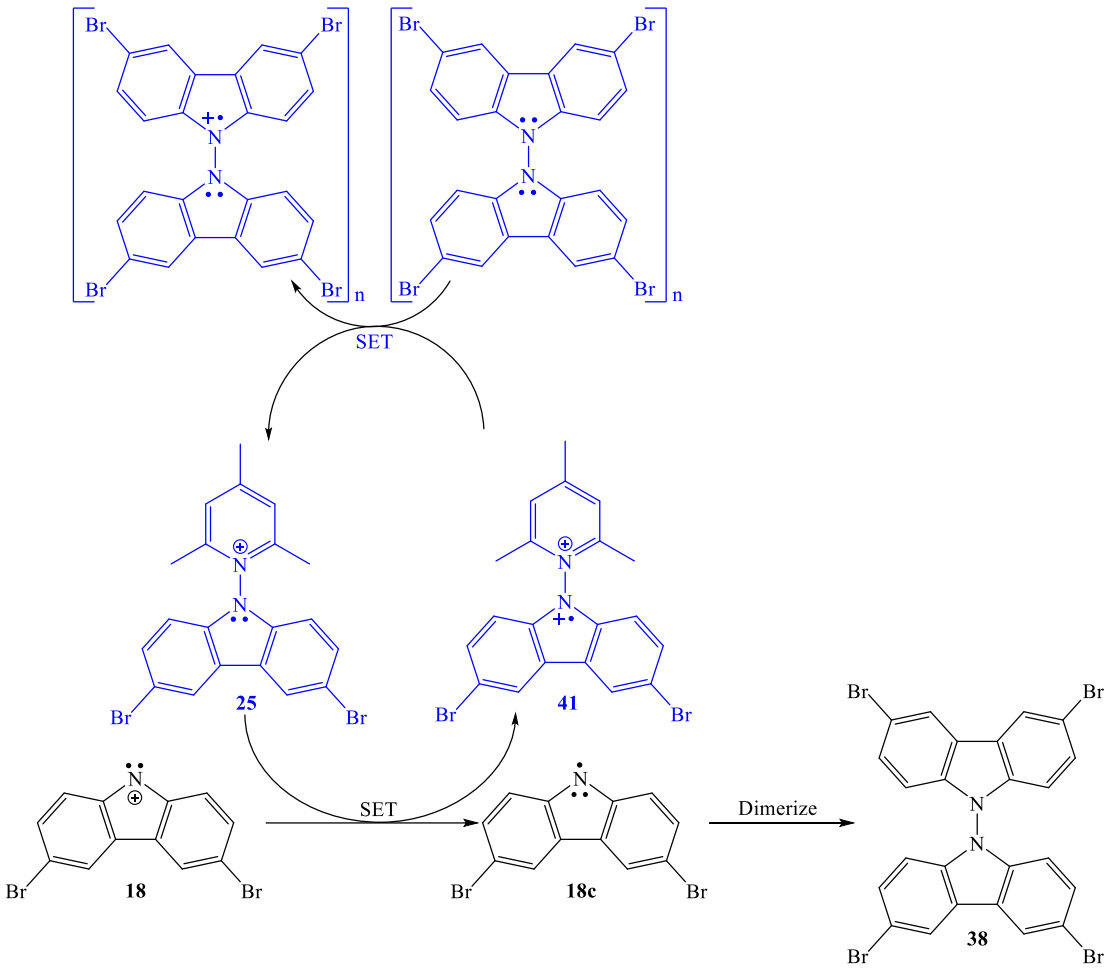

Scheme 4.7. Mechanism for formation of Dimer **38** from nitrenium ion **18**. Additionally, instead of **38** being oxidized to its cation radical, short oligomers could be oxidized as well.

A couple final points need to be made on the formation of **38**. The earlier mechanism proposed for the N-N dimer formation of the nitrenium ions **16** and **17** suggest that the nitrenium ions were reduced by a trace impurity.[17] The issue with this explanation is that it would be dependent on the sample purity. Presumably the more times the reaction is carried out, the concentrations of trace impurities would change, unless they are solvent impurities. In this case, distilling the solvent should change trace impurity concentration. Further, changing the solvent should change the impurities or their concentrations in the solvents as well. None of these changes in nitrenium ion lifetime were observed, so the trace impurity explanation is ruled out.

Second, it is worthwhile to consider why N-N dimers only form as the only product in the cases where the para positions are substituted. Our hypothesis is that in examples where the para position are unsubstituted for electrophilic aromatic substitution, a mixture of N-N dimers (head-to-head) and N-para dimers (head-to-tail), and even possibly para-para dimers (tail-to-tail). This mixture of dimers and even eventually the formation of oligomers make it difficult to isolate and characterize the various products.[11,17,51]

Additionally, it is possible that the dicationic pyridinium ion **41** photolyzes to form nitrenium ion **18** and the cation radical of collidine instead of accepting an electron from **38** or short oligomer. The cation radical of collidine then accepts an electron from the dimer or short oligomer.

In summary, we believe the mechanism of dimer **38** formation's first step is the nitrenium ion **18** oxidizing pyridinium ion **25** to form the neutral radical **18c** and the dicationic pyridinium ion **36**. Two neutral radicals dimerize to make dimer **38**. **41** reforms the pyridinium ion **25** by a subsequent electron transfer presumably from the dimer **38** or oligomers of the dimer **38**.

4.7 Trapping Alkenes with 3,6-Dibromocarbazolyl Nitrenium Ion

The last objective of this study is to determine if the antiaromatic nitrenium ion **18** can react with weak nucleophiles. The nucleophiles investigated are alkenes with different electron density as seen in Figure 4.3. First, nitrenium ion **18** was trapped by the 1-phenyl-1-trimethylsiloxyethylene **30** to give adduct **37** (see Scheme 4.3 above). This trap has previously been used to successfully trap diphenyl nitrenium ion **1**.[15] Surprisingly only the N-adduct was formed as seen in Scheme 4.3, but in the case of **1**, the ortho and para products were isolated.[15] This suggests that **30** could be trapping **18** through a radical mechanism which has been seen in

similar silyl enol ethers with a sufficient oxidant.[108] A proposed mechanism for the formation of adduct **37** can be seen in Scheme 4.8.

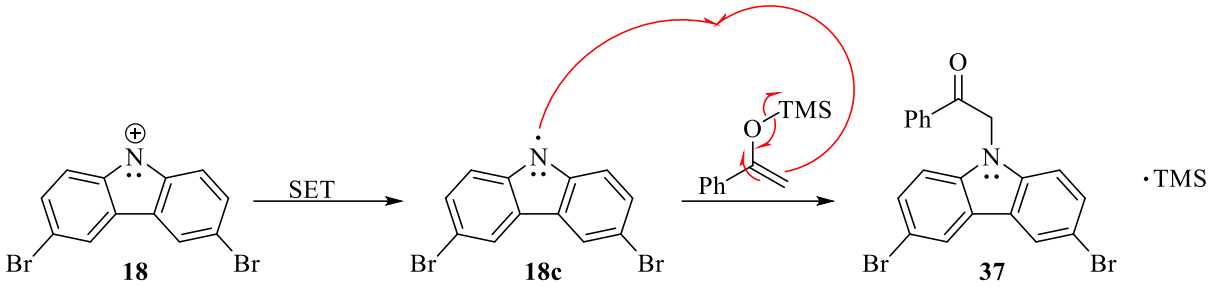

Scheme 4.8. Proposed mechanism for the formation of only the N-adduct **37**.

Since nitrenium ion **18** is reactive with **30**, we decided to test **18**'s reactivity with less electron rich alkenes, namely cis-stilbene **32**, styrene **33**, and cyclohexene **34**. The yields of these traps were obtained with ^{1}H NMR as described in Chapter 6.4.1 and the results can be seen in Table 4.6.

Table 4.6. NMR yields of different alkene traps. Only **30** is reactive with nitrenium ion **18**. EVE **31** makes an insoluble polymeric gel mixture, so its yields were not accurate with ^{1}H NMR as not everything went into solution, so it is not included in this table.

Alkene Trap	Adduct (%)	Amine **39** (%)	Dimer **38** (%)	Total (%)
1-phenyl-1-trimethylsiloxyethylene **30**	82 (Adduct **37**)	Peaks covered up by **30**	Peaks covered up **30**	82
Cis-Stilbene **32**	Not Detected	24.8	29.5	54.3
Styrene **33**	Not Detected	24.0	39.4	63.4
Cyclohexene **34**	Not Detected	8.5	31.8	40.3
No Trap	N/A	0%	Only Product	N/A

Surprisingly, none of the other alkenes were able to trap the nitrenium ion **18**, despite its antiaromaticity. Alkenes **32**, **33**, and **34** did not produce any adducts, but rather the parent amine

39 (yields 8.5-24.8%) and dimer **38** (yields 29.5-31.8%). Since no adducts were observed in ^{1}H NMR, only alkene **30** can form adducts with nitrenium ion **18**. It is possible that the trimethylsilyl (TMS) leaving group may be necessary to achieve trapping at the concentrations of alkene trapping. Ethyl vinyl ether (EVE) **31** was used to probe this hypothesis. Photolysis of pyridinium ion **25** with alkene **31** generated a polymeric gel like mixture. This is not surprising since nitrenium ions will eventually generate an equivalent of acid, and **31** is known to cationically polymerize in the presence of acid[109]. The gel itself is soluble in CH_3CN so ESI-MS was used to identify any adducts with a dibrominated isotopic distribution. No adducts were observed, so **31** is not able to trap the nitrenium ion **18**.

The Mal group has been able to achieve intramolecular trapping of alkenes and intermolecular trapping of a nitrenium ion with aryl rings.[110,111] We interpret our results to mean that a higher concentration of alkene is needed to achieve labeling as nitrenium ion **18** is being reduced before the alkenes can nucleophilically trap it. The pyridinium ion **25** was not soluble in neat alkene solvent like styrene, so the concentration of alkene was kept constant across all alkene traps **30**-**34** and matched the concentrations used for the **1** with silyl enol ethers.[15] It is possible that if the concentration of the alkenes used was maximized that adducts could potentially be isolated.

Therefore, we conclude that the nitrenium ion **18** is reduced so rapidly that either it has to be trapped with a nucleophile that has a 2^{nd} order rate constant close to the diffusion limit like Cl^-, or nitrenium ion **18** can be trapped by a nucleophilic solvent like MeOH. Otherwise, it accepts an electron to form **18c**. Once **18c** is formed alkene **30** can trap it. If there are no acidic protons then it forms the dimer **38**. If there are acidic protons it forms **18b** and eventually the parent amine **39**.

4.8 Conclusions and Future Work

The 3,6-dibromocarbazolyl nitrenium ion **18** can be characterized by LFP and product analysis. It has 2nd order rate constants consistent with **19** with nucleophilic traps and electron donor traps, and H-atom donor traps. In neutral conditions **18** accepts an electron to form **18c** which then dimerizes to form the N-N dimer **38**. In acidic conditions **18c** get protonated to form **18b** which then accept another electron to form the parent amine **39**. Finally, **18** was unable to be trapped with different alkenes except for **30** which is believed to form through a radical mechanism. Therefore, the antiaromaticity of the high energy nitrenium ion does not lead to any new synthetically useful reactivity, but mainly results in electron transfer.

The future work of this project would be to investigate the 3,6-dichlorocarbazolyl nitrenium ion and determine if it follows the same pattern as **18**. Further, synthesizing a new nitrenium ion which alkylates the 3 and 6 positions would isolate the substitution patten of the antiaromatic nitrenium ion from the electronic effects of the lone pairs on the halogens.

Chapter 5: Selective Labeling and Isolating Tryptophan adducts in N-acetyl-L-Tryptophan ethyl ester and Peptide WWCNDGR

The majority of the work in this chapter has been published.

Chinn, E. S.; Li, Y.; Joyce, A. M.; Falvey, D. E. Selective Photo Labeling of Tryptophan with N-Acetyl-L-Tryptophan Ethyl Ester and Peptide WWCNDGR. ***2025****.* *https://doi.org/10.26434/CHEMRXIV-2025-96K9J.* [112]

5.1 Aryl Nitrenium Ions as a Tryptophan Labeling Candidate

Covalent modification of proteins is important for controlling protein activity. To this end it is desirable to develop reagents capable of reacting with specific amino acids. Many methods have been developed for selectively labeling natural occurring amino acids. Some of the amino acids studied include but are not limited to, lysine,[113] glutamine,[114] cysteine,[115] tyrosine,[116–119] arginine,[120] methionine,[121,122] tryptophan,[123–129] as well as the N and C terminus amino acids.[130]

There are many ways to target amino acid labeling in peptides and proteins, but a previously unexplored way is through using nitrenium ions. Aryl nitrenium ions have previously been shown to covalently modify guanosine monophosphate (GMP). This labeling has been suspected to cause mutations in DNA causing cancer.[28,131,132] The advantage of covalently modifying peptides and proteins with aryl nitrenium ions is that aryl nitrenium ions are easily photochemically generated. This allows for both spatial and temporal control of the peptide or protein modification.

In a previous work, the Falvey lab showed that aryl nitrenium ions also react with amino acids, GMP, and proteins. These experimental measurements were done using LFP of 1-(*N*-methyl-*N*-4-biphenylyl)-2,4,6-trimethylpyridinium tetrafluoroborate **42** to its corresponding

nitrenium ion **43** and observing quenching of **43**'s signal by different biomolecules.[133] More recently we designed the 10,11-dihydrodibenz[b,f]azepinyl nitrenium ion **2** and showed that the fastest trapped amino acids are tryptophan, cysteine, and methionine.[10,133] A summary of the important trapping rate constants can be seen in Table 5.1.

Table 5.1. 2nd order rate constants measured using LFP trapping different nitrenium ions with naturally occurring amino acids.

Amino Acid Trap	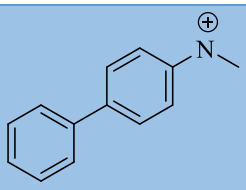 **43**[133]	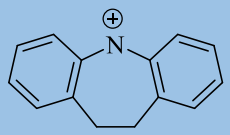 **2**[10]
Tryptophan	(2.91 ± 0.1) x 10^9 M^{-1} s^{-1}	2.52 x 10^9 M^{-1} s^{-1}
Methionine	(1.29 ± 0.7) x 10^9 M^{-1} s^{-1}	8.63 x 10^8 M^{-1} s^{-1}
Cysteine	(2.79 ± 0.2) x 10^8 M^{-1} s^{-1}	3.95 x 10^8 M^{-1} s^{-1}
Lysine	(8.04 ± 1.6) x 10^7 M^{-1} s^{-1}	3.72 x 10^7 M^{-1} s^{-1}
Tyrosine	(2.95 ± 0.7) x 10^8 M^{-1} s^{-1}	2.10 x 10^7 M^{-1} s^{-1}
Arginine	(3.04 ± 0.5) x 10^7 M^{-1} s^{-1}	6.49 x 10^7 M^{-1} s^{-1}
Serine	(7.93 ± 0.7) x 10^6 M^{-1} s^{-1}	
Histidine	(5.39 ± 0.5) x 10^7 M^{-1} s^{-1}	

The LFP experiments in Table 5.1 shows that tryptophan reacts the fastest out of all the amino acids. However, the earlier studies did not distinguish between different mechanisms for this reaction. It is unclear whether the mechanism of trapping the nitrenium ion with tryptophan is by electron transfer, nucleophilic addition, or H-atom transfer. Our expectation is that tryptophan will add to an aryl nitrenium ion through a nucleophilic addition mechanism. Before labeling a peptide with an aryl nitrenium ion, the tryptophan adducts with the aryl nitrenium ion will be characterized. Once we characterize the tryptophan adducts, we hypothesize that we will be able to selectively label tryptophan in a short peptide chain.

Tryptophan is the least abundant naturally occurring amino acid in nature, comprising only about 1% of amino acids in proteins.[134] Tryptophan labeling agents are important to develop to understand protein interactions.[130] Current selective tryptophan labeling reactions use rhodium carbenoids,[126] opening an oxaziridine ring,[127] exciting the tryptophan indole ring to react with short halohydrocarbon,[123] or oxidizing the alpha carbon of the indole ring.[124] Most relevant to this study is the Taylor Lab's work on selectively labeling tryptophan with photoinduced electron transfer from the tryptophan to an N-carbamoylpyridinium salt which results in a group transfer of the N-carbamoyl group to the tryptophan producing collidine as a by-product.[128,129] The Taylor lab discounts the possibility of a nitrenium ion intermediate because they see no rearrangement products and non-aryl nitrenium ions quickly rearrange.[64,129]

5.2 Designing a Nitrenium Ion for Tryptophan and Peptide Adducts

In designing an aryl nitrenium ion to use for labeling a peptide, a dibrominated nitrenium ion is used as the two bromines would give an isotopically unique isotopic distribution in our mass spectra. The *N*,*N*-di(4-bromophenyl)nitrenium ion **16** is a good option. It is also known to be generated from the *N*-(4,4'-dibromodiphenylamino)-2,4,6-trimethylpyridinium ion (**44**) with UV light as can be seen in Scheme 5.1.[17]

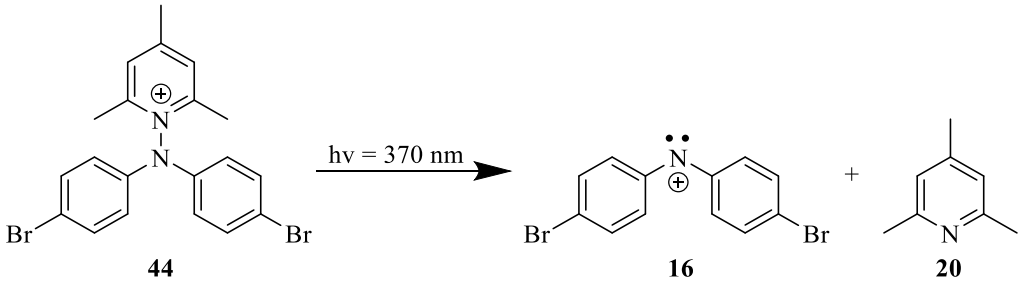

44 **16** **20**

Scheme 5.1. Generation of nitrenium ion **16** from compound **44**.

In this work, we first demonstrate that tryptophan traps nitrenium ion **16** and leading to two major covalent adducts. Further, we show that nitrenium ion **16** covalently bonds to the indole ring in a short peptide WWCNDGR. In using a dibrominated nitrenium ion, we are be able to unambiguously identify labeled fragments in tandem mass spectrometry analysis. We propose that nitrenium ion **16** is representative of aryl nitrenium ions and that aryl nitrenium ions should be considered an option for tryptophan labeling.

5.3 N,N-di(4-bromodiphenyl)nitrenium ion-Tryptophan Adducts Characterized

First, nitrenium ion **16** is used to label *N*-acetyl-L-tryptophan ethyl ester **45**. The trapping of nitrenium ion **16** produces two major adducts **46** and **47**. The identity of these products was established using ^{1}H NMR, ^{13}C NMR, HSQC NMR, and ESI^{+} MS and their formation mechanisms are shown in Schemes 5.2 and 5.3.

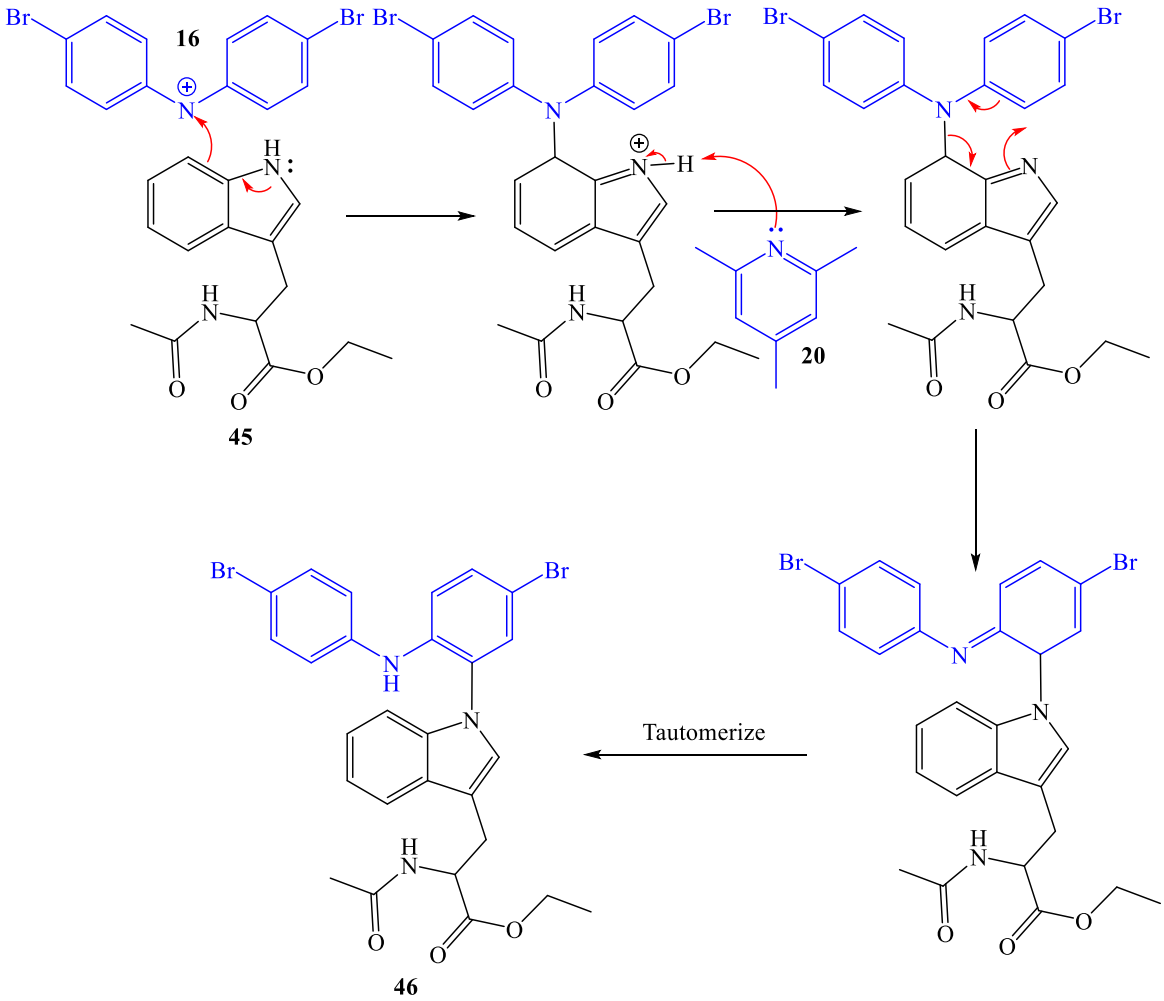

Scheme 5.2. Proposed Mechanism for the labeling of **45** with **16** to make compound **46**.

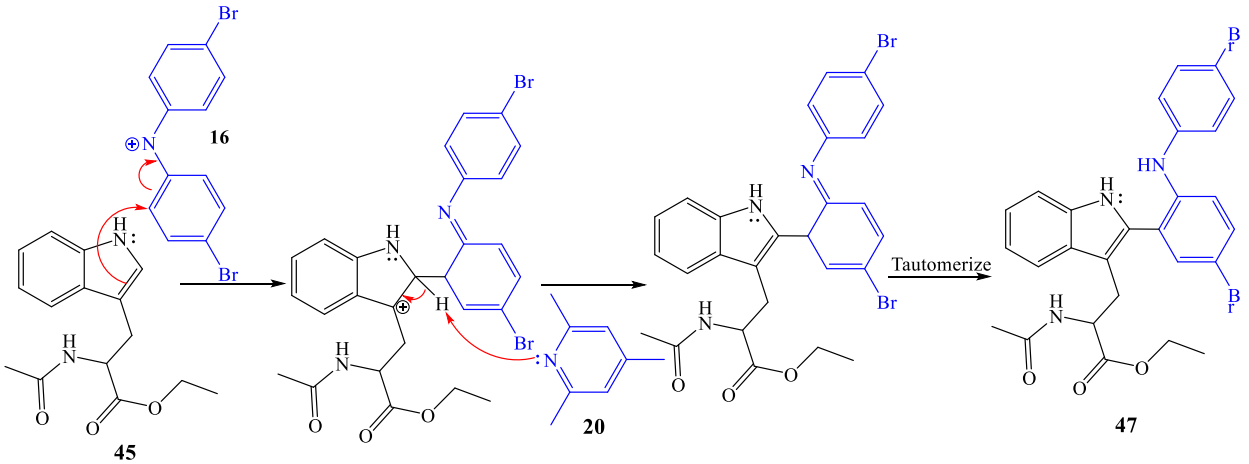

Scheme 5.3. Proposed Mechanism for the labeling of **45** with **16** to make compound **47**.

*5.4 Labeling and Identifying Amino Acid Binding on Peptide WWCNDGR with Nitrenium Ion **16***

Once the tryptophan adducts were isolated and identified, it was assumed that tryptophan in peptides would make the analogous adducts as well. A short peptide containing tryptophan was used to determine if similar adducts could form in a peptide. Photolysis of nitrenium ion **16** was carried out in the presence of peptide WWCNDGR. This peptide was used because it is the T9 trypsin digest fragment of lysozyme.[135] The m/z of the peptide and the labeled peptide can be seen in Figure 5.1.

NT—W—W—C—N—D—G—R

m/z 936.38

NT—W—**W***—C—N—D—G—R

m/z 1261.27

Figure 5.1. The expected m/z values of the peptide and the labeled peptide.

Since the labeled peptide has a unique dibrominated isotopic distribution, we are able to unambiguously identify the labeled peptide in the mass spectrum. After photolyzing the pyridinium ion, an isotopic distribution with m/z 1259.27, 1261.27, 1263.27 was seen. This corresponds to the peptide with one nitrenium ion bonded to it as can be seen in Figure 5.2.

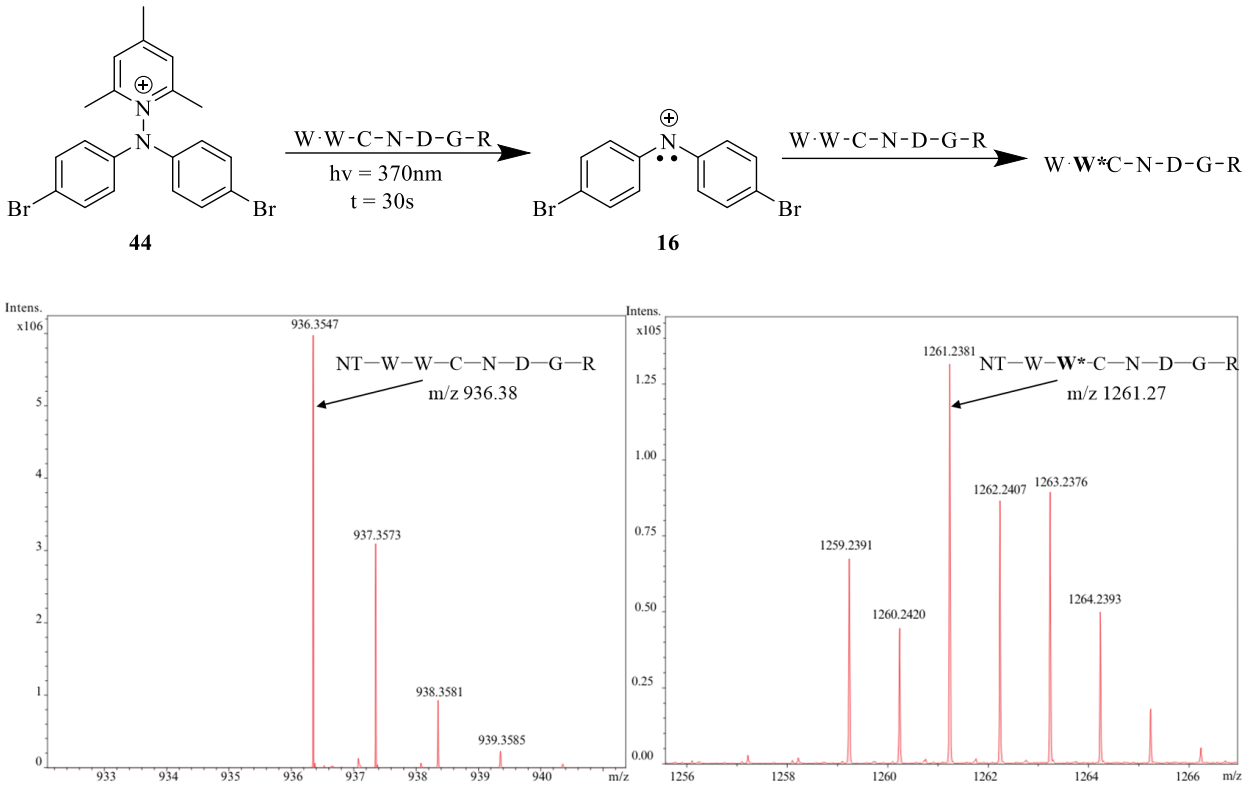

Figure 5.2. Labeling of peptide WWCNDGR. Reaction Scheme (Top), the ESI$^+$ mass spectra of the peptide (left), and of the labeled peptide (right). The labeled peptide shows the characteristic isotopic distribution of having two bromines alongside of the expected second isotopic distribution resulting from ^{13}C isotopes. A full comparison of the calculated mass spectra to measured mass spectra can be seen in Figure 6.33.

After the mass of the labeled peptide has been identified by mass spectrometry, the CID spectrum of the m/z 631.14 ion, which is the doubly charged labeled peptide ion, was obtained to determine which amino acid is labeled. We expect nitrenium ion **16** to label one of the two tryptophans. Figure 5.3 shows that unambiguously there is a labeled fragment from tryptophan. This can be seen by the isotopic distribution m/z 452.95, 454.95, 456.95. These three ions correspond to a labeled fragment from tryptophan which has two bromines on it. Since there are two tryptophans on the peptide, it is unsurprising that the unlabeled fragment from tryptophan with a m/z 130.07 can also be seen. These observations do not identify if the terminal

tryptophan, the interior tryptophan, or a mixture of both are labeled, but it does unambiguously show that tryptophan has been labeled by the nitrenium ion because of the dibrominated ion pattern.

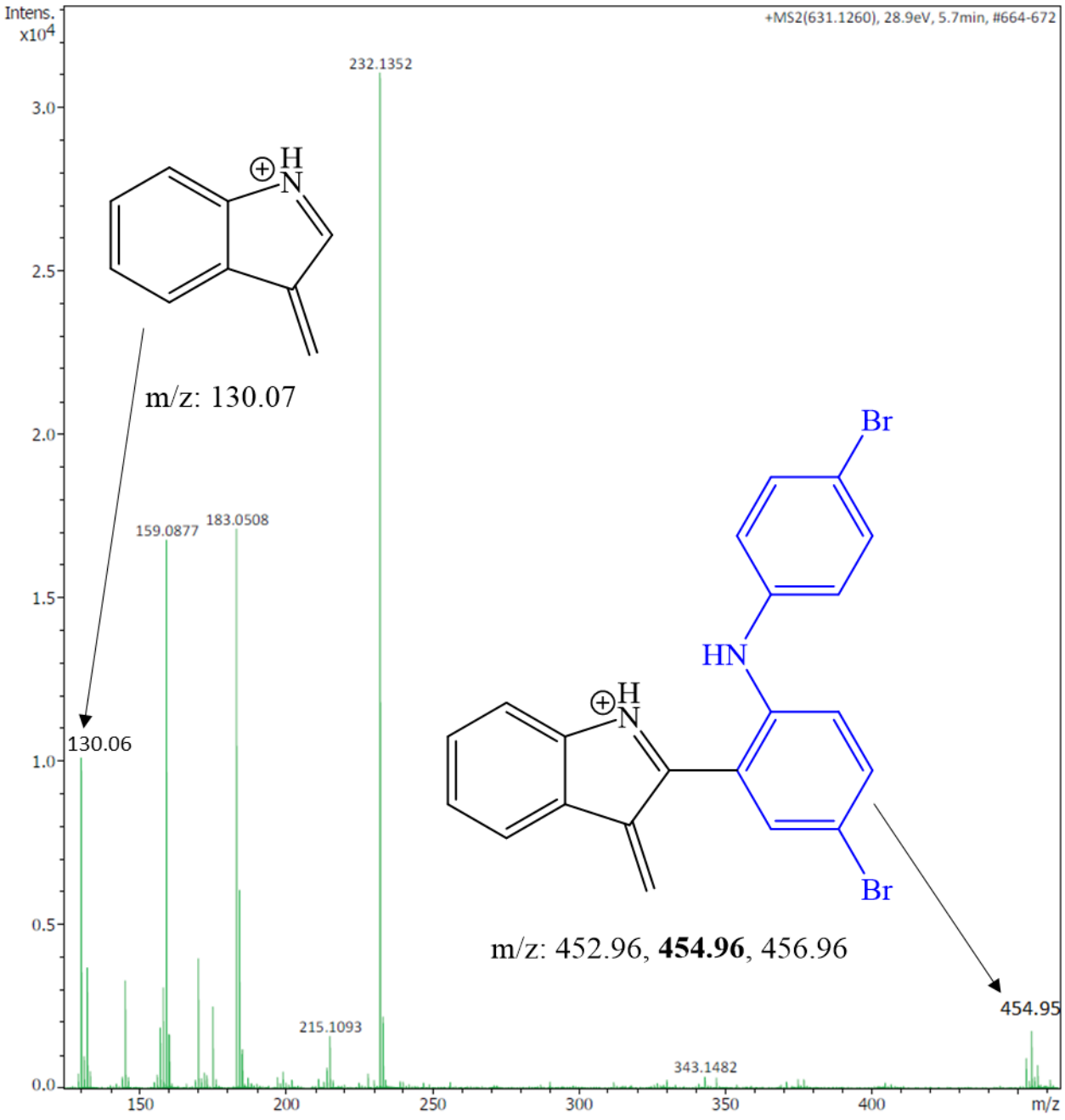

Figure 5.3. CID spectrum of the m/z 631.14 ion provides two tryptophan fragments. A labeled fragment from tryptophan (m/z 454.95) and an unlabeled fragment from tryptophan (m/z 130.07).

A summary of the tandem mass spectrometry data of the peptide and the labeled peptide are given in Figure 5.4. In Taylor's selective tryptophan labeling work, the last seven amino acids in their peptide sequence are the same as ours. The fragmentation pattern seen on these amino acids showed the y_6^+ and the y_5^+ fragments.[129] Figure 5.4 shows that we can further fragment our peptide to make the a_1^+, y_6^+, y_5^+, and y_2^+ fragments (See Figure 6.32).

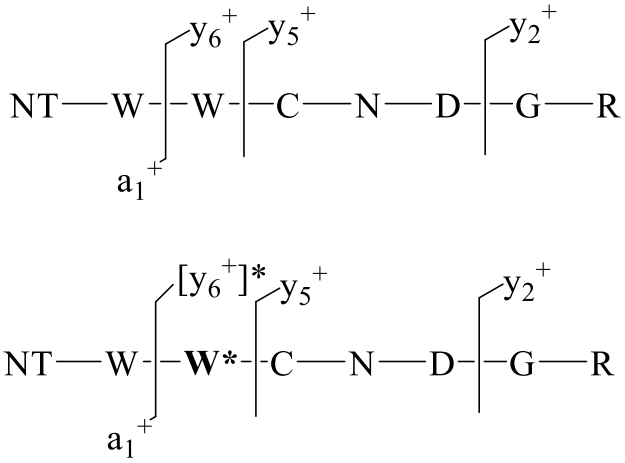

Figure 5.4. Summary of the peptide fragmentation in tandem mass spectrometry. The **W*** is the labeled tryptophan. The $[y_6^+]^*$ fragment is the labeled fragment. The a_1^+, y_5^+, and y_2^+ fragments can be seen in Figure 6.32.

The $[y_6^+]^*$ and the y_6^+ fragments can be seen in Figure 5.5. The isotopic bromine signature in the $[y_6^+]^*$ fragment confirms that the peptide fragment was labeled. The y_5^+ fragment corresponds to all of the amino acids in the peptide except for the two tryptophans on the N-terminus. Since, there is no evidence for labeling the y_5^+ or y_2^+ fragments, there is no detectable labeling of any amino acid except for tryptophan. Therefore, this photolabeling of tryptophan is selective in the peptide.

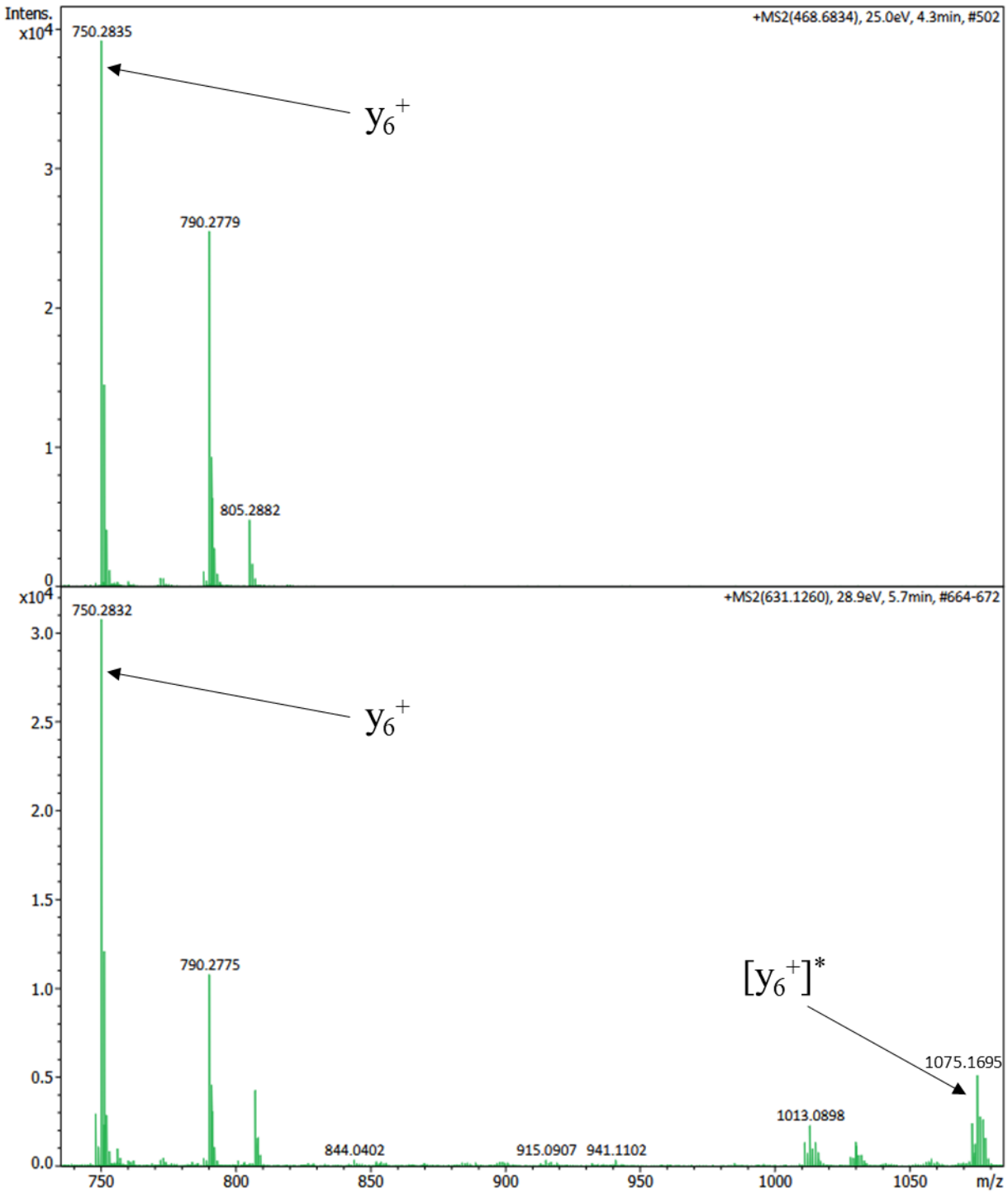

Figure 5.5. CID spectra of the peptide (top) and the labeled peptide (bottom). A comparison of the spectra show that the peptide is labeled on the y_6^+ fragment which contains tryptophan. Also, this labeling is only observed as a result of photolyzing pyridinium ion **44** in the presence of the peptide. The original y_6^+ fragment is (m/z 750.30). The labeled $[y_6^+]^*$ fragment is (m/z 1075.19).

The Taylor Group proposed that even when the pyridinium ion was excited instead of tryptophan, the mechanism still occurred via electron transfer from the tryptophan to the pyridinium ion followed by group transfer.[129] This brings up the question of whether our system's mechanism is the same. LFP of **44** generates transient absorption spectra of the nitrenium ion **16**. If a solution of both **44** and the peptide WWCNDGR is photolyzed and the labeling occurs via the electron transfer mechanism then no nitrenium ion intermediate will be observed. If it occurs through a nitrenium ion then the nitrenium ion signal will be quenched by the peptide WWCNDGR. A spectrum of nitrenium ion **16** in the presence of the peptide WWCNDGR shows that the nitrenium ion's spectrum is the same as is seen in literature (see Figure 5.6).[17] Therefore, we propose that the mechanism of tryptophan labeling proceeds through a nitrenium ion.

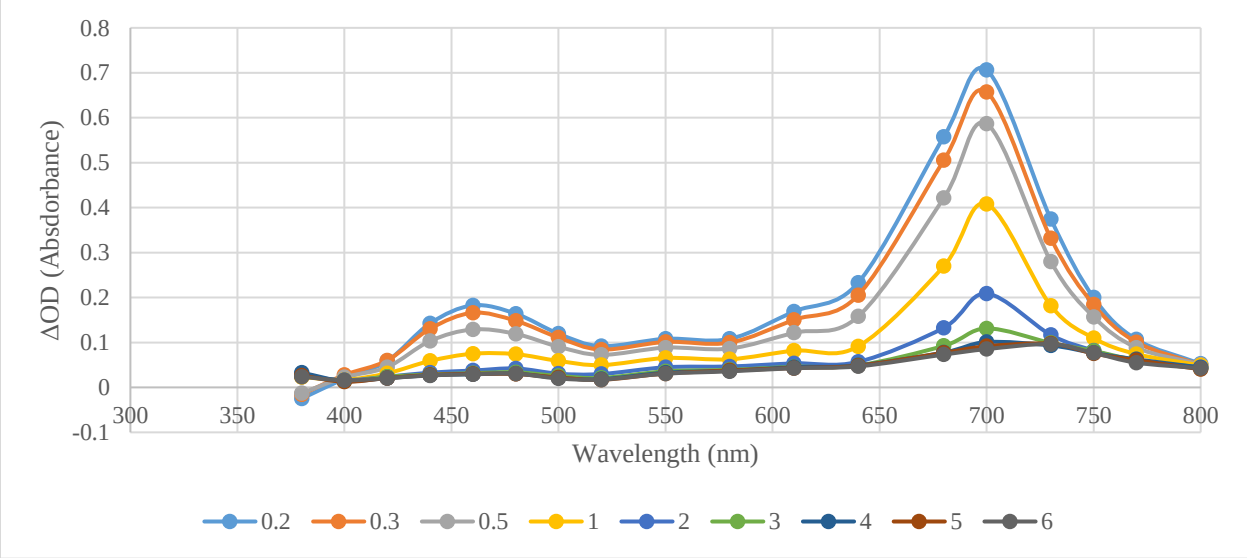

Figure 5.6. Transient Absorption Spectra of nitrenium ion **16** with peptide WWCNDGR concentration of 0.5mM. The spectra match the nitrenium ion spectra previously published.[17] Time slices are in μs.

There is no direct evidence that the terminal tryptophan is not labeled. Ideally the a_1^+ fragment would be paired with an $[a_1^+]^*$ fragment, but this fragment is not observed. Indirectly, the presence of the m/z = 750.30 ion in the labeled peptide CID MS data suggests that the terminal tryptophan labeled with a nitrenium ion has been cleaved off. However, this labeling of the terminal tryptophan is suggestive not definitive. Therefore, nitrenium ion **16** is able to selectively label tryptophan in the peptide WWCNDGR.

5.5 Conclusions and Future Work

Nitrenium ion **16** is able to make two major adducts with *N*-acetyl-L-tryptophan ethyl ester. We assume that tryptophan in a peptide will make the same adducts. We labeled the peptide WWCNDGR with nitrenium ion **16**, and see direct evidence of the labeled fragment from tryptophan and the interior tryptophan being labeled. This shows that nitrenium ions indeed can make sigma bonds with tryptophan in peptides, and these nitrenium ion-peptide/protein interactions must be considered for future nitrenium ion-DNA reactions on a cellular level.

The labeled tryptophan is unstable under 370 nm UV light, absorbing all the way to approximately 470 nm. A nitrenium ion with less conjugation should blue shift the absorption spectrum of the adducts which should minimize or even eliminate this issue. Therefore, new nitrenium ions should be used as labeling agents which have less conjugation than nitrenium ion **16**.

Now that it has been proven that peptides can be labeled with aryl nitrenium ions, the next step is to label a protein. The peptide WWCNDGR was chosen as a model peptide because it is a short trypsin digest fragment of the protein lysozyme with two tryptophans in it.[135] Therefore, a next step would be to label lysozyme with a nitrenium ion as well.

Chapter 6: Supporting Information

6.1 General Methods

6.1.1 General Chemicals and Analytical Methods

All chemicals and solvents were purchased from chemical suppliers and were used without further purification. ^{1}H NMR and ^{13}C NMR spectra were collected on either a Bruker 400 MHz instrument or a Bruker 600MHz instrument. Chemical shifts are reported in parts per million (ppm) and are referenced to the solvent signal. UV-Vis spectra were collected on a Shimadzu UV-1800 spectrometer using UVProbe 2.43 software. Samples were scanned using a fast scanning speed and a sampling interval of 1.0 nm. Each sample was blanked with the solvent of choice used in solvating the compound. Mass spectrometry experiments were performed on a JEOL AccuTOF-CS-ESI-TOF or with a Bruker Maxis-II QTOF, an ultra-high resolution Q-TOF mass spectrometer. Kinetic decay curves were fitted using MATLAB software.

6.1.1 Laser Flash Photolysis Setup

Laser Flash Photolysis experiments were conducted with a Nd:YAG Surelite II laser purchased from Continuum with 4-6 ns excitation pulses. The 3rd harmonic is used to produce a 355 nm laser pulse with 90-100 mJ pulse energy. The laser is spread across the width of the cuvette with a cylindrical lens to ensure even photolysis. A 350 W Xe arc lamp is used as the probe beam with a monochromator and PMT to amplify the detection signal. In this way a difference spectrum of the sample can be measured at any wavelength the monochromator is set to. The transient of each wavelength can be combined with a LabVIEW program to give the full spectra.

6.1.2 Full Spectral Analysis Flow System Setup

The solution is set up in a flow system. All glassware is sealed with rubber septums and parafilmed. Cannulas are used to connect the 100 mL RBF to a quartz cuvette, and the cuvette to a 100 mL graduated cylinder. A bleed needle is added to the graduated cylinder so that there is no buildup of pressure. The 100 mL RBF is connected to a N_2(g) tank via a needle. The solution is purged for 20 min with the N_2(g) bubbling the solution and an additional 10 min with the N_2(g) purging the air gap.

To flow the system the N_2(g) needle is moved to the 100 mL RBF air gap and the canula connecting the RBF to the cuvette is lowered into the solution of the 100 mL RBF. This causes the sample to be continually replenished so that there is no buildup of photoproducts. The full spectrum is measured with a 1 Hz laser pulse frequency with each data point being the average of 20 laser pulses.

6.1.3 Kinetic Trace Experimental Setup

All kinetic trace experiments are performed by making parent pyridinium ion solution in CH_3CN with an absorbance at 355 nm between 1 and 2 as a stock solution. 6 different concentrations of each trap were measured out by serial dilution to make 6 different final cuvettes with identical concentrations of parent pyridinium ion and equidistant concentrations of trap. Each cuvette is analyzed via LFP to obtain a pseudo 1^{st} order rate constant with MATLAB's curve fitter app. These 6 pseudo 1^{st} order rate constants are fitted to give a 2^{nd} order rate constant for each trap.

6.2 Chapter 2 Experimental

6.2.1 Synthesis

5-Nitroso-10,11-dihydro-dibenzo[b,f]azepine:[136]

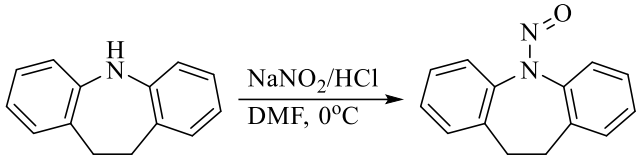

10,11-dihydro-5H-dibenzo[b,f]azepine (3.0006 g, 15.21 mmol) was placed in a 100 mL RBF and dissolved in 8 mL dimethylformamide and 1.3588 g (19.69 mmol) of $NaNO_2$. The solution was then cooled to 0°C. Upon cooling, 15.2 mL of 2M HCl was added dropwise while being stirring. The reaction mixture was stirred in ice bath for 30 minutes. Orange precipitate began to form as the reaction proceeded. The precipitate was collected by vacuum filtration to yield 3.3300 g (97.6%) of pure orange-yellow powder of 5-nitroso-10,11-dihydro-dibenzo[b,f]azepine.

^{1}H NMR: (600 MHz, CD_3OD) δ = 7.64-7.60 (m, 1H), 7.30-7.45 (m, 6H), 7.06 (d, 1H), 2.78-3.14 (m, 4H)

5-Amino-10,11-dihydrodibenzo[b,f]azepine:[17]

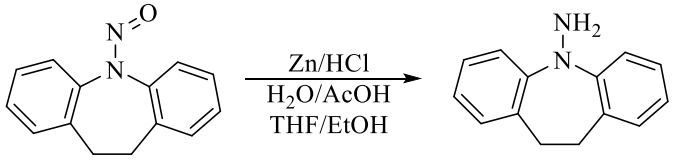

5-nitroso-10,11-dihydro-dibenzo[b,f]azepine was reduced to a hydrazine using zinc dust. In a 100 mL RBF, 9.0 mL H_2O, 9.0 mL glacial acetic acid, 4.5 mL ethanol, 10.3 mL THF and 1.46 mL HCl were cooled in an ice bath for 10 minutes. 2.9496 g (45.11 mmol) of zinc dust was added to the solution. After stirring for 5 min, 1.0055 g (4.524 mmol) of nitrosamine was added to the suspension. The suspension was at first stirred in ice bath for 20 minutes and then at room

temperature for another 10 minutes. Excess zinc was filtered off and the filtrate was neutralized using $NaHCO_3$. The filtrate was extracted two times with diethyl ether. The combined organic extract was washed with H_2O and dried over $MgSO_4$. The solvent was removed under reduced pressure. The resulting crude solid was used as it is and it gave a yield of 0.6501 g (68%) of 5-Amino-10,11-dihydrodibenz[b,f]azepine.

^{1}H NMR: (600 MHz, CD_3OD) δ = 7.38 (dd, 2H), 7.15 (dt, 2H), 7.07 (dd, 2H), 6.89 (dt, 2H), 3.14 (s, 4H)

2,4,6-Trimethylpyrylium tetrafluoroborate:[137]

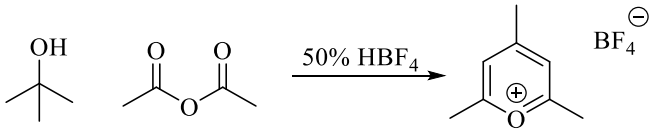

In a 250 mL round bottom flask equipped with a stir bar was added 4 mL of *t*-butyl alcohol and 50 mL of acetic anhydride. 6 mL of 50% tetrafluoroboric acid was added dropwise at such a rate that the final temperature reached 100°C. The reaction mixture was then cooled to 5°C and precipitate began to form. 100 mL of diethyl ether was added to complete precipitation. The precipitate was vacuum filtered and washed with diethyl ether to yield 2.5635 g (42%) of pyrylium salt.

^{1}H NMR: (400 MHz, CD_3OD) δ = 7.88 (s, 2H), 2.87 (m, 6H), 2.70 (m, 3H)

ESI MS$^+$: 123.06

1-(10,11-Dihydro-dibenzo[b,f]azepin-5-yl)-2,4,6-trimethylpyridin-1-ium (3):[17]

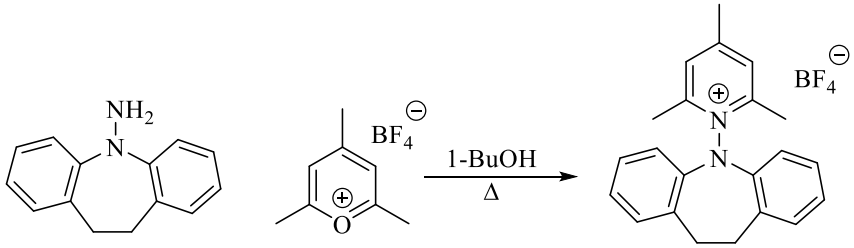

5-Amino-10,11-dihydrodibenz[b,f]azepine (0.6501 g, 3.09 mmol) was suspended in 15 ml of 1-butanol. Freshly prepared 2,4,6-trimethylpyrylium tetrafluroborate 0.1523 g (1.24 mmol) was added to the solution. The color of the reaction mixture changed from dark red to reddish brown. The mixture was heated at reflux for an hour at 70°C and then cooled to room temperature. Green precipitate began to form upon addition of 80mL of diethyl ether. The precipitate was collected and washed with diethyl ether to yield 0.2522 g (50.7%) of pure 1-(10,11-dihydro-dibenzo[b,f]azepin-5-yl)-2,4,6-trimethylpyridin-1-ium.

^{1}H NMR: (600 MHz, CD_3OD) δ = 8.10 (s, 2H), 7.38 (dd, 2H), 7.17 (dt, 2H), 7.09 (t, 2H), 5.89 (d, 2H), 3.25 (s, 4H), 2.79 (s, 3H), 2.55 (s, 6H)

^{13}C NMR: (600 MHz, CD_3OD) δ = 162.48, 157.76, 139.47, 131.24, 130.78, 130.09, 127.55, 122.77, 113.90, 36.12, 20.51, 17.33

ESI MS^{+}: 315.19

2-Chloro-10,11-dihydro-5H-dibenzo[b,f]azepine (5):

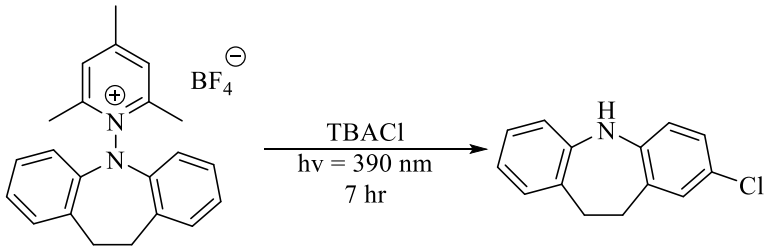

0.1091 g (0.271 mmol) of 1-(10,11-dihydro-dibenzo[b,f]azepin-5-yl)-2,4,6-trimethylpyridin-1-ium **3** is dissolved in CH_3CN with 0.7549 g (2.712 mmol) of TBACl. The solution was irratiated with 390 nm Kessel lamps for 7 hours. The resulting solution was purified twice by column chromatography to result in light-yellow crystals of 2-chloro-10,11-dihydro-dibenzo[b,f]azepine.

^{1}H NMR: (600 MHz, CH_3OD) δ = 7.01 (m, 4H), 6.86 (dt, 2H), 6.71 (dt, 1H), 3.01 (m, 4H)

^{13}C NMR: (600 MHz, CH_3OD) δ = 141.97, 141.46, 129.96, 129.68, 129.29, 127.98, 126.36, 125.88, 122.26, 118.94, 118.72, 117.46, 34.10, 33.93

ESI MS$^+$: 230.11, 232.10

6.2.2 Transient Absorption Spectra

Generation of 10,11-dihydro-dibenzo[b,f]azepinyl cation radical in CH_3CN (2b)

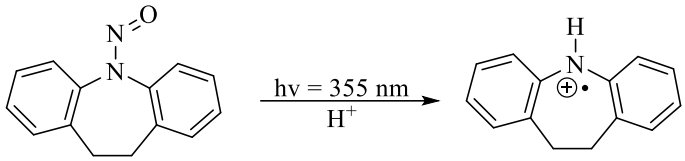

5-Nitroso-10,11-dihydro-dibenzo[b,f]azepine is dissolved in CH_3CN in pH = 2.08 phosphate buffer. The solution was purged with N_2(g) and was analyzed with LFP using a 355 nm laser pulse, resulting in the generation of the cation radical of 10,11-dihydro-5H-dibenzo[b,f]azepine **2b**.

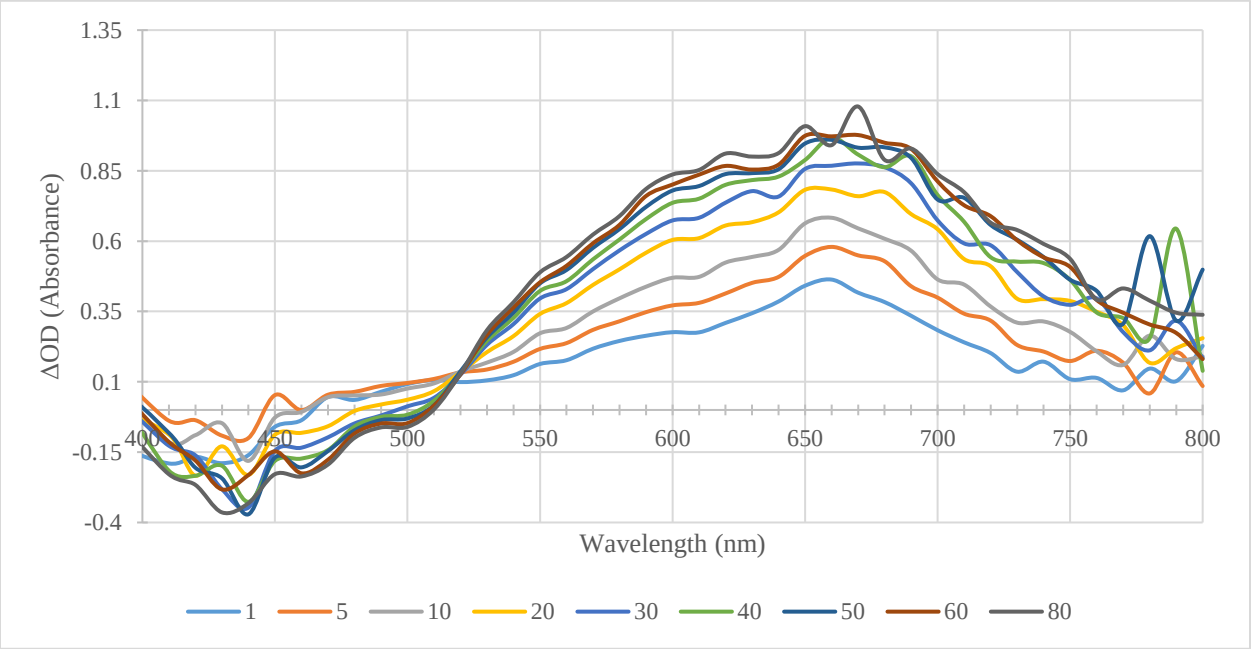

Figure 6.1. Generation of 10,11-dihydro-dibenzo[b,f]azepinyl cation radical **2b** in CH_3CN.

Generation of 10,11-dihydro-dibenzo[b,f]azepinyl radical (2c) in CH_3CN

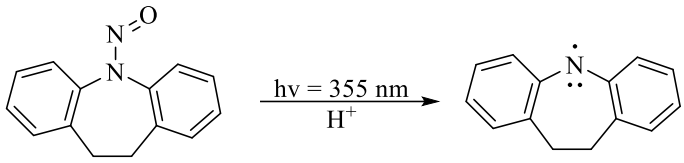

5-Nitroso-10,11-dihydro-dibenzo[b,f]azepine is dissolved in CH_3CN. The solution was purged with N_2(g) and was analyzed with LFP using a 355 nm laser, resulting in the generation of the radical of 10,11-dihydro-5H-dibenzo[b,f]azepine **2c**.

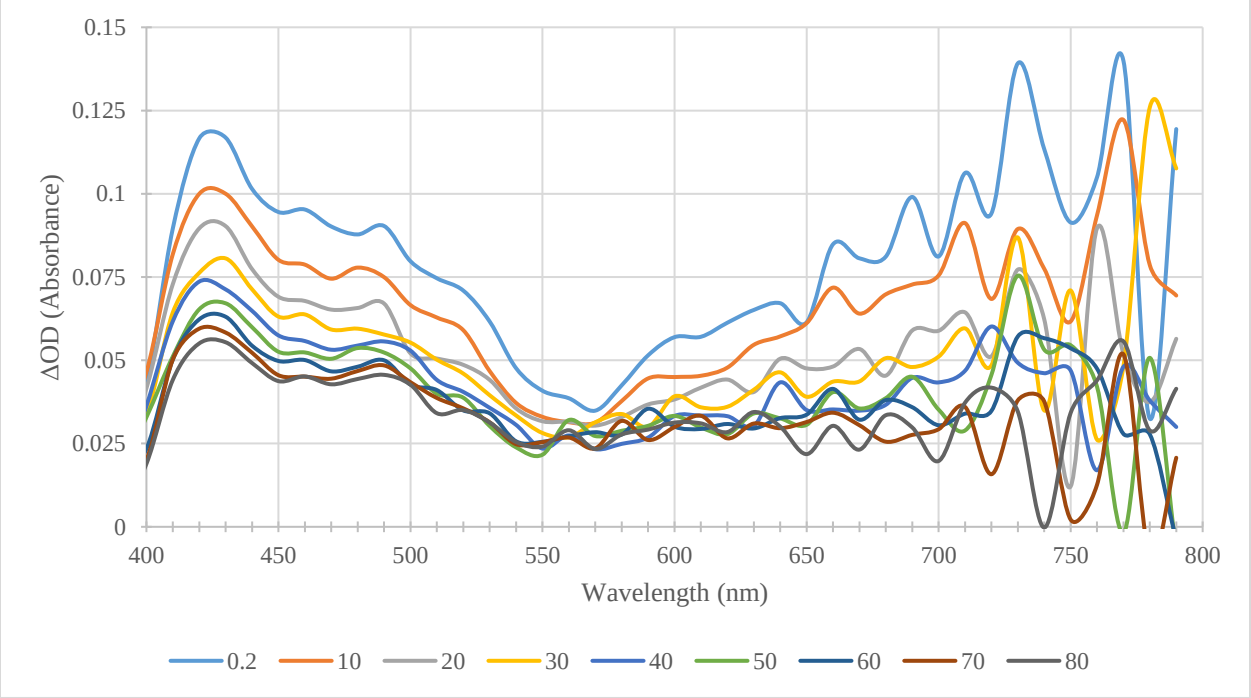

Figure 6.2. Generation of 10,11-dihydro-dibenzo[b,f]azepinyl radical **2c** in CH_3CN.

6.2.3 Kinetic Data from LFP

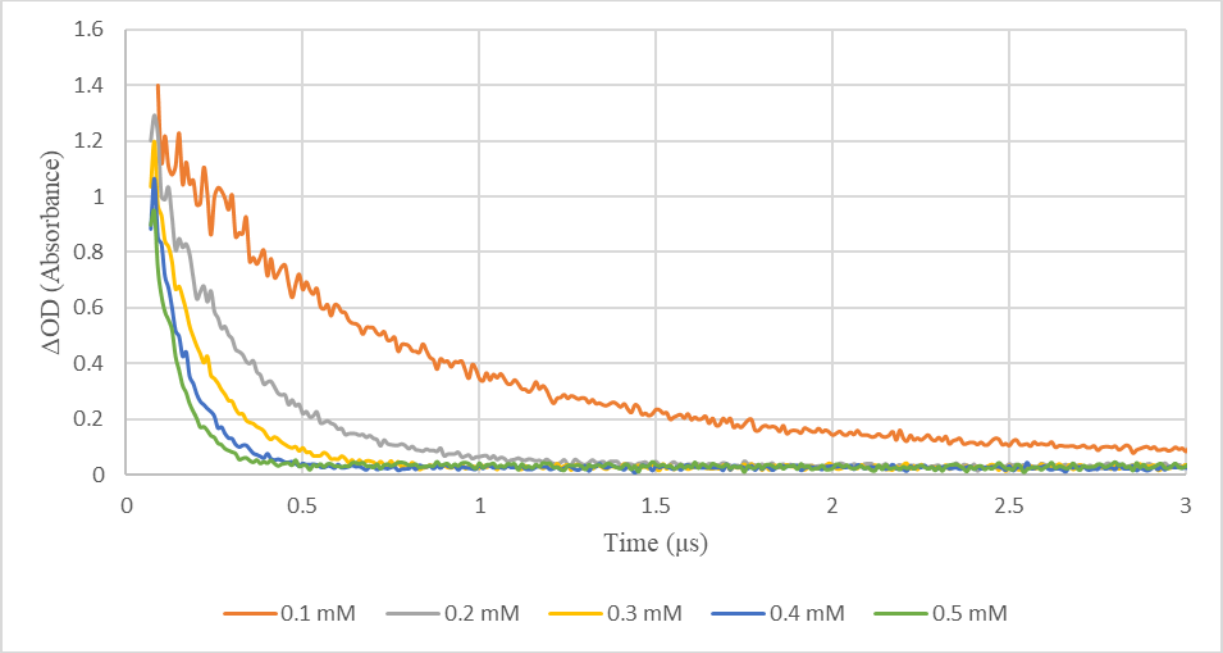

Figure 6.3. Kinetic Trace of TBACl with 10,11-dihydro-dibenzo[b,f]azepinyl nitrenium ion **2**.

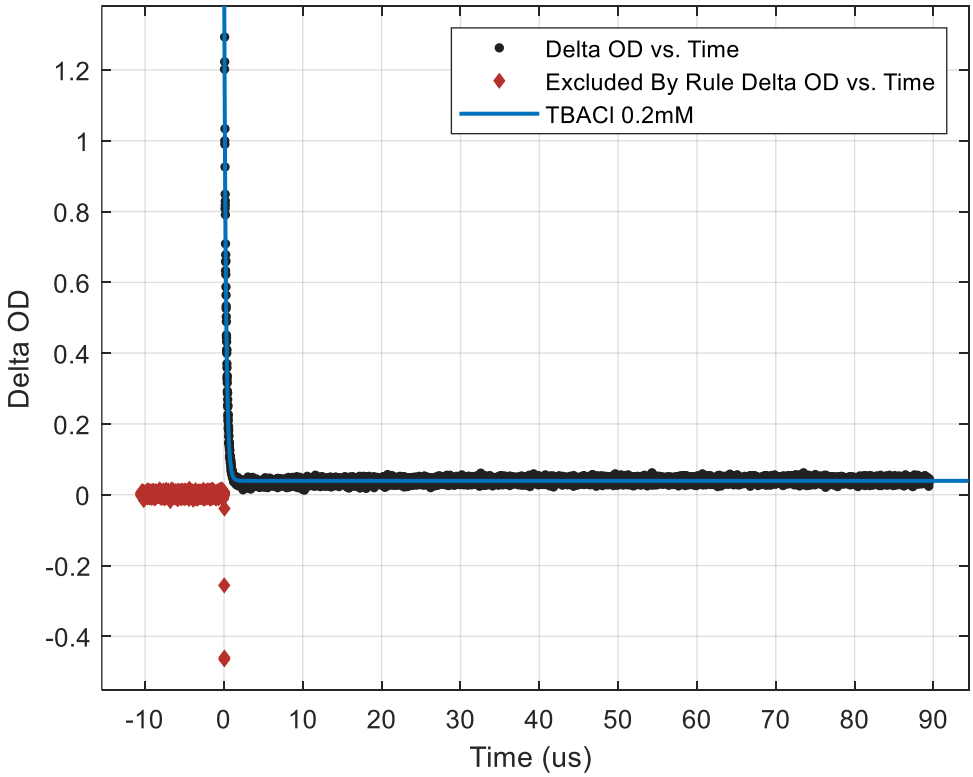

Figure 6.4. Matlab Fitting of TBACl with 10,11-dihydro-dibenzo[b,f]azepinyl nitrenium ion **2**.

Fit Name: TBACl 0.2mM

Custom Curve Fit
f(x) = a*exp(-b*x)+c

Coefficients and 95% Confidence Bounds

	Value	Lower	Upper
a	1.5769	1.5677	1.5862
b	4.2237	4.1969	4.2505
c	0.0392	0.0391	0.0393

Goodness of Fit

	Value
SSE	0.397
R-square	0.9771
DFE	8940
Adj R-sq	0.977
RMSE	0.0067

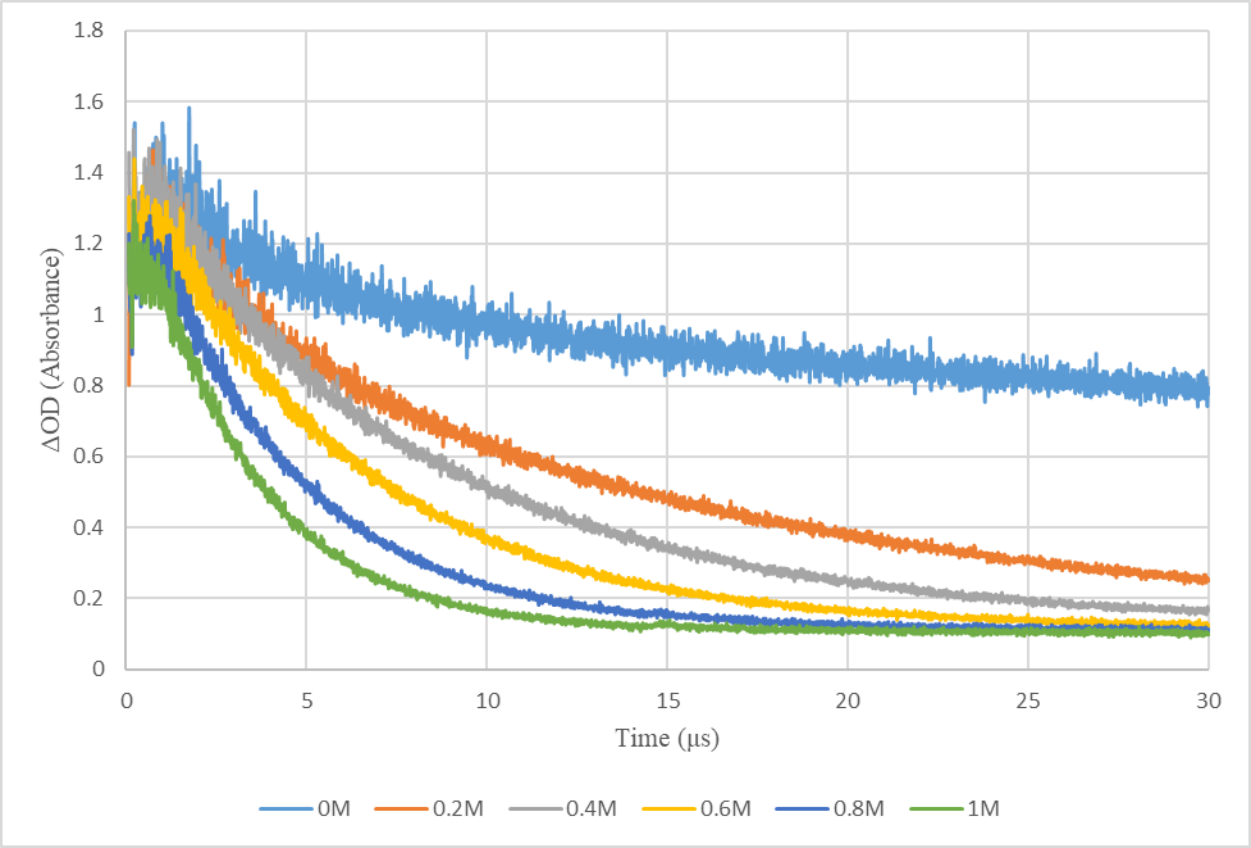

Figure 6.5. Kinetic Trace of CHD with 10,11-dihydro-dibenzo[b,f]azepinyl nitrenium ion **2**.

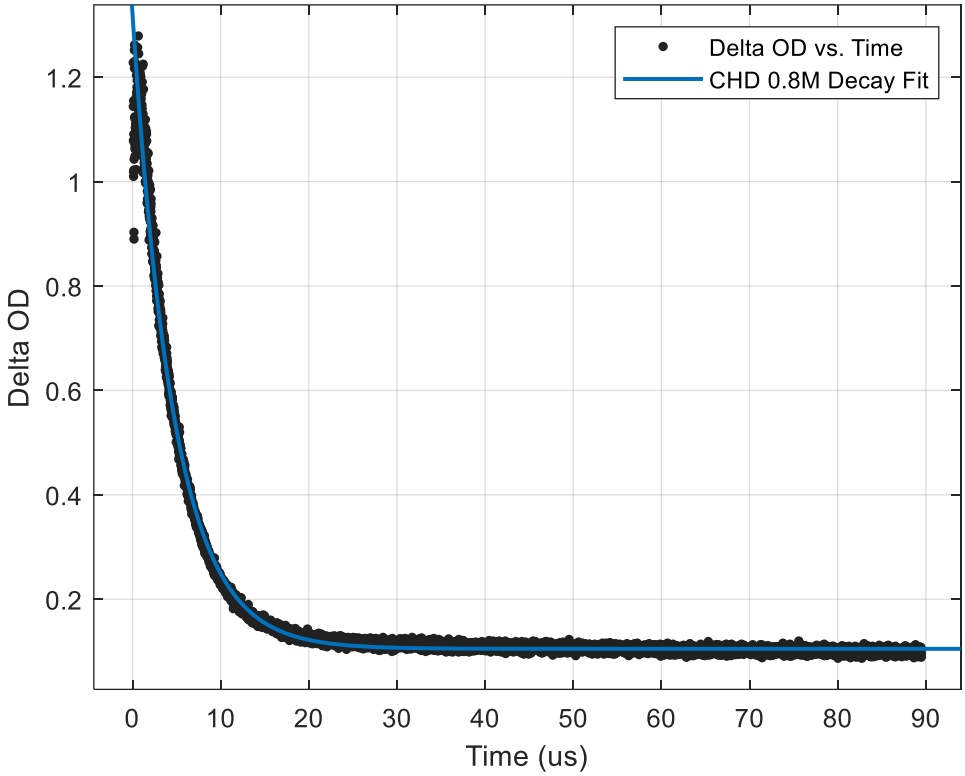

Figure 6.6. Matlab Fitting of CHD with 10,11-dihydro-dibenzo[b,f]azepinyl nitrenium ion **2**.

Fit Name: CHD 0.8M

Custom Curve Fit
f(x) = a*exp(-b*x)+c

Coefficients and 95% Confidence Bounds
Value Lower Upper

	Value	Lower	Upper
a	1.2161	1.213	1.2191
b	0.2133	0.2125	0.2141
c	0.1051	0.1047	0.1055

Goodness of Fit

	Value
SSE	2.3644
R-square	0.9922
DFE	8939
Adj R-sq	0.9922
RMSE	0.0163

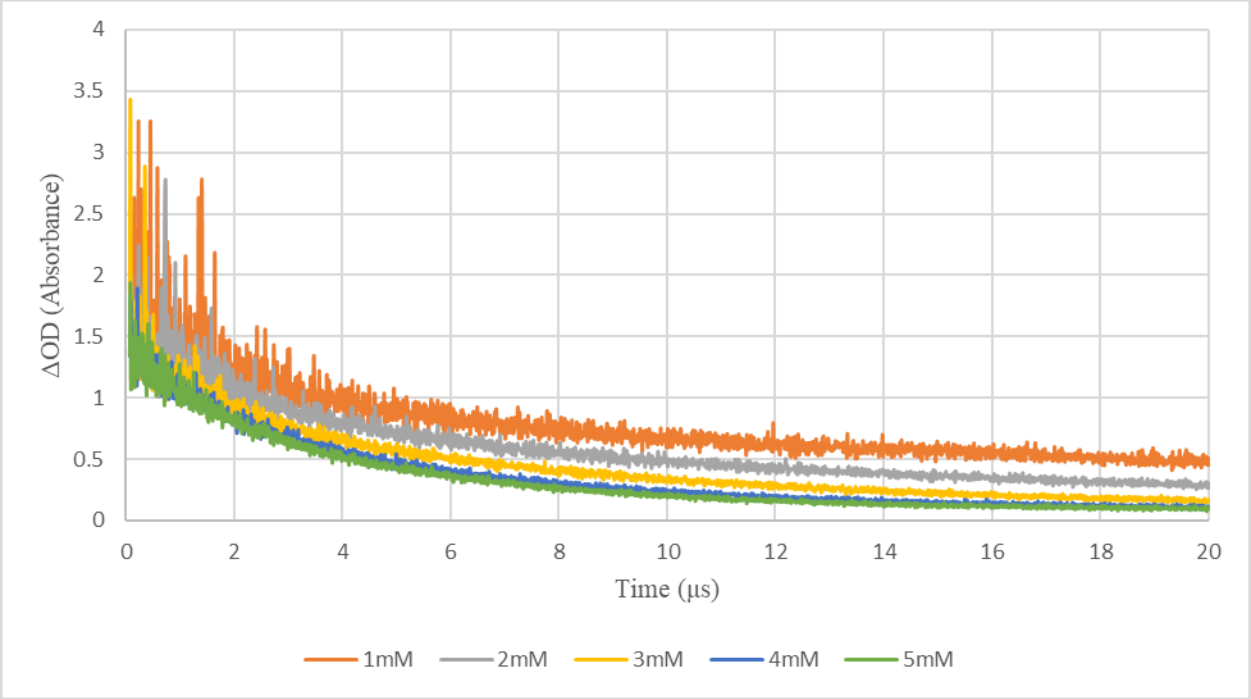

Figure 6.7. Kinetic Trace of H_2O with 10,11-dihydro-dibenzo[b,f]azepinyl nitrenium ion **2**.

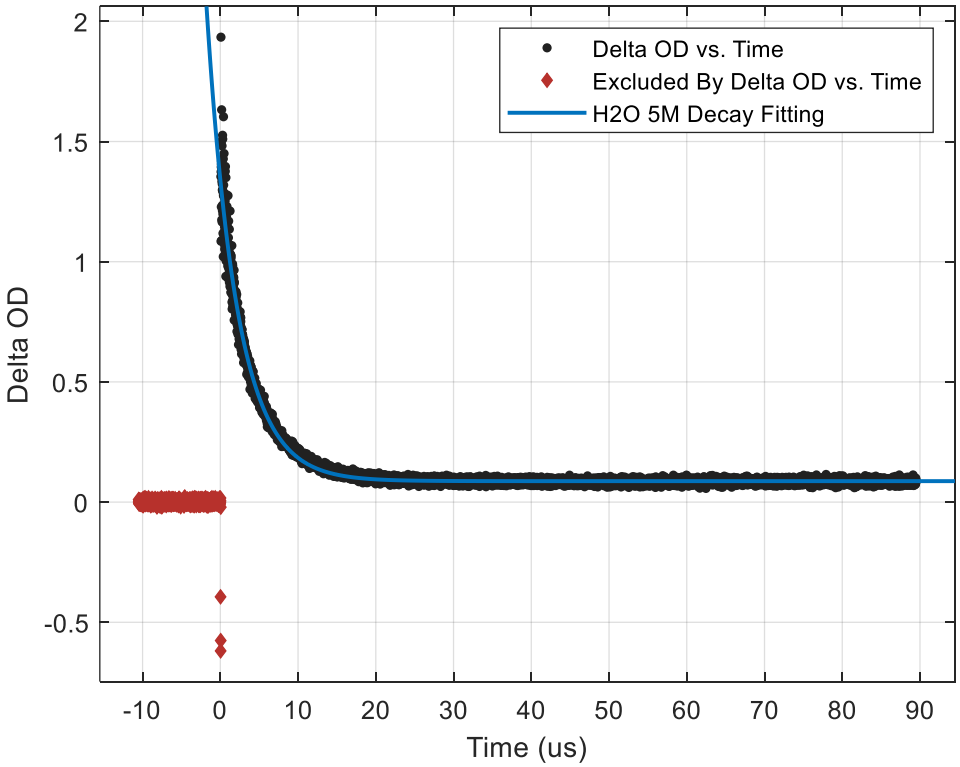

Figure 6.8. Matlab Fitting of H_2O with 10,11-dihydro-dibenzo[b,f]azepinyl nitrenium ion **2**.

Fit Name: H_2O 4M

Custom Curve Fit
f(x) = a*exp(-b*x)+c

Coefficients and 95% Confidence Bounds

	Value	Lower	Upper
a	1.2537	1.2496	1.2578
b	0.2559	0.2546	0.2571
c	0.0872	0.0867	0.0877

Goodness of Fit

	Value
SSE	3.5266
R-square	0.9872
DFE	8940
Adj R-sq	0.9872
RMSE	0.0199

6.2.4 Cartesian Coordinates & Energies

10,11-dihydro-dibenzo[b,f]azepinyl radical (2c)

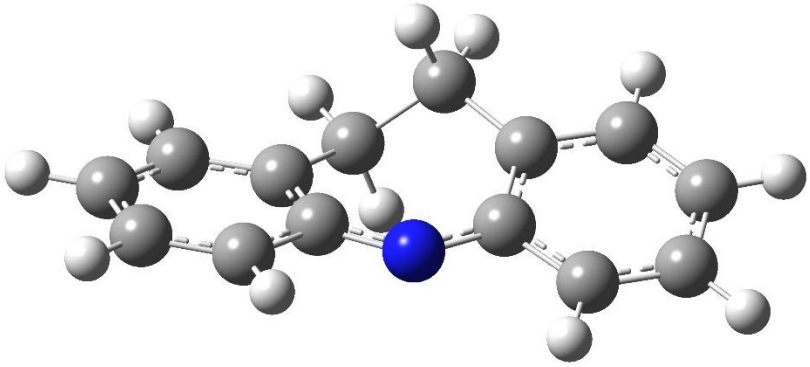

Standard orientation:

Center Number	Atomic Number	Atomic Type	Coordinates (Angstroms) X	Y	Z
1	6	0	-1.602392	-0.726240	0.243842
2	6	0	-1.236391	0.637299	0.000738
3	6	0	-2.952250	-1.067828	0.237592
4	6	0	-2.287815	1.575068	-0.216398
5	6	0	-3.617567	1.203776	-0.228875

6	6	0	-3.959176	-0.131396	0.000913
7	1	0	-3.226793	-2.102914	0.421886
8	1	0	-1.987274	2.603852	-0.376657
9	1	0	-4.389111	1.945434	-0.408403
10	1	0	-4.998717	-0.442447	0.000860
11	6	0	2.952249	-1.067828	-0.237596
12	6	0	3.959176	-0.131396	-0.000920
13	6	0	3.617568	1.203776	0.228871
14	6	0	2.287816	1.575068	0.216399
15	6	0	1.236390	0.637298	-0.000734
16	6	0	1.602392	-0.726240	-0.243840
17	1	0	3.226792	-2.102913	-0.421891
18	1	0	4.998718	-0.442447	-0.000870
19	1	0	4.389113	1.945434	0.408398
20	1	0	1.987275	2.603851	0.376661
21	7	0	0.000000	1.206619	0.000004
22	6	0	-0.572434	-1.790104	0.512981
23	1	0	-0.149590	-1.664677	1.518089
24	1	0	-1.066506	-2.765855	0.510499
25	6	0	0.572434	-1.790106	-0.512976
26	1	0	0.149590	-1.664682	-1.518085
27	1	0	1.066505	-2.765856	-0.510492

Sum of electronic and zero-point Energies= -595.344457
Sum of electronic and thermal Energies= -595.333535
Sum of electronic and thermal Enthalpies= -595.332591
Sum of electronic and thermal Free Energies= -595.381964

10,11-dihydro-dibenzo[b,f]azepinyl cation radical (2b)

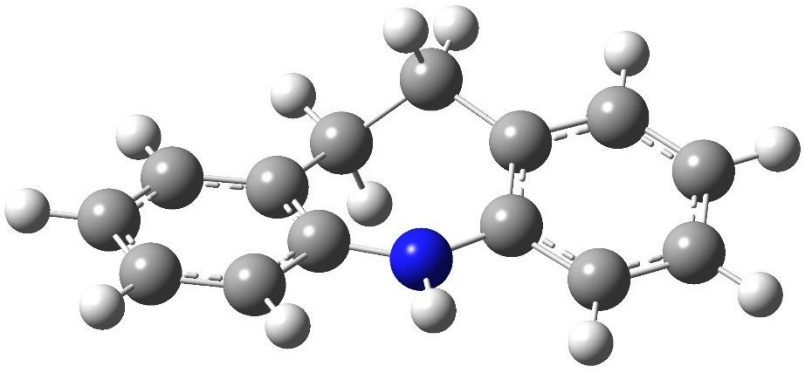

Standard orientation:

Center Number	Atomic Number	Atomic Type	Coordinates (Angstroms) X	Y	Z
1	6	0	-0.108531	1.629087	-0.755522

2	6	0	0.095109	1.280786	0.608520
3	6	0	0.000000	2.974817	-1.089488
4	6	0	0.371147	2.287303	1.571622
5	6	0	0.469796	3.609490	1.201558
6	6	0	0.285944	3.959295	-0.141652
7	1	0	-0.150643	3.266035	-2.123212
8	1	0	0.519106	2.003690	2.609791
9	1	0	0.688612	4.367403	1.943943
10	1	0	0.360800	4.995950	-0.449071
11	6	0	0.000000	-2.974817	-1.089488
12	6	0	-0.285944	-3.959295	-0.141652
13	6	0	-0.469796	-3.609490	1.201558
14	6	0	-0.371147	-2.287303	1.571622
15	6	0	-0.095109	-1.280786	0.608520
16	6	0	0.108531	-1.629087	-0.755522
17	1	0	0.150643	-3.266035	-2.123212
18	1	0	-0.360800	-4.995950	-0.449071
19	1	0	-0.688612	-4.367403	1.943943
20	1	0	-0.519106	-2.003690	2.609791
21	6	0	-0.458812	0.616494	-1.811087
22	1	0	-1.502307	0.298591	-1.691769
23	1	0	-0.405923	1.103394	-2.786479
24	6	0	0.458812	-0.616494	-1.811087
25	1	0	1.502307	-0.298591	-1.691769
26	1	0	0.405923	-1.103394	-2.786479
27	7	0	0.000000	0.000000	1.121453
28	1	0	0.000000	0.000000	2.136016

Sum of electronic and zero-point Energies= -595.721347
Sum of electronic and thermal Energies= -595.710271
Sum of electronic and thermal Enthalpies= -595.709327
Sum of electronic and thermal Free Energies= -595.758249

Singlet State of 10,11-dihydro-dibenzo[b,f]azepinyl nitrenium ion (^{1}2)

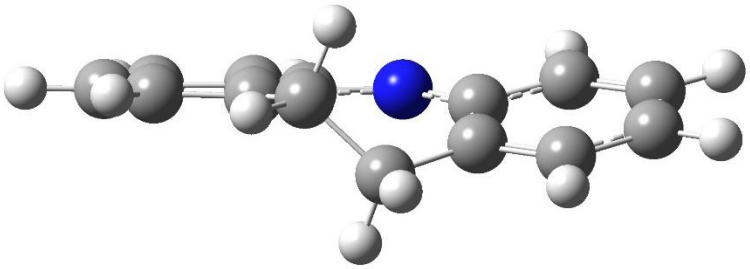

Standard orientation:

Center Number	Atomic Number	Atomic Type	Coordinates (Angstroms) X	Y	Z

1	6	0	1.603637	-0.761699	-0.218255
2	6	0	1.227008	0.615120	0.008644
3	6	0	2.953538	-1.066337	-0.226303
4	6	0	2.256728	1.598173	0.201716
5	6	0	3.586564	1.250545	0.221268
6	6	0	3.932597	-0.088638	0.001689
7	1	0	3.266135	-2.088944	-0.407353
8	1	0	1.930385	2.620873	0.344500
9	1	0	4.353849	1.996931	0.386866
10	1	0	4.977679	-0.380056	-0.000636
11	6	0	-2.953538	-1.066337	0.226302
12	6	0	-3.932597	-0.088638	-0.001689
13	6	0	-3.586564	1.250546	-0.221266
14	6	0	-2.256728	1.598173	-0.201715
15	6	0	-1.227008	0.615120	-0.008643
16	6	0	-1.603637	-0.761700	0.218254
17	1	0	-3.266135	-2.088945	0.407351
18	1	0	-4.977679	-0.380056	0.000636
19	1	0	-4.353849	1.996931	-0.386864
20	1	0	-1.930385	2.620873	-0.344497
21	7	0	0.000000	1.152030	0.000000
22	6	0	0.583164	-1.826635	-0.497358
23	1	0	0.200492	-1.702834	-1.520040
24	1	0	1.074656	-2.801250	-0.480043
25	6	0	-0.583164	-1.826636	0.497356
26	1	0	-0.200492	-1.702836	1.520039
27	1	0	-1.074656	-2.801251	0.480040

Sum of electronic and zero-point Energies= -595.096562
Sum of electronic and thermal Energies= -595.085638
Sum of electronic and thermal Enthalpies= -595.084694
Sum of electronic and thermal Free Energies= -595.133458

Triplet State of 10,11-dihydro-dibenzo[b,f]azepinyl nitrenium ion (^{3}2)

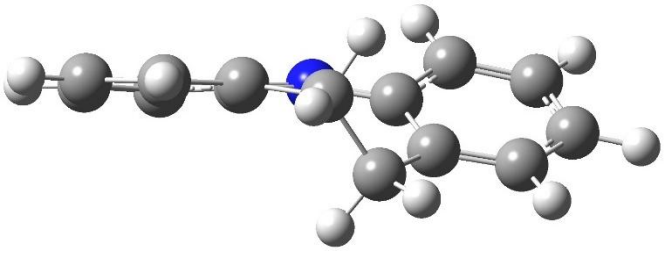

Standard orientation:

Center Number	Atomic Number	Atomic Type	Coordinates (Angstroms) X	Y	Z

1	6	0	-0.364708	1.612532	-0.711924
2	6	0	0.033965	1.256832	0.634481
3	6	0	-0.356435	2.955321	-1.040482
4	6	0	0.472229	2.265278	1.551792
5	6	0	0.427778	3.587335	1.183627
6	6	0	0.000000	3.941065	-0.109118
7	1	0	-0.612848	3.250897	-2.052384
8	1	0	0.782610	1.958402	2.542845
9	1	0	0.720352	4.356791	1.888074
10	1	0	-0.031084	4.985002	-0.398932
11	6	0	0.356435	-2.955321	-1.040482
12	6	0	0.000000	-3.941065	-0.109118
13	6	0	-0.427778	-3.587335	1.183627
14	6	0	-0.472229	-2.265278	1.551792
15	6	0	-0.033965	-1.256832	0.634481
16	6	0	0.364708	-1.612532	-0.711924
17	1	0	0.612848	-3.250897	-2.052384
18	1	0	0.031084	-4.985002	-0.398932
19	1	0	-0.720352	-4.356791	1.888074
20	1	0	-0.782610	-1.958402	2.542845
21	7	0	0.000000	0.000000	1.045784
22	6	0	-0.575243	0.528059	-1.732853
23	1	0	-1.533039	0.020047	-1.571838
24	1	0	-0.636946	0.986234	-2.721149
25	6	0	0.575243	-0.528059	-1.732853
26	1	0	1.533039	-0.020047	-1.571838
27	1	0	0.636946	-0.986234	-2.721149

Sum of electronic and zero-point Energies= -595.066807
Sum of electronic and thermal Energies= -595.055607
Sum of electronic and thermal Enthalpies= -595.054663
Sum of electronic and thermal Free Energies= -595.104243

6.2.5 Calculated UV-VIS Spectra and Oscillator Strength

Singlet State of 10,11-dihydro-dibenzo[b,f]azepinyl nitrenium ion (^{1}2)

Table 6.1. Calculated UV-Vis bands and oscillator strengths for 10,11-dihydro-dibenzo[b,f]azepinyl singlet nitrenium ion ^{1}**2**

State	Energy (eV)	Excitation Wavelength (nm)	Oscillator Strength
S1	2.0050	618.38	0.0384
S2	2.3287	532.42	0.0006
S3	2.4825	499.43	0.0225
S4	3.2256	384.37	0.6305
S5	4.2351	292.76	0.0000
S6	4.3535	284.79	0.0043
S7	4.6650	265.78	0.0030
S8	5.0076	247.59	0.0000
S9	5.0216	246.90	0.0161
S10	5.0645	244.81	0.0046
S11	5.4021	229.51	0.0045
S12	5.4856	226.02	0.0016

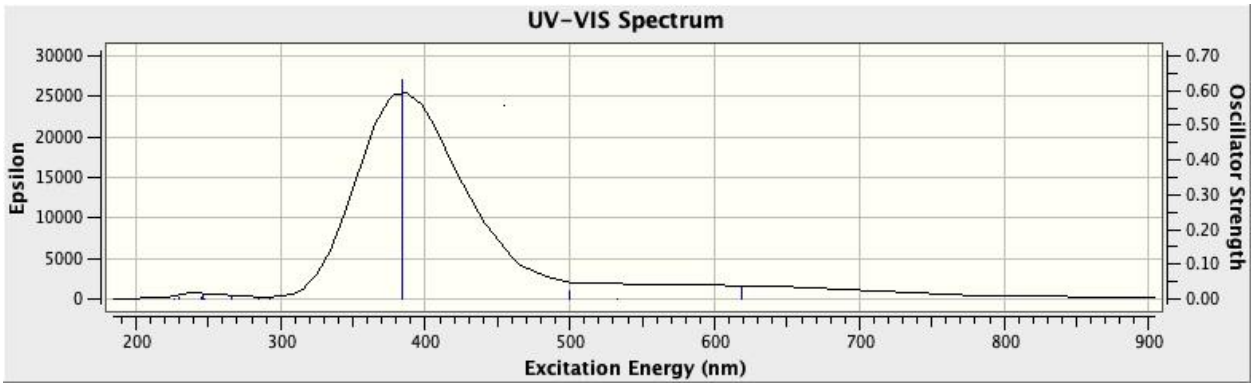

Figure 6.9. 10,11-dihydro-dibenzo[b,f]azepinyl singlet nitrenium ion ^{1}**2** UV-VIS calculated spectrum

Triplet State of 10,11-dihydro-dibenzo[b,f]azepinyl nitrenium ion (^{3}2)

Table 6.2. Calculated UV-Vis bands and oscillator strengths for 10,11-dihydro-dibenzo[b,f]azepinyl triplet nitrenium ion ^{3}**2**

State	Energy (eV)	Excitation Wavelength (nm)	Oscillator Strength
T1	1.2929	958.99	0.0016
T2	1.3372	927.18	0.0001
T3	1.7152	722.86	0.0010
T4	2.3910	518.55	0.0017
T5	2.4790	500.14	0.0044
T6	2.8210	439.51	0.0709
T7	2.9024	427.18	0.0608
T8	3.6429	340.35	0.0048
T9	3.6996	335.13	0.0000
T10	3.8022	326.08	0.0000
T11	3.9307	315.43	0.4246
T12	4.1005	302.36	0.0002

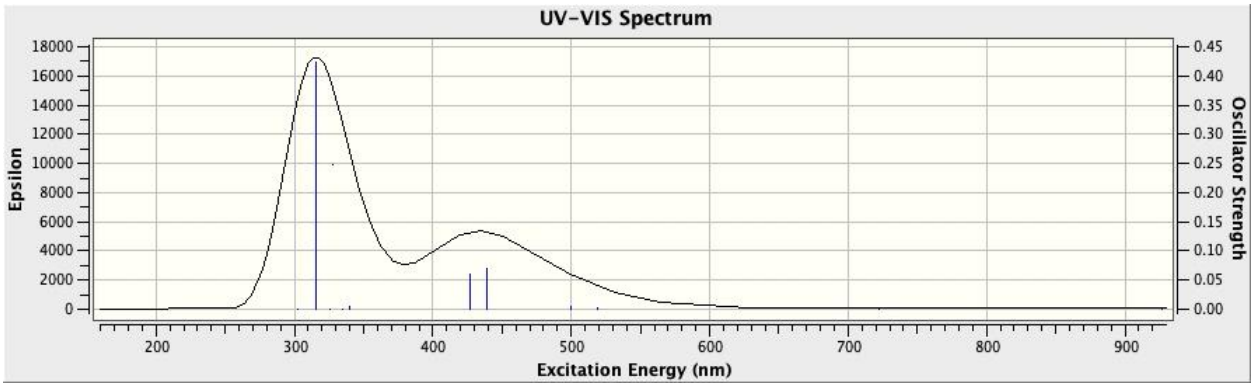

Figure 6.10. 10,11-dihydro-dibenzo[b,f]azepinyl triplet nitrenium ion ^{3}**2** UV-VIS calculated spectrum

Radical of 10,11-dihydro-dibenzo[b,f]azepinyl nitrenium ion (2c)

Table 6.3. Calculated UV-Vis bands and oscillator strengths for 10,11-dihydro-dibenzo[b,f]azepinyl Radical **2c**

State	Energy (eV)	Excitation Wavelength (nm)	Oscillator Strength
1	1.7066	726.52	0.0171
2	2.6129	474.51	0.0105
3	2.7297	454.21	0.0066
4	2.7908	444.27	0.0515
5	3.8082	325.57	0.0107
6	3.8418	322.73	0.3388
7	3.9709	312.23	0.0128
8	4.0090	309.26	0.1527
9	4.2394	292.46	0.0010
10	4.3700	283.72	0.0218
11	4.7526	260.88	0.0002
12	4.8793	254.10	0.0000

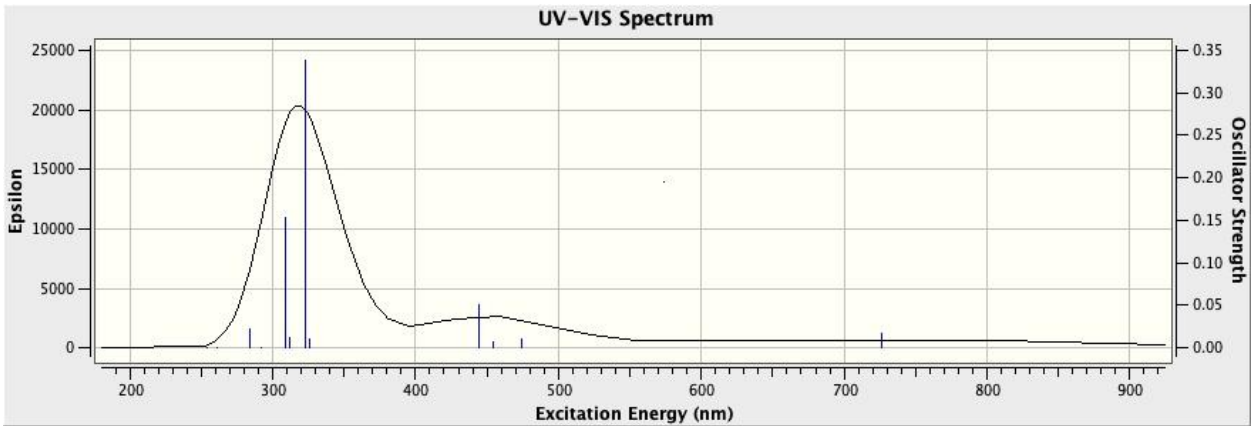

Figure 6.11. 10,11-dihydro-dibenzo[b,f]azepinyl radical **2c** UV-VIS calculated spectrum

Cation Radical of 10,11-dihydro-dibenzo[b,f]azepinyl nitrenium ion (2b)

Table 6.4. Calculated UV-Vis bands and oscillator strengths for 10,11-dihydro-dibenzo[b,f]azepinyl cation radical **2b**

State	Energy (eV)	Excitation Wavelength (nm)	Oscillator Strength
1	1.6763	739.63	0.0077
2	1.8014	688.27	0.0035
3	2.1512	576.35	0.2238
4	3.6914	335.88	0.0017
5	3.9458	314.22	0.2044
6	3.9887	310.84	0.0112
7	4.0679	304.79	0.0001
8	4.1167	301.18	0.0013
9	4.2288	293.19	0.0086
10	4.4871	276.31	0.0316
11	4.5379	273.22	0.0130
12	4.5914	270.03	0.0153

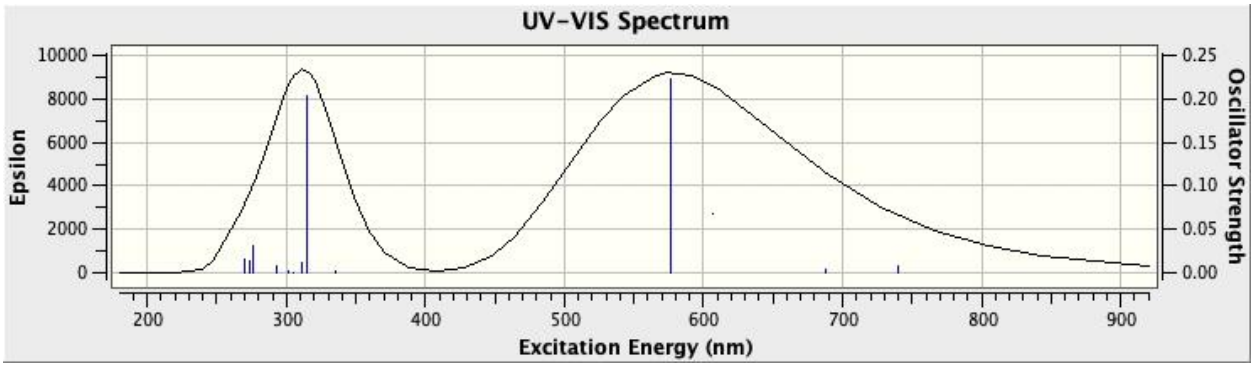

Figure 6.12. 10,11-dihydro-dibenzo[b,f]azepinyl cation radical **2b** UV-VIS calculated spectrum

6.3 Chapter 3 Experimental

6.3.1 Cartesian Coordinates & Energies

Carbazolyl Radical (19c)

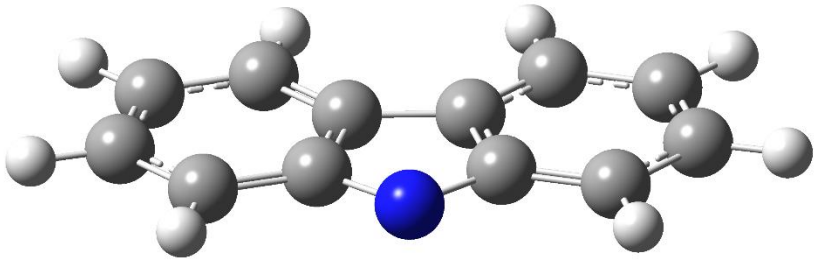

Standard orientation:

Center Number	Atomic Number	Atomic Type	Coordinates (Angstroms) X	Y	Z
1	6	0	3.065324	1.098954	0.000104
2	6	0	3.423190	-0.257813	-0.000001
3	6	0	2.443888	-1.258203	-0.000077
4	6	0	1.711897	1.499627	0.000266
5	1	0	4.480280	-0.534371	0.000049
6	1	0	2.703861	-2.318687	-0.000058
7	1	0	1.451905	2.561396	0.000352
8	6	0	-1.093327	-0.870935	0.000262
9	6	0	-2.443854	-1.258206	0.000485
10	6	0	-3.423201	-0.257814	0.000149
11	6	0	-3.065355	1.098928	-0.000352
12	6	0	-1.711912	1.499623	-0.000226
13	6	0	-0.732262	0.519401	0.000109
14	1	0	-2.703892	-2.318675	0.000893
15	1	0	-4.480269	-0.534440	0.000271
16	1	0	-1.451984	2.561406	-0.000181
17	7	0	0.000007	-1.701462	-0.000664
18	6	0	1.093334	-0.870911	-0.000112
19	6	0	0.732285	0.519360	0.000079
20	1	0	-3.848972	1.860779	-0.000815
21	1	0	3.848978	1.860758	0.000031

Sum of electronic and zero-point Energies= -516.303231
Sum of electronic and thermal Energies= -516.294696
Sum of electronic and thermal Enthalpies= -516.293752
Sum of electronic and thermal Free Energies= -516.337609

Carbazolyl Cation Radical (19b)

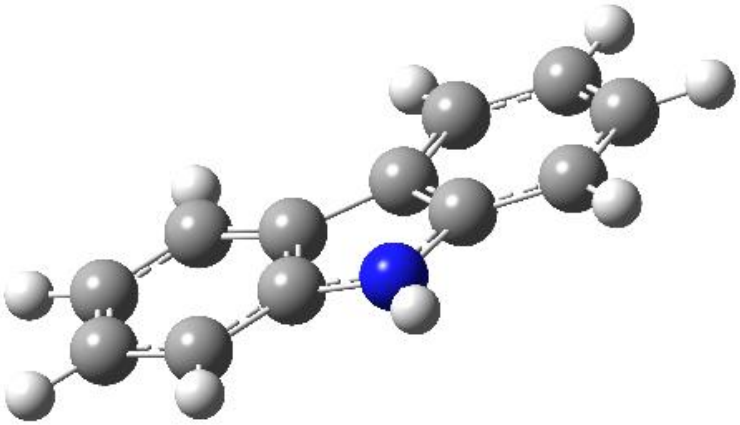

Standard orientation:

Center Number	Atomic Number	Atomic Type	Coordinates (Angstroms) X	Y	Z
1	6	0	-1.125237	0.000103	-3.068468
2	6	0	0.227387	0.000121	-3.445830
3	6	0	1.237420	-0.000010	-2.481323
4	6	0	0.835902	-0.000071	-1.133504
5	6	0	-0.535253	-0.000126	-0.733074
6	6	0	-1.519210	-0.000066	-1.706588
7	1	0	0.492749	0.000220	-4.504624
8	1	0	2.292891	-0.000162	-2.761865
9	1	0	-2.578781	-0.000153	-1.442828
10	6	0	0.835902	-0.000071	1.133504
11	6	0	1.237420	-0.000010	2.481323
12	6	0	0.227387	0.000121	3.445830
13	6	0	-1.125237	0.000103	3.068468
14	6	0	-1.519210	-0.000066	1.706588
15	6	0	-0.535253	-0.000126	0.733074
16	1	0	2.292891	-0.000162	2.761865
17	1	0	0.492749	0.000220	4.504624
18	1	0	-2.578781	-0.000153	1.442828
19	7	0	1.613371	-0.000012	0.000000
20	1	0	2.632070	0.000308	0.000000
21	1	0	-1.895746	0.000269	3.842665
22	1	0	-1.895746	0.000269	-3.842665

Sum of electronic and zero-point Energies= -516.676566
Sum of electronic and thermal Energies= -516.667729
Sum of electronic and thermal Enthalpies= -516.666784
Sum of electronic and thermal Free Energies= -516.711122

Carbazolyl Singlet Nitrenium Ion (^{1}19)

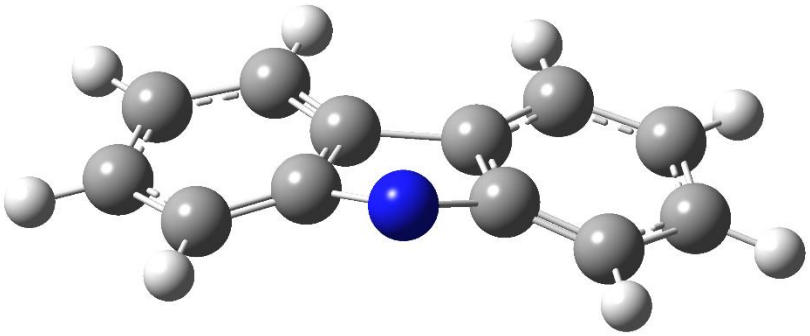

Standard orientation:

Center Number	Atomic Number	Atomic Type	Coordinates (Angstroms) X	Y	Z
1	6	0	3.089756	1.060250	0.000093
2	6	0	3.436394	-0.292720	-0.000229
3	6	0	2.434312	-1.274463	-0.000210
4	6	0	1.726296	1.507980	0.000155
5	1	0	4.488452	-0.583333	-0.000601
6	1	0	2.663710	-2.342340	-0.000320
7	1	0	1.507234	2.577874	0.000218
8	6	0	-1.091292	-0.841488	0.000242
9	6	0	-2.434231	-1.274469	0.000217
10	6	0	-3.436406	-0.292722	-0.000172
11	6	0	-3.089831	1.060196	-0.000269
12	6	0	-1.726312	1.507954	-0.000048
13	6	0	-0.740796	0.556342	0.000191
14	1	0	-2.663683	-2.342335	0.000410
15	1	0	-4.488428	-0.583462	-0.000482
16	1	0	-1.507334	2.577866	0.000239
17	7	0	0.000031	-1.645469	0.000018
18	6	0	1.091289	-0.841484	0.000027
19	6	0	0.740797	0.556325	0.000258
20	1	0	-3.883582	1.811905	-0.000844
21	1	0	3.883554	1.811912	-0.000276

Sum of electronic and zero-point Energies= -516.026888
Sum of electronic and thermal Energies= -516.018187
Sum of electronic and thermal Enthalpies= -516.017242
Sum of electronic and thermal Free Energies= -516.060813

Carbazolyl Triplet Nitrenium Ion (^{3}19)

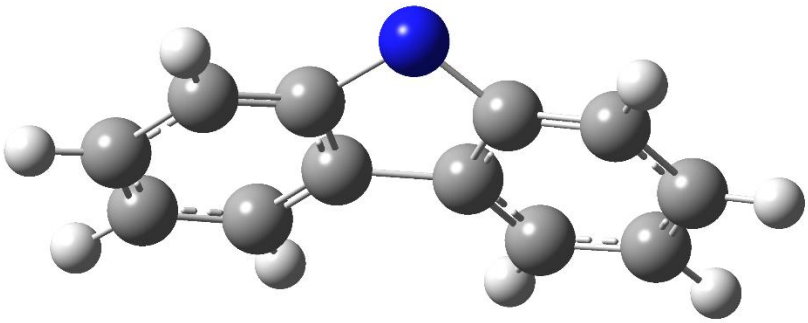

Standard orientation:

Center Number	Atomic Number	Atomic Type	Coordinates (Angstroms) X	Y	Z
1	6	0	3.030915	1.121623	-0.000051
2	6	0	3.390964	-0.261482	0.000017
3	6	0	2.432362	-1.278423	-0.000055
4	6	0	1.698532	1.525790	-0.000024
5	1	0	4.451875	-0.524209	0.000060
6	1	0	2.706942	-2.334572	-0.000169
7	1	0	1.434276	2.585360	0.000011
8	6	0	-1.084690	-0.895611	0.000077
9	6	0	-2.432361	-1.278422	0.000001
10	6	0	-3.390963	-0.261482	-0.000051
11	6	0	-3.030908	1.121634	-0.000092
12	6	0	-1.698527	1.525782	0.000085
13	6	0	-0.712086	0.524931	0.000130
14	1	0	-2.706935	-2.334572	-0.000002
15	1	0	-4.451879	-0.524186	-0.000082
16	1	0	-1.434231	2.585344	0.000135
17	7	0	-0.000003	-1.719536	0.000009
18	6	0	1.084681	-0.895621	0.000022
19	6	0	0.712078	0.524937	-0.000008
20	1	0	-3.825737	1.870819	-0.000252
21	1	0	3.825729	1.870826	-0.000064

Sum of electronic and zero-point Energies= -516.014246
Sum of electronic and thermal Energies= -516.005459
Sum of electronic and thermal Enthalpies= -516.004515
Sum of electronic and thermal Free Energies= -516.049311

3,6-dibromocarbazolyl Radical (18c)

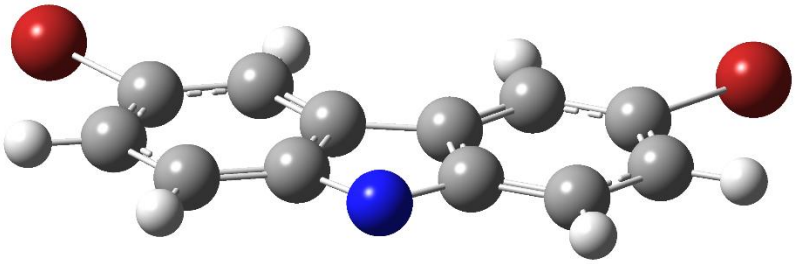

Standard orientation:

Center Number	Atomic Number	Atomic Type	Coordinates (Angstroms) X	Y	Z
1	6	0	-3.053212	-0.022702	0.000131
2	6	0	-3.424453	1.332317	0.000143
3	6	0	-2.443614	2.327100	0.000117
4	6	0	-1.090816	1.946077	0.000079
5	6	0	-0.731875	0.554405	0.000068
6	6	0	-1.702310	-0.432821	0.000092
7	1	0	-4.482123	1.599314	0.000175
8	1	0	-2.712099	3.385234	0.000137
9	1	0	-1.448661	-1.494310	0.000076
10	6	0	1.090816	1.946077	-0.000017
11	6	0	2.443614	2.327100	-0.000095
12	6	0	3.424453	1.332317	-0.000151
13	6	0	3.053212	-0.022702	-0.000136
14	6	0	1.702310	-0.432820	-0.000058
15	6	0	0.731875	0.554405	0.000001
16	1	0	2.712099	3.385234	-0.000097
17	1	0	4.482123	1.599314	-0.000208
18	1	0	1.448661	-1.494310	-0.000046
19	7	0	0.000000	2.774304	0.000071
20	35	0	4.410304	-1.355045	-0.000209
21	35	0	-4.410304	-1.355045	0.000164

Sum of electronic and zero-point Energies= -5662.864110
Sum of electronic and thermal Energies= -5662.852532
Sum of electronic and thermal Enthalpies= -5662.851588
Sum of electronic and thermal Free Energies= -5662.904939

3,6-dibromocarbazolyl Cation Radical (18b)

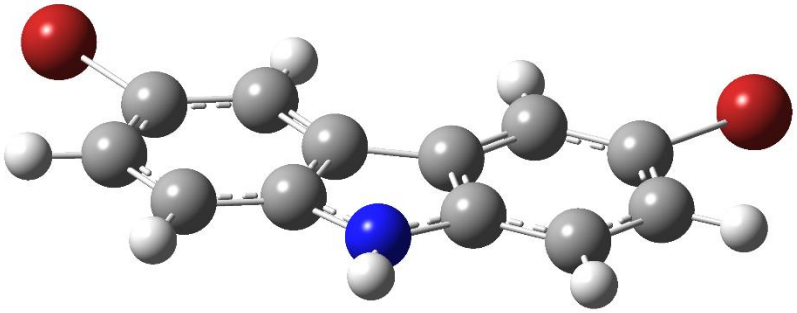

Standard orientation:

Center Number	Atomic Number	Atomic Type	Coordinates (Angstroms) X	Y	Z
1	6	0	-0.050297	-0.000064	-3.057933
2	6	0	1.308043	-0.000375	-3.443689
3	6	0	2.312964	-0.000267	-2.482272
4	6	0	1.924798	0.000178	-1.132093
5	6	0	0.553584	0.000428	-0.732270
6	6	0	-0.440960	0.000234	-1.694238
7	1	0	1.565522	-0.000688	-4.503651
8	1	0	3.365029	-0.000444	-2.774706
9	1	0	-1.498877	0.000334	-1.427364
10	6	0	1.924798	0.000178	1.132093
11	6	0	2.312964	-0.000267	2.482272
12	6	0	1.308043	-0.000375	3.443689
13	6	0	-0.050297	-0.000064	3.057933
14	6	0	-0.440960	0.000234	1.694238
15	6	0	0.553584	0.000428	0.732270
16	1	0	3.365029	-0.000444	2.774706
17	1	0	1.565522	-0.000688	4.503651
18	1	0	-1.498877	0.000334	1.427364
19	7	0	2.703045	0.000352	0.000000
20	35	0	-1.382898	-0.000046	4.376289
21	35	0	-1.382898	-0.000046	-4.376289
22	1	0	3.720593	0.000701	0.000000

Sum of electronic and zero-point Energies= -5663.234600
Sum of electronic and thermal Energies= -5663.222879
Sum of electronic and thermal Enthalpies= -5663.221934
Sum of electronic and thermal Free Energies= -5663.275507

3,6-dibromocarbazolyl Singlet Nitrenium Ion (^{1}18)

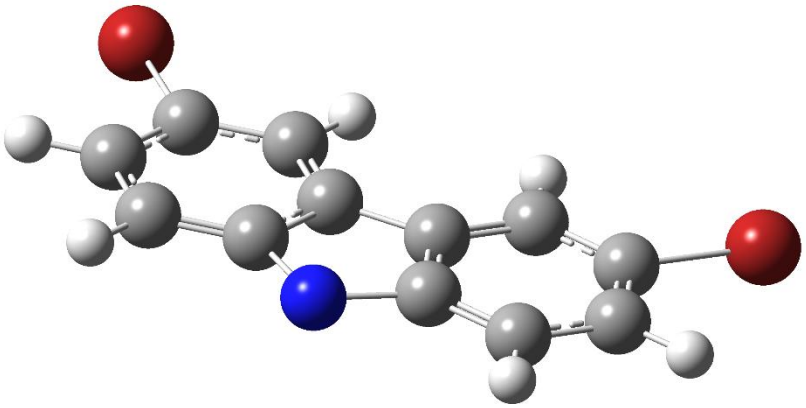

Standard orientation:

Center Number	Atomic Number	Atomic Type	Coordinates (Angstroms) X	Y	Z
1	6	0	-3.082704	-0.021860	0.000130
2	6	0	-3.434657	1.338496	0.000188
3	6	0	-2.436825	2.314048	0.000124
4	6	0	-1.089570	1.896686	-0.000007
5	6	0	-0.740412	0.497002	-0.000055
6	6	0	-1.712462	-0.464529	0.000013
7	1	0	-4.487658	1.623059	0.000277
8	1	0	-2.679111	3.378870	0.000140
9	1	0	-1.489728	-1.532993	0.000005
10	6	0	1.089570	1.896686	-0.000104
11	6	0	2.436825	2.314048	-0.000090
12	6	0	3.434657	1.338496	-0.000108
13	6	0	3.082704	-0.021860	-0.000131
14	6	0	1.712462	-0.464528	-0.000130
15	6	0	0.740413	0.497002	-0.000120
16	1	0	2.679111	3.378870	-0.000097
17	1	0	4.487658	1.623059	-0.000111
18	1	0	1.489728	-1.532993	-0.000113
19	7	0	0.000000	2.699396	-0.000174
20	35	0	4.419403	-1.322168	-0.000150
21	35	0	-4.419403	-1.322168	0.000232

Sum of electronic and zero-point Energies= -5662.589825
Sum of electronic and thermal Energies= -5662.578229
Sum of electronic and thermal Enthalpies= -5662.577284
Sum of electronic and thermal Free Energies= -5662.630122

3,6-dibromocarbazolyl Triplet Nitrenium Ion (^{3}18)

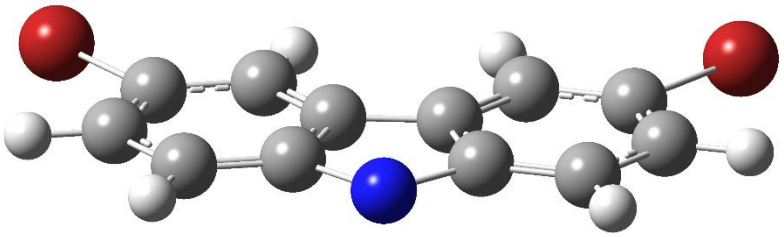

Standard orientation:

Center Number	Atomic Number	Atomic Type	Coordinates (Angstroms) X	Y	Z
1	6	0	-3.035651	-0.059081	0.000140
2	6	0	-3.400461	1.334093	0.000161
3	6	0	-2.438127	2.325679	0.000117
4	6	0	-1.080258	1.931964	0.000055
5	6	0	-0.719321	0.510381	0.000042
6	6	0	-1.692891	-0.477703	0.000084
7	1	0	-4.460594	1.594815	0.000213
8	1	0	-2.703315	3.384071	0.000136
9	1	0	-1.443129	-1.539928	0.000074
10	6	0	1.080258	1.931964	-0.000037
11	6	0	2.438127	2.325678	-0.000085
12	6	0	3.400462	1.334093	-0.000128
13	6	0	3.035651	-0.059081	-0.000129
14	6	0	1.692891	-0.477703	-0.000065
15	6	0	0.719321	0.510381	-0.000022
16	1	0	2.703315	3.384070	-0.000087
17	1	0	4.460595	1.594815	-0.000158
18	1	0	1.443129	-1.539928	-0.000049
19	7	0	0.000000	2.751470	-0.000004
20	35	0	4.403766	-1.327460	-0.000213
21	35	0	-4.403766	-1.327460	0.000187

Sum of electronic and zero-point Energies= -5662.574092
Sum of electronic and thermal Energies= -5662.562372
Sum of electronic and thermal Enthalpies= -5662.561428
Sum of electronic and thermal Free Energies= -5662.615546

3,6-dichloroarbazolyl Radical

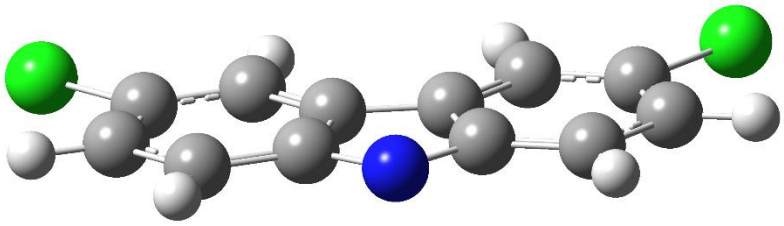

Standard orientation:

Center Number	Atomic Number	Atomic Type	Coordinates (Angstroms) X	Y	Z
1	6	0	-3.053266	-0.464116	0.000124
2	6	0	-3.424215	0.891286	0.000130
3	6	0	-2.443940	1.885657	0.000103
4	6	0	-1.090848	1.504677	0.000068
5	6	0	-0.731723	0.112798	0.000060
6	6	0	-1.702351	-0.873872	0.000087
7	1	0	-4.483770	1.150917	0.000160
8	1	0	-2.711855	2.943900	0.000120
9	1	0	-1.456016	-1.937091	0.000071
10	6	0	1.090848	1.504677	-0.000029
11	6	0	2.443939	1.885657	-0.000110
12	6	0	3.424215	0.891286	-0.000165
13	6	0	3.053267	-0.464116	-0.000144
14	6	0	1.702351	-0.873871	-0.000065
15	6	0	0.731723	0.112798	-0.000007
16	1	0	2.711855	2.943900	-0.000114
17	1	0	4.483770	1.150917	-0.000223
18	1	0	1.456016	-1.937091	-0.000051
19	7	0	0.000000	2.332781	0.000063
20	17	0	4.297352	-1.685944	-0.000197
21	17	0	-4.297352	-1.685944	0.000155

Sum of electronic and zero-point Energies= -1435.259518
Sum of electronic and thermal Energies= -1435.248477
Sum of electronic and thermal Enthalpies= -1435.247532
Sum of electronic and thermal Free Energies= -1435.298193

3,6-dichloroarbazolyl Cation Radical

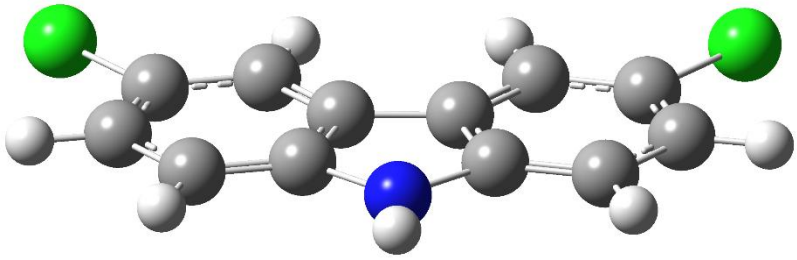

Standard orientation:

Center Number	Atomic Number	Atomic Type	Coordinates (Angstroms) X	Y	Z
1	6	0	-3.058333	-0.495435	0.000132
2	6	0	-3.444500	0.862623	0.000134
3	6	0	-2.482623	1.866513	0.000095
4	6	0	-1.132320	1.476773	0.000055
5	6	0	-0.732535	0.105161	0.000054
6	6	0	-1.694304	-0.888268	0.000093
7	1	0	-4.505993	1.113352	0.000169
8	1	0	-2.774144	2.918786	0.000103
9	1	0	-1.436026	-1.948241	0.000093
10	6	0	1.132319	1.476773	-0.000046
11	6	0	2.482622	1.866513	-0.000117
12	6	0	3.444500	0.862623	-0.000157
13	6	0	3.058333	-0.495435	-0.000138
14	6	0	1.694304	-0.888268	-0.000059
15	6	0	0.732535	0.105162	-0.000014
16	1	0	2.774143	2.918786	-0.000132
17	1	0	4.505993	1.113352	-0.000203
18	1	0	1.436027	-1.948241	-0.000033
19	7	0	0.000000	2.254381	0.000021
20	17	0	4.266080	-1.716150	-0.000192
21	17	0	-4.266080	-1.716150	0.000171
22	1	0	0.000000	3.272215	0.000042

Sum of electronic and zero-point Energies= -1435.628834
Sum of electronic and thermal Energies= -1435.617628
Sum of electronic and thermal Enthalpies= -1435.616684
Sum of electronic and thermal Free Energies= -1435.667617

3,6-dichlorocarbazolyl Singlet Nitrenium Ion

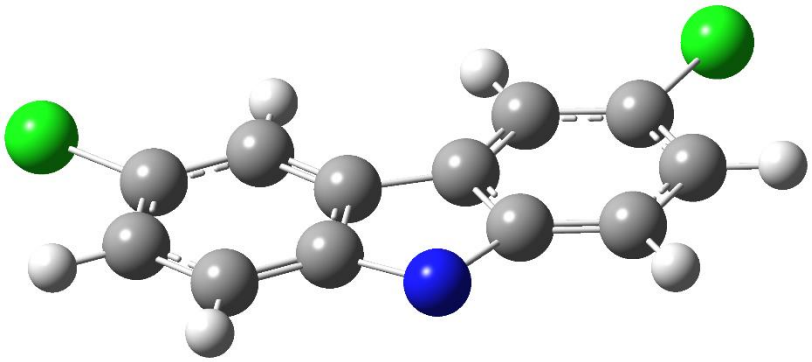

Standard orientation:

Center Number	Atomic Number	Atomic Type	Coordinates (Angstroms) X	Y	Z
1	6	0	-3.082994	-0.451341	0.000153
2	6	0	-3.435569	0.908813	0.000236
3	6	0	-2.437104	1.882898	0.000145
4	6	0	-1.089885	1.464011	-0.000043
5	6	0	-0.740669	0.064059	-0.000111
6	6	0	-1.712615	-0.896342	-0.000012
7	1	0	-4.490518	1.186148	0.000360
8	1	0	-2.677777	2.948099	0.000158
9	1	0	-1.499094	-1.966673	-0.000013
10	6	0	1.089885	1.464011	-0.000140
11	6	0	2.437104	1.882898	-0.000068
12	6	0	3.435569	0.908813	-0.000058
13	6	0	3.082994	-0.451340	-0.000098
14	6	0	1.712615	-0.896342	-0.000151
15	6	0	0.740669	0.064059	-0.000173
16	1	0	2.677777	2.948099	-0.000080
17	1	0	4.490518	1.186148	-0.000030
18	1	0	1.499094	-1.966673	-0.000132
19	7	0	0.000000	2.265758	-0.000311
20	17	0	4.305722	-1.642960	-0.000073
21	17	0	-4.305722	-1.642959	0.000299

Sum of electronic and zero-point Energies= -1434.984248
Sum of electronic and thermal Energies= -1434.973168
Sum of electronic and thermal Enthalpies= -1434.972223
Sum of electronic and thermal Free Energies= -1435.022429

3,6-dichlorocarbazolyl Triplet Nitrenium Ion

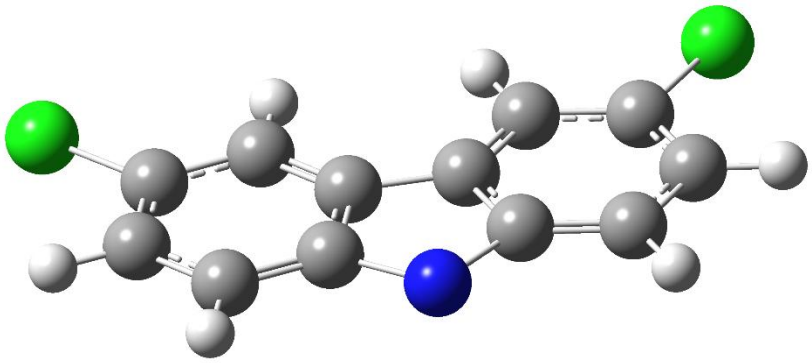

Standard orientation:

Center Number	Atomic Number	Atomic Type	Coordinates (Angstroms) X	Y	Z
1	6	0	3.034238	-0.491062	-0.000131
2	6	0	3.400143	0.903097	-0.000146
3	6	0	2.438755	1.894214	-0.000104
4	6	0	1.080292	1.500191	-0.000048
5	6	0	0.718780	0.077250	-0.000029
6	6	0	1.692208	-0.910696	-0.000072
7	1	0	4.462546	1.155201	-0.000192
8	1	0	2.702041	2.953170	-0.000113
9	1	0	1.450794	-1.974837	-0.000063
10	6	0	-1.080292	1.500191	0.000045
11	6	0	-2.438755	1.894214	0.000103
12	6	0	-3.400143	0.903097	0.000144
13	6	0	-3.034238	-0.491062	0.000129
14	6	0	-1.692208	-0.910696	0.000074
15	6	0	-0.718780	0.077250	0.000033
16	1	0	-2.702041	2.953170	0.000115
17	1	0	-4.462546	1.155201	0.000189
18	1	0	-1.450794	-1.974837	0.000064
19	7	0	0.000000	2.318617	0.000004
20	17	0	-4.286699	-1.652157	0.000186
21	17	0	4.286699	-1.652157	-0.000187

Sum of electronic and zero-point Energies= -1434.967908
Sum of electronic and thermal Energies= -1434.956699
Sum of electronic and thermal Enthalpies= -1434.955755
Sum of electronic and thermal Free Energies= -1435.007261

***N,N*-di(4-bromophenyl) Amine Radical (16c)**

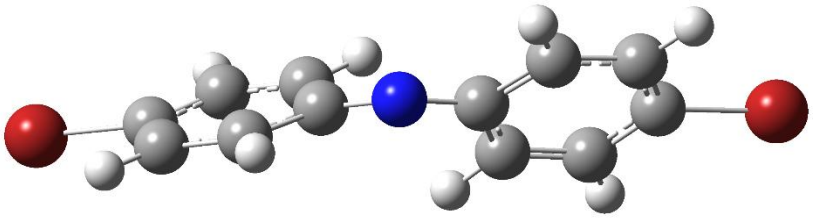

Standard orientation:

Center Number	Atomic Number	Atomic Type	Coordinates (Angstroms) X	Y	Z
1	6	0	-3.794766	-0.023598	-0.026983
2	6	0	-2.724390	-0.744265	-0.576717
3	6	0	-1.446040	-0.200074	-0.563664
4	6	0	-3.594914	1.260806	0.504319
5	1	0	-2.900344	-1.725989	-1.020120
6	1	0	-0.626251	-0.751739	-1.026182
7	1	0	-4.438597	1.818980	0.913741
8	6	0	1.201262	1.093477	0.012518
9	6	0	2.323558	1.814926	-0.489020
10	6	0	3.594786	1.260633	-0.504570
11	6	0	3.794681	-0.023736	0.026966
12	6	0	2.724421	-0.744367	0.576906
13	6	0	1.446069	-0.200128	0.563977
14	1	0	2.145146	2.818128	-0.880938
15	1	0	4.438550	1.818537	-0.914195
16	1	0	2.900455	-1.726032	1.020403
17	7	0	0.000032	1.729189	0.000234
18	6	0	-1.201292	1.093529	-0.012283
19	6	0	-2.323620	1.815079	0.488817
20	1	0	-2.145351	2.818359	0.880594
21	1	0	0.626261	-0.751705	1.026557
22	35	0	-5.537796	-0.783425	-0.025927
23	35	0	5.537835	-0.783334	0.025838

Sum of electronic and zero-point Energies= -5664.036075
Sum of electronic and thermal Energies= -5664.023309
Sum of electronic and thermal Enthalpies= -5664.022365
Sum of electronic and thermal Free Energies= -5664.079445

***N,N*-di(4-bromophenyl) Amine Cation Radical (16b)**

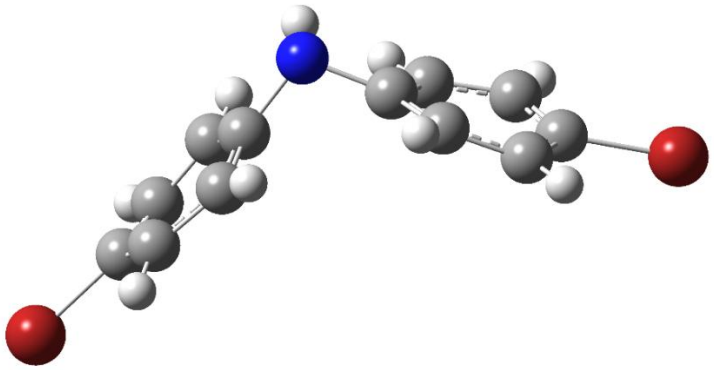

Standard orientation:

Center Number	Atomic Number	Atomic Type	Coordinates (Angstroms) X	Y	Z
1	6	0	-3.857876	-0.041492	0.022049
2	6	0	-3.636963	1.282039	-0.411199
3	6	0	-2.353788	1.798670	-0.405957
4	6	0	-2.782125	-0.830330	0.477785
5	1	0	-4.474849	1.892479	-0.751464
6	1	0	-2.182072	2.821393	-0.752431
7	1	0	-2.968588	-1.837851	0.852918
8	6	0	1.256608	1.001442	-0.014838
9	6	0	1.495635	-0.317612	-0.479010
10	6	0	2.782253	-0.830253	-0.478296
11	6	0	3.857805	-0.041536	-0.022110
12	6	0	3.636754	1.281813	0.411609
13	6	0	2.353626	1.798523	0.406157
14	1	0	0.682415	-0.915630	-0.889386
15	1	0	2.968725	-1.837741	-0.853507
16	1	0	4.474613	1.892059	0.752286
17	7	0	0.000012	1.574717	-0.000256
18	6	0	-1.256555	1.001459	0.014457
19	6	0	-1.495502	-0.317764	0.478338
20	1	0	-0.682205	-0.915929	0.888398
21	1	0	2.181879	2.821158	0.752804
22	1	0	-0.000052	2.594405	-0.000001
23	35	0	5.594379	-0.746353	-0.018687
24	35	0	-5.594355	-0.746421	0.018923

Sum of electronic and zero-point Energies= -5664.409063
Sum of electronic and thermal Energies= -5664.396175
Sum of electronic and thermal Enthalpies= -5664.395231
Sum of electronic and thermal Free Energies= -5664.452504

***N*,*N*-di(4-bromophenyl) Singlet Nitrenium Ion (^{1}16)**

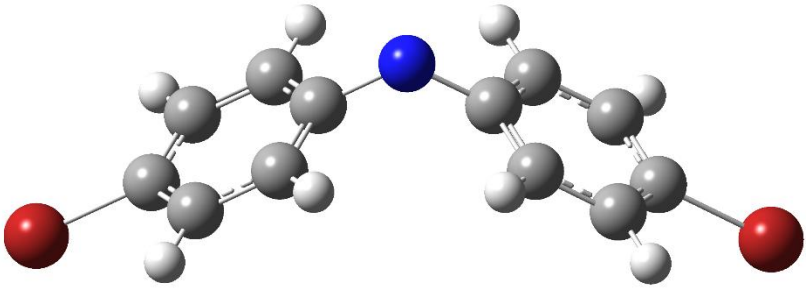

Standard orientation:

Center Number	Atomic Number	Atomic Type	Coordinates (Angstroms) X	Y	Z
1	6	0	-3.820213	-0.025415	0.023710
2	6	0	-3.591991	1.304480	-0.395891
3	6	0	-2.311522	1.813907	-0.348190
4	6	0	-2.758867	-0.837063	0.496215
5	1	0	-4.427505	1.920405	-0.732225
6	1	0	-2.099319	2.842164	-0.647279
7	1	0	-2.973243	-1.837551	0.875669
8	6	0	1.199947	0.991079	-0.041195
9	6	0	2.311630	1.813984	0.348111
10	6	0	3.592079	1.304593	0.395747
11	6	0	3.820258	-0.025361	-0.023710
12	6	0	2.758840	-0.837073	-0.496103
13	6	0	1.471419	-0.346514	-0.498355
14	1	0	2.099259	2.842227	0.647155
15	1	0	4.427644	1.920546	0.731906
16	1	0	2.973334	-1.837547	-0.875532
17	7	0	0.000033	1.580444	0.000123
18	6	0	-1.200026	0.991088	0.041318
19	6	0	-1.471416	-0.346419	0.498506
20	1	0	-0.668675	-0.948449	0.926102
21	1	0	0.668624	-0.948524	-0.925881
22	35	0	-5.555322	-0.711755	0.006573
23	35	0	5.555288	-0.711791	-0.006623

Sum of electronic and zero-point Energies= -5663.778812
Sum of electronic and thermal Energies= -5663.766178
Sum of electronic and thermal Enthalpies= -5663.765234
Sum of electronic and thermal Free Energies= -5663.821367

***N*,*N*-di(4-bromophenyl) Triplet Nitrenium Ion (^{3}16)**

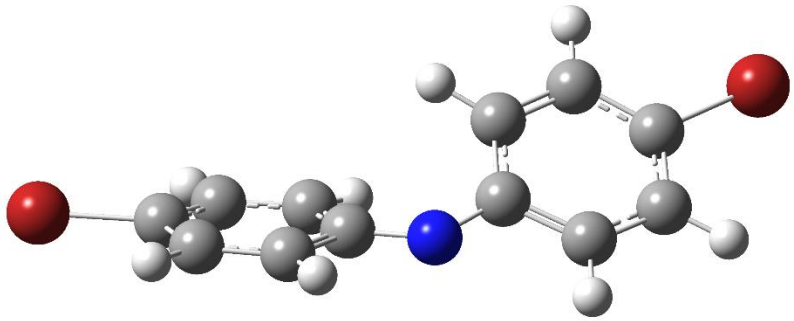

Standard orientation:

Center Number	Atomic Number	Atomic Type	Coordinates (Angstroms) X	Y	Z
1	6	0	-3.963873	-0.017696	0.016313
2	6	0	-3.550726	1.078154	-0.780687
3	6	0	-2.226509	1.454932	-0.797499
4	6	0	-3.028738	-0.734270	0.805355
5	1	0	-4.285563	1.619378	-1.379060
6	1	0	-1.888282	2.298574	-1.401488
7	1	0	-3.366229	-1.576642	1.412057
8	6	0	1.259084	0.738058	0.009917
9	6	0	2.226554	1.455031	0.797405
10	6	0	3.550769	1.078249	0.780570
11	6	0	3.963874	-0.017698	-0.016317
12	6	0	3.028696	-0.734368	-0.805223
13	6	0	1.703030	-0.364472	-0.805861
14	1	0	1.888358	2.298745	1.401311
15	1	0	4.285637	1.619545	1.378839
16	1	0	3.366154	-1.576815	-1.411838
17	7	0	0.000001	1.127052	0.000036
18	6	0	-1.259082	0.738052	-0.009875
19	6	0	-1.703072	-0.364375	0.806017
20	1	0	-0.971565	-0.898800	1.415203
21	1	0	0.971491	-0.898973	-1.414942
22	35	0	-5.762031	-0.523308	0.032364
23	35	0	5.762029	-0.523319	-0.032394

Sum of electronic and zero-point Energies= -5663.763340
Sum of electronic and thermal Energies= -5663.750219
Sum of electronic and thermal Enthalpies= -5663.749274
Sum of electronic and thermal Free Energies= -5663.808273

***N,N*-di(4-chlorophenyl) Amine Radical (17c)**

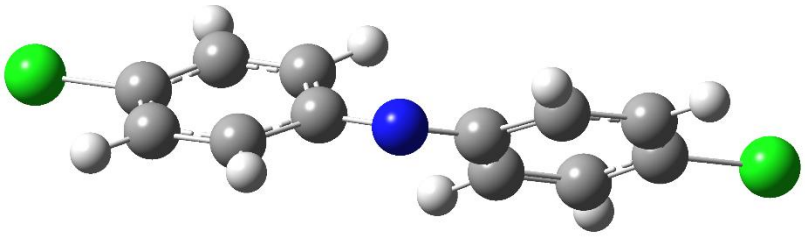

Standard orientation:

Center Number	Atomic Number	Atomic Type	Coordinates (Angstroms) X	Y	Z
1	6	0	-3.799534	-0.273094	-0.037668
2	6	0	-2.728638	-0.998985	-0.579515
3	6	0	-1.448698	-0.459391	-0.562370
4	6	0	-3.597072	1.011716	0.491856
5	1	0	-2.912768	-1.980882	-1.019324
6	1	0	-0.628816	-1.015247	-1.019525
7	1	0	-4.445122	1.568200	0.894311
8	6	0	1.202039	0.835534	0.014229
9	6	0	2.324639	1.561700	-0.480348
10	6	0	3.597170	1.011749	-0.491345
11	6	0	3.799566	-0.273247	0.037743
12	6	0	2.728490	-0.999280	0.579217
13	6	0	1.448625	-0.459641	0.561788
14	1	0	2.144380	2.565588	-0.869517
15	1	0	4.445282	1.568408	-0.893455
16	1	0	2.912572	-1.981184	1.019034
17	7	0	0.000036	1.469959	-0.000260
18	17	0	5.401647	-0.961450	0.045951
19	17	0	-5.401687	-0.961460	-0.045662
20	6	0	-1.201994	0.835555	-0.014746
21	6	0	-2.324504	1.561541	0.480612
22	1	0	-2.144034	2.565266	0.870118
23	1	0	0.628403	-1.015344	1.018531

Sum of electronic and zero-point Energies= -1436.431272
Sum of electronic and thermal Energies= -1436.419016
Sum of electronic and thermal Enthalpies= -1436.418071
Sum of electronic and thermal Free Energies= -1436.472510

***N,N*-di(4-chlorophenyl) Amine Cation Radical (17b)**

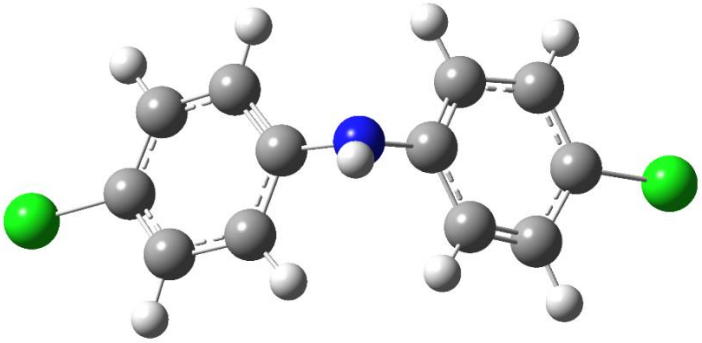

Standard orientation:

Center Number	Atomic Number	Atomic Type	Coordinates (Angstroms) X	Y	Z
1	6	0	-3.859152	-0.276662	0.030221
2	6	0	-3.637489	1.047614	-0.400698
3	6	0	-2.353745	1.560950	-0.397796
4	6	0	-2.784462	-1.070067	0.481443
5	1	0	-4.479705	1.654922	-0.735298
6	1	0	-2.180515	2.584084	-0.742138
7	1	0	-2.979800	-2.076933	0.853666
8	6	0	1.256905	0.759535	-0.016945
9	6	0	1.496972	-0.560918	-0.477906
10	6	0	2.784165	-1.070516	-0.480349
11	6	0	3.859200	-0.276747	-0.030787
12	6	0	3.637694	1.047743	0.399896
13	6	0	2.354012	1.560969	0.397549
14	1	0	0.683664	-1.161713	-0.883871
15	1	0	2.979047	-2.077737	-0.851801
16	1	0	4.480189	1.655280	0.733404
17	7	0	0.000038	1.331494	0.000571
18	6	0	-1.257036	0.759852	0.017892
19	6	0	-1.497343	-0.560415	0.479634
20	1	0	-0.684270	-1.160588	0.886958
21	1	0	2.181039	2.584363	0.741258
22	1	0	0.000039	2.351278	-0.000091
23	17	0	5.451698	-0.917664	-0.032303
24	17	0	-5.451597	-0.917715	0.031185

Sum of electronic and zero-point Energies= -1436.803770
Sum of electronic and thermal Energies= -1436.791387
Sum of electronic and thermal Enthalpies= -1436.790443
Sum of electronic and thermal Free Energies= -1436.845049

***N*,*N*-di(4-chlorophenyl) Singlet Nitrenium Ion (^{1}17)**

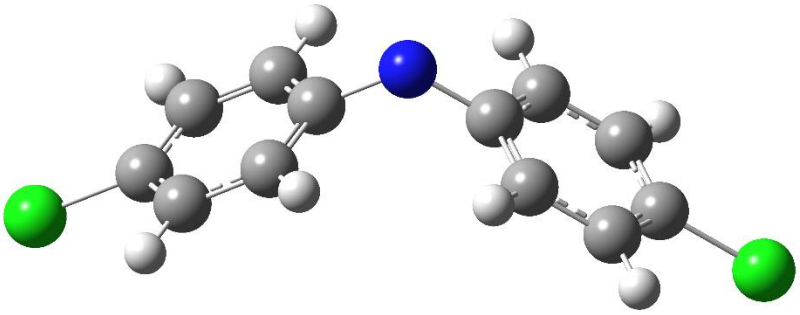

Standard orientation:

Center Number	Atomic Number	Atomic Type	Coordinates (Angstroms) X	Y	Z
1	6	0	-3.823864	-0.250235	0.025206
2	6	0	-3.592797	1.081673	-0.385959
3	6	0	-2.310579	1.584827	-0.338304
4	6	0	-2.765078	-1.070726	0.489575
5	1	0	-4.431668	1.697590	-0.713403
6	1	0	-2.094289	2.614193	-0.630454
7	1	0	-2.990616	-2.071373	0.862006
8	6	0	1.200964	0.754333	-0.042309
9	6	0	2.310615	1.584829	0.338304
10	6	0	3.592856	1.081714	0.385804
11	6	0	3.823867	-0.250252	-0.025212
12	6	0	2.765014	-1.070844	-0.489274
13	6	0	1.476325	-0.585650	-0.491591
14	1	0	2.094340	2.614190	0.630490
15	1	0	4.431756	1.697655	0.713120
16	1	0	2.990531	-2.071571	-0.861501
17	7	0	-0.000006	1.340938	0.000048
18	17	0	5.415029	-0.872086	-0.010312
19	17	0	-5.415012	-0.872100	0.010035
20	6	0	-1.200979	0.754331	0.042423
21	6	0	-1.476378	-0.585542	0.491920
22	1	0	-0.675140	-1.193302	0.914024
23	1	0	0.675033	-1.193542	-0.913393

Sum of electronic and zero-point Energies= -1436.173843
Sum of electronic and thermal Energies= -1436.161711
Sum of electronic and thermal Enthalpies= -1436.160767
Sum of electronic and thermal Free Energies= -1436.214236

***N*,*N*-Di(4-chlorophenyl) Triplet Nitrenium Ion (^{3}17)**

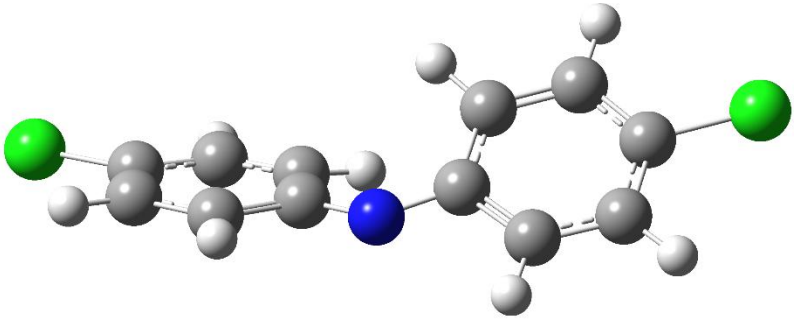

Standard orientation:

Center Number	Atomic Number	Atomic Type	Coordinates (Angstroms) X	Y	Z
1	6	0	-3.965388	-0.182749	0.032985
2	6	0	-3.553060	0.910102	-0.768762
3	6	0	-2.228294	1.282690	-0.791082
4	6	0	-3.030407	-0.900922	0.820956
5	1	0	-4.293906	1.447094	-1.363473
6	1	0	-1.889282	2.123491	-1.398538
7	1	0	-3.375523	-1.739839	1.427926
8	6	0	1.260425	0.564566	0.004304
9	6	0	2.228311	1.282721	0.791051
10	6	0	3.553076	0.910132	0.768720
11	6	0	3.965388	-0.182752	-0.032991
12	6	0	3.030391	-0.900958	-0.820912
13	6	0	1.704385	-0.534749	-0.816501
14	1	0	1.889311	2.123547	1.398480
15	1	0	4.293934	1.447147	1.363394
16	1	0	3.375494	-1.739901	-1.427854
17	7	0	0.000001	0.948499	0.000014
18	17	0	5.613207	-0.642052	-0.054797
19	17	0	-5.613208	-0.642046	0.054777
20	6	0	-1.260424	0.564566	-0.004287
21	6	0	-1.704402	-0.534714	0.816555
22	1	0	-0.972039	-1.069455	1.424354
23	1	0	0.972010	-1.069516	-1.424262

Sum of electronic and zero-point Energies= -1436.158083
Sum of electronic and thermal Energies= -1436.145447
Sum of electronic and thermal Enthalpies= -1436.144503
Sum of electronic and thermal Free Energies= -1436.201029

Diphenyl Amine Radical (1c)

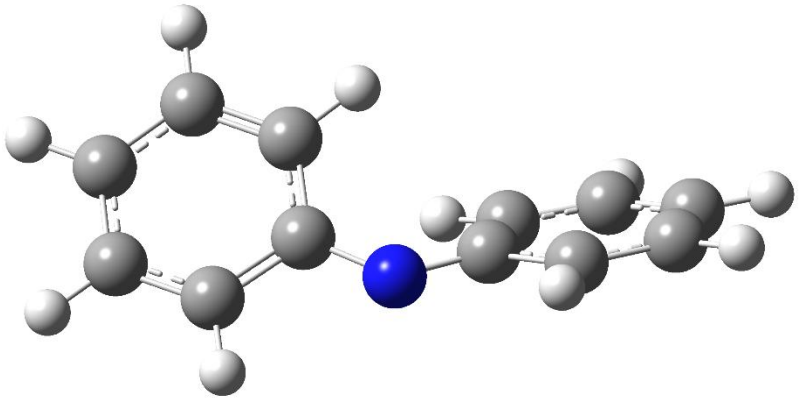

Standard orientation:

Center Number	Atomic Number	Atomic Type	Coordinates (Angstroms) X	Y	Z
1	6	0	3.802334	-0.634963	0.091056
2	6	0	2.715892	-1.340267	0.628052
3	6	0	1.434068	-0.800225	0.597372
4	6	0	3.598935	0.642739	-0.453710
5	1	0	2.876087	-2.321349	1.083354
6	1	0	0.602492	-1.342459	1.050142
7	1	0	4.444986	1.203108	-0.860028
8	6	0	-1.202501	0.489437	-0.031652
9	6	0	-2.329643	1.206316	0.464083
10	6	0	-3.598912	0.642665	0.453797
11	6	0	-3.802323	-0.634937	-0.090949
12	6	0	-2.715863	-1.340239	-0.628095
13	6	0	-1.434143	-0.800182	-0.597476
14	1	0	-2.152619	2.205669	0.866723
15	1	0	-4.444859	1.203127	0.860197
16	1	0	-2.876210	-2.321252	-1.083488
17	7	0	0.000020	1.127742	-0.000118
18	6	0	1.202434	0.489371	0.031756
19	6	0	2.329724	1.206312	-0.464084
20	1	0	2.152370	2.205604	-0.866734
21	1	0	-0.602469	-1.342172	-1.050364
22	1	0	-4.804266	-1.070363	-0.113372
23	1	0	4.804331	-1.070260	0.113498

Sum of electronic and zero-point Energies= -517.474869
Sum of electronic and thermal Energies= -517.465052
Sum of electronic and thermal Enthalpies= -517.464107
Sum of electronic and thermal Free Energies= -517.511707

Diphenyl Amine Cation Radical (1b)

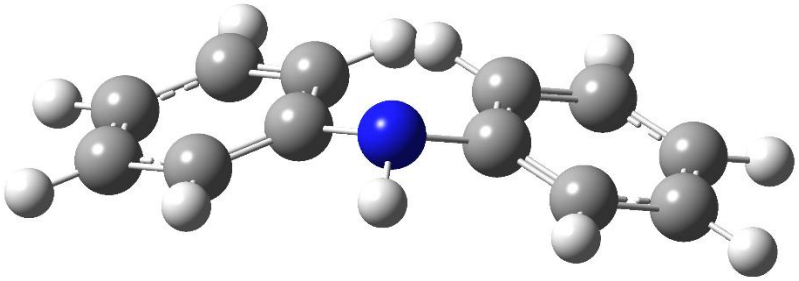

Standard orientation:

Center Number	Atomic Number	Atomic Type	Coordinates (Angstroms) X	Y	Z
1	6	0	3.857972	0.608663	0.063358
2	6	0	3.637694	-0.710484	-0.369742
3	6	0	2.354048	-1.233142	-0.378792
4	6	0	1.257553	-0.427011	0.030090
5	6	0	1.488318	0.893863	0.496896
6	6	0	2.781464	1.397362	0.504339
7	1	0	4.476485	-1.326169	-0.700610
8	1	0	2.177115	-2.255218	-0.724807
9	1	0	2.963526	2.406454	0.879848
10	6	0	-1.257598	-0.426946	-0.029871
11	6	0	-2.354044	-1.233092	0.378803
12	6	0	-3.637743	-0.710472	0.369546
13	6	0	-3.857987	0.608650	-0.063557
14	6	0	-2.781440	1.397366	-0.504387
15	6	0	-1.488266	0.893897	-0.496704
16	1	0	-2.177186	-2.255174	0.724827
17	1	0	-4.476557	-1.326201	0.700275
18	1	0	-2.963447	2.406452	-0.879936
19	7	0	0.000026	-0.998178	0.000111
20	1	0	-0.000009	-2.018717	-0.000195
21	1	0	-4.871658	1.015171	-0.076901
22	1	0	4.871619	1.015252	0.076478
23	1	0	0.668283	1.486692	0.901148
24	1	0	-0.668176	1.486778	-0.900770

Sum of electronic and zero-point Energies= -517.851590
Sum of electronic and thermal Energies= -517.841593
Sum of electronic and thermal Enthalpies= -517.840649
Sum of electronic and thermal Free Energies= -517.888494

Diphenyl Singlet Nitrenium Ion (^{1}1)

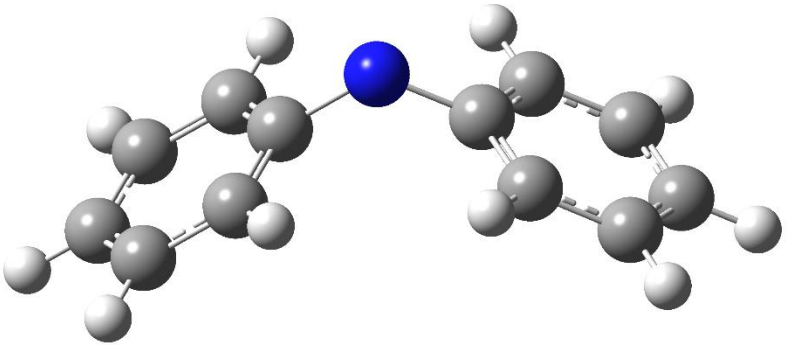

Standard orientation:

Center Number	Atomic Number	Atomic Type	Coordinates (Angstroms) X	Y	Z
1	6	0	3.808173	0.581238	0.037995
2	6	0	3.588039	-0.741672	-0.386707
3	6	0	2.309600	-1.267814	-0.341934
4	6	0	2.747994	1.384247	0.510282
5	1	0	4.425986	-1.353841	-0.726025
6	1	0	2.094875	-2.294520	-0.644441
7	1	0	2.956859	2.385521	0.892963
8	6	0	-1.199201	-0.444736	-0.052679
9	6	0	-2.309626	-1.267797	0.341890
10	6	0	-3.588087	-0.741658	0.386492
11	6	0	-3.808174	0.581288	-0.038133
12	6	0	-2.747939	1.384278	-0.510302
13	6	0	-1.456753	0.893388	-0.517978
14	1	0	-2.095042	-2.294530	0.644400
15	1	0	-4.426088	-1.353847	0.725635
16	1	0	-2.956692	2.385561	-0.893016
17	7	0	-0.000003	-1.037351	0.000163
18	6	0	1.199174	-0.444750	0.052889
19	6	0	1.456809	0.893408	0.518089
20	1	0	0.647402	1.480389	0.954255
21	1	0	-0.647330	1.480339	-0.954148
22	1	0	-4.824150	0.984952	-0.036240
23	1	0	4.824140	0.984925	0.036057

Sum of electronic and zero-point Energies= -517.216921
Sum of electronic and thermal Energies= -517.207131
Sum of electronic and thermal Enthalpies= -517.206187
Sum of electronic and thermal Free Energies= -517.252955

Diphenyl Triplet Nitrenium Ion (^{3}1)

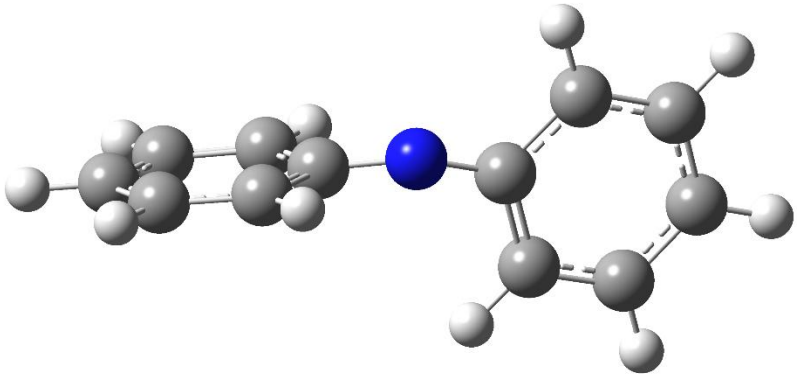

Standard orientation:

Center Number	Atomic Number	Atomic Type	Coordinates (Angstroms) X	Y	Z
1	6	0	3.988608	-0.381781	0.086561
2	6	0	3.065109	-1.107375	0.871218
3	6	0	1.725211	-0.778536	0.856568
4	6	0	3.558451	0.686115	-0.729293
5	1	0	3.413840	-1.932469	1.496335
6	1	0	0.994527	-1.319183	1.461120
7	1	0	4.285093	1.238972	-1.328417
8	6	0	-1.270783	0.301305	-0.015559
9	6	0	-2.223092	1.035778	0.775404
10	6	0	-3.557995	0.685883	0.730176
11	6	0	-3.988551	-0.381561	-0.086090
12	6	0	-3.065568	-1.106866	-0.871521
13	6	0	-1.725600	-0.778012	-0.857203
14	1	0	-1.864888	1.859146	1.395606
15	1	0	-4.284422	1.238328	1.329924
16	1	0	-3.414662	-1.931657	-1.496808
17	7	0	-0.000031	0.647177	-0.000545
18	6	0	1.270616	0.301142	0.015064
19	6	0	2.223617	1.036075	-0.774955
20	1	0	1.865714	1.859776	-1.394902
21	1	0	-0.995104	-1.318574	-1.462058
22	1	0	-5.047523	-0.648548	-0.113450
23	1	0	5.047499	-0.649013	0.114250

Sum of electronic and zero-point Energies= -517.203737
Sum of electronic and thermal Energies= -517.193385
Sum of electronic and thermal Enthalpies= -517.192441
Sum of electronic and thermal Free Energies= -517.242603

Saturated Dibenzoazepinyl Cation Radical (2b)

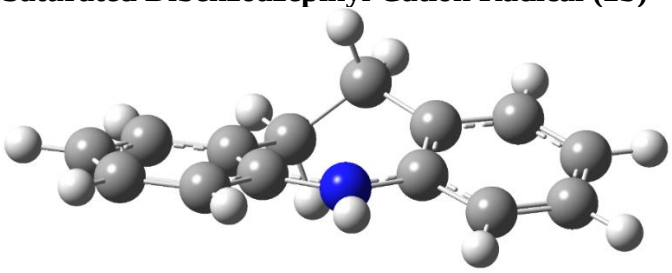

Standard orientation:

Center Number	Atomic Number	Atomic Type	Coordinates (Angstroms) X	Y	Z
1	6	0	-3.980068	-0.143654	-0.001273
2	6	0	-3.643094	1.204836	-0.207195
3	6	0	-2.312272	1.576426	-0.202713
4	6	0	-1.283839	0.610807	-0.000877
5	6	0	-1.619511	-0.758783	0.225769
6	6	0	-2.974430	-1.094997	0.212643
7	1	0	-4.420653	1.953294	-0.370505
8	1	0	-2.037170	2.622507	-0.366981
9	1	0	-3.255105	-2.136949	0.382717
10	6	0	1.283841	0.610842	0.000609
11	6	0	2.312267	1.576506	0.202564
12	6	0	3.643049	1.204863	0.207468
13	6	0	3.980036	-0.143704	0.001863
14	6	0	2.974448	-1.095029	-0.212248
15	6	0	1.619536	-0.758749	-0.225846
16	1	0	2.037103	2.622615	0.366549
17	1	0	4.420630	1.953290	0.370813
18	1	0	3.255106	-2.137020	-0.382117
19	7	0	0.000019	1.120295	-0.000192
20	1	0	0.000014	2.139838	-0.000305
21	1	0	5.027388	-0.453420	0.004011
22	1	0	-5.027425	-0.453357	-0.002980
23	6	0	-0.581025	-1.811545	0.502261
24	1	0	-0.183282	-1.680940	1.525640
25	1	0	-1.071399	-2.795097	0.492056
26	6	0	0.581046	-1.811401	-0.502782
27	1	0	1.071390	-2.794967	-0.492886
28	1	0	0.183361	-1.680372	-1.526117

Sum of electronic and zero-point Energies= -595.201928
Sum of electronic and thermal Energies= -595.190886
Sum of electronic and thermal Enthalpies= -595.189942
Sum of electronic and thermal Free Energies= -595.239552

Saturated Dibenzoazepinyl Singlet Nitrenium Ion (^{1}2)

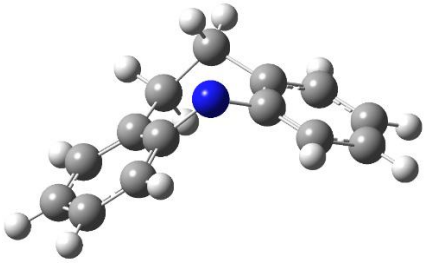

Standard orientation:

Center Number	Atomic Number	Atomic Type	Coordinates (Angstroms) X	Y	Z
1	6	0	3.945328	0.091198	-0.001166
2	6	0	3.598287	-1.252604	-0.224173
3	6	0	2.263858	-1.602735	-0.205053
4	6	0	2.963641	1.071609	0.228961
5	1	0	4.371942	-2.003675	-0.393437
6	1	0	1.935399	-2.633188	-0.351211
7	1	0	3.276728	2.102123	0.412114
8	6	0	-1.230521	-0.617844	0.007915
9	6	0	-2.263848	-1.602758	0.204898
10	6	0	-3.598287	-1.252643	0.224069
11	6	0	-3.945318	0.091230	0.001492
12	6	0	-2.963635	1.071645	-0.228669
13	6	0	-1.608717	0.763779	-0.220490
14	1	0	-1.935356	-2.633203	0.351027
15	1	0	-4.371952	-2.003742	0.393165
16	1	0	-3.276702	2.102196	-0.411656
17	7	0	-0.000008	-1.142476	0.000142
18	6	0	1.230516	-0.617855	-0.007975
19	1	0	-4.998600	0.384588	-0.000288
20	1	0	4.998619	0.384521	0.000927
21	6	0	1.608700	0.763796	0.220438
22	6	0	0.581643	1.822869	0.498886
23	1	0	1.071718	2.806904	0.492420
24	1	0	0.191925	1.684798	1.526156
25	6	0	-0.581648	1.822777	-0.499256
26	1	0	-1.071671	2.806830	-0.492982
27	1	0	-0.191973	1.684387	-1.526484

Sum of electronic and zero-point Energies= -594.571458
Sum of electronic and thermal Energies= -594.560587
Sum of electronic and thermal Enthalpies= -594.559643
Sum of electronic and thermal Free Energies= -594.608313

Saturated Dibenzoazepinyl Triplet Nitrenium Ion (^{3}2)

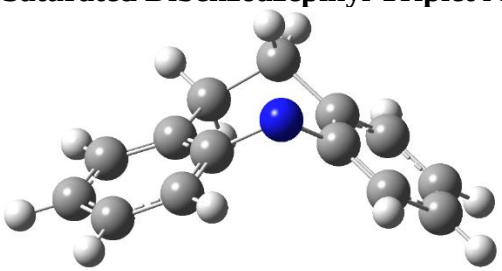

Standard orientation:

Center Number	Atomic Number	Atomic Type	Coordinates (Angstroms) X	Y	Z
1	6	0	3.952192	0.112258	0.070062
2	6	0	3.605869	-1.186498	-0.360192
3	6	0	2.279827	-1.558627	-0.425504
4	6	0	2.956868	1.045993	0.409535
5	1	0	4.386732	-1.896696	-0.639593
6	1	0	1.977152	-2.558010	-0.741591
7	1	0	3.247395	2.066469	0.671725
8	6	0	-1.260664	-0.637617	0.007469
9	6	0	-2.279809	-1.558625	0.425493
10	6	0	-3.605860	-1.186502	0.360205
11	6	0	-3.952182	0.112253	-0.070068
12	6	0	-2.956878	1.045996	-0.409527
13	6	0	-1.609060	0.714278	-0.394874
14	1	0	-1.977145	-2.557999	0.741615
15	1	0	-4.386727	-1.896685	0.639623
16	1	0	-3.247384	2.066476	-0.671713
17	7	0	-0.000001	-1.038538	0.000005
18	6	0	1.260638	-0.637619	-0.007493
19	1	0	-5.003310	0.405752	-0.116957
20	1	0	5.003311	0.405785	0.116954
21	6	0	1.609063	0.714286	0.394868
22	6	0	0.516470	1.731963	0.585072
23	1	0	0.973737	2.728113	0.663692
24	1	0	-0.015022	1.558674	1.537822
25	6	0	-0.516480	1.731969	-0.585067
26	1	0	-0.973743	2.728119	-0.663682
27	1	0	0.015040	1.558731	-1.537814

Sum of electronic and zero-point Energies= -594.544056
Sum of electronic and thermal Energies= -594.532949
Sum of electronic and thermal Enthalpies= -594.532005
Sum of electronic and thermal Free Energies= -594.582076

6.3.2 Calculated UV-VIS Spectra and Oscillator Strength

Singlet state of diphenyl nitrenium ion ^{1}1

Table 6.5. Calculated UV-Vis bands and oscillator strengths for diphenyl singlet nitrenium ion ^{1}**1**

State	Energy (eV)	Excitation Wavelength (nm)	Oscillator Strength
S1	0.4978	2490.56	0.0002
S2	0.8394	1476.99	0.0009
S3	1.0178	1218.13	0.0013
S4	1.3851	895.14	0.1567
S5	3.1515	393.41	0.0165
S6	3.2757	378.49	0.0015
S7	3.5009	354.15	0.0794
S8	3.5451	349.74	0.0082
S9	4.0562	305.67	0.0057
S10	4.1339	299.92	0.0035

Triplet state of diphenyl nitrenium ion ^{3}1

Table 6.6. Calculated UV-Vis bands and oscillator strengths for diphenyl triplet nitrenium ion ^{3}**1**

State	Energy (eV)	Excitation Wavelength (nm)	Oscillator Strength
T1	0.8752	1416.68	0.0046
T2	1.0494	1181.44	0.0080
T3	1.1692	1060.39	0.1210
T4	1.6516	750.68	0.0001
T5	2.0607	601.66	0.0000
T6	2.2271	556.70	0.0000
T7	2.7909	444.25	0.0183
T8	3.1174	397.72	0.0005
T9	3.4242	362.08	0.0021
T10	3.5699	347.30	0.0239

Singlet state of *N*,*N*-di(4-bromophenyl)nitrenium ion ^{1}**16**

Table 6.7. Calculated UV-Vis bands and oscillator strengths for *N*,*N*-di(4-bromophenyl) singlet nitrenium ion ^{1}**16**

State	Energy (eV)	Excitation Wavelength (nm)	Oscillator Strength
S1	0.4606	2691.89	0.0002
S2	1.2481	993.39	0.1494
S3	1.2862	963.92	0.1484
S4	1.4434	858.96	0.0034
S5	1.6969	730.66	0.0053
S6	1.7283	717.39	0.0045
S7	2.4311	510.00	0.0496
S8	2.7895	444.47	0.0631
S9	3.7655	329.26	0.0010
S10	3.8349	323.31	0.0002

Triplet state of *N*,*N*-di(4-bromophenyl)nitrenium ion ^{3}**16**

Table 6.8. Calculated UV-Vis bands and oscillator strengths for *N*,*N*-di(4-bromophenyl)nitrenium ion ^{3}**16**

State	Energy (eV)	Excitation Wavelength (nm)	Oscillator Strength
T1	0.9131	1357.80	0.2035
T2	1.2462	994.90	0.0024
T3	1.4164	875.38	0.0007
T4	1.4659	845.80	0.0001
T5	1.5074	822.53	0.0000
T6	1.5385	805.86	0.0000
T7	1.9090	649.46	0.0333
T8	2.2555	549.69	0.0004
T9	2.4423	507.65	0.0000
T10	2.4955	496.83	0.0313

Singlet state of *N*-(4,4'-dichlorodiphenyl)nitrenium ion ^{1}**17**

Table 6.9. Calculated UV-Vis bands and oscillator strengths for *N*-(4,4'-dichlorodiphenyl)nitrenium ion ^{1}**17**

State	Energy (eV)	Excitation Wavelength (nm)	Oscillator Strength
S1	-1.1058	-1121.25	-0.0000
S2	-0.3494	-3548.75	-0.0000
S3	0.4534	2734.70	0.0002
S4	0.8839	1402.75	0.0000
S5	0.9696	1278.69	0.0000
S6	1.1615	1067.46	0.0000
S7	1.2451	995.81	0.0132
S8	1.3442	922.34	0.2500
S9	1.4297	867.18	0.0124
S10	2.1412	579.05	0.0000

Triplet state of *N*-(4,4'-dichlorodiphenyl)nitrenium ion ^{3}**17**

Table 6.10. Calculated UV-Vis bands and oscillator strengths for *N*-(4,4'-dichlorodiphenyl)nitrenium ion ^{3}**17**

State	Energy (eV)	Excitation Wavelength (nm)	Oscillator Strength
T1	0.9736	1273.44	0.1801
T2	1.2169	1018.83	0.0044
T3	1.3870	893.89	0.0010
T4	1.4707	843.03	0.0001
T5	2.0544	603.50	0.0000
T6	2.0880	593.80	0.0001
T7	2.2056	562.13	0.0315
T8	2.3708	522.97	0.0000
T9	2.4550	505.03	0.0003
T10	2.6119	474.69	0.0001

Singlet State of carbazolyl nitrenium ion ^{1}**19**

Table 6.11. Calculated UV-Vis bands and oscillator strengths for carbazolyl nitrenium ion ^{1}**19**

State	Energy (eV)	Excitation Wavelength (nm)	Oscillator Strength
S1	0.3165	3917.49	0.0000
S2	0.6080	2039.13	0.0000
S3	0.8077	1535.10	0.0011
S4	0.9090	1363.97	0.0000
S5	1.7017	728.58	0.0000
S6	2.0696	599.08	0.0022
S7	2.1234	583.90	0.1877
S8	2.1374	580.06	0.0000
S9	2.3805	520.84	0.0063
S10	3.5087	353.36	0.0000

Triplet state of carbazolyl nitrenium ion ^{3}**19**

Table 6.12. Calculated UV-Vis bands and oscillator strengths for carbazolyl nitrenium ion ^{3}**19**

State	Energy (eV)	Excitation Wavelength (nm)	Oscillator Strength
T1	0.6122	2025.33	0.0002
T2	0.6478	1913.86	0.0001
T3	1.4714	842.65	0.0370
T4	1.9084	649.66	0.0045
T5	2.0364	608.83	0.0701
T6	2.8093	441.33	0.1301
T7	3.0423	407.53	0.0008
T8	3.2223	384.77	0.0005
T9	3.2473	381.80	0.0012
T10	3.4986	354.38	0.0019

Singlet state of 3,6-dibromocarbazolyl nitrenium ion **^{1}18**

Table 6.13. Calculated UV-Vis bands and oscillator strengths for 3,6-dibromocarbazolyl singlet nitrenium ion **^{1}18**

State	Energy (eV)	Excitation Wavelength (nm)	Oscillator Strength
S1	1.1681	1061.44	0.0362
S2	2.2070	561.77	0.0006
S3	2.3769	521.61	0.3931
S4	2.4402	508.10	0.0000
S5	2.4641	503.17	0.0000
S6	2.8613	433.32	0.0952

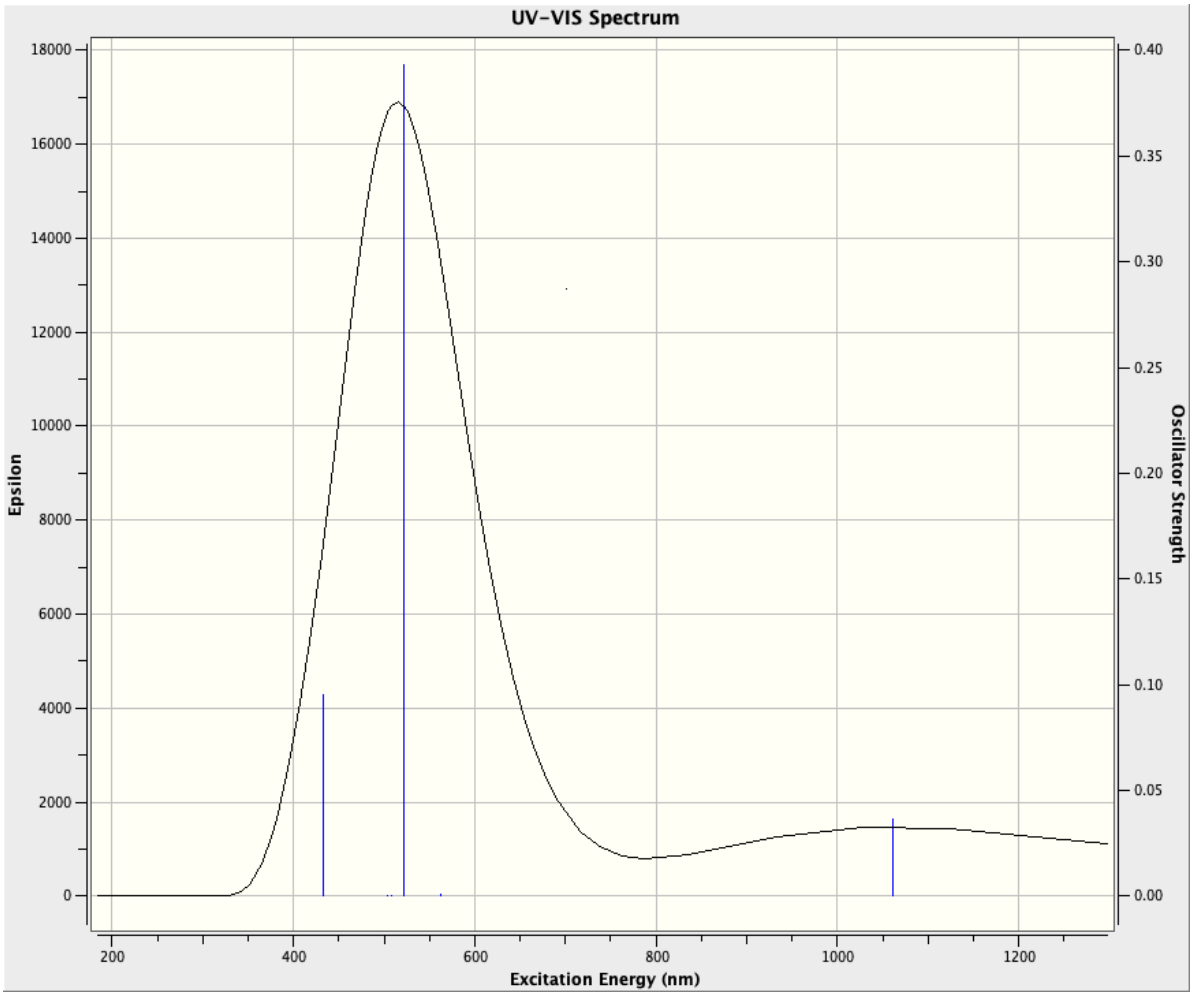

Figure 6.13. Calculated Singlet state UV-Vis Spectrum of 3,6-dibromocarbazolyl nitrenium ion **^{1}18**

Table 6.14. Calculated UV-Vis bands and oscillator strengths for 3,6-dibromocarbazolyl triplet nitrenium ion ^{3}**18**

State	Energy (eV)	Excitation Wavelength (nm)	Oscillator Strength
T1	0.5958	2081.05	0.0000
T2	1.1495	1078.56	0.0042
T3	1.3524	916.75	0.0000
T4	1.3710	904.31	0.0000
T5	1.4050	882.43	0.0003
T6	1.5062	823.19	0.1221
T7	2.3122	536.21	0.0702
T8	2.3280	532.59	0.0000
T9	2.6398	469.68	0.1581
T10	2.6952	460.01	0.0698

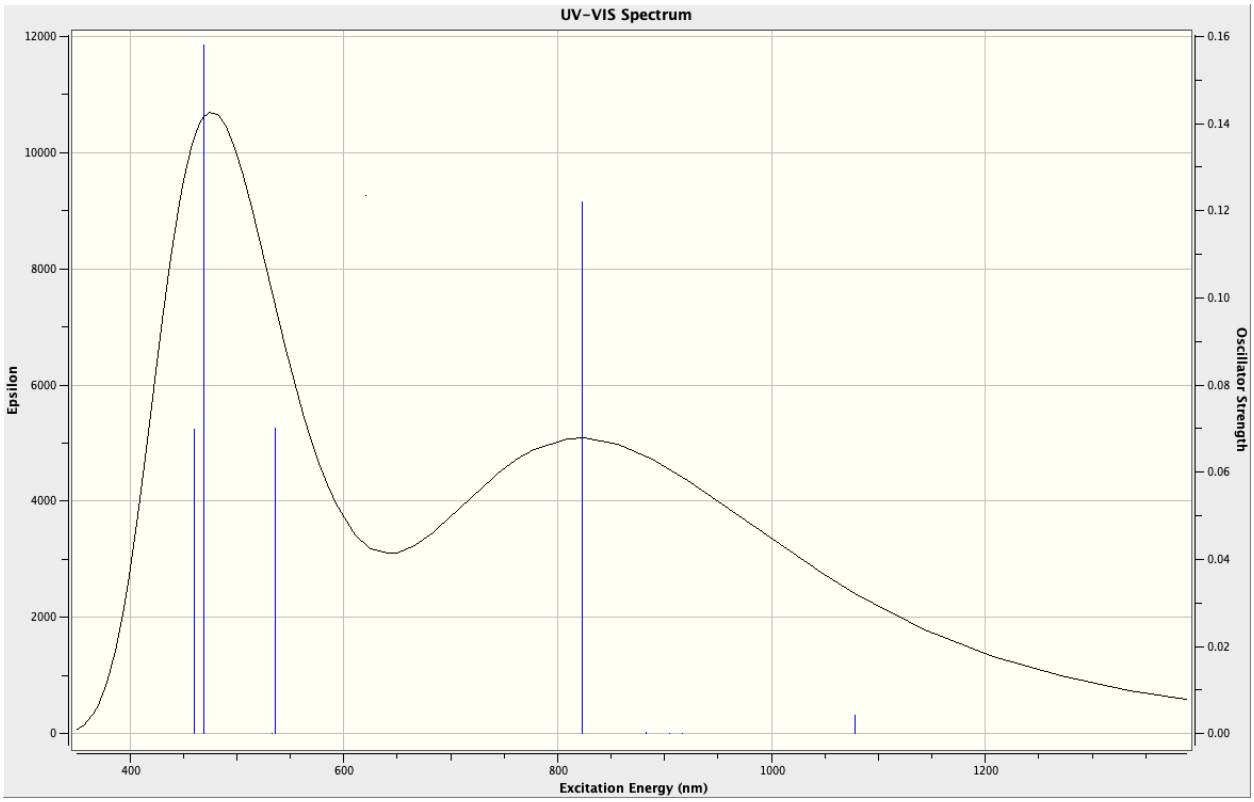

Figure 6.14. Calculated Triplet state UV-Vis Spectrum of 3,6-dibromocarbazolyl nitrenium ion ^{3}**18**

Radical of 3,6-dibromocarbazole

Table 6.15. Calculated UV-Vis bands and oscillator strengths for 3,6-dibromocarbazole radical **18c**

State	Energy (eV)	Excitation Wavelength (nm)	Oscillator Strength
1	1.2998	953.85	0.0151
2	1.8587	667.04	0.0005
3	2.2634	547.79	0.1179
4	2.9117	425.81	0.0285
5	3.3176	373.71	0.0000
6	3.3480	370.32	0.0000

Cation radical of 3,6-dibromocarbazole

Table 6.16. Calculated UV-Vis bands and oscillator strengths for 3,6-dibromocarbazole cation radical **18b**

State	Energy (eV)	Excitation Wavelength (nm)	Oscillator Strength
1	0.7362	1684.22	0.0219
2	1.4714	842.65	0.1605
3	1.9209	645.45	0.0000
4	1.9401	639.06	0.0000
5	2.1422	578.76	0.0433
6	2.7945	443.68	0.0173

6.4 Chapter 4 Experimental

6.4.1 Synthesis

The (carbazolylamino)-2,4,6-trimethylpyridinium tetrafluoroborate **24** was synthesized using the method developed in our previous publication.[11]

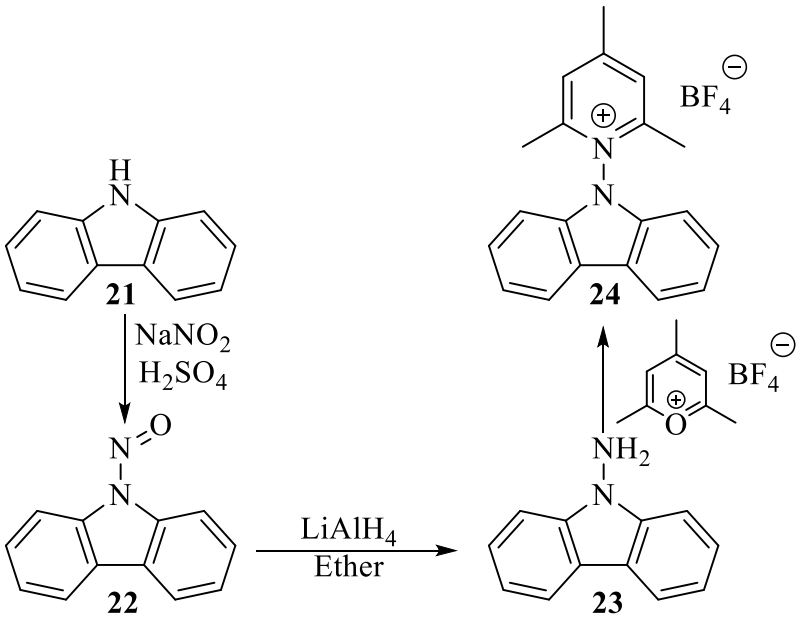

Scheme 6.1. Synthesis of 1-(carbazol-9-yl)-2,4,6-trimethylpyridinium tetrafluoroborate **24**

Synthesis of (3,6-dibromocarbazolylamino)-2,4,6-trimethylpyridinium tetra-fluoroborate 25

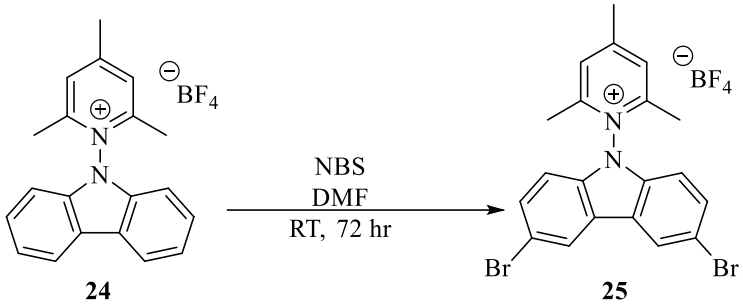

5 g (13.4 mmol) of (carbazolylamino)-2,4,6-trimethylpyridinium tetrafluoroborate was added to 5 mL of DMF. 23.8 g (134 mmol) of NBS is added to 45 mL of DMF and added with an addition funnel. The mixture is stirred for 3 days. The solvent is evaporated and the resulting solid is dissolved in 15 mL of 1-BuOH and stirred for 1 hr. approximately 80 mL of ether is added to the solution and cooled on ice. The precipitate is filtered over a Buchner funnel. This precipitate is

dissolved in CH_3CN and copious amounts of styrene and $AgBF_4$ are added to remove any remaining Br_2 or Br^-. The CH_3CN is evaporated and 15 mL of 1-BuOH and 80 mL of diethyl ether are used to precipitate out 1 g (14% yield) of the (3,6-dibromocarbazolylamino)-2,4,6-trimethylpyridinium tetrafluoroborate **25**.

^{1}H NMR (600 MHz, CD_3CN) δ = 8.51 (d, 2H), 7.94 (s, 2H), 7.77 (dd, 2H), 7.15 (d, 2H), 2.75 (s, 3H), 2.26 (s, 6H)

^{13}C NMR (600 MHz, CD_3CN) δ = 17.27, 21.21, 110.05, 115.56, 122.50, 124.39, 129.32, 130.91, 135.48, 157.65, 163.67

Synthesis of 3,6-dibromo-1-chloro-9H-carbazole (35):

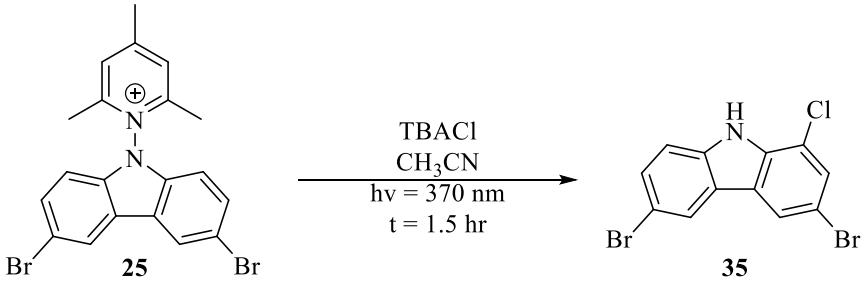

0.100 g (0.19mmol) (3,6-dibromocarbazolylamino)-2,4,6-trimethylpyridinium tetrafluoroborate **25** and 1.05 g (3.8mmol) of TBACl is added to 20 mL of CH_3CN. The solution was photolyzed with 370 nm Kessil Lamps at full power for 90 min. The solvent was evaporated then purified on a silica column with 15:85 ethyl acetate:hexane mixture to give the 2-chloro-3,6-dibromo-9H-carbazole (**35**)

^{1}H NMR (600 MHz, CD_3CN) δ = 8.25 (d, 1H), 7.68 (dd, 1H), 7.59 (d, 1H), 7.56 (d, 1H), 7.51 (dd, 1H)

DART MS$^+$: 359.78

Synthesis of 3,6-dibromo-1-methoxy-9H-carbazole (36)

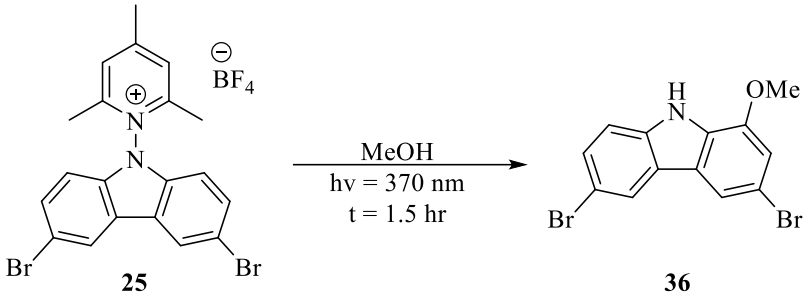

0.2 g (3,6-dibromocarbazolylamino)-2,4,6-trimethylpyridinium tetrafluoroborate **25** is added to 20 mL of neat MeOH. The solution was photolyzed with 370 nm Kessil Lamps at full power for 90 min. The solvent was evaporated then purified on a silica column with 15:85 ethyl acetate:hexane mixture to give the 3,6-dibromo-1-methoxy-9H-carbazole (**36**)

^{1}H NMR (600 MHz, CD_3CN) δ = 8.25 (d, 1H), 7.88 (d, 1H), 7.56 (dd, 1H), 7.50 (d, 1H), 7.15 (d, 1H), 4.03 (s, 3H)

Synthesis of 2-(3,6-dibromo-9H-carbazol-9-yl)-1-phenylethan-1-one (37)

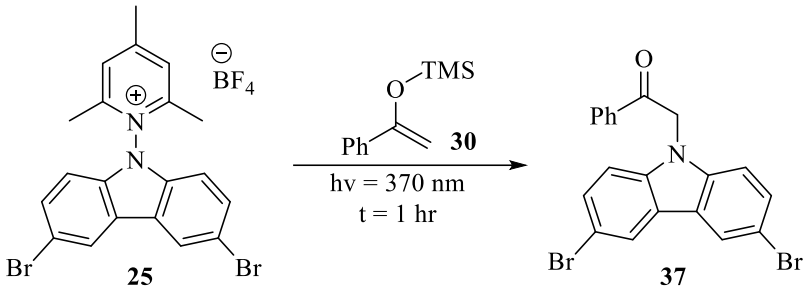

100 mg (0.019mmol) (3,6-dibromocarbazolylamino)-2,4,6-trimethylpyridinium tetrafluoroborate **25** and 0.038 mL (0.036 g, 0.19 mmol) of 1-phenyl-1-trimethylsiloxyethylene **30** is added to 10 mL of CH_3CN. The solution was photolyzed with 370 nm Kessil Lamps at full power for 60 min. The solvent was evaporated then purified on a silica column with 30:70 ethyl acetate:hexane mixture to give crude 2-(3,6-dibromo-9H-carbazol-9-yl)-1-phenylethan-1-one (**37**). The crude 2-

(3,6-dibromo-9H-carbazol-9-yl)-1-phenylethan-1-one **37** was further purified by recrystallizing with 10% ethyl acetate and hexane.

^{1}H NMR (600 MHz, CD_3CN) δ = 8.34 (d, 2H), 8.15 (d, 2H), 7.76 (t, 1H), 7.64 (t, 2H), 7.60 (dd, 2H), 7.38 (d, 2H), 5.92 (s, 2H)

^{13}C NMR (600 MHz, DMSO) δ 49.19, 110.77, 111.45, 122.87, 123.14, 127.68, 128.45, 128.61, 133.60, 134.48, 139.77, 211.50 ppm

Synthesis of 3,3',6,6'-tetrabromo-9,9'-bicarbazole (38)

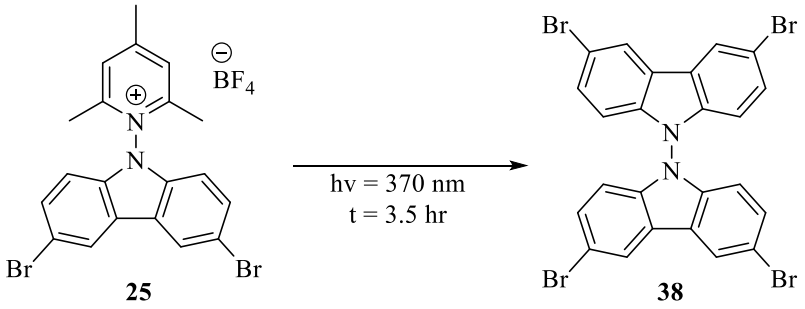

10 mg (0.002 mmol) (3,6-dibromocarbazolylamino)-2,4,6-trimethylpyridinium tetrafluoroborate **25** is added to 1 mL of CH_3CN in an NMR tube. The solution was photolyzed with 370 nm Kessil Lamps at full power for 210 min. The product was purified on a silica column with ethyl acetate:hexane mixture to give 3,3',6,6'-tetrabromo-9,9'-bicarbazole **38**. The ^{1}H NMR and DART MS^+ matched perfectly with the literature.[104]

^{1}H NMR (600 MHz, CD_3CN) δ = 8.34 (d, 2H), 8.15 (d, 2H), 7.76 (t, 1H), 7.64 (t, 2H), 7.60 (dd, 2H), 7.38 (d, 2H), 5.92 (s, 2H)

DART MS^+ 647.61

Synthesis of 3,6-dibromocarbazole (39):

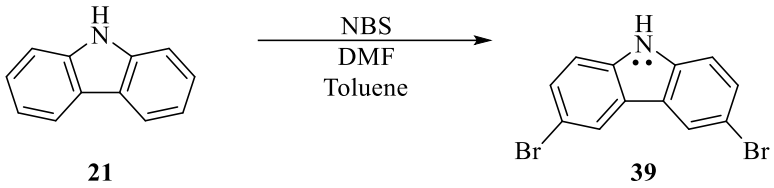

21 **39**

2.03 g (12.1 mmol) carbazole **21** is added to 10 mL of toluene in a 250 mL RBF. The solution was cooled to 0 ^{o}C. 4.68 g (26.3 mmol) is dissolved in 30 mL DMF and added by an addition funnel dropwise to the carbazole solution. After addition is complete, the reaction was stirred for 30 minutes at room temperature. Then 100 mL of H_2O is added to crash out the 3,6-carbazole product. The product was filtered and washed with ice cold MeOH to give 2.03 g (51%) the pure 3,6-carbazole **39**.

^{1}H NMR: (600 MHz, CD_3CN) δ = 8.26 (d, 2H), 7.56 (dd, 2H), 7.48 (d, 2H)

^{13}C NMR: (600 MHz, CD_3CN) δ = 138.47, 128.48, 123.24, 122.64, 112.50, 111.05

6.4.2 Methods and Transient Absorption Spectra from LFP

Generation of 3,6-dibromocarbazolyl nitrenium ion 18 in CH_3CN

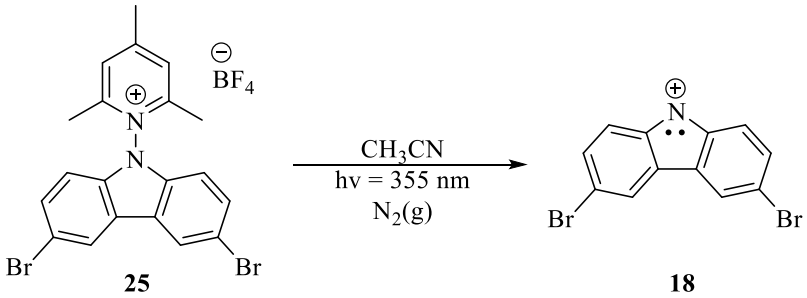

25 **18**

200 mg of (3,6-dibromocarbazolylamino)-2,4,6-trimethylpyridinium tetrafluoroborate **25** is added to 40 mL of CH_3CN in a 100 mL RBF. The spectrum is obtained by the method described in Full Spectrum Solutions section above.

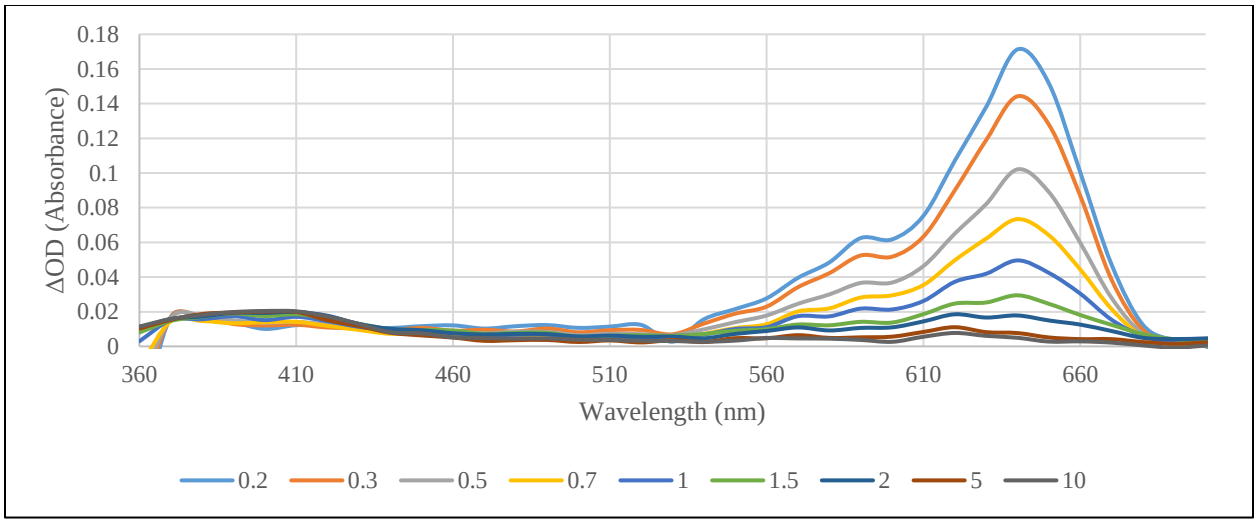

Figure 6.15. Transient spectra of 3,6-dibromocarbazolyl nitrenium ion **18** in CH_3CN.

Generation of 3,6-dibromocarbazolyl nitrenium ion 18 in DCM

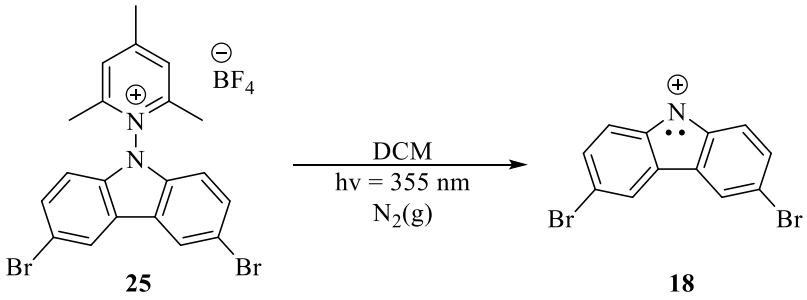

160 mg of (3,6-dibromocarbazolylamino)-2,4,6-trimethylpyridinium tetrafluoroborate **25** is added to 55 mL of DCM in a 100 mL RBF. The spectrum is obtained by the method described in Full Spectrum Solutions section above.

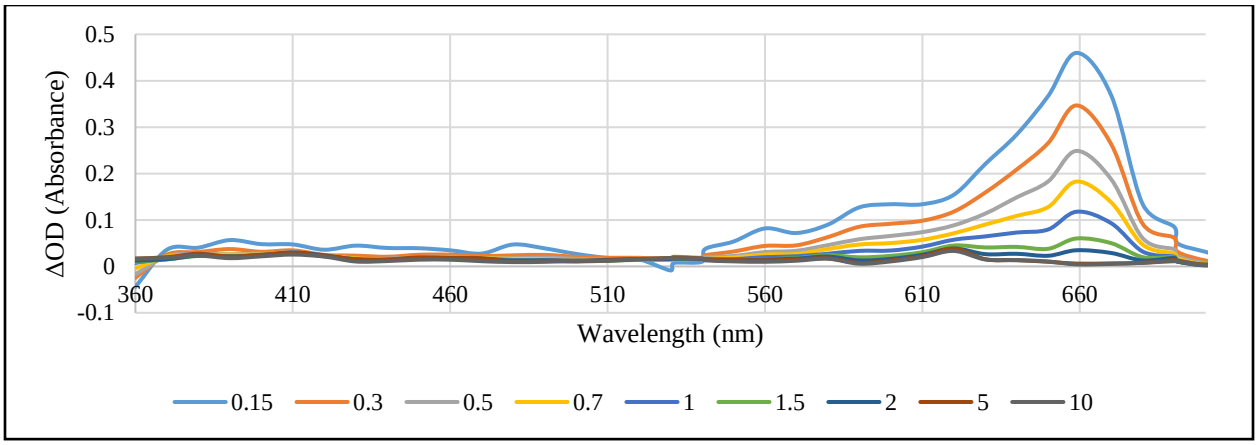

Figure 6.16. Transient spectra of 3,6-dibromocarbazolyl nitrenium ion **18** in DCM.

Generation of 3,6-dibromocarbazolyl radical (18c)

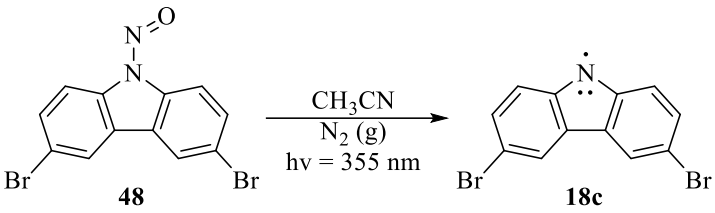

5 mg of 3,6-dibromo-9-nitrosocarbazole is added to 50 mL of CH_3CN in a 100 mL RBF.

The spectrum is obtained by the method described in Full Spectrum Solutions section above.

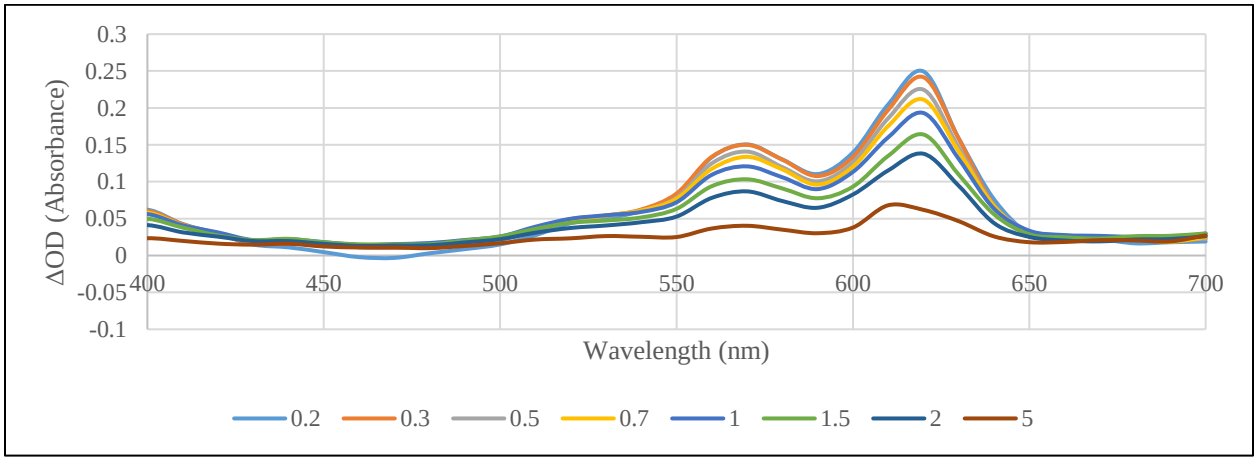

Figure 6.17. Transient spectra of 3,6-dibromocarbazolyl radical **18c** in CH_3CN.

Generation of 3,6-dibromocarbazolyl cation radical 18b

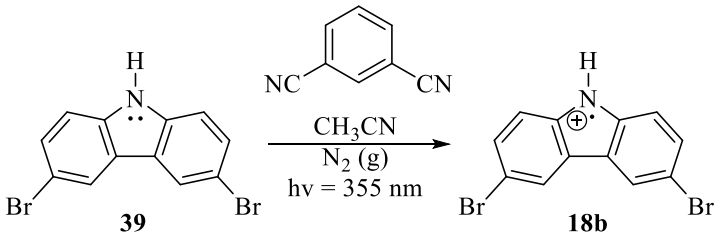

27 mg of 3,6-dibromocarbazole **39** and 57 mg of 1,3-dicyanobenzene is added to 80 mL of CH_3CN in a 100 mL RBF. The spectrum is obtained by the method described in Full Spectrum Solutions section above with N_2(g) purge.

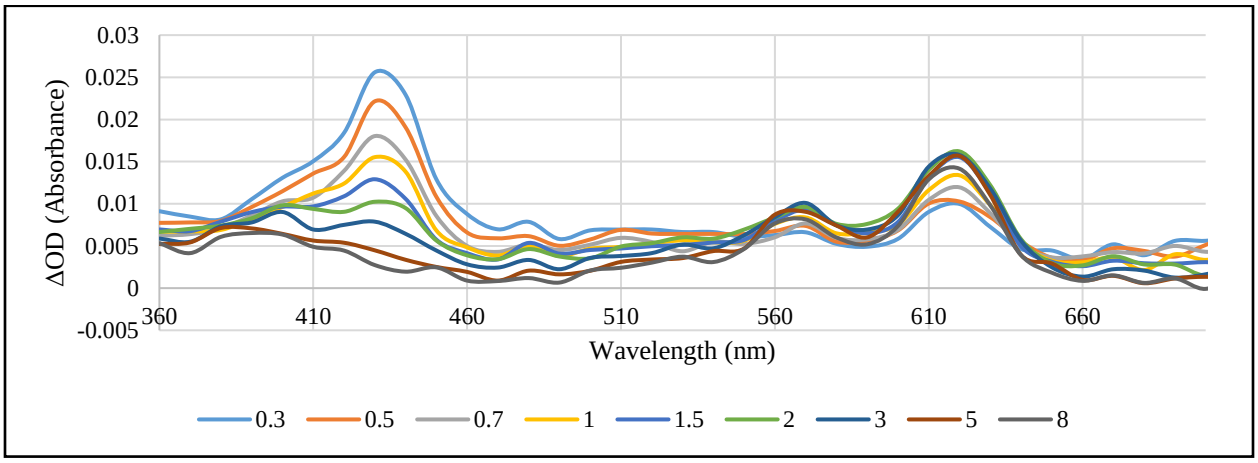

Figure 6.18. Transient Spectra of 3,6-dibromocarbazolyl cation radical **18b** in CH_3CN purged with N_2.

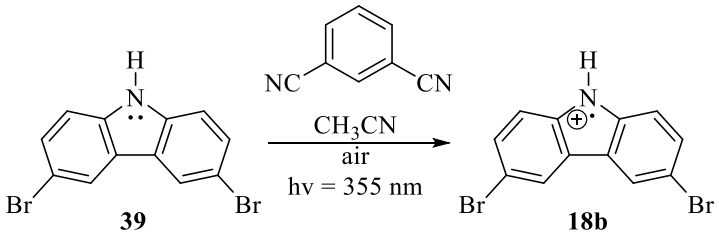

27 mg of 3,6-dibromocarbazole **39** and 57 mg of 1,3-dicyanobenzene is added to 80mL of CH_3CN in a 100 mL RBF. The spectrum is obtained by the LFP method describe above, but

instead of a purged flow system, static cuvettes open to the atmosphere were used for the air trial.

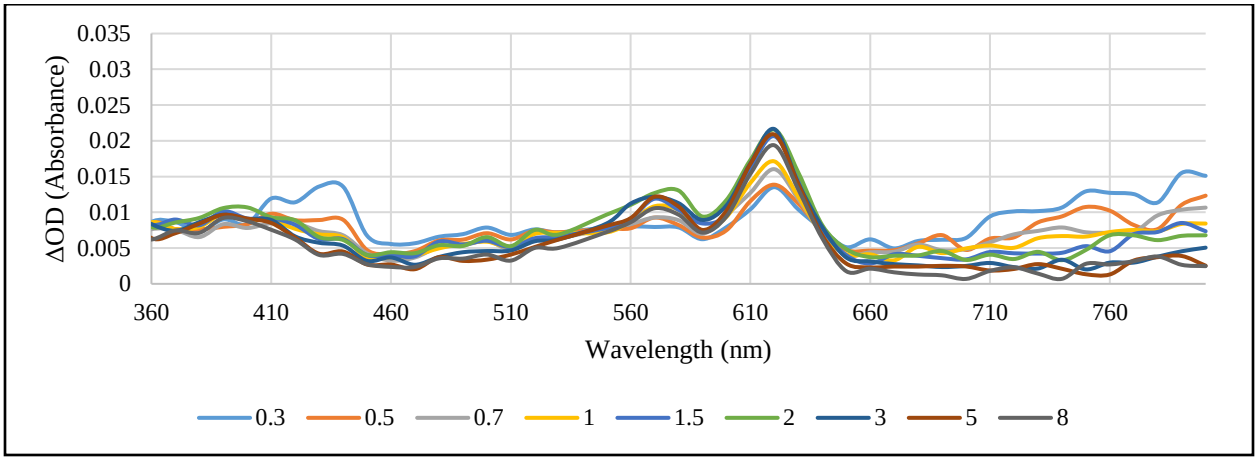

Figure 6.19. Transient Spectra of 3,6-dibromocarbazolyl cation radical **18b** in CH_3CN without purge.

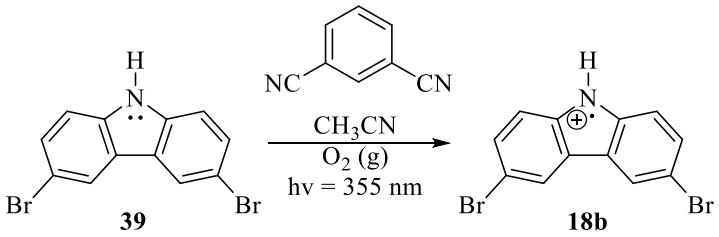

27 mg of 3,6-dibromocarbazole **39** and 57 mg of 1,3-dicyanobenzene is added to 80 mL of CH_3CN in a 100 mL RBF. The spectrum is obtained by the method described in Full Spectrum Solutions section above with O_2(g) purge.

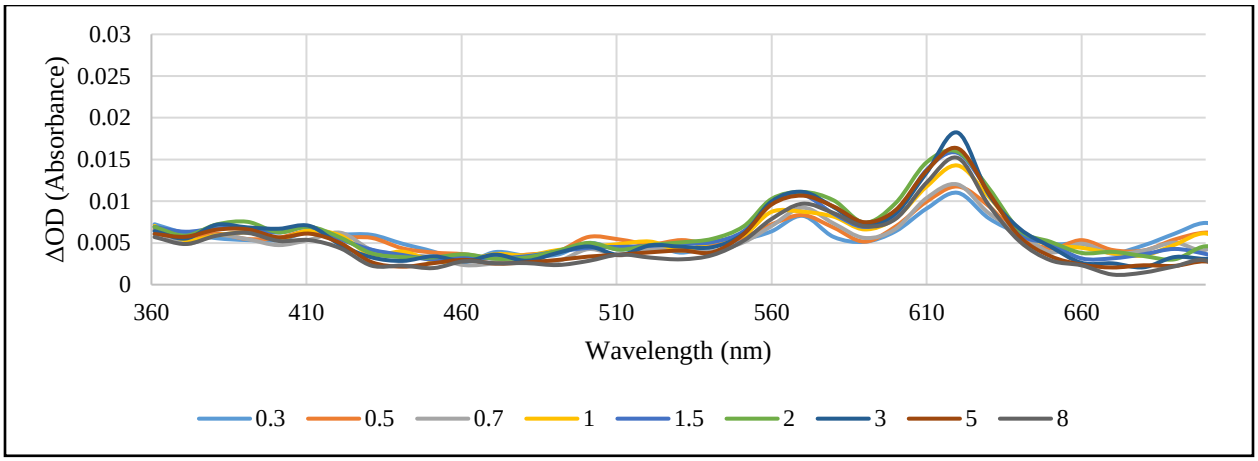

Figure 6.20. Transient Spectra of 3,6-dibromocarbazolyl cation radical **18b** in CH_3CN purged with O_2.

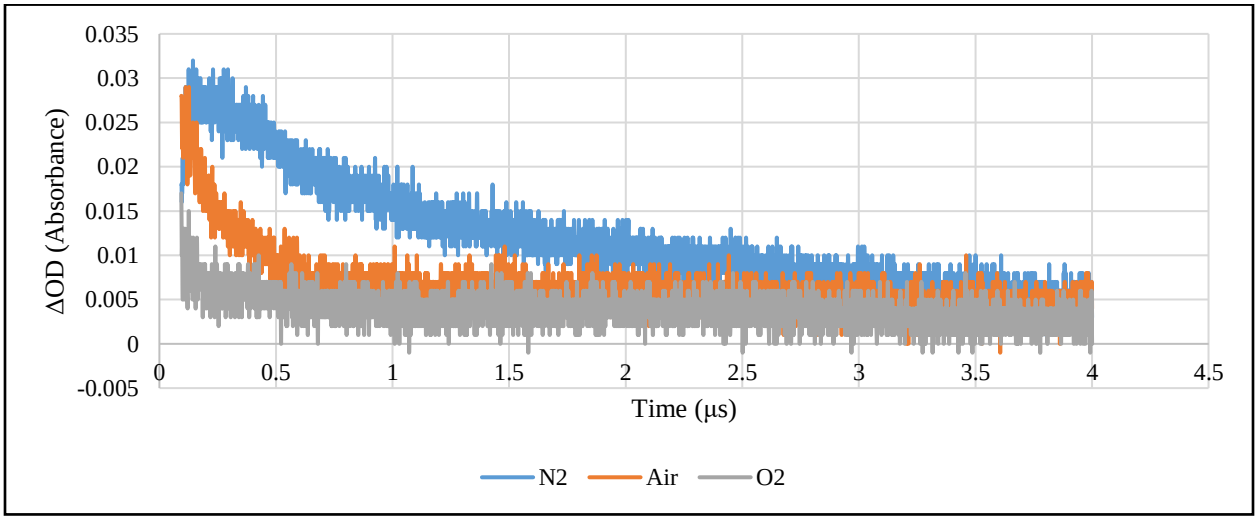

Figure 6.21. 1st order decays of 3,6-dibromocarbazolyl cation radical **18b** in different atmospheres at 430 nm.

Generation of 3,6-dibromocarbazolyl nitrenium ion 18 in the presence of DABCO

165 mg of (3,6-dibromocarbazolylamino)-2,4,6-trimethylpyridinium tetrafluoroborate **25** and 1 mL of 10 mM solution of DABCO in CH_3CN is added to 32 mL of CH_3CN in a 100 mL

RBF. The spectrum is obtained by the method described in Full Spectrum Solutions section above.

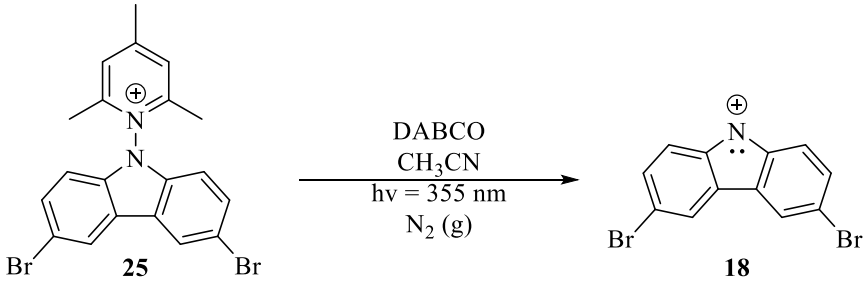

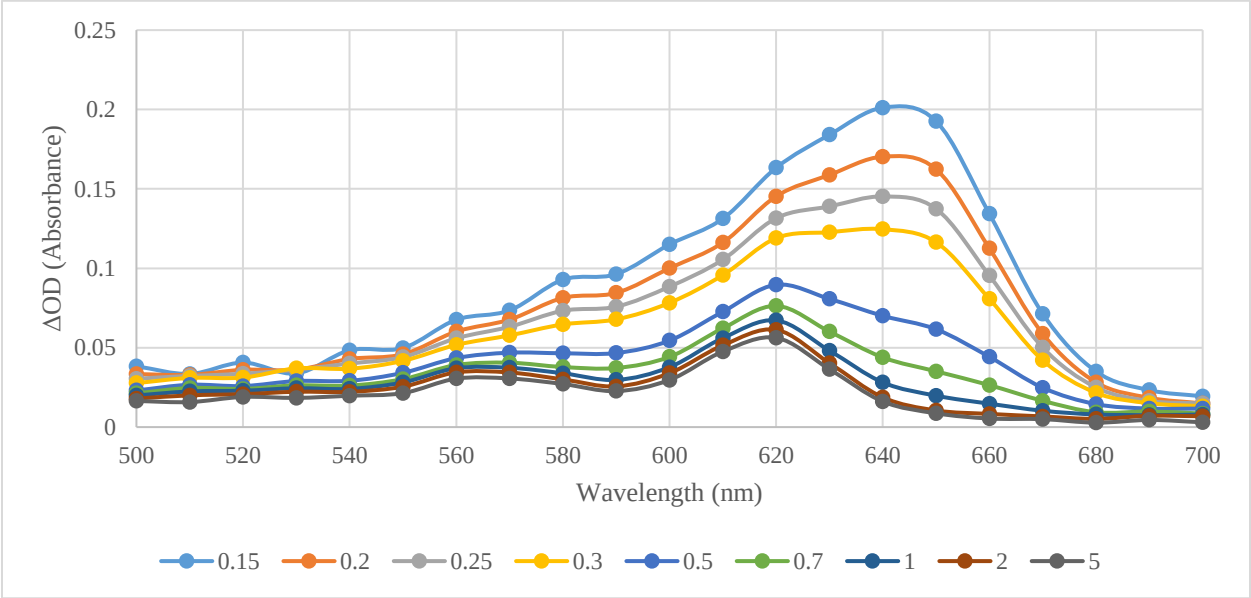

Figure 6.22. Transient Absorption Spectra of 3,6-dibromocarbazolyl nitrenium ion **18** quenched by 0.1mM DABCO. It can be seen that the nitrenium ion max at 640 nm decays to the radical maxes at 620 nm, and 560 nm.

6.4.3 Kinetic Data from LFP

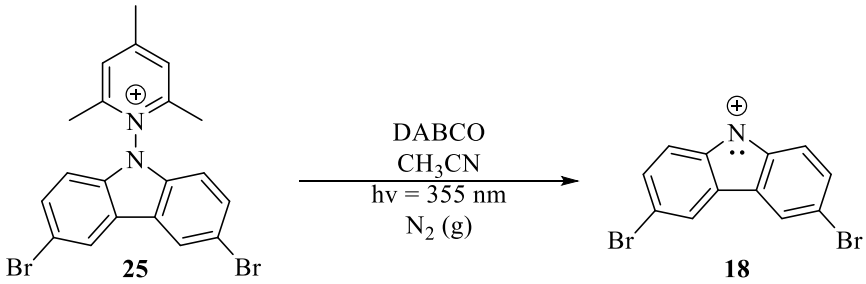

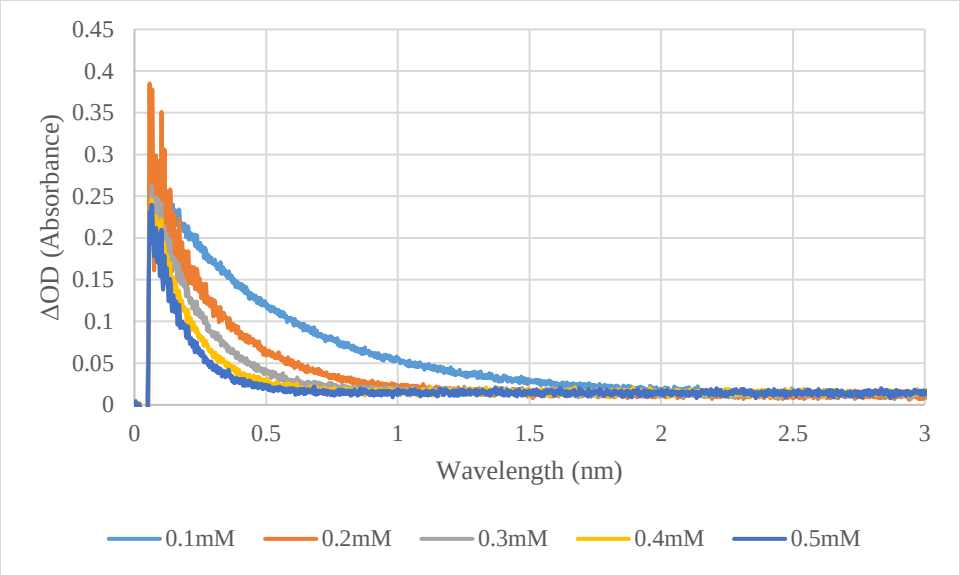

Figure 6.23. 3,6-dibromocarbazolyl nitrenium ion **18** being trapped by DABCO.

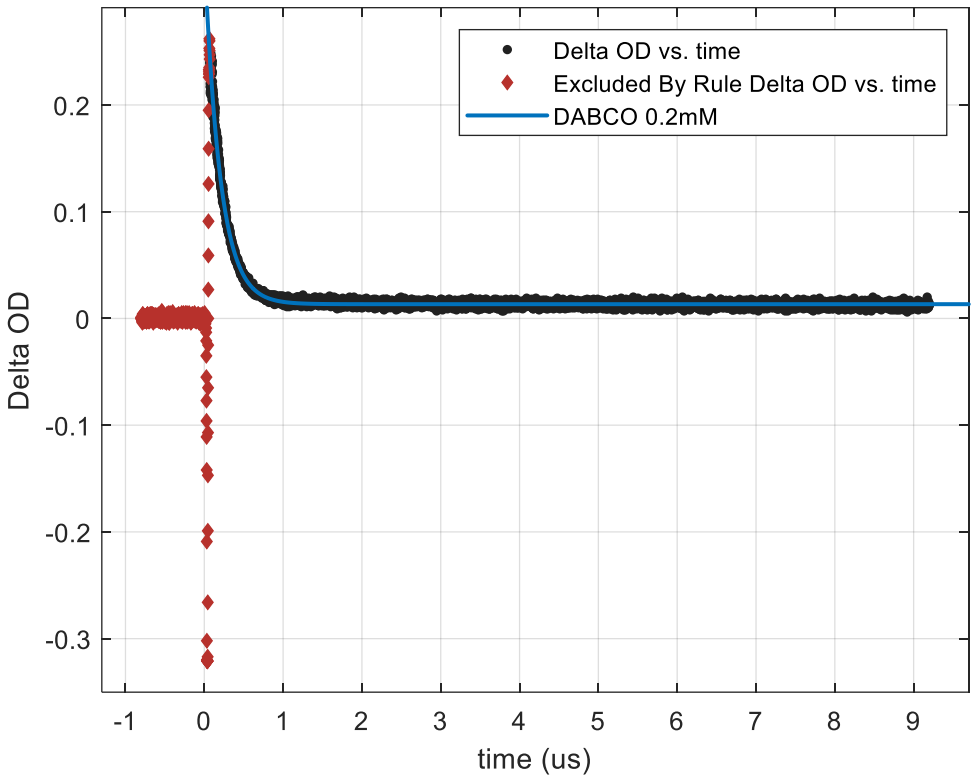

Figure 6.24. 3,6-dibromocarbazolyl nitrenium ion **18** being trapped by DABCO Matlab Fitting.

Fit Name: DABCO 0.2mM

Custom Curve Fit
f(x) = a*exp(-b*x)+c

Coefficients and 95% Confidence Bounds

	Value	Lower	Upper
a	0.3305	0.3291	0.3318
b	5.0208	4.9997	5.0419
c	0.0134	0.0133	0.0134

Goodness of Fit

	Value
SSE	0.054
R-square	0.9897
DFE	9127
Adj R-sq	0.9897
RMSE	0.0024

.

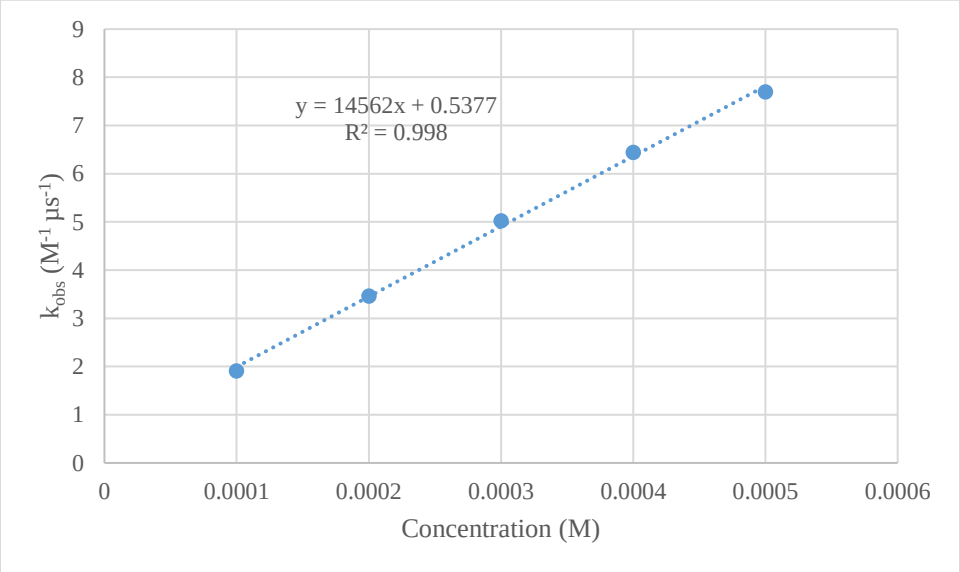

Figure 6.25. Determining 2nd order rate constant for 3,6-dibromocarbazolyl nitrenium ion **18** and DABCO.

6.4.4 Mechanistic Considerations for Dimer Formation in the Absence of Trap

Fluorine NMR Procedure

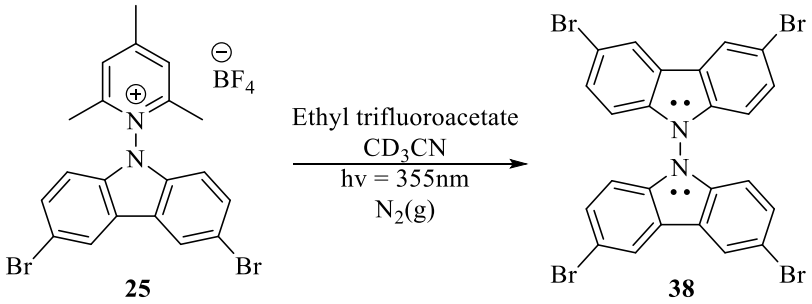

10 mg of (3,6-dibromocarbazolylamino)-2,4,6-trimethylpyridinium tetrafluoroborate **25** and 20 μL of ethyl trifluoroacetate were combined with 400 μL of CD_3CN. ^1H NMR was monitored to ensure complete conversion of (3,6-dibromocarbazolylamino)-2,4,6-trimethylpyridinium tetrafluoroborate **25** to dimer **38**. ^{19}F NMR was used to monitor the BF_4^- during the reaction. 370 nm Kessil lamps were used at full power to photolyze the solution in an NMR tube for 80 minutes. Ethyl trifluoroacetate has a literature reference chemical shift of -75.8ppm.[138] The BF_4^- peak varies by 0.06 ppm during the course of the reaction which is within the acceptable range for ^{19}F NMR shifts with an internal standard.[139]

Kinetic Isotope Effect Experiments

CH_3CN/CD_3CN

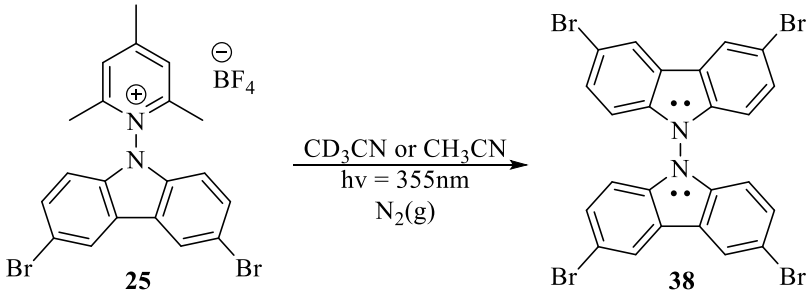

25 mg of 3,6-dibromocarbazolylamino)-2,4,6-trimethylpyridinium tetrafluoroborate **25** is added to 3 mL of either CH_3CN or CD_3CN with a stir bar in a quartz cuvette. The cuvette was sealed with a septum and parafilm and purged with $N_2(g)$ for 15 min in the solution and 5 min in the air gap. The solutions were analyzed with the procedure outlined in the Transient Absorption

Spectroscopy section above. There was no significant difference if new CH_3CN or distilled CH_3CN is used.

Phenol/d1-Phenol

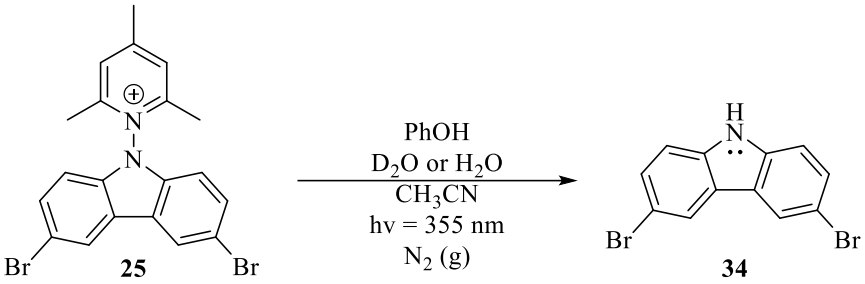

25 mg of 3,6-dibromocarbazolylamino)-2,4,6-trimethylpyridinium tetrafluoroborate **25** is added to 3 mL of CH_3CN with a H_2O or D_2O concentration of 10mM and PhOH concentration of 1 mM with a stir bar in a quartz cuvette. The cuvette is allowed to stir for 30 minutes to ensure that the D_2O converts the phenol to d1-phenol. The solutions were analyzed with the procedure outlined in the Transient Absorption Spectroscopy section above. There was no significant difference in k_{obs} from the 10 mM H_2O and D_2O solutions if the H_2O or D_2O concentration was raised to 170 mM

Ruling out counter ion BF_4^- from being a reducing agent.

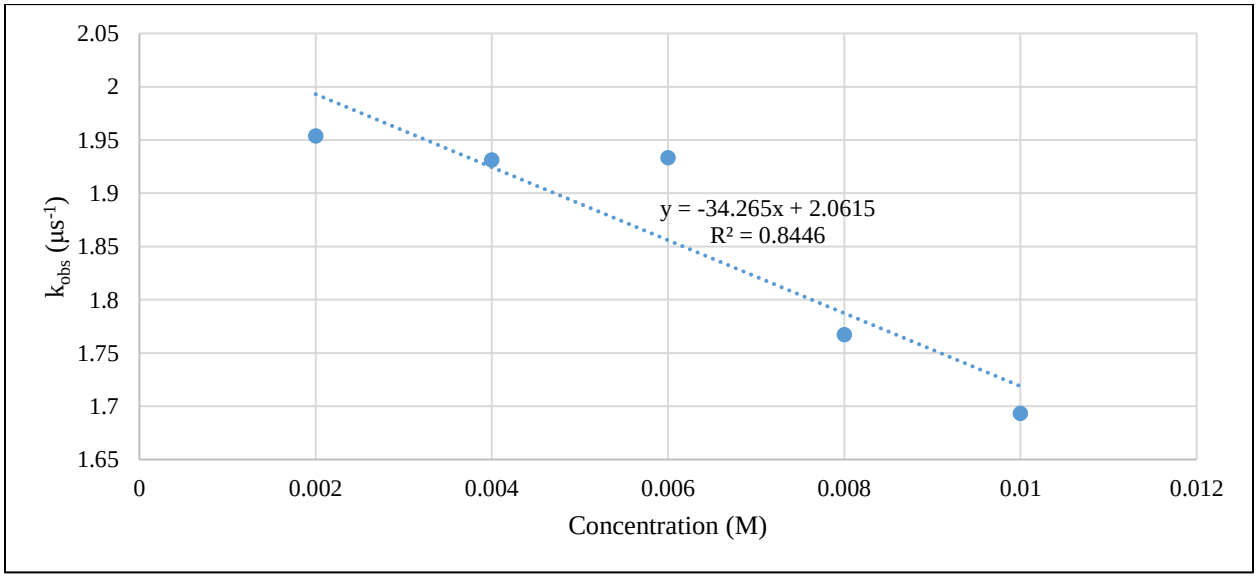

Figure 6.26. LFP 3,6-dibromocarbazolyl nitrenium ion **18** with added tetrabutylammonium tetrafluoroborate.

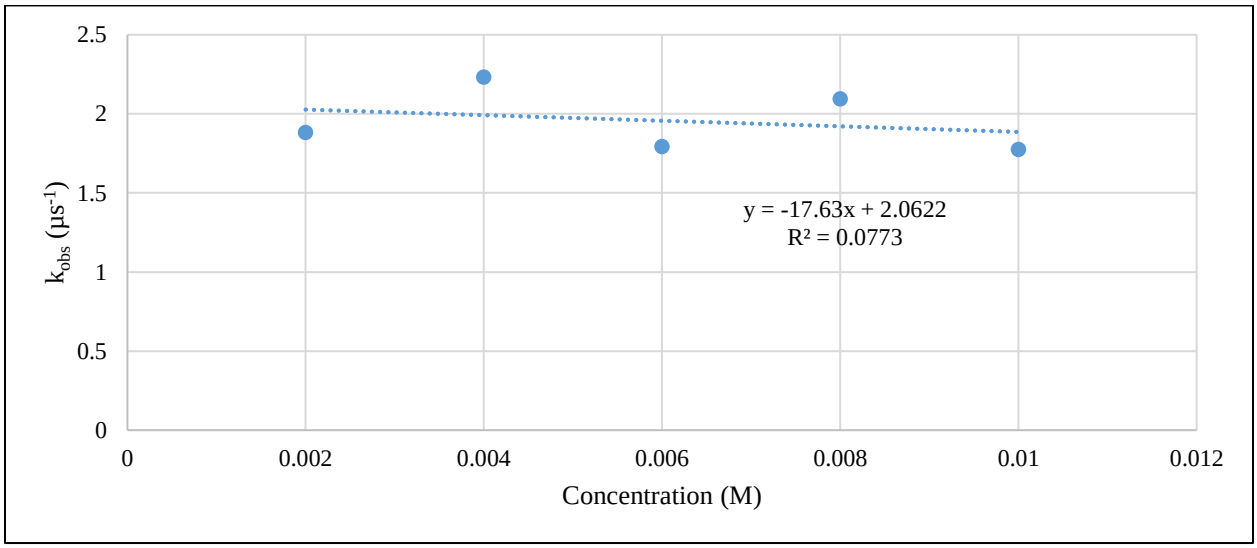

Figure 6.27. LFP of 3,6-dibromocarbazolyl nitrenium ion **18** with added tetrabutylammonium perchlorate.

6.4.5 NMR Yield Analysis

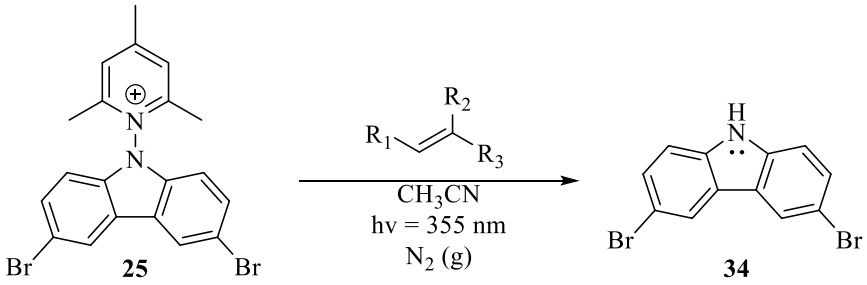

20 mg of (3,6-dibromocarbazolylamino)-2,4,6-trimethylpyridinium tetrafluoroborate **25** (0.0375 mmol) and 0.375 mmol of alkene is added to 2 mL of CH_3CN. The solution is split into two 1mL solutions and both are purged with N_2(g) for 15 min. One of the solutions is photolyzed for 30 min with 370 nm Kessil lamps. Both solutions are evaporated. 350 µL of $CDCl_3$ is added to each solution and ^{1}H NMR is used to determine the yields of products. The yields are compared to the $CDCl_3$ peak used to dissolve the ^{1}H NMR samples.

6.5 Chapter 5 Experimental

6.5.1 Synthesis and General Methods

The *N*-(4,4'-dibromodiphenylamino)-2,4,6-trimethylpyridinium ion **44** was synthesized using the same procedure used in our previous publication.[17]

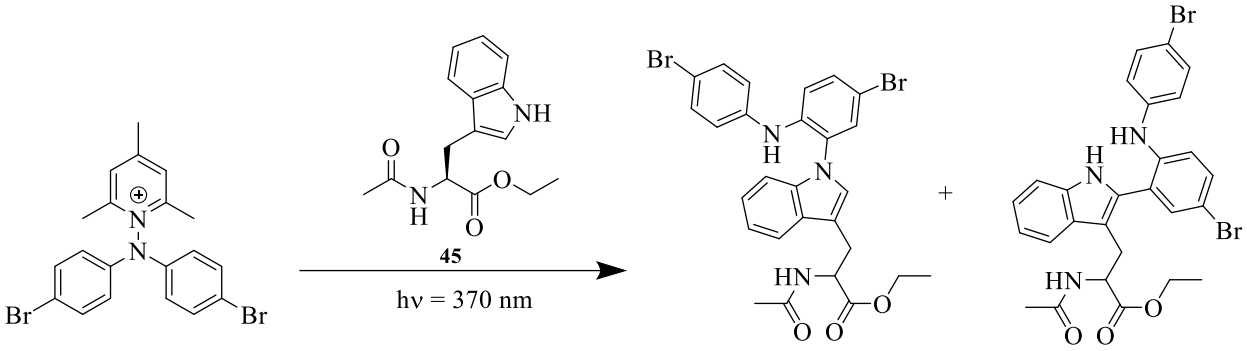

44 **46** **47**

N-Acetyl-L-tryptophan ethyl ester **45** (0.80 g, 2.9 mmol) and **44** (0.31 g 0.59 mmol) are added to 30 mL of CH_3CN and photolyzed for 2 hr with 370 nm Kessil lamps. The reaction was stopped when ESI-MS showed that the pyridinium ion was consumed. Next a silica column was run with a solvent mixture of 60:40 hexane:ethyl acetate. Two major adducts were isolated and identified by ^{1}H NMR, ^{13}C NMR, HSQC NMR, and Accutof ESI^{+} MS.

Compound **46**

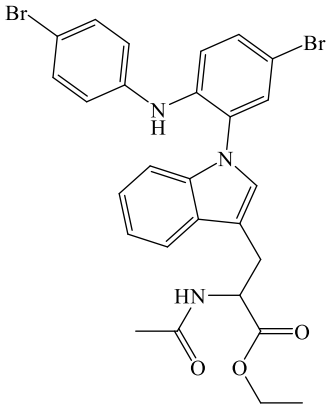

^{1}H NMR (CD_3CN, 600 MHz): δ 7.55 (d, 2H, J = 0.014ppm), 7.50 (d, 1H, *J* = 0.004ppm), 7.40 (d, 1H, *J* = 0.014ppm), 7.26 (d, 1H, *J* = 0.014ppm), 7.24 (dd, 1H, *J* = 0.014ppm, 0.004ppm), 7.06 (t, 1H), 6.92 (d, 1H), 6.79 (t, 1H), 6.63 (t, 1H), 6.07 (d, 1H), 4.25 (m, 1H), 3.97-4.07 (m, 2H,), 2.73 (dd, 1H,), 2.29 (dd, 1H,), 1.51 (s, 3H,), 1.20 (t, 3H,)

^{13}C NMR (CD_3CN, 600 MHz): δ 172.94, 170.66, 150.35, 142.44, 137.46, 133.35, 133.14, 132.87, 131.76, 129.53, 127.79, 124.31ppm, 122.50, 120.31, 115.61, 112.11, 111.75, 110.71, 88.38, 62.20, 58.86, 50.76, 39.87, 22.47, 14.43

ESI-MS m/z 599.92

Compound **47**

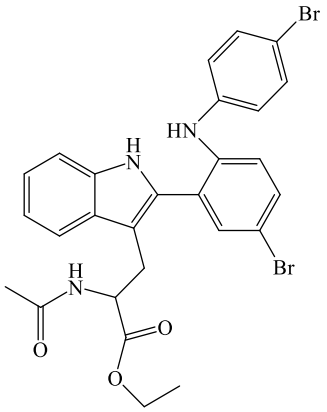

^{1}H NMR (CD_3CN, 600 MHz): δ 7.61 (d, 1H, J = 0.020ppm), 7.53 (d, 1H, *J* = 0.006ppm), 7.46 (dd, 1H, *J* = 0.022ppm, *J* = 0.006ppm), 7.38 (d, 2H, *J* = 0.022ppm), 7.31 (d, 1H, *J* = 0.022ppm), 7.18 (t, 1H, J = 0.020ppm), 7.11 (t, 1H, 0.020ppm), 7.05 (d, 2H, J = 0.022ppm), 6.64 (broad s, 1H), 6.57 (d, 1H), 4.53 (m, 1H), 3.88-4.03 (m, 2H,), 3.25 (dd, 1H,), 3.09 (dd, 1H,), 1.61 (s, 3H,), 1.11 (t, 3H,)

^{13}C NMR (CD_3CN, 600 MHz): δ 171.03, 168.96, 141.57, 141.06, 135.96, 133.80, 131.55, 131.44, 131.10, 128.18, 123.90, 121.58, 120.00, 118.71, 118.34, 117.85, 112.10, 111.27, 110.61, 109.04, 60.45, 52.52, 26.60, 21.24, 12.77

ESI-MS m/z 600.08

The peptide WWCNDGR was custom made and purchased from the Genscript company. A 100 μL of 90% CH_3CN, 10% H_2O solvent mixture was used to make a 1.8 mM peptide concentration and a 12.25 mM of compound **44** concentration. This solution was photolyzed for 30 s with 370 nm kessel lamps. After photolysis the solutions were evaporated with a speed vacuum. The supernatant was washed twice with 50 μL of CH_3CN was added to the Eppendorf tube then decanted. Since the peptide is insoluble in CH_3CN, 300 μL of H_2O was added and 20μL of CH_3CN was added to make the final solution for QTOF Mass Spectrometry analysis.

Samples were analyzed with a Bruker Maxis-II QTOF, an ultra-high resolution Q-TOF mass spectrometer coupled with a Waters Acquity I-Class PLUS LC system. Liquid chromatography separation was performed on an Agilent Zorbax XDB-C18 LC Column (50 x 2.1 mm, 5 μm particle size) with a mobile phase A (water with 0.1% formic acid) and mobile phase B (acetonitrile with 0.1% formic acid). The gradient program was initially set at 10% B in 3 minutes. The linear gradient increased to 90% B in 6 minutes followed by maintenance of 3 minutes before returning to 10% in 1 minute. The column was kept at 30°C. The flow rate was 0.25 ml/min and the injection volume was 5 μl. Mass spectra were acquired under positive electrospray ionization with a needle voltage of 4,500 V. The mass range from 250 to 2000 Da was used for the LC-MS measurements, and from 100 to 1400 Da for the LC-MS/MS, respectively. The ion source temperature (dry gas) was set to 220°C with a flow rate of 5.0

L/min. The collision energy used for the LC-MS/MS measurements was from 25 to 50 eV, depending on the m/z values of the parent ions. All data were visualized and analyzed using the Bruker Compass Analysis software.

6.5.2 Methods and Transient Absorption Spectra from LFP

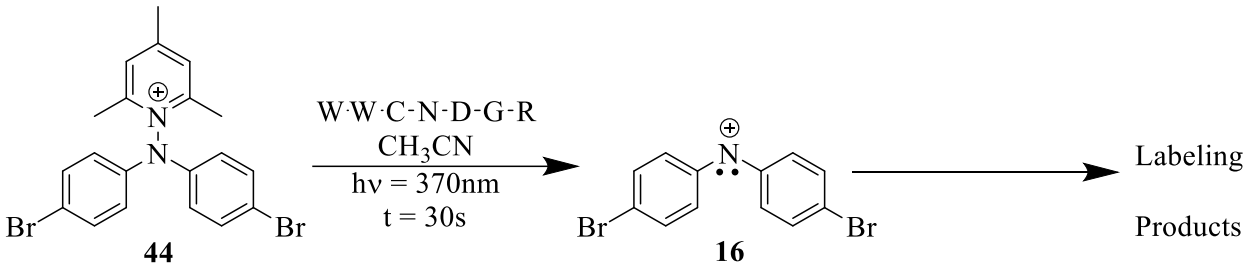

20 mg of *N*-(4,4'-dibromodiphenylamino)-2,4,6-trimethylpyridinium ion and **44** 9.36 mg of peptide WWCNDGR is added to 20 mL of CH_3CN in a 100mL RBF. The spectrum is obtained by the method described in Full Spectrum Solutions section above.

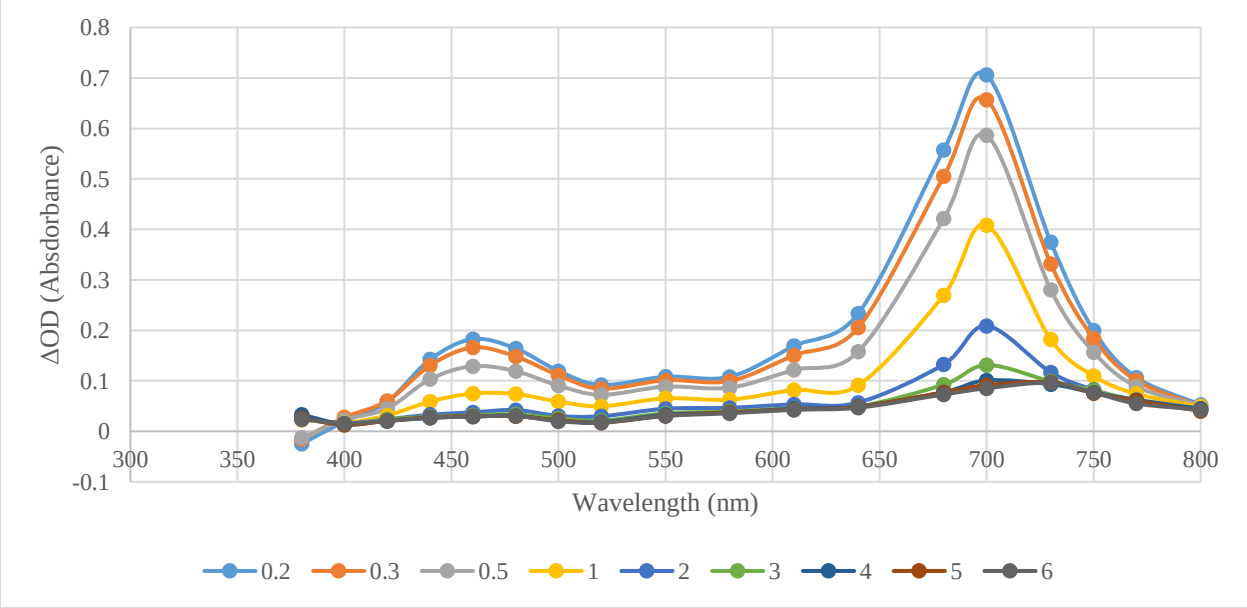

Figure 6.28. Transient Absorption Spectra of nitrenium ion **16** with peptide WWCNDGR concentration of 0.5mM. The spectra match the nitrenium ion spectra previously published.[17] Time slices are in μs.

6.5.3 ESI MS^+ Labeling and MS/MS

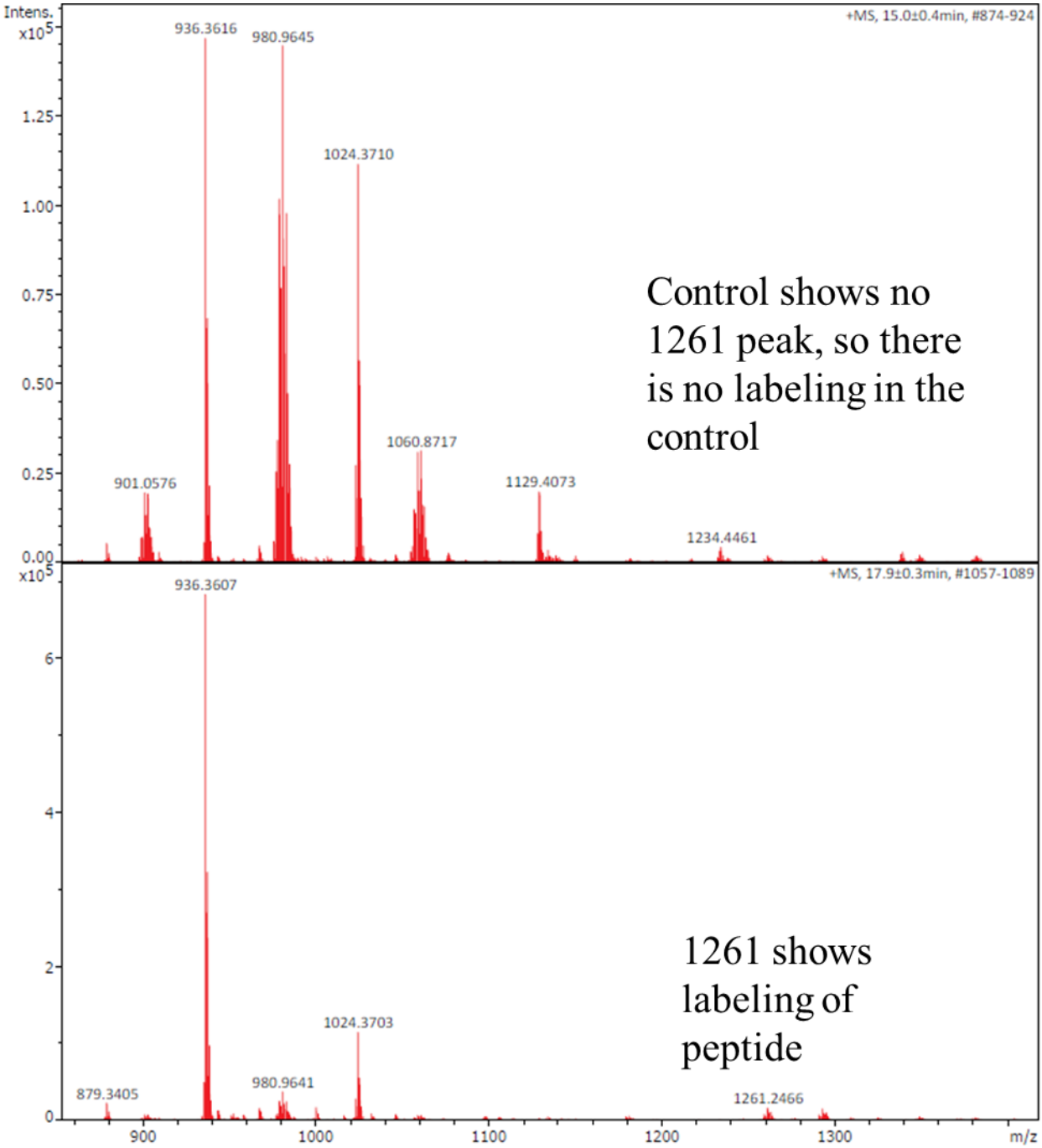

Figure 6.29. ESI^+-MS shows that the peptide was labeled at m/z 1261.27 (bottom) which is not seen in the control (top).

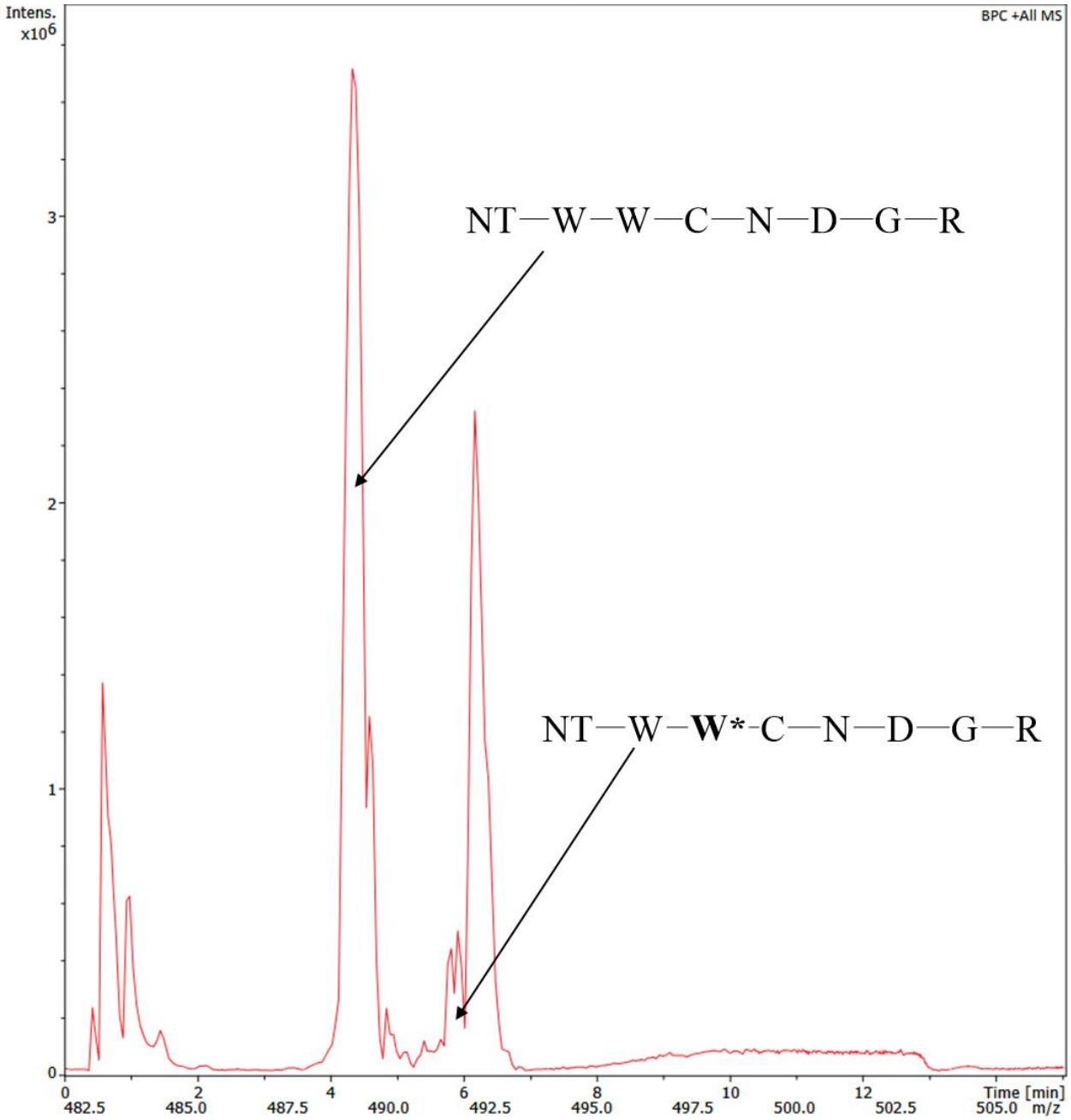

Figure 6.30. Chromatogram Showing Separation of Peptide Solution for MS/MS.

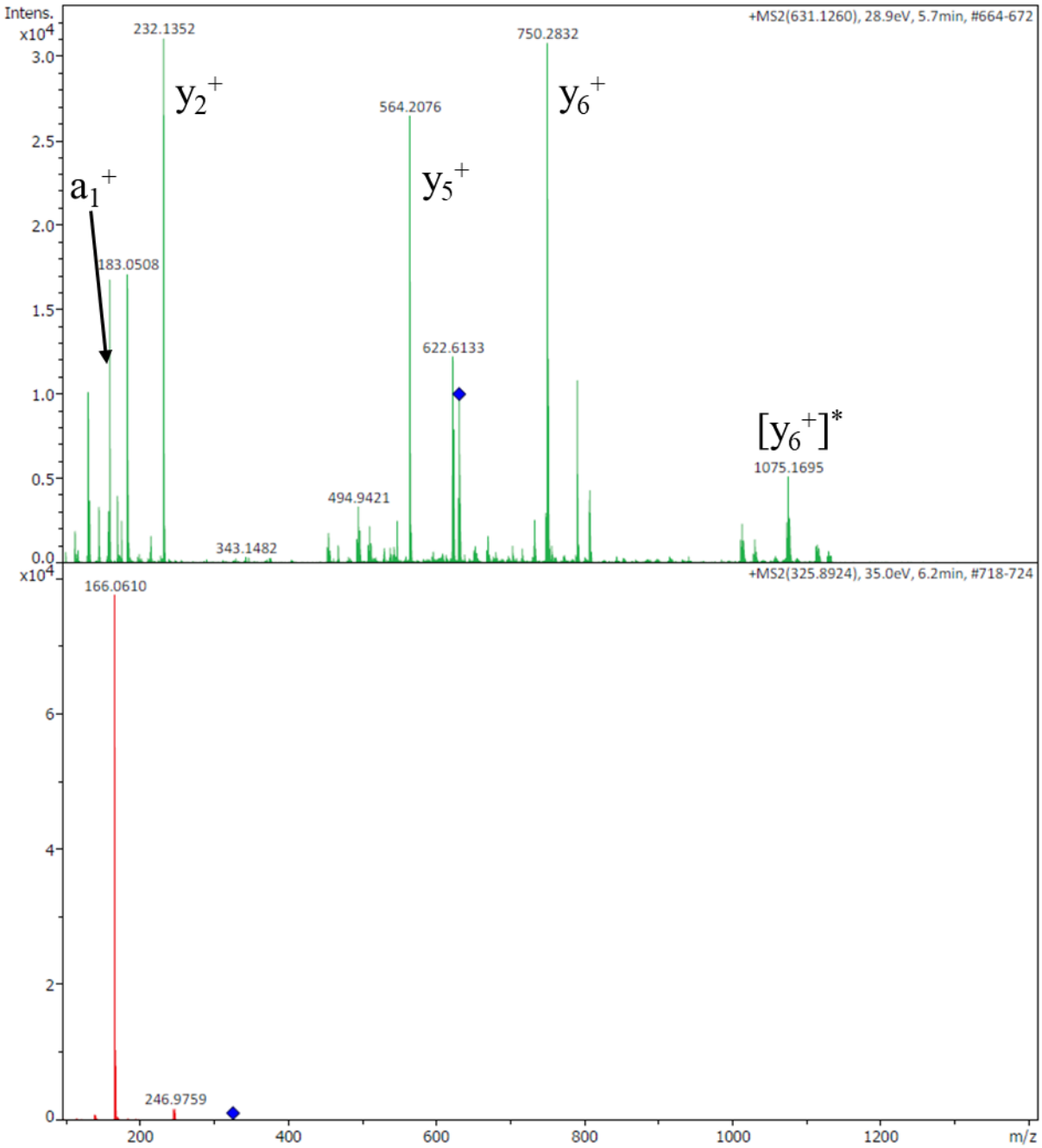

Figure 6.31. MS/MS Control shows that the nitrenium ion **16** (bottom) does not fragment to make any important peptide fragments (top).

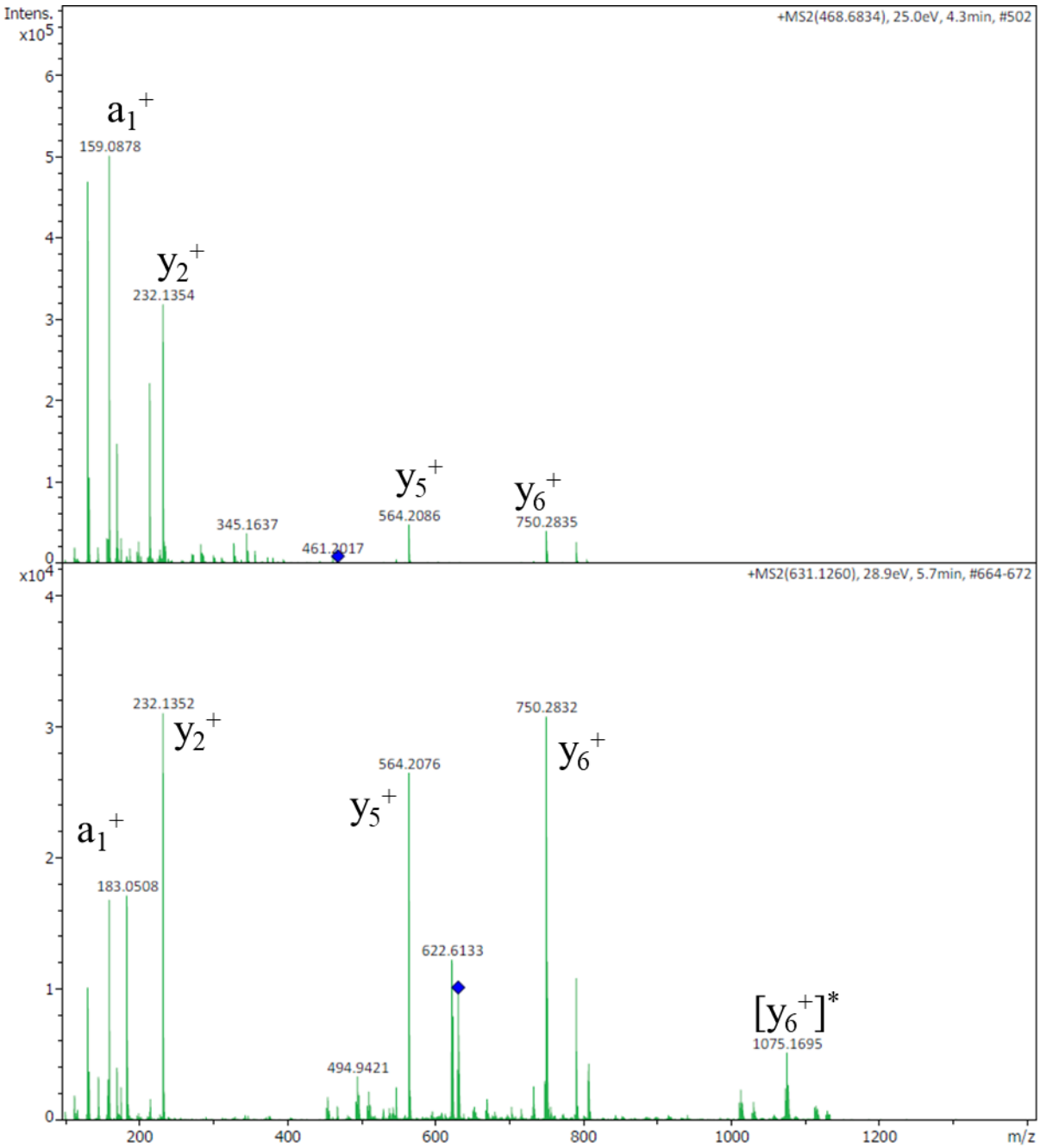

Figure 6.32. MS/MS Full Spectrum of the peptide m/z 468.68 (top) and the labeled peptide m/z 631.14 (bottom). All fragments are labeled.

6.5.4 Simulated Isotopic Distribution of Labeled Peptide

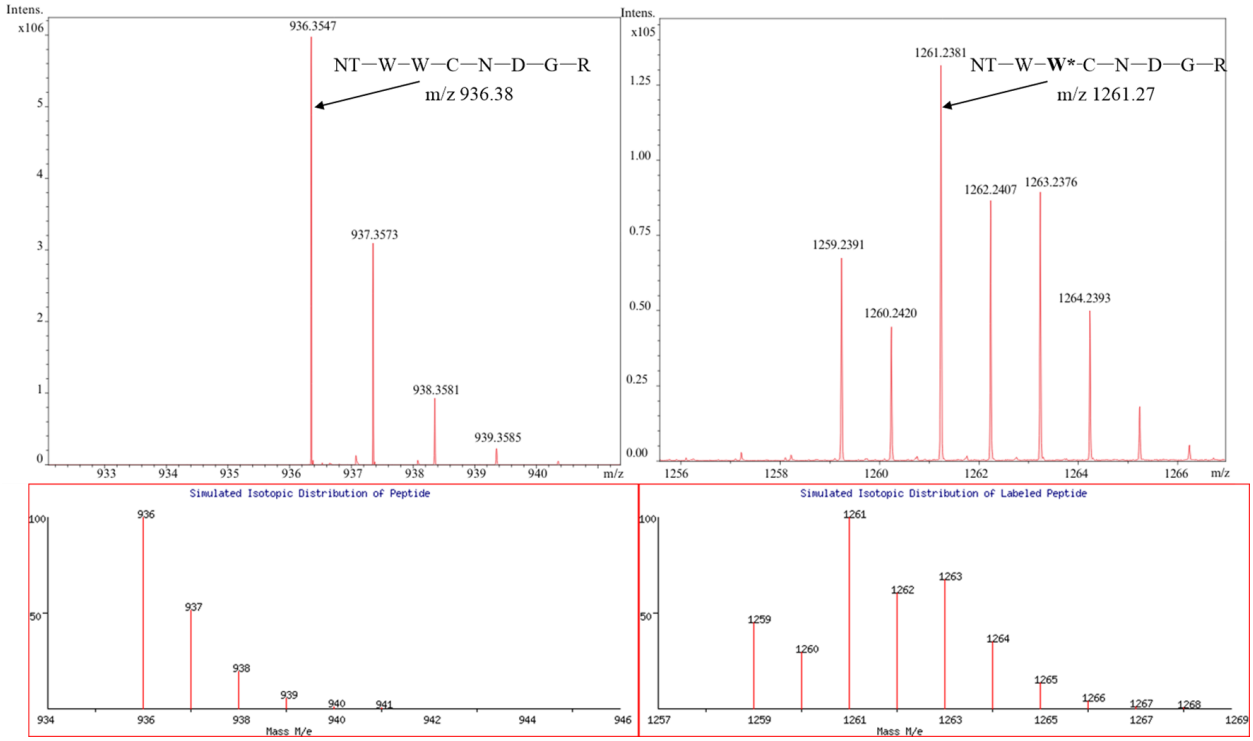

Figure 6.33. Comparison of peptide and peptide labeling to computer generated isotopic distributions. Simulated data was done with Scientific Instrument Services (SIS)'s Isotope Distribution Calculator and Mass Spec Plotter.

References

(1) Falvey, D. E. Nitrenium Ions. In *Reactive Intermediate Chemistry*; Moss, R. A., Platz, M. S., Jones Jr., M., Eds.; John Wiley And Sons, Inc.: Hoboken, 2004; pp 593–650.

(2) Falvey, D. E. Electronic Properties of Nitrenium Ions. In *Nitrenes And Nitrenium Ions*; Falvey, D. E., Gudmundsdottir, A. D., Eds.; John Wiley And Sons, Inc.: New York, 2013; Vol. 6, pp 191–216.

(3) Novak, M.; Rajagopal, S. N-Arylnitreniurn Ions. *Adv Phys Org Chem* **2001**, *36*, 167–254. https://doi.org/10.1016/S0065-3160(01)36005-7.

(4) Novak, M.; Zhang, Y. Antitumor Drugs And Nitrenium Ions. *Adv. Phys. Org. Chem.* **2012**, *46*, 121–164.

(5) Zhu, P.; Ong, S. Y.; Chan, Y.; Poon, Y. F.; Leung, K. H.; Phillips, D. L. Transient-Resonance Raman and Density Functional Theory Investigation of 4-Biphenylylnitrenium, 2-Fluorenylnitrenium, and Diphenylnitrenium Ions. *Chemistry - A European Journal* **2001**, *7* (22), 4928–4936. https://doi.org/10.1002/1521-3765(20011119)7:22.

(6) Srivastava, S.; Toscano, J. P. Experimental Confirmation of the Iminocyclohexadienyl Cation-like Structure of Arylnitrenium Ions: Time-Resolved IR Studies of Diphenylnitrenium Ion [9]. *J Am Chem Soc* **1997**, *119* (47), 11552–11553. https://doi.org/10.1021/JA9729342/ASSET/IMAGES/LARGE/JA9729342F00003.JPEG.

(7) Moran, R. J.; Falvey, D. E. Singlet And Triplet State Dynamics of Diphenylnitrenium Ions. *Abstracts of Papers of the American Chemical Society* **1997**, *214*, 151-ORGN.

(8) McIlroy, S.; Falvey, D. E. Reactions of Nitrenium Ions with Arenes: Laser Flash Photoylsis Detection of a σ-Complex between N,N-Diphenylnitrenium Ion and

Alkoxybenzenes [1]. *J Am Chem Soc* **2001**, *123* (45), 11329–11330. https://doi.org/10.1021/JA016557B/ASSET/IMAGES/LARGE/JA016557BH00001.JPEG .

(9) McIlroy, S.; Moran, R. J.; Falvey, D. E. Photogenerated Nitrenium Ions: A Search for Triplet-State Reactivity in the Chemistry of the Diphenylnitrenium Ion. *Journal of Physical Chemistry A* **2000**. https://doi.org/10.1021/jp002756q.

(10) Chinn, E. S.; Falvey, D. E. Photochemical Generation and Characterization of the 5-Endo-10,11-Dihydrodibenzoazepine Nitrenium Ion. *Photochemical & Photobiological Sciences* **2022**, *21*, 1907–1914.

(11) Winter, A. H.; Gibson, H. H.; Falvey, D. E. Carbazolyl Nitrenium Ion: Electron Configuration and Antiaromaticity Assessed by Laser Flash Photolysis, Trapping Rate Constants, Product Analysis, and Computational Studies. *Journal of Organic Chemistry* **2007**. https://doi.org/10.1021/jo0708184.

(12) Winter, A. H.; Falvey, D. E.; Cramer, C. J. Effect of Meta Electron-Donating Groups on the Electronic Structure of Substituted Phenyl Nitrenium Ions. *J Am Chem Soc* **2004**, *126* (31), 9661–9668. https://doi.org/10.1021/JA047677X/SUPPL_FILE/JA047677XSI20040422_100730.PDF.

(13) Winter, A. H.; Thomas, S. I.; Kung, A. C.; Falvey, D. E. Photochemical Generation of Nitrenium Ions from Protonated 1,1-Diarylhydrazines. **2004**. https://doi.org/10.1021/ol048250y.

(14) Qiu, Y.; Du, L.; Cady, S. D.; Phillips, D. L.; Winter, A. H. Optical and EPR Detection of a Triplet Ground State Phenyl Nitrenium Ion. *J Am Chem Soc* **2024**, *146* (15), 10679–10686. https://doi.org/10.1021/JACS.4C00511/SUPPL_FILE/JA4C00511_SI_001.PDF.

(15) Moran, R. J.; Cramer, C.; Falvey, D. E. Reactions of Diarylnitrenium Ions with Electron Rich Alkenes: An Experimental and Theoretical Study. *Journal of Organic Chemistry* **1997**, *62* (9), 2742–2751. https://doi.org/10.1021/JO9623649/SUPPL_FILE/JO2742.PDF.

(16) Fishbein, J. C.; McClelland, R. A. Azide Ion Trapping of the Intermediate in the Bamberger Rearrangement. Lifetime of a Free Nitrenium Ion in Aqueous Solution. *J Am Chem Soc* **1987**, *109* (9), 2824–2825. https://doi.org/10.1021/JA00243A045/ASSET/JA00243A045.FP.PNG_V03.

(17) Thomas, S. I.; Falvey, D. E. N,N-Di(4-Halophenyl)Nitrenium Ions: Nucleophilic Trapping, Aromatic Substitution, and Hydrogen Atom Transfer. *Journal of Organic Chemistry* **2007**. https://doi.org/10.1021/jo062578i.

(18) Takeuchi, H.; Hayakawa, S.; Tanahashi, T.; Kobayashi, A.; Adachi, T.; Higuchi, D. *Novel Generation of Parent, Alkyl, Dialkyl and Alicyclic Nitrenium Ions in Photolyses of Pyrid i Ni Um, Quinol in Ium, B Ipyrid i Nium and Phenant Hrol i Nium Salts and Aromatic A/-Substitution by Nitrenium Lonst*; 1991; Vol. 2.

(19) Gibson, S. T.; Greene, J. P.; Berkowitz, J. Photoionization of the Amidogen Radical. *J Chem Phys* **1985**, *83* (9), 4319–4328. https://doi.org/10.1063/1.449045.

(20) Van Huis, T. J.; Leininger, M. L.; Sherrill, C. D.; Schaefer, H. F. Full Configuration Interaction Energies, Geometries, and Quartic Force Fields of the Nitrenium Ion. *Collect Czechoslov Chem Commun* **1998**, *63* (8), 1107–1142. https://doi.org/10.1135/CCCC19981107.

(21) Stephens, J. C.; Yamaguchi, Y.; Schaefer, H. F. The Adiabatic and Vertical Ionization Potentials of NH2 to the Three Lowest-Lying States of NH2+. *Journal of Molecular*

Structure: THEOCHEM **1999**, *461–462*, 41–53. https://doi.org/10.1016/S0166-1280(98)00420-5.

(22) Falvey, D. E. Discrete Existence of Singlet Nitrenium Ions Revisited: Computational Studies of Non-Aryl Nitrenium Ions and Their Rearrangements. *ACS Omega* **2018**, *3* (8), 10418–10432. https://doi.org/10.1021/ACSOMEGA.8B01038/SUPPL_FILE/AO8B01038_SI_001.PDF.

(23) Yang, Z. Z.; Qi, S. F.; Zhao, D. X.; Gong, L. D. Insight into Mechanism of Formation of C8 Adducts in Carcinogenic Reactions of Arylnitrenium Ions with Purine Nucleosides. *Journal of Physical Chemistry B* **2009**, *113* (1), 254–259. https://doi.org/10.1021/JP804128S/SUPPL_FILE/JP804128S_SI_001.PDF.

(24) Yang, Z. Z.; Qi, S. F. Mechanism of Direct Conversion between C8 Adducts and N7 Adducts in Carcinogenic Reactions of Arylnitrenium Ions with Purine Nucleosides: A Theoretical Study. *Journal of Physical Chemistry B* **2007**, *111* (47), 13444–13450. https://doi.org/10.1021/JP0765143/SUPPL_FILE/JP0765143SI20070911_031542.PDF.

(25) Stavros, K. M.; Hawkins, E. K.; Rizzo, C. J.; Stone, M. P. Base-Displaced Intercalation of the 2-Amino-3-Methylimidazo[4,5-f]Quinolone N2-DG Adduct in the NarI DNA Recognition Sequence. *Nucleic Acids Res* **2014**, *42* (5), 3450–3463. https://doi.org/10.1093/NAR/GKT1109.

(26) Skipper, P. L.; Kim, M. Y.; Patty Sun, H. L.; Wogan, G. N.; Tannenbaum, S. R. Monocyclic Aromatic Amines as Potential Human Carcinogens: Old Is New Again. *Carcinogenesis* **2010**, *31* (1), 50–58. https://doi.org/10.1093/CARCIN/BGP267.

(27) Reynisson, J.; Stiborová, M.; Martínek, V.; Da Costa, G. G.; Phillips, D. H.; Arlt, V. Mutagenic Potential of Nitrenium Ions of Nitrobenzanthrones: Correlation between

Theory and Experiment. *Environ Mol Mutagen* **2008**, *49* (8), 659–667. https://doi.org/10.1002/EM.20411.

(28) McClelland, R. A.; Ahmad, A.; Dicks, A. P.; Licence, V. E. Spectroscopic Characterization of the Initial C8 Intermediate in the Reaction of the 2-Fluorenylnitrenium Ion with 2'-Deoxyguanosine. *J Am Chem Soc* **1999**. https://doi.org/10.1021/ja9836702.

(29) Guengerich, F. P. N-HYDROXYARYLAMINES. *Drug Metab Rev* **2002**, *34* (3), 607–623. https://doi.org/10.1081/DMR-120005663.

(30) Cui, L.; Sun, H. L.; Wishnok, J. S.; Tannenbaum, S. R.; Skipper, P. L. Identification of Adducts Formed by Reaction of N-Acetoxy-3,5- Dimethylaniline with DNA. *Chem Res Toxicol* **2007**, *20* (11), 1730–1736. https://doi.org/10.1021/TX700306C/SUPPL_FILE/TX700306C-FILE002.PDF.

(31) Cheng, B.; McClelland, R. A. Reaction of Arylnitrenium Ions with Guanine Derivatives: N1-Methylguanosine and N2,N2-Dimethylguanosine. *https://doi-org.proxy-um.researchport.umd.edu/10.1139/v01-179* **2011**, *79* (12), 1881–1886. https://doi.org/10.1139/V01-179.

(32) Zhou, J.; Liu, L. L.; Cao, L. L.; Stephan, D. W. Nitrogen-Based Lewis Acids: Synthesis and Reactivity of a Cyclic (Alkyl)(Amino)Nitrenium Cation. *Angewandte Chemie International Edition* **2018**, *57* (13), 3322–3326. https://doi.org/10.1002/ANIE.201713118.

(33) Winter, D. K.; Drouin, A.; Lessard, J.; Spino, C. Photochemical Rearrangement of N -Chlorolactams: A Route to N -Heterocycles through Concerted Ring Contraction. *Journal of Organic Chemistry* **2010**, *75* (8), 2610–2618. https://doi.org/10.1021/JO100181H/SUPPL_FILE/JO100181H_SI_002.PDF.

(34) Wardrop, D. J.; Burge, M. S. Nitrenium Ion Azaspirocyclization-Spirodienone Cleavage: A New Synthetic Strategy for the Stereocontrolled Preparation of Highly Substituted Lactams and N-Hydroxy Lactams. *Journal of Organic Chemistry* **2005**, *70* (25), 10271–10284. https://doi.org/10.1021/JO051252R/SUPPL_FILE/JO051252RSI20050727_023704.PDF.

(35) Wardrop, D. J.; Bowen, E. G. Nitrenium Ion-Mediated Alkene Bis-Cyclofunctionalization: Total Synthesis of (-)-Swainsonine. *Org Lett* **2011**, *13* (9), 2376–2379. https://doi.org/10.1021/OL2006117/SUPPL_FILE/OL2006117_SI_002.PDF.

(36) Plater, M. J.; Harrison, W. T. A. The Isolation of N-Tert-Butyl-p-Toluidine Hydrochloride and the Synthesis of Mauveine. *J Chem Res* **2014**, *38* (11), 651–654. https://doi.org/10.3184/174751914X14136446204529.

(37) Murai, K.; Matsuura, K.; Aoyama, H.; Fujioka, H. Oxidative Rearrangement via in Situ Generated N-Chloroamine: Synthesis of Fused Tetrahydroisoquinolines. *Org Lett* **2016**, *18* (6), 1314–1317. https://doi.org/10.1021/ACS.ORGLETT.6B00233/SUPPL_FILE/OL6B00233_SI_002.CIF.

(38) Maiti, S.; Bose, A.; Mal, P. Oxidative N-Arylation for Carbazole Synthesis by C-C Bond Activation. *Journal of Organic Chemistry* **2018**. https://doi.org/10.1021/acs.joc.8b00921.

(39) Maiti, S.; Mal, P. Dehydrogenative Aromatic Ring Fusion for Carbazole Synthesis via C-C/C-N Bond Formation and Alkyl Migration. *Org Lett* **2017**, *19* (9), 2454–2457. https://doi.org/10.1021/ACS.ORGLETT.7B01117/SUPPL_FILE/OL7B01117_SI_003.CIF.

(40) Voskresenska, V.; Wilson, R. M.; Panov, M.; Tarnovsky, A. N.; Krause, J. A.; Vyas, S.; Winter, A. H.; Hadad, C. M. Photoaffinity Labeling via Nitrenium Ion Chemistry: Protonation of the Nitrene Derived from 4-Amino-3-Nitrophenyl Azide to Afford Reactive Nitrenium Ion Pairs. *J Am Chem Soc* **2009**, *131* (32), 11535–11547. https://doi.org/10.1021/JA902224M/SUPPL_FILE/JA902224M_SI_001.PDF.

(41) Panov, M. S.; Voskresenska, V. D.; Ryazantsev, M. N.; Tarnovsky, A. N.; Wilson, R. M. 5-Azido-2-Aminopyridine, a New Nitrene/Nitrenium Ion Photoaffinity Labeling Agent That Exhibits Reversible Intersystem Crossing between Singlet and Triplet Nitrenes. *J Am Chem Soc* **2013**, *135* (51), 19167–19179. https://doi.org/10.1021/JA405637B/SUPPL_FILE/JA405637B_SI_001.PDF.

(42) Michalak, J.; Zhai, H. Bin; Platz, M. S. The Photochemistry of Various Para-Substituted Tetrafluorophenyl Azides in Acidic Media and the Formation of Nitrenium Ions. *Journal of Physical Chemistry* **1996**, *100* (33), 14028–14036. https://doi.org/10.1021/JP961100N/ASSET/IMAGES/LARGE/JP961100NFD17H.JPEG.

(43) Winter, A. H.; Falvey, D. E.; Cramer, C. J.; Gherman, B. F. Benzylic Cations with Triplet Ground States: Computational Studies of Aryl Carbenium Ions, Silylenium Ions, Nitrenium Ions, and Oxenium Ions Substituted with Meta π Donors. *J Am Chem Soc* **2007**, *129* (33), 10113–10119. https://doi.org/10.1021/JA070143M/SUPPL_FILE/JA070143MSI20070620_041738.PDF .

(44) Wang, J.; Burdzinski, G.; Zhu, Z.; Platz, M. S.; Carra, C.; Bally, T. Ultrafast Spectroscopic and Matrix Isolation Studies of P-Biphenylyl, o-Biphenylyl, and 1-

Naphthylnitrenium Cations. *J Am Chem Soc* **2007**, *129* (26), 8380–8388. https://doi.org/10.1021/JA071325J/SUPPL_FILE/JA071325JSI20070416_112825.PDF.

(45) Sullivan, M. B.; Cramer, C. J. Quantum Chemical Analysis of Heteroarylnitrenium Ions and Mechanisms for Their Self-Destruction. *J Am Chem Soc* **2000**, *122* (23), 5588–5596. https://doi.org/10.1021/JA0005486/SUPPL_FILE/JA0005486_S.PDF.

(46) Qiu, Y.; Fischer, L. J.; Dutton, A. S.; Winter, A. H. Aryl Nitrenium and Oxenium Ions with Unusual High-Spin π,Π* Ground States: Exploiting (Anti)Aromaticity. *J Org Chem* **2017**, *82* (24), 13550–13556. https://doi.org/10.1021/acs.joc.7b02698.

(47) McIlroy, S.; Cramer, C. J.; Falvey, D. E. Singlet - Triplet Energy Gaps in Highly Stabilized Nitrenium Ions: Experimental and Theoretical Study of 1,3-Dimethylbenzotriazolium Ion. *Org Lett* **2000**, *2* (16), 2451–2454. https://doi.org/10.1021/OL006106G/ASSET/IMAGES/LARGE/OL006106GF00002.JPEG.

(48) Lim, M. H.; Worthington, S. E.; Dulles, F. J.; Cramer, C. J. Density-Functional Calculations of Radicals and Diradicals. In *Chemical Applications of Density-Functional Theory*; Laird, B. B., Ross, R. B., Ziegler, T., Eds.; American Chemical Society: Washington, 1996; Vol. 629, pp 402–422.

(49) Gonzalez, C.; Restrepo-Cossio, A.; Márquez, M.; Wiberg, K. B.; De Rosa, M. Ab Initio Study of the Solvent Effects on the Singlet-Triplet Gap of Nitrenium Ions and Carbenes. *Journal of Physical Chemistry A* **1998**, *102* (16), 2732–2738. https://doi.org/10.1021/JP981150N/ASSET/IMAGES/LARGE/JP981150NF00003.JPEG.

(50) Falvey, D. E. Singlet and Triplet States in the Reactions of Nitrenium Ions. *Journal of Physical Organic Chemistry*. John Wiley and Sons Ltd 1999, pp 589–596. https://doi.org/10.1002/(SICI)1099-1395(199908)12:8<589::AID-POC170>3.0.CO;2-T.

(51) Kung, A. C.; Mcilroy, S. P.; Falvey, D. E. Diphenylnitrenium Ion: Cyclization, Electron Transfer, and Polymerization Reactions. **2005**. https://doi.org/10.1021/jo050598z.

(52) Ren, D.; McClelland, R. A. Carbocation-like Reactivity Patterns in X'-Substituted-4-Biphenylylnitrenium Ions. *Canadian Journal Chemistry* **1998**, *76* (1), 78–84. https://doi.org/10.1139/V97-204.

(53) Ramlall, P.; McClelland, R. A. Photochemical Generation and Lifetimes in Water of P-Aryloxy- and p-Alkoxyphenylnitrenium Ions. *Journal of the Chemical Society, Perkin Transactions 2* **1999**, No. 2, 225–232. https://doi.org/10.1039/A807567K.

(54) Dicks, A. P.; Ahmad, A. R.; D'Sa, R.; McClelland, R. A. Tautomers and Conjugate Base of the Nitrenium Ion Derived from N-Acetylbenzidine. *Journal of the Chemical Society, Perkin Transactions 2* **1999**, No. 1, 1–4. https://doi.org/10.1039/A808322C.

(55) Sullivan, M. B.; Brown, K.; Cramer, C. J.; Truhlar, D. G. Quantum Chemical Analysis of Para-Substitution Effects on the Electronic Structure of Phenylnitrenium Ions in the Gas Phase and Aqueous Solution. *J. Am. Chem. Soc.* **1998**, *120* (45), 11778–11783. https://doi.org/10.1021/ja982542a.

(56) Albright, T. R.; Winter, A. H. A Fine Line Separates Carbocations from Diradical Ions in Donor-Unconjugated Cations. *J Am Chem Soc* **2015**, *137* (9), 3402–3410. https://doi.org/10.1021/JACS.5B00707/SUPPL_FILE/JA5B00707_SI_001.PDF.

(57) Chiapperino, D.; McIlroy, S.; Falvey, D. E. Reactions of N-Methyl-N-(4-Biphenylyl)Nitrenium Ion with Electron-Rich Arenes: Laser Flash Photolysis and Product

Studies. *J Am Chem Soc* **2002**, *124* (14), 3567–3577. https://doi.org/10.1021/JA011049N/SUPPL_FILE/JA011049N_S.PDF.

(58) Chiapperino, D.; Falvey, D. E. N-Methyl-N-Phenylnitrenium Ion from Photolysis of N-(Methylphenylamino)-2,4,6-Trimethylpyridinium Tetrafluoroborate. *J Phys Org Chem* **1998**, *10* (12), 917–924.

(59) Chiapperino, D.; Anderson, G. B.; Robbins, R. J.; Falvey, D. E. Photochemically Generated Arylnitrenium Ions: Laser Flash Photolysis and Product Studies of the Photochemistry of N-Tert-Butyl-3-Methyl-6-Chloroanthranilium Ions. *Journal of Organic Chemistry* **1996**, *61* (9), 3195–3199. https://doi.org/10.1021/JO952149C/ASSET/IMAGES/JO952149C.SOCIAL.JPEG_V03.

(60) Srivastava, S.; Falvey, D. E. Reactions of a Triplet Arylnitrenium Ion: Laser Flash Photolysis and Product Studies of N-Tert-Butyl(2-Acetyl-4-Nitrophenyl)Nitrenium Ion. *J Am Chem Soc* **1995**, *117* (41), 10186–10193. https://doi.org/10.1021/JA00146A003/ASSET/JA00146A003.FP.PNG_V03.

(61) Zeppuhar, A. N.; Falvey, D. E. Generation of N,N-Di(4-Bromophenyl)Nitrenium Ion under Acidic Conditions: Search for a Nitrenium Dication. *Cite This: J. Org. Chem* **2020**, *85*, 8850. https://doi.org/10.1021/acs.joc.0c00686.

(62) Robbins, R. J.; Yang, L. L. N.; Anderson, G. B.; Falvey, D. E. Photogenerated Arylnitrenium Ions: Reactions of N-Tert-Butyl (2-Acetyl-4-Substituted)Phenyl Nitrenium Ions with Alcohols and Water Studied by Laser Flash Photolysis. *J Am Chem Soc* **1995**, *117* (24), 6544–6552. https://doi.org/10.1021/ja00129a019.

(63) Anderson, G. B.; Falvey, D. E. Photogenerated Arylnitrenium Ions: Absorption Spectra and Absolute Rate Constants for Tert-Butyl(4-Halo-2-Acetylphenyl)Nitrenium Ions

Measured by Time-Resolved Laser Spectroscopy. *J Am Chem Soc* **1993**, *115* (21), 9870–9871. https://doi.org/10.1021/ja00074a092.

(64) Falvey, D. E. Discrete Existence of Singlet Nitrenium Ions Revisited: Computational Studies of Non-Aryl Nitrenium Ions and Their Rearrangements. *ACS Omega* **2018**, *3* (8), 10418–10432. https://doi.org/10.1021/ACSOMEGA.8B01038/SUPPL_FILE/AO8B01038_SI_001.PDF.

(65) Huh, C. W.; Aubé, J. Aryl Nitrenium Ions from N-Alkyl-N-Arylamino-Diazonium Precursors: Synthesis and Reactivity. *Chem Sci* **2014**. https://doi.org/10.1039/c3sc52805g.

(66) Srivastava, S.; Kercher, M.; Falvey, D. E. On the Solution Chemistry of Parent Nitrenium Ion NH 2 + : The Role of the Singlet and Triplet States in Its Reactions with Water, Methanol, and Hydrocarbons. *J. Org. Chem.* **1999**, *64* (16), 5853–5857. https://doi.org/10.1021/jo990324.

(67) Onozato, M.; Ohshima, S. ANALYSIS OF MUTAGENICITY OF NITROBENZANTHRONES BY MOLECULAR ORBITAL CALCULATIONS. *Polycycl Aromat Compd* **2006**, *26* (2), 93–101. https://doi.org/10.1080/10406630600642113.

(68) Chapman, M. C. The First Law of Photochemistry. *Journal of the Chemical Society, Transactions* **1924**, *125* (0), 1521–1526. https://doi.org/10.1039/CT9242501521.

(69) Rohatgi-Mukherjee. The Second Law of Photochemistry. In *Fundamentals of Photochemistry*; New Age International: New Delhi, India, 2013; p 370.

(70) Anslyn, E.; Dougherty, D. Photochemistry. In *Modern Physical Organic Chemistry*; Murdzek, J., Ed.; University Science, 2004; pp 935–992.

(71) Jaffé, H. H.; Miller, A. L. The Fates of Electronic Excitation Energy. *J Chem Educ* **1966**, *43* (9), 469–473. https://doi.org/10.1021/ED043P469.

(72) Chakraborty, M.; Jin, K. J.; Brewer, S. C.; Peng, H. L.; Platz, M. S.; Novak, M. Indirect and Direct Detection of the 4-(Benzothiazol-2-Yl)Phenylnitrenium Ion from a Putative Metabolite of a Model Anti-Tumor Drug. *Org Lett* **2009**, *11* (21), 4862–4865. https://doi.org/10.1021/OL901959Z/SUPPL_FILE/OL901959Z_SI_001.PDF.

(73) Wang, J.; Kubicki, J.; Platz, M. S. An Ultrafast Study of Phenyl Azide: The Direct Observation of Phenylnitrenium Ion. *Org Lett* **2007**, *9* (20), 3973–3976. https://doi.org/10.1021/OL701598M/SUPPL_FILE/OL701598M-FILE002.PDF.

(74) McClelland, R. A.; Kahley, M. J.; Davidse, P. A.; Hadzialic, G. Acid-Base Properties of Arylnitrenium Ions. *J Am Chem Soc* **1996**, *118* (20), 4794–4803. https://doi.org/10.1021/JA954248D/ASSET/IMAGES/LARGE/JA954248DF00006.JPEG.

(75) Xue, J.; Guo, Z.; Chan, P. Y.; Chu, L. M.; But, T. Y. S.; Phillips, D. L. Time-Resolved Resonance Raman Study of the Reaction of the 2-Fluorenylnitrenium Ion with 2-Fluorenylazide. *Journal of Physical Chemistry A* **2007**, *111* (8), 1441–1451. https://doi.org/10.1021/JP066699Y/SUPPL_FILE/JP066699YSI20061205_104916.PDF.

(76) Kwok, W. M.; Chan, P. Y.; Phillips, D. L. Direct Observation of the 2-Fluorenylnitrene and 4-Methoxyphenylnitrene Reactions with Water Using Picosecond Kerr-Gated Time-Resolved Resonance Raman Spectroscopy. *Journal of Physical Chemistry B* **2004**, *108* (49), 19068–19075. https://doi.org/10.1021/JP0467292/SUPPL_FILE/JP0467292SI20040723_120650.PDF.

(77) Chan, P. Y.; Zhu, P.; Phillips, D. L. Transient Resonance Raman and Density Functional Theory Study of the 7-Bromo-2-Fluorenylnitrenium Cation. *Research on Chemical Intermediates* **2005**, *31*, 73–84. https://doi.org/10.1163/1568567053146913/METRICS.

(78) Chan, P. Y.; Ong, S. Y.; Zhu, P.; Zhao, C.; Phillips, D. L. Transient Resonance Raman and Density Functional Theory Investigation of 4-Methoxyphenylnitrenium and 4-Ethoxyphenylnitrenium Ions. *Journal of Physical Chemistry A* **2003**, *107* (40), 8067–8074. https://doi.org/10.1021/JP0224261/SUPPL_FILE/JP0224261_S.PDF.

(79) Kirmse, W. Carbene Chemistry. *J Organomet Chem* **1972**, *37* (1), C27–C28. https://doi.org/10.1016/s0022-328x(00)89252-9.

(80) Magid, R. M. Carbenes . Vol. 1. M. Jones, Jr., and R. A. Moss, Eds. Wiley, New York, 1973. *Science (1979)* **1973**. https://doi.org/10.1126/science.181.4098.435.a.

(81) Magid, R. M. Carbenes. Vol. 2. M. Jones, Jr., and R. A. Moss, Eds. Wiley, New York, 1975. *Science (1979)* **1975**. https://doi.org/10.1126/science.181.4098.435-a.

(82) Herzberg, G.; Shoosmith, J. Spectrum and Structure of the Free Methylene Radical. *Nature* **1959**. https://doi.org/10.1038/1831801a0.

(83) Herzberg, G; Johns, J. W. C. The Bakerian Lecture, The Spectra and Structures of Free Methyl and Free Methylene. *Proc R Soc Lond A Math Phys Sci* **1961**. https://doi.org/10.1098/rspa.1961.0120.

(84) Herzberg, G; Johns, J. W. C. The Spectrum and Structure of the Free BH2 Radical. *Society* **1967**, *298* (1453), 142–159.

(85) Herzberg, G.; Johns, J. W. C. On the Structure of CH2 in Its Triplet Ground State. *The Journal of Chemical Physics*. 1971. https://doi.org/10.1063/1.1675164.

(86) Skell, P. S.; Woodworth, R. C. Methylene, CH2. Stereospecific Reaction with Cis-and Trans-2-Butene. *J Am Chem Soc* **1959**, *81* (12), 3383–3386.

(87) Platz, M.; Maloney, V. *Kinetics and Spectroscopy of Carbenes and Biradicals*; Platz, M., Ed.; Plenum Press: New York, 1990.

(88) Closs, G. *Topics in Stereochemistry Vol. 3*; Eliel, E. L.; Allinger, N. L., Ed.; Interscience Publishers, 1968.

(89) Paddon-Row, M. N.; Santiago, C.; Houk, K. N. Dynamics and Energetics of the Singlet-Triplet Interconversion of Diphenyl Carbene. *Journal of American Chemical Society* **1980**, *102* (21), 6563–6566.

(90) Griller, D.; Nazran, A. S.; Scaiano, J. C. Flash Photolysis Studies of Carbenes and Their Reaction Kinetics. *Acc Chem Res* **1984**. https://doi.org/10.1021/ar00104a004.

(91) Hadel, L. M.; Maloney, V. M.; Platz, M. S.; McGimpsey, W. G.; Scaiano, J. C. The Absolute Kinetics of Several Reactions of Substituted Diphenylcarbenes. *J Phys Chem* **1986**. https://doi.org/10.1021/j100402a044.

(92) Robbins, R. J.; Laman, D. M.; Falvey, D. E. Substituent Effects on the Lifetimes and Reactivities of Arylnitrenium Ions Studied by Laser Flash Photolysis and Photothermal Beam Deflection. *J Am Chem Soc* **1996**, *118* (34), 8127–8135. https://doi.org/10.1021/ja961518z.

(93) Bogdal, D. CARBAZOLYL NITRENIUM CATIONS: GENERATION AND REACTIONS. *Heterocycles* **2000**, *53* (12), 2679–2688.

(94) Chinn, E.; Falvey, D. Generation of the Antiaromatic 3,6-Dibromocarbazolyl Nitrenium Ion: Mechanistic Studies and Alkene Trapping.

(95) Bogdal, D. Microwave-Assisted Generation of Carbazolyl Nitrenium Cation. *ARKIVOC* **2001**, *6*, 109–115.

(96) Thomas, S. I.; Falvey, D. E. N,N-Di(4-Halophenyl)Nitrenium Ions: Nucleophilic Trapping, Aromatic Substitution, and Hydrogen Atom Transfer. *Journal of Organic Chemistry* **2007**. https://doi.org/10.1021/jo062578i.

(97) Zeppuhar, A. N.; Falvey, D. E. Generation of N, N-Di(4-Bromophenyl)Nitrenium Ion under Acidic Conditions: Search for a Nitrenium Dication. *Journal of Organic Chemistry* **2020**. https://doi.org/10.1021/acs.joc.0c00686.

(98) Thomas, S. I.; Falvey, D. E. Fast Reactions of Arylnitrenium Ions with Amino Acids and Proteins: A Laser Flash Photolysis Study. *J Phys Org Chem* **2006**. https://doi.org/10.1002/poc.1031.

(99) Platz, M.; Maloney, V. Laser Flash Photolysis Studies of Triplet Carbenes. In *Kinetics and Spectroscopy of Carbenes and Biradicals*; Plenum Press: New York, 1990; p 266.

(100) Platz, M.; Maloney, V. Laser Flash Photolysis Studies of Triplet Carbenes. In *Kinetics and Spectroscopy of Carbenes and Biradicals*; Plenum Press: New York, 1990; p 287.

(101) Burkey, T. J.; Majewski, M.; Griller, D. Heats of Formation of Radicals and Molecules by a Photoacoustic Technique. *J Am Chem Soc* **1986**, *108* (9), 2218–2221. https://doi.org/10.1021/JA00269A017/ASSET/JA00269A017.FP.PNG_V03.

(102) Roth, H. G.; Romero, N. A.; Nicewicz, D. A. Experimental and Calculated Electrochemical Potentials of Common Organic Molecules for Applications to Single-Electron Redox Chemistry. *Synlett* **2016**, *27* (5), 714–723. https://doi.org/10.1055/S-0035-1561297/ID/JR000-2/BIB.

(103) Saraswat, M.; Portela-Gonzalez, A.; Mendez-Vega, E.; Sander, W.; Hemberger, P. N-Carbazolyl π-Radical and Its Antiaromatic Nitrenium Ion: A Threshold Photoelectron Spectroscopic Study. *Journal of Physical Chemistry A* **2024**. https://doi.org/10.1021/ACS.JPCA.4C05855/SUPPL_FILE/JP4C05855_SI_001.PDF.

(104) Balakrishna, B.; Mossin, S.; Kramer, S. Photo-Induced Metal-Free Dehydrogenative N–N Homo-Coupling. *Chemical Communications* **2022**, *58* (78), 10977–10980. https://doi.org/10.1039/D2CC04204E.

(105) Kundu, S.; Behera, B.; Giri, A.; Saha, N.; Patra, A. N,N′-Bicarbazole-Benzothiadiazole-Based Conjugated Porous Organic Polymer for Reactive Oxygen Species Generation in Live Cells. *Chemical Communications* **2021**, *57* (56), 6875–6878. https://doi.org/10.1039/D1CC02352G.

(106) Zweig, A.; Hodgson, W. G.; Jura, W. H. The Oxidation of Methoxybenzenes. *J Am Chem Soc* **1964**, *86* (19), 4124–4129. https://doi.org/10.1021/JA01073A043/ASSET/JA01073A043.FP.PNG_V03.

(107) Da Silva Santos, B. M.; dos Santos Dupim, M.; de Souza, C. P.; Cardozo, T. M.; Finelli, F. G. DABCO-Promoted Photocatalytic C–H Functionalization of Aldehydes. *Beilstein Journal of Organic Chemistry 17:205* **2021**, *17* (1), 2959–2967. https://doi.org/10.3762/BJOC.17.205.

(108) Mikami, K.; Tomita, Y.; Ichikawa, Y.; Amikura, K.; Itoh, Y. Radical Trifluoromethylation of Ketone Silyl Enol Ethers by Activation with Dialkylzinc. *Org Lett* **2006**, *8* (21), 4671–4673. https://doi.org/10.1021/OL0611301/SUPPL_FILE/OL0611301SI20060912_014105.PDF.

(109) Decker, C.; Bianchi, C.; Decker, D.; Morel, F. Photoinitiated Polymerization of Vinyl Ether-Based Systems. *Prog Org Coat* **2001**, *42* (3–4), 253–266. https://doi.org/10.1016/S0300-9440(01)00203-X.

(110) Bal, A.; Maiti, S.; Mal, P. Intermolecular C-Arylation of 2-Amidobiphenyls Overcoming Intramolecular N-Arylation. *Asian J Org Chem* **2020**, *9* (11), 1783–1786.

(111) Zhao, C.-Y.; Li, K.; Pang, Y.; Li, J.-Q.; Liang, C.; Su, G.-F.; Mo, D.-L. Iodine(III) Reagent-Mediated Intramolecular Amination of 2-Alkenylanilines to Prepare Indoles. *Adv Synth Catal* **2018**, *360* (10), 1919–1925.

(112) Chinn, E. S.; Li, Y.; Joyce, A. M.; Falvey, D. E. Selective Photo Labeling of Tryptophan with N-Acetyl-L-Tryptophan Ethyl Ester and Peptide WWCNDGR. **2025**. https://doi.org/10.26434/CHEMRXIV-2025-96K9J.

(113) Pham, G. H.; Ou, W.; Bursulaya, B.; DiDonato, M.; Herath, A.; Jin, Y.; Hao, X.; Loren, J.; Spraggon, G.; Brock, A.; Uno, T.; Geierstanger, B. H.; Cellitti, S. E. Tuning a Protein-Labeling Reaction to Achieve Highly Site Selective Lysine Conjugation. *ChemBioChem* **2018**, *19* (8), 799–804. https://doi.org/10.1002/CBIC.201700611.

(114) Fontana, A.; Spolaore, B.; Mero, A.; Veronese, F. M. Site-Specific Modification and PEGylation of Pharmaceutical Proteins Mediated by Transglutaminase. *Adv Drug Deliv Rev* **2008**, *60* (1), 13–28. https://doi.org/10.1016/J.ADDR.2007.06.015.

(115) Misterkiewicz, B.; Salmain, M.; Jaouen, G. Site-Selective and Covalent Labelling of the Cysteine-Containing Peptide Glutathione with a Ferrocenyl Group. *Tetrahedron Lett* **2004**, *45* (40), 7511–7513. https://doi.org/10.1016/J.TETLET.2004.07.143.

(116) Ban, H.; Gavrilyuk, J.; Barbas, C. F. Tyrosine Bioconjugation through Aqueous Ene-Type Reactions: A Click-Like Reaction for Tyrosine. **2024**, *14*, 52. https://doi.org/10.1021/ja909062q.

(117) Ban, H.; Nagano, M.; Gavrilyuk, J.; Hakamata, W.; Inokuma, T.; Barbas, C. F. Facile and Stabile Linkages through Tyrosine: Bioconjugation Strategies with the Tyrosine-Click Reaction. **2013**. https://doi.org/10.1021/bc300665t.

(118) Tilley, S. D.; Francis, M. B. Tyrosine-Selective Protein Alkylation Using π-Allylpalladium Complexes. **2006**. https://doi.org/10.1021/ja057106k.

(119) Jones, M. W.; Mantovani, G.; Blindauer, C. A.; Ryan, S. M.; Wang, X.; Brayden, D. J.; Haddleton, D. M. Direct Peptide Bioconjugation/PEGylation at Tyrosine with Linear and Branched Polymeric Diazonium Salts. **2012**. https://doi.org/10.1021/ja211855q.

(120) Gauthier, M. A.; Klok, A. Arginine-Specific Modification of Proteins with Polyethylene Glycol. https://doi.org/10.1021/bm101272g.

(121) Kramer, J. R.; Deming, T. J. Reversible Chemoselective Tagging and Functionalization of Methionine Containing Peptides †. *This journal is Cite this: Chem. Commun* **2013**, *49*, 5144. https://doi.org/10.1039/c3cc42214c.

(122) Carlsson, F. H. H. The Selective S-Alkylation of a Methionine Residue in an Elapid Venom Cardiotoxin. *International Journal of Biochemistry* **1987**, *19* (10), 915–921. https://doi.org/10.1016/0020-711X(87)90172-8.

(123) Ladner, C. L.; Turner, R. J.; Edwards, R. A. Development of Indole Chemistry to Label Tryptophan Residues in Protein for Determination of Tryptophan Surface Accessibility. https://doi.org/10.1110/ps.062728407.

(124) Petersen, J.; Christensen, K. E.; Nielsen, M. T.; Mortensen, K. T.; Komnatnyy, V. V; Nielsen, T. E.; Qvortrup, K. Oxidative Modification of Tryptophan-Containing Peptides. **2018**. https://doi.org/10.1021/acscombsci.8b00014.

(125) Petersen, J.; Christensen, K. E.; Nielsen, M. T.; Mortensen, K. T.; Komnatnyy, V. V; Nielsen, T. E.; Qvortrup, K. Oxidative Modification of Tryptophan-Containing Peptides. **2018**. https://doi.org/10.1021/acscombsci.8b00014.

(126) Antos, J. M.; Francis, M. B. *Selective Tryptophan Modification with Rhodium Carbenoids in Aqueous Solution*; UTC, 2004; Vol. 126, p 40. https://doi.org/10.1021/ja047272c.

(127) *A chemical method for selective labelling of the key amino acid tryptophan*. https://www.nature.com/articles/d41586-024-00452-7 (accessed 2024-10-30).

(128) Orellana, N. V.; Taylor, M. T. Targeting Tryptophan for Tagging through Photoinduced Electron Transfer. *Synlett* **2021**, *32* (14), 1371–1378. https://doi.org/10.1055/A-1479-6366/ID/JR000-2/BIB.

(129) Tower, S. J.; Hetcher, W. J.; Myers, T. E.; Kuehl, N. J.; Taylor, M. T. Selective Modification of Tryptophan Residues in Peptides and Proteins Using a Biomimetic Electron Transfer Process. *J Am Chem Soc* **2020**, *142* (20), 9112–9118. https://doi.org/10.1021/JACS.0C03039/ASSET/IMAGES/LARGE/JA0C03039_0004.JPEG.

(130) Hamachi, I.; Sakamoto, S. Recent Progress in Chemical Modification of Proteins. *Analytical Sciences* **2019**, *35*, 5–27.

(131) Novak, M.; Rajagopal, S.; Xu, L.; Kazerani, S.; Toth, K.; Brooks, M.; Nguyen, T. M. Chemistry of Carcinogenic and Mutagenic Metabolites of Heterocyclic Aromatic Amines. *J Phys Org Chem* **2004**. https://doi.org/10.1002/poc.765.

(132) Dipple, A. Dna Adducts of Chemical Carcinogens. *Carcinogenesis*. 1995. https://doi.org/10.1093/carcin/16.3.437.

(133) Thomas, S. I.; Falvey, D. E. Fast Reactions of Arylnitrenium Ions with Amino Acids and Proteins: A Laser Flash Photolysis Study. *J Phys Org Chem* **2006**. https://doi.org/10.1002/poc.1031.

(134) *UniProtKB/Swiss-Prot protein knowledgebase*. http://web.expasy.org/docs/relnotes/relstat.html.

(135) CANFIELD, R. E. The Amino Acid Sequence of Egg White Lysozyme. *Journal of Biological Chemistry* **1963**, *238* (8), 2698–2707. https://doi.org/10.1016/S0021-9258(18)67888-3.

(136) Christopher Cattanach, B. J.; Cohen, A.; Heath-Brown, B.; Products Limited, R.; Galantay, E. E.; Hoffman, C.; Paolella, N.; Gogerty, J.; Iorio, L.; Leslie, G.; Trapold, J. H.; Broadbent, H. S.; Burnham, W. S.; Olsen, R. K. Studies in the Indole Series. Part VII. Indolo[1,7-Ab][1]Benzazepines and Related Compounds. *J Chem Soc Perkin 1* **1973**, *12* (0), 1041–1047. https://doi.org/10.1039/P19730001041.

(137) Greulich, T. W.; Daniliuc, C. G.; Studer, A. N -Aminopyridinium Salts as Precursors for N-Centered Radicals - Direct Amidation of Arenes and Heteroarenes. *Org Lett* **2015**, *17* (2), 254–257. https://doi.org/10.1021/OL503338B/SUPPL_FILE/OL503338B_SI_002.CIF.

(138) Thermofischer Scientific - Materials & Structural Analysis. *Using Benchtop 19F NMR to Evaluate Fluoroorganic Compounds*. https://www.azom.com/article.aspx?ArticleID=14942 (accessed 2025-02-14).

(139) Rosenau, C. P.; Jelier, B. J.; Gossert, A. D.; Togni, A. Exposing the Origins of Irreproducibility in Fluorine NMR Spectroscopy. *Angewandte Chemie International Edition* **2018**, *57* (30), 9528–9533. https://doi.org/10.1002/ANIE.201802620.